CANADIAN THESES ON MICROFICHE

I.S.B.N.

THESES CANADIENNES SUR MICROFICHE

National Library of Canada
Collections Development Branch

Canadian Theses on
Microfiche Service

Ottawa, Canada
K1A 0N4

Bibliothèque nationale du Canada
Direction du développement des collections

Service des thèses canadiennes
sur microfiche

NOTICE

The quality of this microfiche is heavily dependent upon the quality of the original thesis submitted for microfilming. Every effort has been made to ensure the highest quality of reproduction possible.

If pages are missing, contact the university which granted the degree.

Some pages may have indistinct print especially if the original pages were typed with a poor typewriter ribbon or if the university sent us a poor photocopy.

Previously copyrighted materials (journal articles, published tests, etc.) are not filmed.

Reproduction in full or in part of this film is governed by the Canadian Copyright Act, R.S.C. 1970, c. C-30. Please read the authorization forms which accompany this thesis.

THIS DISSERTATION
HAS BEEN MICROFILMED
EXACTLY AS RECEIVED

AVIS

La qualité de cette microfiche dépend grandement de la qualité de la thèse soumise au microfilmage. Nous avons tout fait pour assurer une qualité supérieure de reproduction.

S'il manque des pages, veuillez communiquer avec l'université qui a conféré le grade.

La qualité d'impression de certaines pages peut laisser à désirer, surtout si les pages originales ont été dactylographiées à l'aide d'un ruban usé ou si l'université nous a fait parvenir une photocopie de mauvaise qualité.

Les documents qui font déjà l'objet d'un droit d'auteur (articles de revue, examens publiés, etc.) ne sont pas microfilmés.

La reproduction, même partielle, de ce microfilm est soumise à la Loi canadienne sur le droit d'auteur, SRC 1970, c. C-30. Veuillez prendre connaissance des formules d'autorisation qui accompagnent cette thèse.

LA THÈSE A ÉTÉ
MICROFILMÉE TELLE QUE
NOUS L'AVONS REÇUE

NL-339 (r. 82/08)

Canada

192 0-315-12505-5

National Library of Canada
Canadian Theses Division
Ottawa, Canada
K1A 0N4

Bibliothèque nationale du Canada
Division des thèses canadiennes

60416

PERMISSION TO MICROFILM — AUTORISATION DE MICROFILMER

- Please print or type — Écrire en lettres moulées ou dactylographier

Full Name of Author — Nom complet de l'auteur

Paul C Weerdenburg

Date of Birth — Date de naissance December 5, 1953	Country of Birth — Lieu de naissance Canada

Permanent Address — Résidence fixe

466 Hillside Park
51112 Range Road 222
Sherwood Park, Alberta T8C 1G9

Title of Thesis — Titre de la thèse

Analytical Study of Time-Dependent Deformation in Permafrost

University — Université

University of Alberta

Degree for which thesis was presented — Grade pour lequel cette thèse fut présentée

Master of Science

Year this degree conferred — Année d'obtention de ce grade 1982	Name of Supervisor — Nom du directeur de thèse N. R. Morgenstern

Permission is hereby granted to the NATIONAL LIBRARY OF CANADA to microfilm this thesis and to lend or sell copies of the film.

The author reserves other publication rights, and neither the thesis nor extensive extracts from it may be printed or otherwise reproduced without the author's written permission.

L'autorisation est, par la présente, accordée à la BIBLIOTHÈQUE NATIONALE DU CANADA de microfilmer cette thèse et de prêter ou de vendre des exemplaires du film.

L'auteur se réserve les autres droits de publication; ni la thèse ni de longs extraits de celle-ci ne doivent être imprimés ou autrement reproduits sans l'autorisation écrite de l'auteur.

Date Oct 12, 1982	Signature Paul Weerdenburg

NL-91 (4/77)

THE UNIVERSITY OF ALBERTA

ANALYTICAL STUDY OF TIME-DEPENDENT DEFORMATION IN PERMAFROST

by

©

PAUL C. WEERDENBURG

A THESIS

SUBMITTED TO THE FACULTY OF GRADUATE STUDIES
AND RESEARCH IN PARTIAL FULFILLMENT OF THE
REQUIREMENTS FOR THE DEGREE OF
MASTER OF SCIENCE

DEPARTMENT OF CIVIL ENGINEERING
EDMONTON, ALBERTA
FALL, 1982

Micro

THE UNIVERSITY OF ALBERTA

RELEASE FORM

NAME OF AUTHOR: Paul C. Weerdenburg

TITLE OF THESIS: Analytical Study of Time-Dependent Deformation in Permafrost

DEGREE FOR WHICH DEGREE WAS GRANTED: Master of Science

YEAR THIS DEGREE WAS GRANTED: Fall 1982

Permission is hereby granted to THE UNIVERSITY OF ALBERTA LIBRARY to reproduce single copies of this thesis and to lend or sell such copies for private, scholarly or scientific research purposes only.

The author reserves other publication rights, and neither the thesis nor extensive extracts from it may be printed or otherwise reproduced without the author's written permission.

(Signed) Paul Weerdenburg

PERMANENT ADDRESS:
466 Hillside Park
51112 Range Road 222
Sherwood Park, Alberta
T8C 1G9

DATED: October 4, 1982

THE UNIVERSITY OF ALBERTA

FACULTY OF GRADUATE STUDIES AND RESEARCH

The undersigned certify that they have read, and recommend to the Faculty of Graduate Studies and Research, for acceptance, a thesis entitled 'ANALYTICAL STUDY OF TIME-DEPENDENT DEFORMATION IN PERMAFROST' submitted by Paul C. Weerdenburg, in partial fulfillment of the degree of Master of Science in Civil Engineering.

N.R. Morgenstern
Supervisor

DC Sego
D.C. Sego

T. Hrudey
T.M. Hrudey

JR Colbourne.
J.R. Colbourne

DATE: October 4, 1982

ABSTRACT

This thesis describes an analytical study of in-situ creep behavior in ice-rich permafrost. An incremental initial strain procedure was formulated to solve steady state creep problems using the finite element method. Two case histories were analyzed where naturally occurring creep had been monitored for several years.

The numerical analyses of the left bank of the Great Bear River at the proposed Arctic Gas crossing has shown that the steady state creep in the ice-rich glaciolacustrine clay at the site can be modelled by a simple power law with an exponent of 3.0 and a coefficient of 3.33×10^{-9} kPa^{-3} yr^{-1}. This strain rate is six times slower than the value for polycrystalline ice at an equivalent temperature. The exact form of the constitutive relationship for the glaciodeltaic sand overlying the clay remains unclear.

A review of the available in-situ deformation studies carried out at the Fox Tunnel near Fairbanks, Alaska, showed that attenuating creep behavior extended well over one year and contributed significantly to the total room closure. In this case, the flow law for polycrystalline ice did not yield an upper bound solution to the observed room closure measurements. However, it is felt that the difference lies in time-dependent failure caused by stress release which was not accounted for in the numerical model.

ACKNOWLEDGEMENTS

The author would like to thank his supervisor, Dr. N.R. Morgenstern, for suggesting this thesis topic and providing guidance and encouragement throughout this reserch.

Financial assistance was provided by the National Research Council of Canada, the Department of National Defence, and the University of Alberta. EBA Engineering Consultants Ltd. generously provided personnel and facilities for typing, drafting and duplication of the manuscript. This support is gratefully acknowledged.

The author is grateful to Mr. F. Sayles of the U.S. Army Cold Regions Research and Engineering Laboratory in Hanover, N.H., for providing the room closure measurements of the Fox Tunnel. Special thanks are extended to Dr. K.W. Savigny for guidance provided during the Great Bear River study and to Dr. W.D. Roggensack for his valued comments on portions of the manuscript. A word of thanks is also due to the staff and my fellow graduate students within the Department of Civil Engineering.

Typing of the manuscript by E. Bishop, N. Teixeira, and C. Zuk is acknowledged, with thanks. Drafting services provided by L. Marquis and B. Regan are gratefully appreciated.

In closing, the author would like to express sincere thanks to my wife, Genia, for her continual encouragement and patience has made the past twelve months possible and to my daughter, Kirstin, who made the busiest moments seem a little easier.

TABLE OF CONTENTS

Page

Abstract iv

Acknowledgements v

List of Tables viii

List of Figures ix

CHAPTER I INTRODUCTION 1

1.1 General 1
1.2 Scope of Thesis 2

CHAPTER II RHEOLOGICAL BEHAVIOR OF FROZEN SOILS 4

2.1 General 4
2.2 Composition of Frozen Soil 5
2.3 Creep of Ice 6
2.4 Creep of Frozen Soil 11
2.5 Conclusions 19

CHAPTER III FINITE ELEMENT CREEP ANALYSIS 25

3.1 General 25
3.2 Incremental Initial Strain Procedure 29
3.3 Cumulative Creep Rule 33
3.4 Finite Element Formulation of Incremental Initial Strain Method 36
3.5 Time Increment Selection 39
3.6 Finite Element Programme 42

CHAPTER IV IN-SITU CREEP ANALYSIS OF A SLOPE IN ICE-RICH PERMAFROST 48
4.1 General 48
4.2 Site Geology 49
4.3 Field Instrumentation 50
4.4 Finite Element Analyses 54
4.5 Assessment of Analytical Results 59
4.6 Modelling Ice-Rich Permafrost as a Two-Phase Continuum 61

TABLE OF CONTENTS (cont'd)

Page

CHAPTER V ANALYSES OF IN-SITU CREEP AT FOX TUNNEL 86

5.1 General 86
5.2 Site Geology 87
5.3 In-Situ Deformation Studies 88
5.4 Assessment of In-Situ Deformation Behavior 98
5.5 Underground Circular Cavities in Permafrost 107

CHAPTER VI CONCLUDING REMARKS 132

6.1 General 132
6.2 Conclusions 133
6.2.1 Great Bear River 133
6.2.2 Fox Tunnel 134
6.3 Recommendations for Further Study 135

REFERENCES 137

APPENDIX A Formulation of Finite Element Equations for Incremental Initial Procedure 147

APPENDIX B Calculation of Fictitious Nodal Forces 153

APPENDIX C Users' Manual for Creep 157

APPENDIX D Programme Listing for Creep 172

APPENDIX E Thick Wall Cylinder Closed Form Solution 222

LIST OF TABLES

Table	Description	Page
2.1	Definitions of Effective Stress and Effective Strain Rate	9
2.2	Creep Parameters for Polycrystalline Ice	11
2.3	Frozen Soil Classification System	14
4.1	Elastic Material Properties for Frozen Glaciodeltaic Sand and Glaciolacustrine Clay	55
5.1	Elastic Material Properties for Frozen Silt and Gravel, Fox Tunnel, Alaska	97

LIST OF FIGURES

Figure	Description	Page
2.1	Typical Constant Stress Creep Curves	21
2.2	Comparison of Definitions of Effective Stress	22
2.3	Axial Stress versus Axial Strain Rate	23
2.4	Deviatoric Stress versus Strain Rate	23
2.5	Steady-State Creep Data for Ice-Rich Glaciolacustrine Clay from Various Locations in the Mackenzie River Valley, N.W.T.	24
3.1	Approximation of a Smooth Stress-Time Curve for Incremental Procedure	44
3.2	Strain Hardening Cumulative Creep Rule	45
3.3	Time Hardening Cumulative Creep Rule	46
3.4	Calculation of Increment of Creep Strain for Varying Stress Conditions	47
4.1	Site Plan of Left Bank of Great Bear River at Proposed Arctic Gas Crossing	69
4.2	Site Plan of Proposed Arctic Gas Crossing of Great Bear River (Left Bank)	70
4.3	Stratigraphic Cross-section; Left Bank of Great Bear River at Proposed Arctic Gas Crossing	71
4.4	Thermal Cross-section; Left Bank of Great Bear River at Proposed Arctic Gas Crossing	72
4.5	Site Plan of Inclinometer Locations on Left Bank of Great Bear River at Proposed Arctic Gas Crossing	73
4.6	Velocity versus Depth Profiles for GB1A, GB2, and GB3 Inclinometer Locations	74
4.7	Finite Element Discretization; Left Bank of Great Bear River at Arctic Gas Crossing	75

LIST OF FIGURES (cont'd)

Page

4.8 Predicted Steady State Creep Velocity Profiles, First Creep Analysis 76

4.9 Predicted Steady State Creep Velocity Profiles, Factored Velocities from First Creep Analysis 77

4.10 Comparison of In-Situ Creep Law and Steady State Creep Data for Ice-Rich Glaciolacustrine Clay for Various Locations in the Mackenzie River Valley, N.W.T. 78

4.11 Deformed Grid for Steady State Creep in Sand and Clay 79

4.12 Predicted Creep Velocity Profiles, Creep in Galciolacustrine Clay Only 80

4.13 Deformed Grid for Steady State Creep in Clay Only 81

4.14 Horizontal Stress Contours for Steady State Creep in the Clay Only 82

4.15 Thaw Settlement Data for Norman Wells and Landing Lake Ice Variability Test Sites 83

4.16 Probability Relationship for Thaw Settlement in Lacustrine Silt and Clay 84

4.17 Auto-Correlation Function for Thaw Settlement in Ice-Rich Lacustrine Silt and Clay 85

5.1 Site Plan of Fox Tunnel Site, Alaska 111

5.2 Plan of Fox Tunnel Showing Second Stage of Excavation 112

5.3 Geologic Cross Section, Fox Tunnel Site 113

5.4 Closure Measurements of Main Tunnel Following 1965 Construction Season 114

5.5 Closure Measurements of Main Tunnel Following Installation of Ventilation Shaft 115

5.6 Vertical Closure of the USBM Room in the Fox Tunnel 116

5.7 Vertical Closure of the USA CRREL Room in the Fox Tunnel 117

LIST OF FIGURES (cont'd)

		Page
5.8	Horizontal Closure of the USA CRREL Room in the Fox Tunnel	118
5.9	Vertical and Horizontal Closure Rate of the USA CRREL Room in the Fox Tunnel	119
5.10	Finite Element Discretization of USA CRREL Room in the Fox Tunnel	120
5.11	Rendulic Plot of Normally Consolidate Plastic Frozen Soil Stressed Beyond its Long Term Strength	121
5.12	Stress Paths for Normally Consolidated Plastic Frozen Soil Stressed Beyond its Long Term Strength	122
5.13	Stress Paths for Soil Elements Above an Underground Opening	123
5.14	Finite Element Mesh for Tunnel at H/D=2.0	124
5.15	Tunnel Closure Velocity Versus Depth of Overburden	125
5.16	Velocity Vector Plot for Tunnel at H/D=2.0	126
5.17	Velocity Vector Plot for Tunnel at H/D=3.0	127
5.18	Effective Strain Rate Contours for Tunnel at H/D=2.0	128
5.19	Effective Strain Rate Contours for Tunnel at H/D=3.0	129
5.20	Finite Element Mesh for Lined Tunnel at H/D=2.0	130
5.21	Velocity Vector Plot for Lined Tunnel at H/D=2.0	131
B-1	Statically Equivalent Nodal Forces for Constant Strain Triangle	156
E-1	Thick Wall Cylinder Finite Element Mesh	224
E-2	Steady State Creep Velocity	225

CHAPTER I

INTRODUCTION

1.1 General

Depletion of conventional oil and gas reserves has led to an increase in resource exploration activity in the northern frontier lands of Canada and the United States during the past decade and into the foreseeable future. Rising world energy prices has enhanced the economic feasibility of exploiting these reserves and transporting them to market. The largest such project completed to date is the Alyeska Pipeline which transports Alaskan North Slope oil to a shipping terminal at Valdez. The first major northern oil pipeline to be completed in Canada will be the 900 km long pipeline forecast to be in place by 1985 to transport oil south from the expanded oil field in Norman Wells, N.W.T. to Zama, Alberta where it will connect with an existing pipeline.

Resource exploration and development will require major civil works to be constructed on or within permafrost. These structures will present unique problems to engineers as the strength and deformation behavior in frozen soil will respond in both the time and thermal domain. The presence of ice as either discrete segregated structures or in the pore spaces, imparts a major influence on the creep behavior that characterizes frozen soil.

The in-situ creep behavior of frozen soil will have a major influence on establishing geotechnical design guidelines that ensure serviceable foundation performance for structures founded in permafrost. Ladanyi (1972) has developed an engineering theory for creep in frozen soils. The finite element technique is now routinely used for solving a large class of engineering problems. The aim of the research reported herein was to use the finite element technique to predict the in-situ creep deformation patterns in ice-rich permafrost foundation soils.

To date, these are only two documented case histories comparing long term in-situ and laboratory creep behavior of frozen soil. An analytical study was carried out by Thompson and Sayles (1972) in conjunction with a field program of the U.S. Army Cold Regions Research and Engineering Laboratory (USA CRREL) in the Fox Tunnel north of Fairbanks, Alaska. In-situ measurement of creep deformations were carried out for three and one half years. Savigny (1980) reported the results of an extensive field and laboratory program on the proposed Arctic Gas crossing of the Great Bear River near Fort Norman, N.W.T. Naturally occurring creep movements in the left bank of the Great Bear River were recorded for a two year period.

1.2 Scope of Thesis

Chapter II presents a review of the rheological behavior of frozen soil. Since the deformation behavior of frozen soil is governed by the amount of ice present, a detailed review of the deformation behavior of polycrystalline ice is presented. This is followed by a review of the deformation behavior for reconstituted frozen soil and natural permafrost. The existing constitutive relationships for creep in natural permafrost samples are examined. An upper bound flow law for the creep in ice-rich fine-grained permafrost is presented at the conclusion of this chapter.

Chapter III presents the theoretical basis for the incremental initial strain procedure for solving for the stress state in a non-linear viscous medium. The treatment is restricted to steady state creep problems since the empirically developed constitutive relationship for frozen soil is given by a simple power law relating strain rate to stress. The development of the plane strain finite element programme CREEP is also presented.

Finite element analyses of the in-situ creep behavior of the left bank of the Great Bear River at the proposed Arctic Gas crossing is presented in Chapter IV. These analyses were carried out in an attempt to verify the simple power law as the constitutive equation governing the behavior of frozen ice-rich, fine-grained permafrost soils.

The in-situ deformation behavior at the Fox Tunnel at Fairbanks, Alaska is examined in Chapter V. A synthesis of all the in-situ deformation studies reported in the literature for the Fox Tunnel was carried out in an attempt to gain some insight into the deformation processes surrounding underground openings in frozen ground.

The final chapter presents a summary of the results of this research as well as the limitations of the current analytical approach. Recommended suggestions for future analytical and laboratory creep studies in frozen soils are also presented.

The formulation of the finite element equations for solving creep problems with the incremental initial strain procedure is presented in Appendices A and B. A user's manual and programme listing for the finite element programme CREEP are given in Appendices C and D, respectively. The accuracy of the finite element programme is compared with a thick wall cylinder closed form solution in Appendix E.

CHAPTER II

RHEOLOGICAL BEHAVIOR OF FROZEN SOILS

2.1 General

An understanding of the deformation behavior of frozen ground over a wide range of stress and temperature conditions is required before a numerical analysis can be carried out. Deformation behavior of frozen ground is generally governed by the amount of ice present and its temperature.

Laboratory studies over the past two decades have focussed attention on deriving empirical constitutive relationships describing the stress-strain-time behavior of frozen soils. Many of the early studies were restricted to short duration creep tests on ice and remoulded frozen soils at stresses and temperatures well beyond the range of interest of practical geotechnical problems. As the major factors influencing the creep behavior of frozen soil have been delineated, specifically the soil temperature and ice structure, the need for high quality, long term, low stress creep tests on natural permafrost samples has arisen.

The following sections will present a brief review of the time-dependent load-deformation behavior of ice, remoulded frozen soil and natural permafrost soils as it relates to low stress creep behavior. Unless otherwise mentioned, stress and temperature conditions commonly encountered in geotechnical engineering are assumed.

2.2 Composition of Frozen Soil

Frozen soil can be considered as a complex, four phase, natural formation, consisting of solid mineral particles, ice, unfrozen water and gases. The solid mineral particles present in a frozen soil have an important influence on its geotechnical properties. The primary factors are the grain size and shape as well as the physicochemical nature of the mineral surfaces, which are determined by the mineralogical composition and the cations present. The gaseous phase consists of water vapour and has an insignificant influence on the behavior of frozen soils.

Unfrozen water is present in two states as strongly bound and loosely bound water. The strongly bound water is adjacent to the soil particle. The very high electro-molecular forces present in this layer of water suppresses the formation of ice crystals, even at very low temperatures. The intermolecular forces are also present in the loosely bound water surrounding the strongly bound water. However, this layer is capable of releasing the heat of crystallization at temperatures below 0°C.

The amount of unfrozen water present in a frozen soil depends on its temperature, specific surface and type of soil mineral present and chemistry of the pore water. Each frozen soil is characterized by a specific curve relating its unfrozen water content and temperature.

Of all the phases present in frozen soil, ice is the most important component in the rate, time and temperature dependent properties which characterize frozen soil. Ice can be present both as discrete segregated structures and in the pore spaces of the soil mass. Ice present in frozen soils is generally polycrystalline.

The reader is referred to Anderson and Morgenstern (1973) for a complete summary of conditions affecting the state of frozen ground.

2.3 Creep of Ice

The presence of ice dominates the time-dependent characteristics of frozen soil. Ice 1H is the predominant ice type found in frozen soil. The structure of ice 1H is hexagonal. Each crystal consists of layers of hexagonal rings, referred to as the basal planes. The perpendicular direction to the basal plane is the optic or 'C' axis.

Single crystals of ice deform readily at low stresses along discrete bands parallel to the basal plane of the crystal structure. This type of deformation is referred to as basal glide (easy glide). Single ice crystals will also deform in the perpendicular or non-basal direction (hard glide). However, for a given strain rate, the applied stress can be as much as 20 times greater for hard glide than for easy glide.

Polycrystalline ice is composed of randomly oriented single ice crystals. Physical processes observed during the deformation of polycrystalline ice are dislocation climb, grain boundary slip, cavity formation at the grain boundaries, recrystallization and microcracks developing into ice grains (Michel, 1978).

The deformation response of polycrystalline ice subjected to a load consists of four distinct regions as illustrated by curve II in Figure 2.1. Each of these regions consist of:

1) instantaneous elastic strain (OA)
2) creep strain in a primary mode at a decreasing strain (AB)

3) secondary creep at a constant minimum strain rate (BC)
4) tertiary creep at an accelerating strain rate leading to failure (CD)

The shape of the creep curve is a function of the stress level and ice temperature. For a given temperature, secondary creep is suppressed at high stress levels (undamped creep) while primary creep (damped creep) dominates at low stress levels.

Creep tests on polycrystalline ice in compression, tension, shear and other specialized loading configurations have been carried out to evaluate the form of the constitutive equation. Glen (1975) has recognized two possible ways of identifying a flow law. The first flow law would relate stress to strain rate at a very long time under the application of load allowing recrystallization to occur. The second form of the flow law relates the secondary strain rate to stress before any recrystallization of the ice. At higher stresses, the first flow law would produce deformation rates greater than the minimum (or secondary) rate because recrystallization may produce a grain size and orientation more favorable for plastic flow.

The constitutive equation of polycrystalline ice is most commonly represented empirically by the simple power law. Experimental evidence has shown that the power creep law represents the steady state creep data in the low to intermediate stress range. From a practical viewpoint, this mathematical representation of creep behavior is simpler to use than a physical theory (i.e. rate process theory) because the material parameters are kept to a minimum.

The simple power law relating strain rate to stress is given by:

$$\dot{\varepsilon} = A\sigma^n \tag{2.1}$$

where $\dot{\varepsilon}$ = axial strain rate $(\text{time})^{-1}$
σ = axial stress
A = coefficient (function of temperature and ice type)
n = creep exponent

In order to extend uniaxial creep data to multi-axial stress states, it is common practice to adopt the concept of effective stress, σ_e, and effective creep strain rate, $\dot{\varepsilon}_e$. Several definitions of effective stress and strain rate have been put forward in the metal and ice creep literature. Some of these are listed in Table 2.1.

The definition of effective stress is defined by the square root of the second invariant of the deviatoric stress tensor multiplied by a constant. Likewise, the effective strain rate is defined in a similar manner except that the second invariant of the strain rate tensor is used. The difference between the alternate definitions lies in the value of the constant. Since the stress is raised to an exponent in the simple power law, the magnitude of the constant will influence the effective strain rate in a non-linear manner as shown in Figure 2.3. As shown in the figure, the effective strain rate can change by a complete order of magnitude depending on which definition of effective stress is chosen. The steady state creep law for ice at -2°C (Morgenstern et al., 1980) is plotted in Figure 2.3.

TABLE 2.1 DEFINITIONS OF EFFECTIVE STRESS AND EFFECTIVE STRAIN RATE

Source	Effective Stress	Effective Strain Rate
Odqvist (1966) Dorn et al (1945) Ladanyi (1972) Finnie & Heller (1959)	$\sqrt{3}\sqrt{\overset{\sigma}{J}_2}$	$\frac{2}{\sqrt{3}}\sqrt{\overset{\cdot\varepsilon}{J}_2}$
Nye (1957)	$\sqrt{\overset{\sigma}{J}_2}$	$\sqrt{\overset{\cdot\varepsilon}{J}_2}$
Meier (1959)	$\sqrt{\frac{2}{3}}\sqrt{\overset{\sigma}{J}_2}$	$\sqrt{\frac{2}{3}}\sqrt{\overset{\cdot\varepsilon}{J}_2}$
Vialov (1962)	$\sqrt{\overset{\sigma}{J}_2}$	$\sqrt{2}\sqrt{\overset{\cdot\varepsilon}{J}_2}$

where $\overset{\sigma}{J}_2$ = second invariant of deviatoric stress tensor

$\overset{\cdot\varepsilon}{J}_2$ = second invariant of strain rate tensor

In this work, the effective stress and strain rate as defined by Odqvist (1966) has been used, i.e.:

$$\sigma_e = \sqrt{3}\,\sqrt{J_2^{\sigma}} = \sqrt{\frac{3}{2}\, s_{ij}\, s_{ij}} \qquad (2.2)$$

$$\dot{\varepsilon}_e = \frac{2}{\sqrt{3}}\sqrt{J_2^{\varepsilon}} = \sqrt{\frac{2}{3}\,\dot{\varepsilon}_{ij}\,\dot{\varepsilon}_{ij}} \qquad (2.3)$$

These definitions are adopted because they recover Norton's law, i.e. equation 2.1, for the special case of uniaxial stress. The flow law now becomes:

$$\dot{\varepsilon}_e = A\sigma_e^{\,n} \qquad (2.4)$$

Since the effective stress is a function of the deviatoric stress only, the strain rate is independent of the hydrostatic state of stress.

An extensive review of the secondary creep data of polycrystalline ice was carried out by Morgenstern et al. (1980). Based on this review, the authors presented the values shown in Table 2.2 for the parameters A and n in the power law.

A more detailed review of the rheological characteristics of polycrystalline ice has been prepared by Glen (1975), Roggensack (1977) and Sego (1980).

TABLE 2.2 CREEP PARAMETERS FOR POLYCRYSTALLINE ICE

Temperature (°C)	A($kPa^{-3}yr^{-1}$)	n
-1	4.5×10^{-8}	3.0
-2	2.0×10^{-8}	3.0
-5	1.0×10^{-8}	3.0
-10	5.6×10^{-9}	3.0

2.4 Creep of Frozen Soil

Vialov (1963) described the physical processes involved in the time dependent plastic deformation of frozen soils. The application of a load causes local stress concentrations at soil-ice contacts leading to pressure melting of the ice. A pressure gradient resulting from differences in surface tensions causes the water to migrate to regions of lower stress where it then refreezes. The pressure melting process is accompanied by a breakdown of the ice and structural bonds of the soil grains and plastic deformation of the ice, causing a rearrangement of the mineral particles. The end result is the process known as creep.

Many laboratory studies have been carried out in order to determine the empirical creep parameters for reconsituted frozen soils and natural permafrost soils. The creep tests carried out on remoulded frozen soils are helpful in determining the various factors that influence the creep rate of frozen soils. However, many of these tests were carried out beyond the temperature and stress range of practical interest in geotechnical engineering.

A second difficulty encountered when applying the creep parameters of reconstituted frozen soils to natural permafrost soils is reproducability of the ice facies in the remoulded samples. In natural permafrost samples, the ice is present in the pore spaces as well as in the form of reticulate and segregated ice. Laboratory evidence of Savigny (1980) shows deformations localized along segregated ice in natural permafrost soils. Since the reticulate ice structure can not be reproduced in reconstituted frozen samples, natural permafrost samples must be tested.

Vialov (1959) describes the stress-strain response of a frozen soil as damped or undamped creep. Damped deformations occur when the applied stress is less than the long term strength of the frozen soil. Damped creep behavior is characterized by an instantaneous elastic displacement followed by primary creep where the deformation rate continuously decreases with time. Curve III in Figure 2.1 is typical of damped creep behavior. Undamped deformations occur when the applied stress exceeds the long term strength. In undamped creep, the transient stage gives way to a steady state period where the strain rate reaches a minimum value. The deformations continue to grow until they reach a limiting value or the onset of tertiary creep where the deformation rate will accelerate to failure. A typical undamped deformation response is given by curves I and II in Figure 2.1.

Damped creep deformations are prevalent in dense, ice-poor frozen soils. Since ice has a zero long term strength, its deformation behavior is characterized by undamped creep. The deformation response of ice-rich frozen soils will lie somewhere between these two limiting cases.

Weaver (1979) proposed a classification system for frozen soils based on frozen bulk density that relates to low stress creep behavior. This classification system is shown in Table 2.3.

A generalized theory of creep of frozen soil put forward by Ladanyi (1972) advocates a mathematical rather than a physical treatment of undamped creep behavior. The proposed uniaxial power creep law describing steady state creep is defined as:

$$\dot{\varepsilon}_e = \dot{\varepsilon}_c(\sigma_e/\sigma_c)^n \qquad (2.5)$$

where: σ_c = temperature dependent creep coefficient

ε_c = secondary strain rate corresponding to the application of the stress, σ_c

n = creep exponent

This form of the power law is similar to that given by equation 2.4 except that it is given in a normalized form. Making use of the definitions of effective stress (equation 2.2), the strain rate for an axially symmetric state of stress (i.e. $\sigma_2 = \sigma_3$) is given by:

$$\dot{\varepsilon}_e = \dot{\varepsilon}_c[(\sigma_1-\sigma_3)/\sigma_c]^n \qquad (2.6)$$

where: $\sigma_1 - \sigma_3$ = principal stress difference

TABLE 2.3 FROZEN SOIL CLASSIFICATION SYSTEM
(Proposed by Weaver, 1979)

SOIL TYPE	DESCRIPTION
Dirty Ice	- applies to ice that has a low solids concentration - $\gamma = 0.9 - 1.0$ Mg/m^3 - the soil particles present reduce the average grain size of the ice crystals resulting in higher creep rates than pure ice
Very Dirty Ice	- applies to ice that has medium to high solids concentration - $\gamma = 0.9 - 1.0$ and $1.6 - 1.8$ Mg/m^3 - very little grain to grain contact between soil particles - lower secondary creep rates than polycrystalline ice because soil impedes dislocation movement
Ice-Poor Frozen Soil	- applies to saturated frozen soil whose deformation patterns are characterized by primary creep - $\gamma = 1.7 - 1.8$ and $1.9 - 2.0$ Mg/m^3
Ice-Rich Frozen Soil	- applies to soils that have a continuous network of segregated ice - the overall creep response is complex and is very sensitive to the reticulate structure of the segregated ice, bulk density grain size and ground temperature

The strain rate derived from equation 2.6 is independent of the hydrostatic pressure. The hydrostatic stress can be expected to influence the stress-strain rate behavior up to failure of unconsolidated frictional earth materials. Ladanyi (1972) extended the stress-strain rate constitutive law to account for the mean normal stress using a two or three parameter failure theory.

Vialov (1962) proposed that the strength of a frozen soil can be represented by a series of Mohr failure envelopes, each one corresponding to a specific time to failure. Assuming validity of the Mohr-Coulomb failure criterion in the pre-failure state, the dependence of strain rate on mean normal pressure for an axially symmetric stress state is expressed as:

$$\dot{\varepsilon}_e = \dot{\varepsilon}_c\left[\frac{(f+2)(\sigma_1-\sigma_3) - 3(f-1)\sigma_m}{3\sigma_c}\right]^n \qquad (2.7)$$

where: $f = (1 + \sin\phi)/(1 - \sin\phi)$

$\sigma_m = (\sigma_1+\sigma_2+\sigma_3)/3$

ϕ = angle of internal friction

For a frictionless soil, $f = 1$, equation 2.7 simplifies to equation 2.6. Equation 2.7 assumes full mobilization of internal friction over the pre-failure state. This assumption leads to a non-zero strain rate at a zero stress difference. Thus, application of equation 2.7 should be restricted to strains close to failure. This limitation may also be overcome by assuming a time dependent angle of internal friction.

Ladanyi (1972) used the extended von Mises failure criterion to account for effect of mean normal stress on strain rate for frozen soils with low internal friction. For an axially symmetric state of stress, the strain rate can be expressed in terms of mean normal stress and principal stress difference as:

$$\dot{\varepsilon}_e = \dot{\varepsilon}_c \left[\frac{(r+1)(\sigma_1-\sigma_3) - 3(r-1)\sigma_m}{2\sigma_c} \right]^n \qquad (2.8)$$

where r = ratio of uniaxial compressive strength to uniaxial tensile strength

Equation 2.8 is subject to the same limitations as equation 2.7 in that a zero stress difference gives a non-zero strain rate assuming a constant strength ratio, r. The limitation of equations 2.7 and 2.8 are overcome by simply assuming the strain rate in a pre-failure state is independent of hydrostatic stress and only the creep strength is made a function of the mean normal stress. This is consistent with the experimental findings of Sayles (1973) at higher strain rates and confining pressures.

From a practical viewpoint, the engineering theory is more favourable than a theory describing creep in terms of more fundamental laws of physics because the required number of experimental material parameters are kept to a minimum.

Tests on ice-rich remoulded frozen soils have been carried by Vialov (1962), Perkins and Ruedrich (1973) and Sayles and Haines (1974) and others. Although the existence of a true steady state in the shorter duration tests is questionable. The longer duration tests generally show creep exponent values approaching a value of 3.0.

A comprehensive study of creep of frozen sands carried out by Sayles (1968) showed that strain rates continued to attenuate with time for tests carried out at stress levels below the long term strength. Damped creep behavior was also observed by Sayles and Haines (1974) in unconfined compression creep on fine-grained remoulded frozen samples when the strain did not exceed 20% over the test duration.

The influence of confining pressure on the creep rate of remoulded frozen Ottawa sand was studied by Sayles (1973). The findings of this study reported that the amount of creep strain can be reduced by increasing the confining pressure. Primary creep was still evident at strains exceeding 20%. A separate study carried out by Alkire and Andersland (1973) showed an exponential decrease in creep strain rate with an increase in confining pressure. Application of confining pressure enhances the frictional behavior of the sand.

Many recent laboratory studies have focussed attention on measuring the empirical parameters in the constitutive equation for natural permafrost soils. Thompson and Sayles (1972) studied the in-situ horizontal and vertical closure of the Fox Tunnel in Alaska. The roof of the tunnel was overlain with 17 m of frozen ice-rich Fairbanks silt. Samples of the silt were tested in unconfined compression at stress levels between 250 and 2000 kPa. The test temperature was 1.7°C. They concluded the constitutive equation for the frozen silt has the same form as equation 2.4 with an exponent of 4. Numerical analysis of the room predicted a closure rate more than 3 times faster in the field than that measured in the laboratory.

Roggensack (1977) tested ice-rich fine-grained glaciolacustrine clay from the Mackenzie River Valley. Triaxial constant stress creep tests were carried out at deviatoric stress levels between 20 and 400 kPa and temperatures close to -1°C. This data is shown in Figure 2.3. Although the data showed considerable scatter, especially at stresses below 100 kPa, a bilinear flow law was fit to the data. A power law fit to the data above 100 kPa gives an exponent of 2.75 which is slightly faster, but consistent with the value for polycrystalline ice. In the low stress range, transient processes play a dominant role in the overall deformation response of the sample. Increasing the confining pressure did not have as a significant effect on decreasing the creep rate as was reported for coarse-grained soils (e.g. Sayles, 1973; Alkine and Andersland, 1973).

McRoberts et al. (1978) tested undisturbed ice-rich silt from Norman Wells, N.W.T. Constant stress creep tests were carried out in a triaxial cell at deviatoric stress levels between 10 and 690 kPa. Test temperatures ranged from -1 to -3°C. Their results are shown in Figure 2.4, adjusted to a reference temperature of -1°C. An upper bound to their data is given in terms of a bilinear flow law:

$$\dot{\varepsilon}_a = \frac{1.6 \times 10^{-7}}{(1-T)^{1.8}} \sigma_d^3 + \frac{1.5 \times 10^{-14}}{(1-T)^{1.8}} \sigma_d^6 \qquad (2.9)$$

where $\dot{\varepsilon}_a$ = axial strain rate (yr^{-1})

σ_d = deviatoric stress (kPa)

T = temperature (°C)

All but one of the samples tested at a deviatoric stress exceeding 400 kPa terminated in failure.

In the low stress range the value of the creep exponent is 3.0, consistent with polycrystalline ice. Tertiary creep may be influencing the strain rates in the high stress range.

Savigny (1980) tested fine-grained, ice-rich glaciolacustrine clay samples from the proposed Arctic Gas crossing of the Great Bear River, N.W.T. Constant stress triaxial creep tests were carried out at stress and temperature conditions simulating field behavior. The laboratory results reported showed no correlation with the flow law for polycrystalline ice (Morgenstern et al., 1980). Savigny (1980) attributed this scatter to the ground ice structure and the generation of a non-uniform stress fields within the specimens in response to application of confining pressure.

Nixon (1978) reviewed the data of Roggensack (1977) and McRoberts et al. (1978). He proposed a tentative upper bound to the creep rates of McRoberts et al. (1978) at a temperature of -2.5°C and stress less than 100 kPa:

$$\dot{\varepsilon}_z = 2.135 \times 10^{-8} \sigma^3 \qquad (2.10)$$

where the units are in $(\text{years})^{-1}$ and kPa.

2.5 Conclusions

The combined results of Roggensack (1977), McRoberts et al. (1978) and Savigny (1980) are shown in Figure 2.5. The two flow laws shown in this figure are:

1) flow laws for polycrystalline ice (Morgenstern et al., 1980)

2) tentative upper bound to soil data of fine-grained ice-rich soil proposed by Nixon (1978) extended above 100 kPa.

With a few exceptions, the laboratory data fall within a narrow band at stress levels exceeding 75 kPa. Below this stress, transient processes may still dominate.

Based on the data presented in Figure 2.5, it can be concluded that the creep law of polycrystalline ice represents a reasonable upper bound to the constitutive behavior of fine-grained, ice-rich permafrost. Exceptions to this occur in the high stress range where the creep tests terminated in failure.

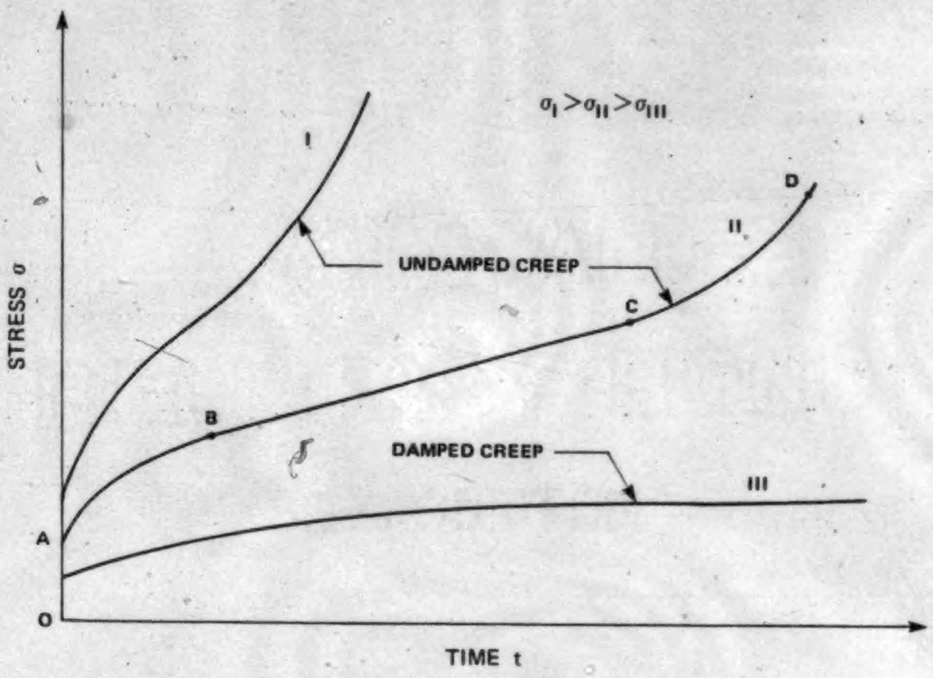

FIGURE 2.1 TYPICAL CONSTANT STRESS CREEP CURVES

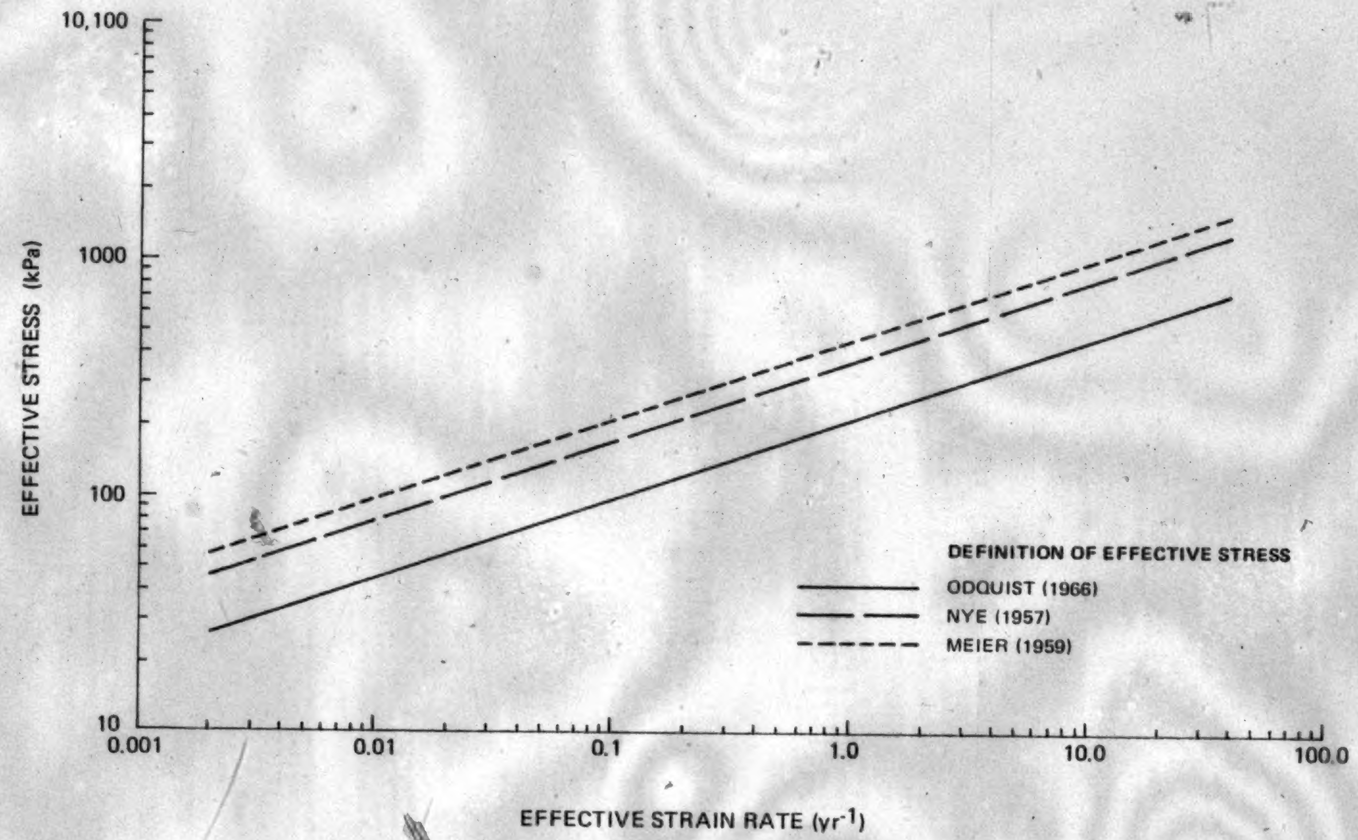

FIGURE 2.2 COMPARISON OF DEFINITION OF EFFECTIVE STRESS

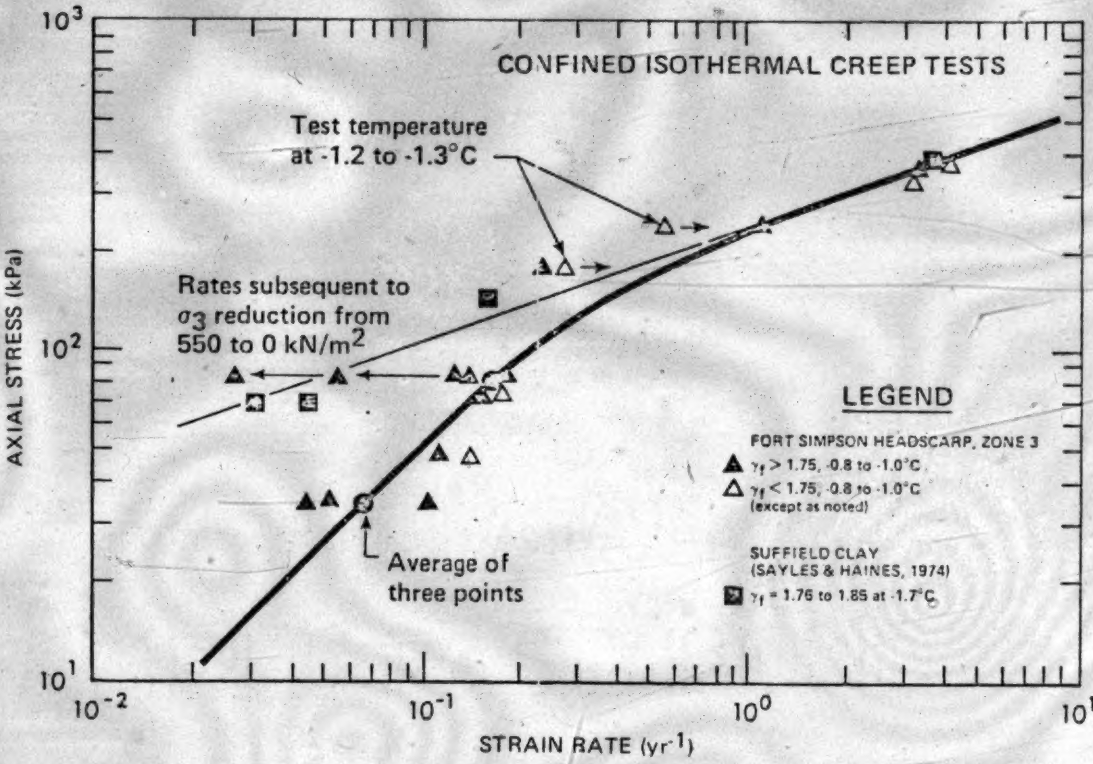

FIGURE 2.3 AXIAL STRESS VERSUS STRAIN RATE (Roggensack, 1977)

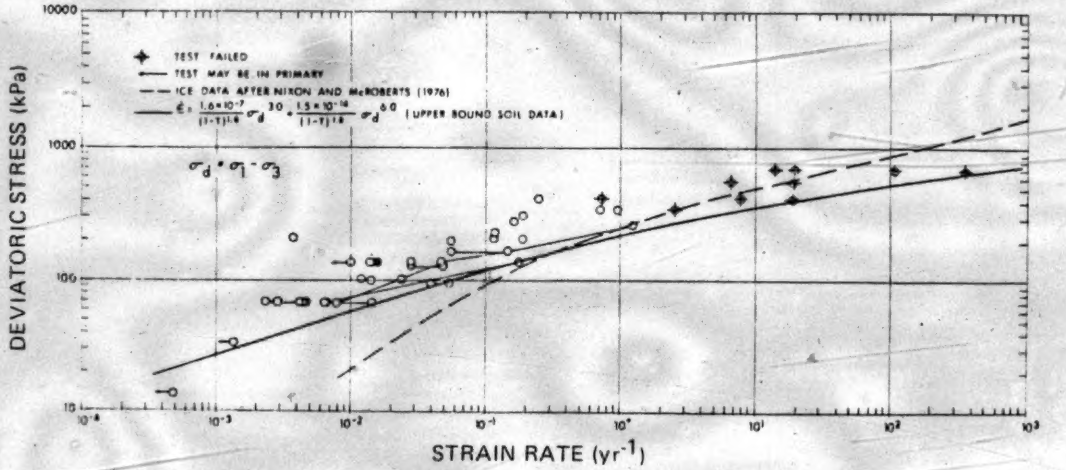

FIGURE 2.4 DEVIATORIC STRESS VERSUS STRAIN RATE (McRoberts etal., 1978)

COPIE DE QUALITEE INFERIEURE

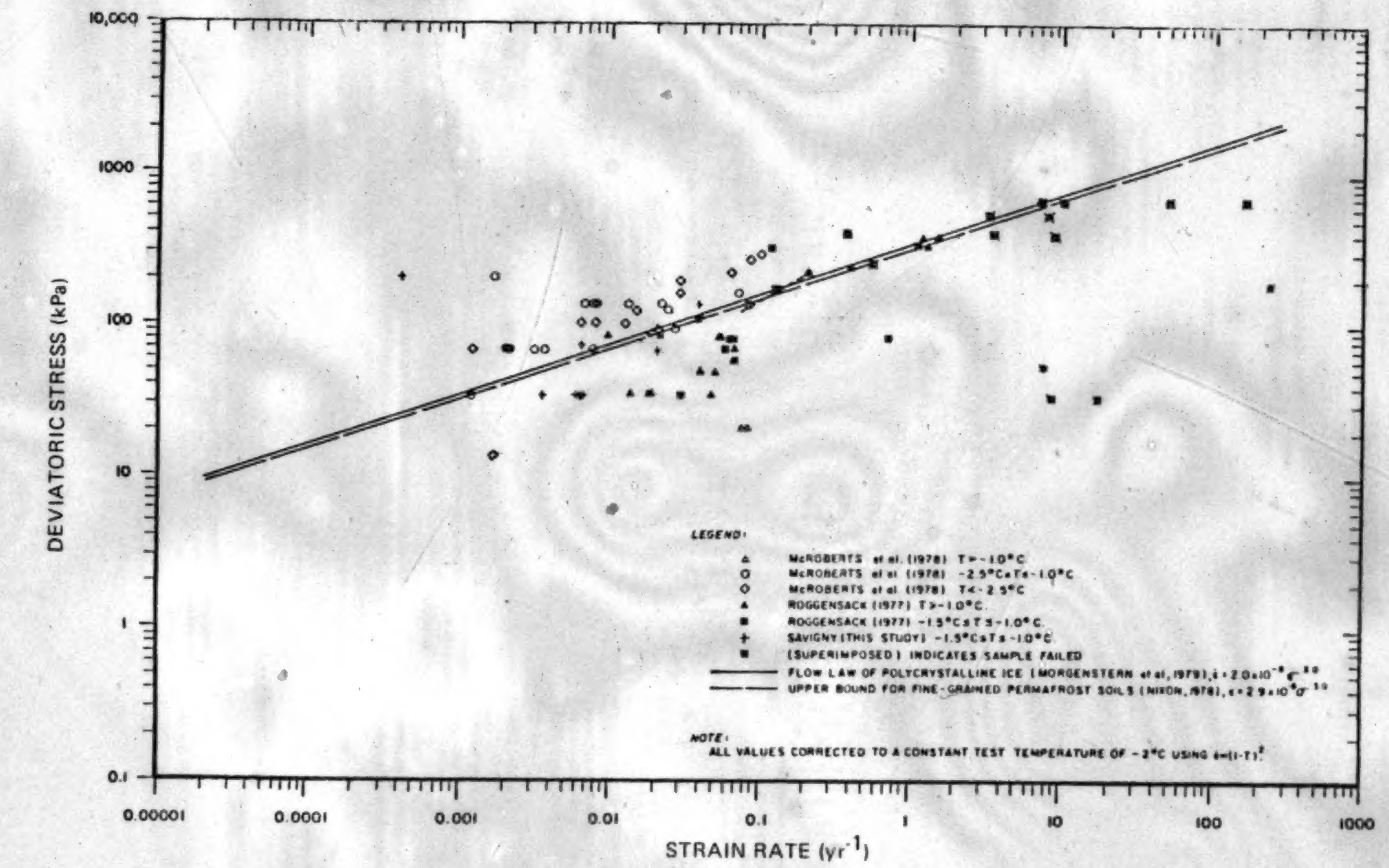

FIGURE 2.5 STEADY - STATE CREEP DATA FOR ICE - RICH GLACIOLACUSTRINE CLAY FROM VARIOUS LOCATIONS IN THE MACKENZIE RIVER VALLEY, N.W.T. (Savigny, 1980)

CHAPTER III

FINITE ELEMENT CREEP ANALYSIS

3.1 General

The primary problem faced by geotechnical engineers concerned with the design and construction of large structures founded on permafrost is the determination of the stress state in the frozen soil. Experimental evidence has shown that time-dependent deformations govern the behavior of frozen soils. The viscous nature of the ice present in discrete layers and in the pore spaces will cause ice-rich soils to creep at very low deviatoric stress levels.

Hoff (1954) simplified the determination of the stress state in a non-linear viscous medium by proposing the elastic analogue. The analogue simply states that:

> "The stress distribution in a body whose deformations are governed by a generalized version of a non-linear creep law is the same as that in a non-linear perfectly elastic body provided that the stress-strain law and the boundary conditions are suitably chosen".

There are two methods which can be used to solve creep problems:

1) direct iteration procedure - the final solution is obtained by an iterative solution of the non-linear equations

2) incremental procedure - the final solution is obtained by solving a number of linearized problems between the initial and final time.

In the finite element method, the inclusion of creep behavior is most easily handled by using an incremental procedure and treating the creep strains as initial strains.

The formulation of the incremental procedure was presented by Mendelson et al (1959). In their approach, they extended the solution of plastic flow problems using the method of successive approximations to include creep behavior with arbitrary creep laws. In this method, the elastic solution is used to calculate the first approximation to the creep strains. These strains are then used to calculate a new stress and total strain state within the body. An improved creep strain approximation is then computed and the procedure is repeated until convergence is obtained for that time interval. Essentially, this solution technique is iterative within each time increment. Creep solutions were presented for uniaxial creep in a flat plate and a biaxial case of rotating disks.

Lin (1962) also presented an incremental procedure for analyzing plates subject to bending with arbitrary creep characteristics. However, in this approach the creep strain increments were treated as equivalent loads and edge moments. This procedure is much less complicated than the method presented by Mendelson et al. (1959) since the method of successive approximations may require several iterations within the same time interval.

The application of the finite element method for solving non-linear creep problems using an incremental procedure where the creep strains are treated as initial strains has been studied by many researchers over the past 15 years. The incremental initial strain procedure is widely used because:

1) it is independent of the type of creep law used;

2) it provides a description of the intermediate stages of creep

3) it is quite simple to extend basic finite element codes to include nonlinear effects arising from creep.

Gerstenkorn and Kobayashi (1966) used the method to solve for creep deformations in a thick-walled cylinder subjected to an internal pressure. Greenbaum and Rubinstein (1968) developed a finite element procedure to study the time-dependent behavior of axisymmetric bodies such as thick-walled cylinders fitted with different types of end closures. Sutherland (1970) extended the work of Greenbaum and Rubinstein (1968) to include problems subject to plane stress and plane strain conditions.

The incremental initial strain procedure was used by Emery (1971) to study the creep behavior of slopes and excavations in rock, cohesive soils and ice. Nair and Boresi (1970) used the incremental solution method to study the time-dependent behavior of circular cavities in rock subjected to a hydrostatic pressure. This procedure was also used by Van Winkel et al. (1972), to predict time-dependent deformation of circular openings in salt media.

A variable stiffness method for creep analysis was presented by Kim and Kuhlemeyer (1977). This method allows the use of relatively large time intervals for which the initial strain procedure would become unstable. However, the disadvantage of this method is the additional computer time associated with regeneration of the structure stiffness matrix at the end of each time interval. This method has proven useful in soil-structure interaction problems where the structure exhibits material non-linearity.

Thompson and Sato (1976) and Dawson and Tillerson (1977) reported a finite element formulation for simulating the creeping flow of an incompressible material. The stress-strain rate response of the material can either be linear (i.e. Newtonian fluid) or non-linear (i.e. non-Newtonian fluid). This method allows the ability to follow the flow through very large changes in material geometry. Velocity components are chosen as the primary variables.

The velocity field is constrained by the material incompressibility condition. This constraint is incorporated into the potential energy functional through the use of a Lagrange multiplier. The multiplier is physically interpreted as the mean normal stress or the pressure within the element. Thus, approximating functions for the pressure as well as the velocity for each element must be chosen. This adds greatly to the solution time required to solve the field equations.

Numerical difficulties arise when trying to satisfy the material incompressibility constraint. To ensure complete incompressibility everywhere within the element, the approximating functions chosen for the pressure within the element must be the same degree as that used for the element strain. Thus, if a linear approximation to the pressure field is chosen, a full quadratic approximating function must be chosen for the components of the velocity field. The complete incompressibility restriction on the velocity field has been shown to be give slow convergence for coarse element grids.

Material incompressibility can be satisfied in an average sense over the entire element. This is accomplished by assuming a constant pressure and linear variation for the strain rates and dilatation within each element. In this approach, the total volume of the element remains unchanged although local incompressibilities within the element are still free to exist. Relaxation of the incompressibility constraint will give more accurate results for coarse element layouts. However, the constant pressure assumption requires a fine element layout in situations where an accurate evaluation of element stresses are desired.

3.2 Incremental Initial Strain Procedure

As a material undergoes creep, the stresses, σ_{ij}, in the body will change with time as shown schematically in Figure 3.1. In the incremental procedure, the smooth stress-time curve is replaced by a series of incremental steps. Each step consists of a constant stress period, Δt, followed by an instantaneous increment of stress.

The fundamental assumption in the incremental creep solution technique is that the time can be subdivided into sufficiently small time intervals such that the stress can be assumed constant within each time interval. If valid, the non-linear creep problem can be solved as a series of linear problems for each time interval using the stresses of the previous time interval to calculate new increments of creep strain and treating them as initial strains for the current time period.

The following assumptions are made in order to establish a stress-strain relationship for a creeping material:

1) there is no volume change associated with the creep strains
2) for an isotropic material the principal directions of the strain rate and stress tensors coincide;
3) the creep rate is independent of any superimposed hydrostatic state of stress;

4) the generalization of the uniaxial creep laws to the multiaxial state of stress should recover the uniaxial relationship for the case of uniaxial stress.

Assumptions 1, 2 and 3 can be stated mathematically as:

$$\Delta\dot{\varepsilon}_{ij} = \alpha\, s_{ij} \qquad (3.1)$$

where: α = constant of proportionality

This equation states that the increments of creep strain rate are proportional to the instantaneous values of the deviatoric stress tensor and are independent of stress history.

Substituting equation 3.1 into Odqvist's definition of effective strain rate (i.e. equation 2.3) and making use of the definition of effective stress yields:

$$\alpha = \frac{3}{2}(\Delta\dot{\varepsilon}^{C}_{e}/\sigma_{e}) \qquad (3.2)$$

Substituting equation 3.2 into 3.1 gives the stress-strain rate relationship for a creeping material:

$$\Delta\dot{\varepsilon}^{C}_{ij} = \frac{3}{2}\,(\Delta\dot{\varepsilon}^{C}_{e}/\sigma_{e})s_{ij} \qquad (3.3)$$

For the plane strain case, the following equations are valid:

$$\sigma_e^2 = \frac{1}{2}[(\sigma_x-\sigma_y)^2 + (\sigma_y-\sigma_z)^2 + (\sigma_z-\sigma_x)^2 + 6\tau_{xy}^2] \tag{3.4}$$

$$\Delta\dot{\varepsilon}_e^2 = \frac{4}{3}[(\Delta\dot{\varepsilon}_x^C)^2 + (\Delta\dot{\varepsilon}_y^C)^2 + \Delta\dot{\varepsilon}_x^C\Delta\dot{\varepsilon}_y^C + (\Delta\dot{\gamma}_{xy}/2)^2] \tag{3.5}$$

$$\Delta\dot{\varepsilon}_x^C = (\Delta\dot{\varepsilon}_e^C/\sigma_e)(2\sigma_x-\sigma_y-\sigma_z)/2 \tag{3.6}$$

$$\Delta\dot{\varepsilon}_y^C = (\Delta\dot{\varepsilon}_e^C/\sigma_e)(2\sigma_y-\sigma_z-\sigma_x)/2 \tag{3.7}$$

$$\Delta\dot{\varepsilon}_z^C = (\Delta\dot{\varepsilon}_e^C/\sigma_e)(2\sigma_z-\sigma_x-\sigma_y)/2 \tag{3.8}$$

$$\Delta\dot{\gamma}_{xy}^C = 3(\Delta\dot{\varepsilon}_e^C/\sigma_e)\tau_{xy} \tag{3.9}$$

The essential feature of the incremental procedure is to proceed in small intervals of time and relate an increment of strain to an increment of stress. The final stress and strain state in the body is obtained by summing each increment.

At the beginning of each time interval, the stresses, elastic strains and creep strains are known from the calculations of the previous time increments. At time t=0, the elastic solution is used as the starting point. The incremental procedure for each increment of time can be summarized by the following five steps:

1) obtain the value of the effective stress (σ_e) from the stresses (σ_{ij}) determined from the previous time step;

2) calculate the effective creep strain increment ($\Delta\varepsilon_e$) by substituting the effective stress (σ_e) (determined from step 1) into the appropriate creep relationship;

3) calculate creep strain increments ($\Delta\varepsilon_{ij}^{C}$) in each direction with the stresses (σ_{ij}) of the preceding time step, the effective stress (σ_e) (from step 1) and the effective creep strain increment ($\Delta\varepsilon_e$) (determined in step 2);

4) treating the creep strain increments ($\Delta\varepsilon_{ij}^{C}$) (calculated in step 3) as initial strains and using the constitutive equations, boundary conditions and equilibrium equations for the particular problem, calculate the increment of stress ($\Delta\sigma_{ij}^{C}$) at the end of the time interval; (the initial strains are converted to ficticious creep forces applied at the nodal points);

5) the incremental stresses ($\Delta\varepsilon_{ij}^{C}$) (obtained in step 4) are added to the stress of the previous time increment to obtain a new stress distribution for the current time interval.

This procedure is repeated for each time interval until either the final time is reached or until the stress distribution does not change (i.e. a steady state condition has been achieved). As long as the incremental stresses are small compared to the previous stresses, the basic assumption of the incremental procedure is not violated. Generally, this condition can be met by selecting time increments small enough to yield the desired accuracy without employing iterative techniques.

3.3 Cumulative Creep Rule

In general, the effective incremental creep strain rate is a function of the effective stress, total effective creep strain, temperature and the strain history of the material. Thus, a general functional form of $\Delta\varepsilon^C_e$ is expressed as follows:

$$\Delta\varepsilon_e^C = F(\sigma_e, \varepsilon_e^C, T, t) \tag{3.10}$$

where: T = temperature

t = time

Materials exhibiting damped creep response have a strain rate that is a function of time as well as applied stress. An expression must be obtained from constant stress creep tests that is able to predict the strain rate under varying states of stress. Assume the damped constant stress creep data can be presented by an empirical relationship of the form:

$$\varepsilon_e = A\sigma_e^n t^m \tag{3.11}$$

where: m = time exponent

The creep strain rate can be obtained by differentiating equation 3.11 with respect to time:

$$\dot{\varepsilon}_e = f(\sigma_e, t) = mA\sigma_e t^{m-1} \tag{3.12}$$

where: $f(\sigma_e, t)$ = general function form expressing the creep strain rate as a function of applied stress and time.

The time variable can be eliminated from the creep strain rate expression by substituting equation 3.11 into equation 3.12:

$$\dot{\varepsilon}_e = g(\sigma_e, \varepsilon_e) = mA^{1/m} \sigma_e^{n/m} \varepsilon_e^{(1-1/m)} \tag{3.13}$$

where: $g(\sigma_e, \varepsilon_e)$ = general function form expressing the creep strain rate as a function of applied stress and total creep strain.

It is clear that integration of equation 3.12 and 3.13 will not give the same result for the general case. Two basic rules that are currently used to describe the time dependency of strain for creep in metals, plastics and concrete are the strain hardening law and the time hardening law.

The strain hardening law for a set of isothermal constant stress curves is illustrated in Figure 3.2. This hypothesis implies the creep strain rate is a function only of the instantaneous value of stress and the total accumulated creep strain. A change in stress state is represented by a horizontal line from one constant stress curve to the new stress curve at the same total creep strain. The total time is given by the sum of all constant stress time intervals. This concept assumes a mechanical-equation-of-state exists for a creeping material relating the variables stress, strain and strain rate. The behavior is independent of the stress history the material was subjected to in the early stages of creep. This is analogous to the theorem proposed by Odquist (1966) which stated:

> "If a test piece is subjected to a series of positive stress values, σ_1, σ_2, ..., σ_n, each acting during a time period Δt_1, Δt_2, ..., Δt_n, then the resulting total creep is independent of the order in which the stress values were applied, each during its respective time period".

The time hardening concept for a set of isothermal constant stress creep curves is illustrated in Figure 3.3. This cumulative rule assumes the creep strain rate is governed by the instantaneous value of the stress and total time from the beginning of the test and is independent of the stress history of the material prior to any point in time. A change in stress state is represented by a vertical line from one constant stress curve to the new stress curve at the same total elapsed time. The total accumulated creep strain is given by the sum of the creep strain increments during each time interval.

The validity of these two hypothesis have not been specifically studied in creep tests on permafrost samples. Experience gained in metal and plastic creep as well as undrained creep behavior of cohesive soils suggests that the strain hardening cumulative creep law adequately describes the creep strain rate under varying stress conditions. Ladanyi and Johnston (1973) used the strain hardening hypothesis to determine the in-situ creep parameters for a frozen varved silty clay from multistage pressuremeter data. The strain hardening cumulative creep law can also be used to predict the creep rate of a material under varying temperature conditions (Dorn, 1961).

Derivation of a cumulative creep law which included all the factors governing the creep rate of a material would be a formidable task. Cumulative creep laws have been put forward in the metal creep literature which take stress and temperature history into account. However, these can lead to untractable mathematical expressions.

3.4 Finite Element Formulation of Incremental Initial Strain Method

The basis of the finite element method is to represent the continuum as an assemblage of finite elements. These elements are interconnected at a finite number of points referred to as nodal points. Approximating functions are chosen to represent the variation of the field variable over the element. A variational principle of mechanics is used to derive the equilibrium equations for each element. The equilibrium equations for the entire body are obtained by summing all the individual element equations with proper regard to displacement continuity at the nodal points. The boundary conditions are applied and the entire set of equations are solved to obtain the unknown displacements at the nodal points.

In the present study, the Theorem of Minimum Potential Energy is used to formulate the equilibrium equations. The elements used are constant strain triangles. Within each element, displacement functions are chosen such that inter-element compatability is maintained. The displacements are assumed to be linear functions of the coordinates. The potential energy of an element is calculated by subtracting the work done by the external forces from the stored strain energy. Minimization of the potential energy yields the equilibrium equations for the element. The equilibrium equations for the entire assemblage are obtained by summing the individual element contributions. The resulting set of linear algebraic equations are solved for the unknown displacements. A detailed derivation of the equilibrium equations for the constant strain triangle element can be found in numerous standard finite element texts [see e.g. Desai and Abel (1972) and Zienkewicz (1977)].

The creep problem is solved by assuming the change in total strain during one time interval is composed of a change in elastic and creep strains.

$$\Delta\varepsilon_x^T = \Delta\varepsilon_x^E + \Delta\varepsilon_x^C = \frac{1}{E}[\Delta\sigma_x - \nu(\Delta\sigma_y + \Delta\sigma_z)] + \Delta\varepsilon_x^C$$

$$\Delta\varepsilon_y^T = \Delta\varepsilon_x^E + \Delta\varepsilon_x^C = \frac{1}{E}[\Delta\sigma_y - \nu(\Delta\sigma_z + \Delta\sigma_x)] + \Delta\varepsilon_y^C \tag{3.14}$$

$$\Delta\varepsilon_z^T = \Delta\varepsilon_x^E + \Delta\varepsilon_x^C = \frac{1}{E}[\Delta\sigma_z - \nu(\Delta\sigma_x + \Delta\sigma_y)] + \Delta\varepsilon_z^C$$

where the superscript T, E and C denote total, elastic and creep respectively.

Plane strain problems have a kinematic constraint placed on the strain in the Z direction (i.e. $\Delta\varepsilon^T{}_z=0$). Thus, the third expression in equation 3.14 gives the value for the stress in the Z direction:

$$\Delta\sigma_z = \nu(\Delta\sigma_x + \Delta\sigma_y) - E\Delta\varepsilon_z^C \tag{3.15}$$

Substituting equation 3.15 into the first two expressions in equation 3.14 yields:-

$$\Delta\varepsilon_x^T = \frac{1}{E}[(1-\nu^2)\Delta\sigma_x - \nu(1+\nu)\Delta\sigma_y] + \Delta\varepsilon_x^C + \nu\Delta\varepsilon_z^C$$

$$\Delta\varepsilon_y^T = \frac{1}{E}[(1-\nu^2)\Delta\sigma_y - \nu(1+\nu)\Delta\sigma_x] + \Delta\varepsilon_y^C + \nu\Delta\varepsilon_z^C \qquad (3.16)$$

Equation 3.16 shows that to account for plane strain, a strain equal to $\nu\Delta\varepsilon_z^C$ must be added to the strains in the X and Y directions. The increments of creep strain $\Delta\varepsilon_{ij}^C$ are calculated from equation 3.3.

The strain-displacement relations and application of the Theorem of Minimum Potential Energy yields the equilibrium equations for one time interval as:

$$[K]\{\Delta q\} = \{P\} + \{F_c\} \qquad (3.17)$$

where: $[K]$ = structure stiffness matrix
$\{\Delta q\}$ = incremental nodal displacements
$\{P\}$ = nodal load vector
$\{F_c\}$ = vector of 'fictitious' nodal loads due to an increment of creep strain.

The introduction of creep strain increments into the equilibrium equations using the initial strain method is given in Appendix A.

At the end of each time interval, the vectors {P} and {F_c} and boundary conditions are known. Equation 3.17 is solved for the unknown displacement increments by the Choleski square root method for symmetrically banded matrices. For linear elastic analysis, the structure stiffness matrix does not change with time and need only be generated once for the initial time increment and stored to be used for each successive time increment. Should the magnitude of the displacements become excessive, the geometry may need to be updated and the stiffness matrix regenerated to reflect the new grid geometry. This was not necessary for the small displacement problems considered in this research.

3.5 Time Increment Selection

The selection of a time increment to ensure the solution process remain stable is very important in the incremental procedure. During the early or transient stages of creep, the stresses are changing very rapidly so it is necessary to select small time increments. As the solution approaches a steady state condition, the magnitude of the time interval can be increased.

Experience of Greenbaum and Rubinstein (1968), Sutherland (1970) and Emery (1971) shows that the solution process becomes unstable if the maximum change in creep strain is larger than the effective creep strain. The magnitude of time intervals chosen is a function of the stress state in the body and the specific form of the creep law.

The initial time increment is chosen such that the maximum ratio of the effective creep strain increment to the effective elastic strain is equal to or less than η_o, i.e.:

$$[\Delta\varepsilon_e^C/\Delta\varepsilon_e^E]_{max} < \eta_o \qquad (3.18)$$

where: $.04 < \eta_o < .10$

Successive time increments are computed on the basis of the fractional change in maximum effective stress allowed per time interval, i.e.:

$$\Delta t_{i+1} = [\omega/(\Delta\sigma_e/\sigma_e)_{max}]\ \Delta t_i \qquad (3.19)$$

where: i) $.035 < \omega < .10$
or ii) $1.2 < \omega/(\Delta\sigma_e/\sigma_e)_{max} < 2.0$

The maximum ratio of effective creep strain increment to the effective elastic strain for successive time increments must also satisfy:

$$[\Delta\varepsilon_e^C/\Delta\varepsilon_e^E]_{max} < \eta_1 \qquad (3.20)$$

where: $0.1 < \eta_1 < 1.0$

The optimum values for η_o, η_1 and ω are a function of the specific creep law and the stress state that exists in the body. Thus, it is advantageous to compute the value for the time interval internally.

The manner in which the program calculates the time interval is as follows:

1) Assume for generality the creep behavior of the material is governed by the creep relationship given by equation 3.11, i.e.: (the steady state creep law is derived from this expression by setting m = 1.0), i.e.:

$$\Delta\varepsilon_e^C = A\sigma_e^n t^m$$

2) The initial time interval is computed by combining equation 3.18 with the above primary creep relationship:

$$\Delta\varepsilon_1 = [\eta_o(\sigma_e)_{max}^{(1-n)}/AE]^{1/m} \qquad (3.21)$$

where: E = Young's modulus

The effective stress is calculated based on the elastic stress distribution at $t = 0$.

3) Succeeding time intervals are obtained by computing the maximum ratio $(\Delta\sigma_e/\sigma_e)_{max}$ and satisfying the conditions given by equation 3.19. A further restriction on succeeding time intervals to prohibit divergence is satisfaction of equation 3.20.

A ficticious time, t_f, is introduced for materials governed by a primary creep law and obeying a strain hardening cumulative creep law. The fictitious time is required to calculate the effective creep strain increments for all increments i (where i = 2, 3, ..., n) total number of increments):

$$\Delta\varepsilon_e^C = A\sigma_e^n[(t_f+\Delta t)^m - t_f^m] \qquad (3.22)$$

where the fictitious time is given by:

$$t_f = [\varepsilon_e^C/(A\sigma_e^n)]^{1/m} \qquad (3.23)$$

The ficticious time concept is illustrated in Figures 3.4 for an increasing and decreasing stress case.

Once a steady state condition is reached the stresses do not change with time and the creep strains can be extrapolated to the final time. Two tests can be made to check for the existence of steady state creep:

1) Check the maximum fractional change in effective stress, i.e.:

$$[\Delta\sigma_e/\sigma_e]_{max} < \rho \qquad (3.24)$$

2) Check the maximum change in effective stress per unit time, i.e.:

$$[\Delta\sigma_e/\Delta t_i]_{max} < \chi \qquad (3.25)$$

Values of ρ and χ depend on the specific problem to be solved.

The steady state condition checks can also be used to monitor the stability of the solution procedure. Erratic fluctuations of the maximum fractional change in effective stress or the maximum change in effective stress per unit time would indicate solution instability. To alleviate this problem, smaller values of η_o, η_1, and ω are required.

3.6 Finite Element Programme

The finite element programme for time dependent creep deformation analysis was originally developed by Emery (1971) at the University of British Columbia. Minor changes were made to the programme after it was obtained by the University of Alberta.

The incremental initial strain method described in a previous section, is used to solve the creep response. The programme is capable of solving isothermal creep problems with linear elastic material behavior in plane strain situations only. The element type used is the constant strain triangle. External loads consist of nodal point loads and/or gravity loading.

The general form of the flow law implemented into the programme is given by:

$$\dot{\varepsilon}_e = [A_1\sigma_e^{n_1} + A_2\sigma_e^{n_2}]t^m \qquad (3.26)$$

where: $\dot{\varepsilon}_e$ = effective strain rate
σ_e = effective stress
t = time
A_1, A_2 = creep coefficients
n_1, n_2 = creep stress exponents
m = creep time exponent

The parameters A_1, A_2, n_1, n_2 and m are material constants. This general form of flow law was selected because it degenerates to a simple power law, a bilinear flow law and a primary (i.e. transient) power law.

A stop and restart capability has been implemented into the finite element program. This feature allows the creep solution to be interrupted after a specified time or number of increments. Solution results up to that point may be examined, or material properties and/or externally applied loads altered to reflect changes in the creep simulation.

A users' manual for the program CREEP is presented in Appendix C. The programme listing is given in Appendix D. A comparison of the closed-form thick wall cylinder solution with the finite element results is presented in Appendix E.

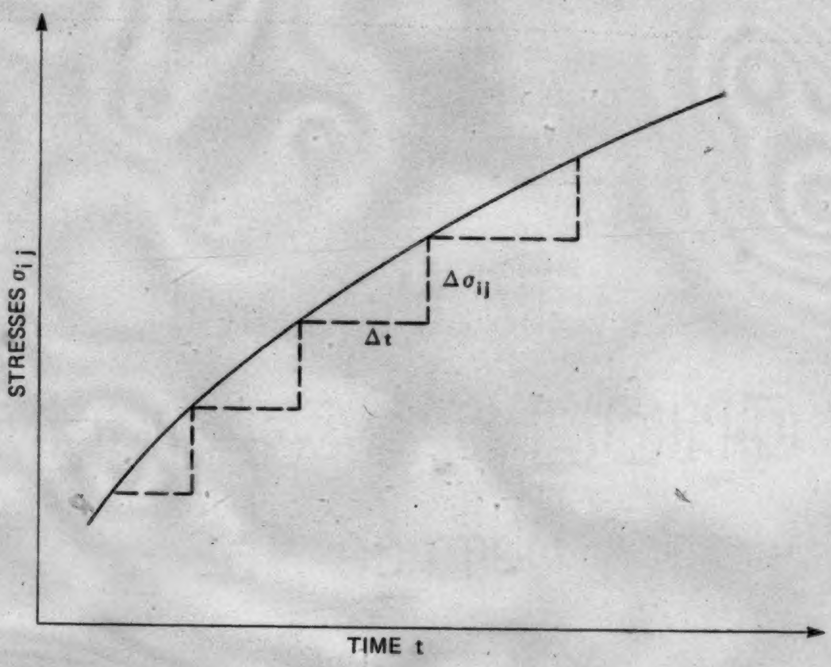
STRESSES σ_{ij}
TIME t
$\Delta\sigma_{ij}$
Δt

FIGURE 3.1 APPROXIMATION OF A SMOOTH STRESS-TIME CURVE FOR INCREMENTAL PROCEDURE

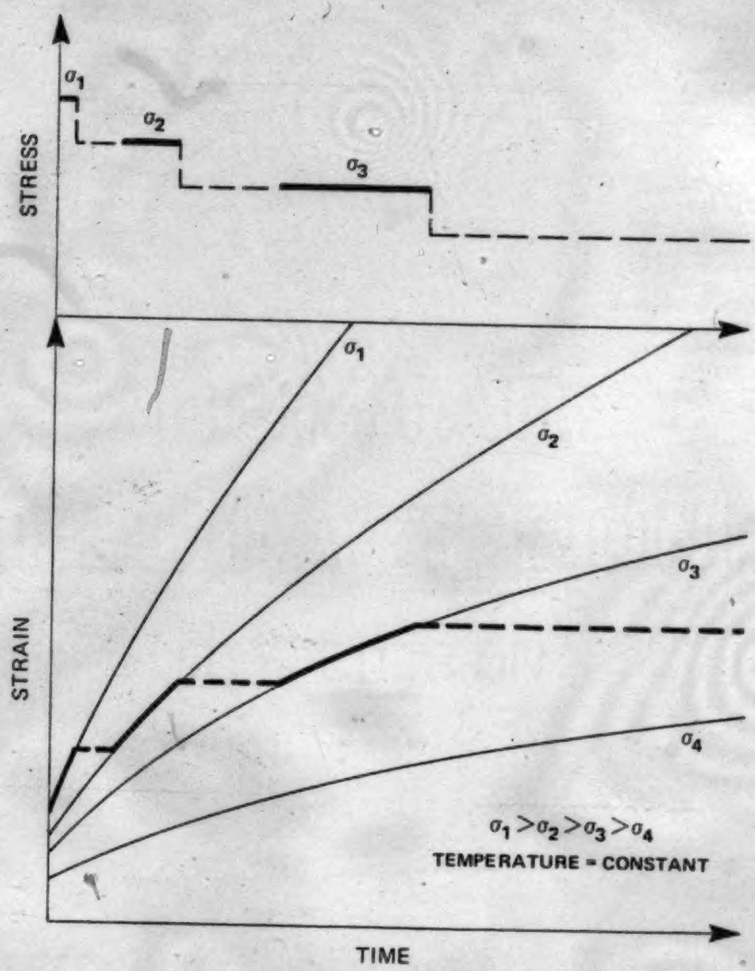

FIGURE 3.2 STRAIN HARDENING CUMULATIVE CREEP RULE

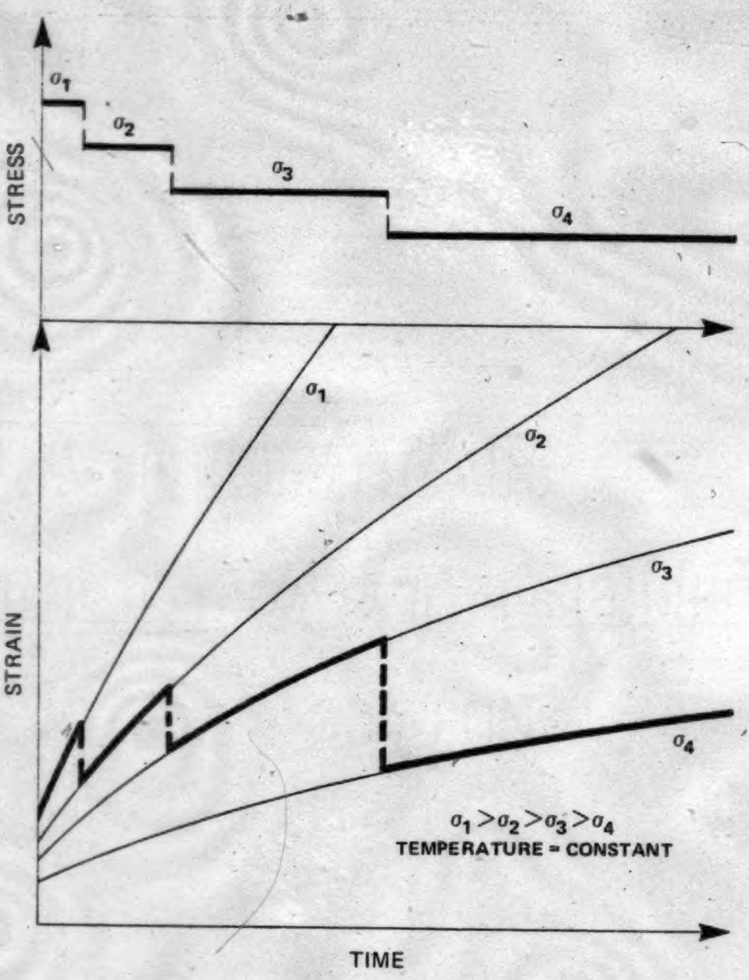

FIGURE 3.3 TIME HARDENING CUMULATIVE CREEP RULE

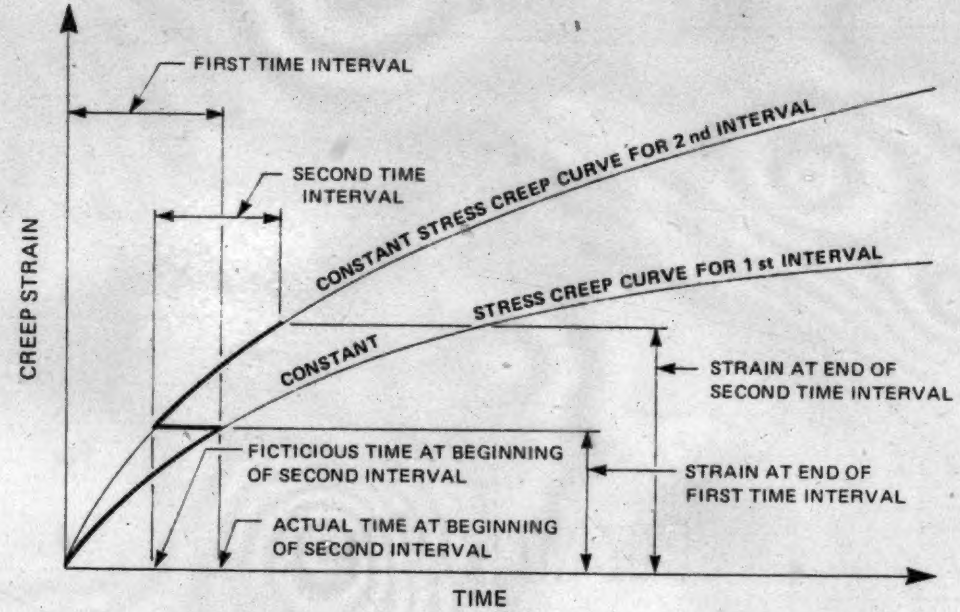
FIRST TIME INTERVAL
SECOND TIME INTERVAL
CONSTANT STRESS CREEP CURVE FOR 2 nd INTERVAL
CONSTANT STRESS CREEP CURVE FOR 1 st INTERVAL
CREEP STRAIN
STRAIN AT END OF SECOND TIME INTERVAL
FICTICIOUS TIME AT BEGINNING OF SECOND INTERVAL
STRAIN AT END OF FIRST TIME INTERVAL
ACTUAL TIME AT BEGINNING OF SECOND INTERVAL
TIME

a) INCREASING STRESS

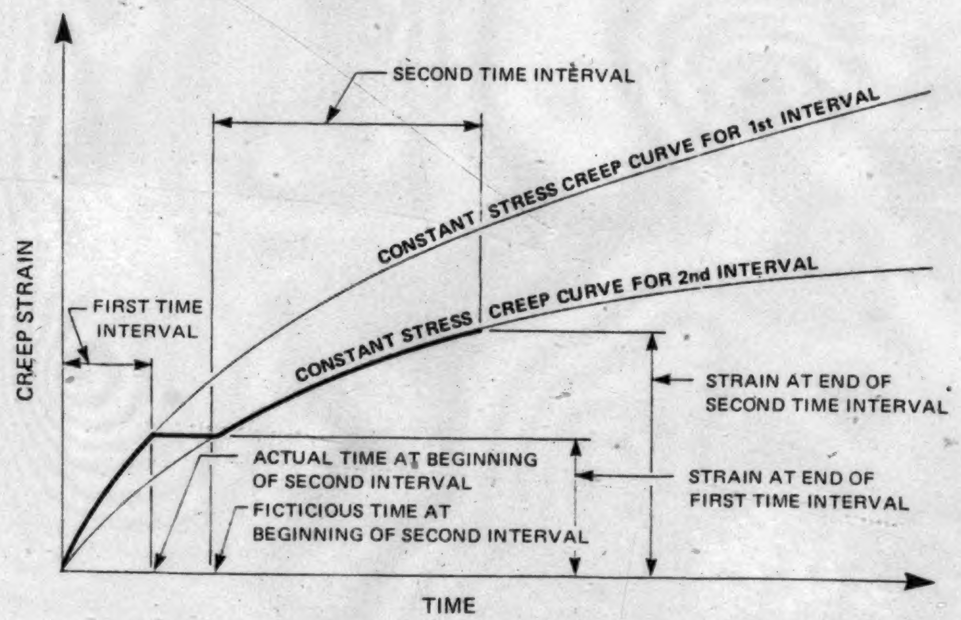
SECOND TIME INTERVAL
CONSTANT STRESS CREEP CURVE FOR 1st INTERVAL
CONSTANT STRESS CREEP CURVE FOR 2nd INTERVAL
CREEP STRAIN
FIRST TIME INTERVAL
STRAIN AT END OF SECOND TIME INTERVAL
ACTUAL TIME AT BEGINNING OF SECOND INTERVAL
STRAIN AT END OF FIRST TIME INTERVAL
FICTICIOUS TIME AT BEGINNING OF SECOND INTERVAL
TIME

b) DECREASING STRESS

FIGURE 3.4 CALCULATION OF INCREMENT OF CREEP STRAIN FOR CHANGING STRESS CONDITIONS

CHAPTER IV

IN SITU CREEP ANALYSIS OF A SLOPE IN ICE-RICH PERMAFROST

4.1 General

The proposed Arctic Gas pipeline route crosses the Great Bear River 7.2 km above the confluence of the Mackenzie and Great Bear Rivers (see Figure 4.1). The left bank of the Great Bear River is consistently steeper than the right bank for several kilometres upstream or downstream from the crossing. Naturally occurring creep was a concern at this particular site because the left bank rises at an average slope 22 degrees over 46 m from river level to the local plain level (see Figure 4.2). Mean river elevation is 56 m a.m.s.l. The local plain elevation is 102 m a.m.s.l. The top of the plain has very little topographic relief south of the slope crest.

The left bank of the Great Bear River at the proposed Arctic Gas crossing was studied by Savigny (1980). An extensive site investigation programme including drilling, sampling and instrumentation was carried out. Undisturbed permafrost core samples were obtained for high quality laboratory testing. The instrumentation was carefully monitored for a two year period. This chapter presents the results of a finite element prediction of the in-situ creep behavior of the proposed Arctic Gas crossing of the Great Bear River.

4.2 Site Geology

The sequence of geologic sediments encountered at the boreholes drilled at this site are shown in Figure 4.3. The slope is composed mainly of sand and clay. Till outcrops near river level. The river has formed in interbedded clay and sand which overlies shale and siltstone bedrock.

The shale and siltstone bedrock are highly weathered and soft. These rocks can be likened to an overconsolidated soil. The bedrock is overlain by an alluvial deposit of interbedded silty clay and sand approximately 6.7 m thick. The two major components of this unit are highly plastic silty clay and clayey silt. Ground ice is present in either reticulate or segregated forms.

A dense glacial till of Wisconsin age lies unconformably on the alluvial deposits. The soil matrix consists of a low to medium plastic sand-silt-clay mixture. The till is highly fissured where it outcrops along the valley wall. Pore ice and reticulate ice are the two most common types of ground ice present.

A fine-grained glaciolacustrine clay rests on the till and is overlain by glaciodeltaic sand. The glaciolacustrine clay was deposited in ice dammed lakes in late Wisconsin time. The soil matrix consists of a medium to highly plastic silty clay. This deposit is approximately 18 m thick at the proposed crossing site. The glaciolacustrine clay is ice-rich. Reticulate ice is most common with primary vertical veins and secondary horizontal veins. Ice veins up to 20 cm thick have been observed. Stratified ice is also common at the till contact. The ice content of this unit increases where the clay outcrops along the valley wall.

The uppermost unit at this site is a 20 m thick stratum of glaciodeltaic sand. This material was deposited following the disappearance of the large ice dams upstream on the Mackenzie River near Fort Good Hope, N.W.T. The sand is medium to fine grained with thin layers of low plastic silt common throughout. Excess pore ice is the dominant type of ground ice.

Some steeply dipping ice veins are also present but not to any great extent. The thickness of the active layer in the sand varies anywhere from .3 to 5 m.

4.3 Field Instrumentation

The field instrumentation installed on the left bank of the Great Bear River at the proposed pipeline crossing consisted of:

1) borehole inclinometers to record in-situ downslope creep velocities in ice-rich permafrost soils (boreholes GB1A, GB2 and GB3);

2) thermistors to measure the in-situ geothermal gradient (boreholes GB1A, GB2 and GB3);

3) piezometers to measure pore pressures below the base of the permafrost (boreholes GB1B and GB3A).

The location of all the boreholes is shown on Figure 4.2.

The pore pressures measured at borehole GB3A show a close correspondence between river level elevation and hydrostatic pore pressure. This is to be expected because the coarse alluvium that lies on top of the bedrock at this site provides a free drainage path.

The ground temperature contours below the depth of zero mean temperature fluctuation for the left bank of the Great Bear River at the proposed pipeline crossing are shown in Figure 4.4. These contours were inferred from the thermistors installed in boreholes GB1A, GB2 and GB3. The temperature data indicate that the permafrost at this site is warm (i.e. warmer than -3°C).

At the top of the slope (GB1A) the active layer is approximately 3 m thick and the depth of annual zero mean temperature fluctuation is 9 to 10 m. The depth of permafrost inferred from the geothermal gradient is at least 61 m. The temperature readings over the two year period show that removal of the surface vegetal cover has initiated a warming trend.

The thermal regime of the slope differs from that on top of the slope. This is primarily due to the aspect of the slope and the difference in vegetation. Along the slope the active layer is approximately 1.2 m thick and the depth of annual zero mean temperature fluctuation is 6 to 7 m. At approximately mid-height of the slope, the mean ground surface temperature is -3.3°C and near the toe of the slope, the warming effect of the Great Bear River increases the mean ground surface temperature to -2.5°C. The steeper thermal gradient measured near the toe of the slope (borehole GB3) is also a result of the thermal disturbance offered by the Great Bear River. The base of the permafrost rises to the river bed elevation as permafrost is absent below the Great Bear River.

Three inclinometers were installed to monitor downslope creep movements:

i) inclinometer GB1A was installed at the top of the slope through the glaciofluvial sand and glaciolacustrine clay and terminates in the silty clay till;

ii) inclinometer GB2 was installed at mid-height of the slope where the glaciolacustrine clay outcrops along the valley wall and terminates at the base of the till;

iii) inclinometer GB3 was installed near the toe of the slope through the glaciolacustrine clay and till and terminates at the base of the interbedded clay and sand.

The location of each inclinometer is shown in Figure 4.5. The inclinometers were read on twelve occasions over a two year period extending from May 6, 1975 to June 14, 1977.

The inclinometer data show a strong correlation between deformations and ice lenses in the glaciolacustrine clay. In zones containing large ice lenses separated 1 to 2 m apart, the movements were large and abrupt and are concentrated at the ice lense location. In zones where the ice lenses are spaced closer than 1 m, the movements are generally smaller and more gradual through the zone. No net transverse slope movements of any practical value were recorded.

Movements recorded in the overlying sand are much more inconsistent than those measured in the clay. Savigny (1980) attributes this to drilling difficulties encountered in the granular material causing disturbed zones around the hole which lead to non-uniform stress distributions in the frozen sand.

The velocity versus depth profiles for all three inclinometer locations are shown in Figure 4.6. A net downslope velocity was recorded through the medium to high plastic glaciolacustrine clay at hole GB1A. The maximum velocity was recorded near the sand-clay contact. Erratic movements were recorded between the 29 m and 34 m depth.

Examination of the GB1A borehole stratigraphy reveals that this depth interval corresponds to a zone containing large pervasive ice lenses spaced greater than 1 m apart. The velocity maxima within this zone coincide with the location of large ice lenses. Above the 29 m depth and below the 34 m depth, there is a pseudo-linear increase in velocity with increasing distance away from the base of the clay layer. The steeper velocity gradient above 29 m is a result of large ice lenses spaced closely together. Below 34 m, the ice lenses are much smaller.

A uniform downslope velocity was recorded in the upper 12 m of the overlying sand at hole GB1A. The magnitude of this velocity is approximately one half of the velocity recorded in the clay just below the sand/clay contact. The 12 to 20 m depth interval of the sand predominantly shows an upslope velocity. The abrupt change at 12 m from upslope to downslope velocity could possibly be due to a large ice vein. At borehole GB1, a large ice vein was observed 13 m below the surface.

No net creep movements were recorded in the transverse-to-slope direction at the GB1A inclinometer.

The velocities recorded through the medium to high plastic clay are very erratic at the GB2 inclinometer location. Savigny (1980) describes two causes for the erratic in-situ velocity:

1) difficulties encountered in installation and monitoring of instrumentation

2) existence of in-situ sheared material as evidenced by the numerous slickensides in the core samples retrieved from this hole.

A small net downslope creep movement is evident in the silty clay till at the GB2 location. There is a pseudo-linear increase in creep velocity from the base of the till up to the till/glaciolacustrine clay contact.

A net downstream creep velocity was recorded in the glaciolacustrine clay at the GB3 inclinometer location. The velocity gradient appears to be fairly uniform. Erratic fluctuations in velocity exist between 2 and 4 m. The GB3 borehole description reveals that this depth interval coincides with a zone of small ice lenses that are widely spaced.

4.4 Finite Element Analyses

The stratigraphy of the left bank of the Great Bear River at the proposed crossing site was discretized for the finite element analysis as shown in Figure 4.7. The finite element grid consisted of 22.5 m of sand overlying 15.5 m of medium to high plastic glaciolacustrine clay. The stiff glacial till that underlies the clay was not discretized. The finite element grid was fixed at the clay/till interface to account for the very high in-situ modulus of the till.

The finite element programme CREEP computes movements in the plane of the slope only. Transverse-to-slope movements are assumed to be zero. The inclinometer data reveals that no net transverse-to-slope movements were recorded at hole locations GB1A and GB3. At hole GB2, the transverse-to-slope velocity recorded in the glaciolacustrine clay is greater than the parallel-to-slope velocity. However, for reasons noted in the previous section, the data for hole GB2 is not considered reliable.

Elastic material properties were assigned on the basis of data presented in the literature. Mean values of bulk unit weight for the sand and clay were assigned on the basis of measured values obtained from the frozen core samples. The elastic material properties for the sand and clay are summarized in Table 4.1.

TABLE 4.1

ELASTIC MATERIAL PROPERTIES FOR FROZEN GLACIODELTAIC
SAND AND GLACIOLACUSTRINE CLAY

PROPERTY	SAND	CLAY
Young's Modulus	4900 MPa	785 MPa
Poisson's Ratio	.495	.495
Unit Weight	1.84 Mg/m^3	2.04 Mg/m^3

Creep properties of the sand and clay were altered to obtain close agreement with the in-situ behavior. Two finite element creep simulations were carried out.

The first creep analysis assumed that the sand and clay would creep at the same rate. A review of the rheological behavior of frozen soils presented in Chapter II concluded that the stress versus strain-rate relationship for polycrystalline ice represents an upper bound to the constitutive behavior of fine-grained, ice-rich permafrost soils. Using this argument, the flow law used in the first analysis was:

$$\dot{\varepsilon} = 2.0 \times 10^{-8} \sigma^{3} \tag{4.1}$$

It was expected that this flow law would overestimate the creep velocities in the sand and clay. The degree of overestimation would be greatest in the sand. Laboratory samples of the sand could not be obtained for laboratory creep testing because of sampling difficulties.

The predicted creep velocity profiles for all three inclinometer locations are shown in Figure 4.8. The in-situ creep velocities are also shown in this figure. At inclinometer locations GB1A and GB3, the predicted velocity profile generally has a similar form to the in-situ profiles. However, the magnitude is much greater. As expected, there is no correlation between measured and observed creep velocities at inclinometer location GB2.

A close examination of the magnitude of predicted velocities versus the observed values revealed that the difference between the two is a constant factor. The creep strain rate varies linearly with the coefficient in the simple power law. Hence, a proportional change in the coefficient will reduce the predicted velocities to the observed values.

The predicted velocities were approximately six times greater than the in-situ values. To reduce the predicted velocities proportionately, the coefficient in the simple power law was set equal to one sixth of its original value. Thus, the flow law for the sand and clay now becomes:

$$\dot{\varepsilon} = .33 \times 10^{-8} \sigma^{3} \tag{4.2}$$

The exponent was left unchanged from its original value of 3.0.

The predicted velocities reduced by a factor of six are shown in Figure 4.9. There is good agreement between the predicted and in-situ velocity profiles for the GB1A and GB3 inclinometer locations through the clay stratum. There is some discrepancy in the upper 2 to 3 m of the GB3 hole due to the influence of the steel casing (Savigny, 1980). Also, the datum for the finite element zero velocity at the GB1A and GB3 holes were translated horizontally to account for the in-situ movement which occurred in the underlying till.

The predicted in-situ creep law is shown in Figure 4.10 along with the flow law for ice (Morgenstern et al., 1980) and the upper bound for soil data as proposed by Nixon (1978). The predicted flow law shows good agreement with the laboratory data. As shown in this figure, the laboratory data overestimate the in-situ creep rate.

The accumulated creep displacement pattern after a steady state condition was achieved is shown in Figure 4.11. The displacement profiles versus depth are indicative of non-Newtonian fluid behavior.

The preliminary finite element creep analysis has shown that the insitu creep behavior of the ice-rich glaciolacustrine clay can be modelled with the simple power law. However, the agreement between predicted and observed velocities through the sand at inclinometer GB1A is less convincing. At the outset, there was some doubt regarding the form of the constitutive behavior of the sand and whether the sand would creep at all. The ice-rich glaciolacustrine clay was expected to creep much faster than the overlying sand. This would set up tensile stresses in the sand near the sand/clay interface. Evidence of a complex stress state at this interface is revealed by the observed erratic movements at the base of the sand.

Selection of a suitable constitutive relationship for the sand is difficult due to the lack of long term low stress creep data for natural coarse-grained permafrost soils. Creep tests on reconsituted frozen sands have shown that the deformations continue to attenuate with time at stress levels below the long term strength (Sayles, 1968). Creep deformations in sand have also been shown to be a function of confining pressure (Sayles, 1973; Alkire and Andersland, 1973). There is also the question of the form of the constitutive relationship for the sand under tensile stresses. Since unfrozen sand has zero tensile strength, all the tensile stresses must be transmitted through the ice phase. Hawkes and Mellor (1972) have shown that the uniaxial strength of polycrystalline ice is similar in tension and compression at slow strain rates. However, the creep behavior of coarse-grained ice-poor frozen soils may differ considerably in tension and compression. In a compression creep test on a coarse-grained frozen soil, there are two components which resist deformation. First, there are the time-dependent deformations occurring in the ice phase and secondly, interparticle friction must also be overcome. In a tension creep test only the ice phase will resist the application of load since the interparticle friction has been reduced to zero. To investigate these points, a second creep analysis was carried out in which the sand was restricted to deform elastically. The clay was assigned the flow law given by equation 4.2.

The predicted velocity profiles for this analysis at all three inclinometer locations is shown in Figure 4.12. Restricting the sand to deform elastically impedes the creep deformations in the clay at the GB1A and GB2 inclinometer locations. At these two inclinometer locations, the predicted velocities do not agree either in form or magnitude with the observed data. The predicted velocities at the GB3 inclinometer are only slightly reduced from the analysis assuming uniform creep properties because this region is well beyond the influence of the sand stratum.

The displacement pattern for the second creep analysis is shown in Figure 4.13. In this case, the clay is being extruded out between the sand and underlying till. As the distance downslope from the point the sand pinches out increases, the displacement pattern begins to resemble non-Newtonian fluid behavior as it did in the first creep analysis.

The extrusion of the clay leads to very high horizontal tensile stresses in the sand as shown in Figure 4.14. The magnitude of the tensile stresses indicate the formation of tensile failure zones propagating through the sand as it restricts the downslope movement of the underlying clay.

4.5 Assessment of Analytical Results

On the basis of the finite element creep analysis of the left bank of the Great Bear River at the proposed Arctic Gas crossing, it can be concluded that the in-situ creep behavior of the glaciolacustrine clay can be accurately represented by the simple power law. The flow law given by equation 4.2 provided the best fit between observed and predicted velocities. The exponent in the power law is the same as that for polycrystalline ice, however, the coefficient is one sixth of the ice value (Morgenstern et al. 1980).

The in-situ creep behavior of the sand may also be represented by the simple power law. However, this remains inconclusive until further insight is gained into the in-situ stress state in the sand. Confining the sand to behave elastically poses much too serious a restriction on creep movements in the clay. The in-situ creep behavior indicates the clay creeps at a faster rate than the sand. The dissimilar in-situ creep behavior in the clay and sand would set up a complicated stress field at the sand/clay interface. It is believed that the faster creep movements in the clay is causing tensile failure in the sand. Thus, to more accurately model the in-situ behavior of the sand, inclusion of a tensile failure criterion would be necessary. Approximate numerical techniques are available for treating soil and rock as either a 'no tension' or 'limited tension' material. Application of such procedures is severely limited in frozen soil mechanics since very little is known about their constitutive behavior under tensile stress conditions.

The largest discrepencies between observed and predicted velocity profiles appear to coincide with regions that have experienced failure. Two such zones are the base of the sand at inclinometer GB1A and the entire thickness of clay at GB2 inclinometer location. It is believed that the abrupt change in the in-situ creep properties between the clay and sand has lead to the development of a zone of tensile failure in the lower 8 m of sand. The upper 12 m of the sand, which is well beyond the zone of influence of the sand/clay interface, generally shows a uniform downslope velocity.

Another such zone occurs at the GB2 inclinometer location. The sand deposit pinches out just upslope of this borehole. The stiffer sand appears to impede the creep velocity in the underlying clay. Downslope of the GB2 inclinometer, the in-situ creep behavior of the clay is not influenced by the overlying sand and creeps at a faster velocity than the clay underlying the sand. The upslope restraint offered by the sand and the downslope pull of the unrestrained creep in the clay would lead to horizontal stress relaxation at GB2. It is believed that numerous slickensided surfaces observed in the core of borehole GB2 occurred as a result of continued horizontal stress relief while the vertical stress remained constant at the overburden pressure.

The in-situ creep behavior of the clay at inclinometer GB3 is not influenced by the sand. The steady state stress field in the clay in the vicinity of GB3 lies well beyond the disturbing influence of the sand.

4.6 Modelling Ice-Rich Permafrost as a Two-Phase Continuum

At the proposed Arctic Gas crossing of the Great Bear River, the data gathered from inclinometer locations GB1A and GB3 clearly show that velocities are erratic and more movement is associated with the large ice lenses where they are widely separated (Savigny, 1980). The constant stress creep tests carried out on samples obtained from the field program all showed that the deformation behavior was affected by the ground ice stucture. Savigny (1980) reported that samples tested with a reticulate ice structure all failed along the soil/ice interface with virtually no shearing through the soil. One sample tested with stratified ice oriented perpendicular to the direction of load application failed by radial tensile failure in the soil. It is clear from the foregoing points, the ice structures present in an ice-rich permafrost play an important role in establishing the overall deformation behavior of the soil mass. Thus, there is good reason to believe that the segregated ice features can be treated as discontinuities in a frozen soil matrix.

In the field of rock mechanics, the presence of discontinuities has long been recognized by engineers designing structures in the rock. The behavior of a rock mass is not only a function of the intact rock but also the nature and extent of the discontinuities present.

Generally, all rock masses contain planes of potential weakness which come in all lengths and spacings and have varying degrees of influence on the overall rock mass properties. A geological field investigation can accurately map the orientation and absolute position of the more important discontinuities so that their influence on the rock mass behavior can be adequately evaluated.

Conventional finite element analysis utilizes the continuum approach which enforces material compatability throughout the body being analyzed. The continuum approach may be entirely adequate when dealing with small joint spacings relative to the size of the structure being analyzed. Situations where rocks deform along preexisting planes of weakness present additional degrees of freedom to the rock mass. Thus, the analytical model must allow relative movement to obtain a realistic solution.

When dealing with a single very important discontinuity whose orientation and position are known with confidence, it is possible to represent plane of weakness explicitly and calculate the resulting stresses and deformations in the rock mass. Several interface elements have been developed over the past ten years for solving problems that involve relative movement.

Goodman et al. (1968) introduced a four node displacement discontinuity element. Zienkiewicz et al. (1970) presented a continuous isoparatric interface element with linear strain along the element and uniform strain across its thickness. Ghaboussi et al. (1973) advocates the use of relative displacement as an independent variable to prevent adjacent blocks of continuous elements from penetrating into each other. Simmons (1981) used a thin linear strain isoparametric continuum element to model shearband yielding and strain weakening in dense, structured soils.

The essential feature in using these interface elements is to be able to predict the location of a shearzone or map a through-going discontinuity. Little is known about the aerial extent of individual lenses of segregated ice or reticulate ice veins. The ice lenses may vary from hairline cracks to massive ice bodies with vast horizontal and vertical extent. The factors governing the amount and distribution of ground ice are the type of host material, availability of moisture, rate of freezing and geologic history of events. The most common form of segregated ice in the glaciolacustrine clay at the proposed Arctic Gas Crossing site was reticulate ice with smaller amounts of segregated and stratified ice. The thicker primary veins in the reticulate ice structure are typically vertical making lateral correlation of these ice features very difficult.

The variability of ground ice is of major significance when studying the stability of buried, warm pipelines operating through permafrost. Determination of the amount and distribution of ground ice is essential for evaluating the configuration of the thawed ditch bottom profile. The lateral variation of ground ice can be determined by visual examination of ditch walls or detailed logging of continuous undisturbed samples obtained from closely spaced boreholes.

Mapping of ground ice structures found on ditch walls will provide the most reliable estimate of the continuity of individual ice features. However, an undertaking of this sort would be very costly. Ditch wall disturbance as a result of overbreak would preclude the use of a blast and backhoe operation to excavate the ditch. Large diameter bucket wheel ditchers produce a smooth and relatively undisturbed ditch wall ideal for observing the ground ice structure. Very few ditching trials have been carried out and reported in the public literature. Also, the few trials that have taken place were primarily concerned with the ability of the ditcher to excavate frozen permafrost rather than mapping the ground ice structures.

Detailed logging of the ice structures observed in undisturbed permafrost core samples obtained from closely spaced boreholes would be much more expedient. The ground ice may appear to be much more variable in the undisturbed core samples than that actually present in the soil mass. However, an estimate of the variability of ground ice in the soil mass can be obtained by a statistical evaluation of the observations at individual boreholes.

Use of statistical analysis to solve variability problems in geotechnical engineering is relatively recent. Quality control on construction projects and to a lesser extent the analysis of laboratory test data are two areas where much of the application of statistical techniques has taken place. Ideally, a known statistical model would be used to describe the population under consideration. Holtz and Krizek (1971) studied several foundation case histories and found that the laboratory test data essentialy conform to the Gaussian or normal distribution.

Speer et al. (1973) reported the results of a ground ice variability study undertaken by Mackenzie Valley Pipeline Research Limited (MVPRL). The purpose of the ice variability study was to assess the amount of ground ice and its distribution in the thawed zone below a warm oil pipeline buried in ice-rich permafrost. The thaw settlement potential of representative geologic units through which the propsed pipeline might be buried is required to compute pipe stresses under operating conditions.

When fine-grained ice-rich permafrost soil thaws, water is released and settlements develop as the water is expelled from the pore space due to the soils self weight and applied loads. Laboratory studies have shown that for light loadings in relatively ice-rich soils, a major portion of the thaw settlement occurs during the thaw stage. This component of settlement is independent of external loading and is caused by excess water draining away. A rough estimate of the thaw settlement for ice-rich soils can be obtained from the thickness of visible ice lenses. Thus, it would seem reasonable to assume that the variation in thaw settlement provides an estimate of the variability of ground ice.

Field and laboratory studies were carried out by MVPRL to study ground ice variability in silt and clay soils. The lateral variation of ground ice content was studied in rectangular arrays of closely spaced borings. An estimate of the total potential settlement was calculated from an empirical correlation between frozen bulk density and thaw strain derived from laboratory tests on undisturbed core samples obtained during the field investigation.

Two arrays were drilled in lacustrine silts and clays deposited in a proglacial lake. These deposits are considered texturally similar to those encountered at the proposed Arctic Gas crossing of the Great Bear River.

The Norman Wells study site is located approximately 3 km northwest of the airport runway at Norman Wells. The Landing Lake array is located approximately 53 km northwest of Norman Wells on the east bank of the Mackenzie River. At both sites, reticulate and segregated ground ice structures were present in the lacustrine silt and clay. Massive ice structures were not observed.

The estimated total thaw settlement for the Norman Wells and Landing Lake study sites are shown in Figure 4.15. The depth interval that thaw settlements were calculated was 2 to 13 m. There is good reason to believe that for a uniform stratigraphic unit, the ground ice will be a normally distributed variable. The combined data for the Norman Wells and Landing Lake arrays plotted in terms of a thaw settlement probability distribution on normal probability paper is shown in Figure 4.16. The observed data shows little scatter about the theoretical normal distribution. Also shown in the figure are the results of the Kolmogorov-Smirnov goodness of fit test evaluated for normality at the 20% significance level. This test indicates that the thaw settlement in lacustrine silts and clays of the Mackenzie River Valley can be described by a normal distribution.

Although the foregoing has shown that the variability of ground ice in a uniform stratigraphic unit can be considered to be normally distributed, it has done little to elucidate the lateral extent of individual ice lenses. One method of estimating the applicable horizontal scale for a given depth interval is to observe the surface profile of ground which was once frozen but has subsequently thawed such as seismic cutlines, highways and airstrips.

A mathematical description of the overall ground ice correlation between pairs of points at various arbitrary spacings is through the concept of an auto-correlation function. This function is defined as the product of the deviations from the mean thaw settlement measured at pairs of points spaced an arbitrary distance, ℓ, apart averaged over the entire population, ie:

$$R(k) = \frac{1}{n-k}\left[\sum_{i=1}^{n-k} (x_i-\bar{x})(x_{i+k}-\bar{x})\right] \qquad (4.3)$$

where: $R(k)$ = auto-correlation at spacing k
n = total number of observations
x_i = observation at point i
$\bar{x}$ = mean

For the thaw settlement data, the auto-correlation function expresses the dependence of the correlation between settlements measured at boreholes i and i + k on the distance, kℓ, between boreholes. The distance at which the auto-correlation falls to zero indicates the horizontal scale over which the thaw settlements can be correlated. The product of the deviations from the mean thaw settlement spaced further than this distance can be expected to be as often positive as it is negative. Thus, the expected value of the sum of these products should be zero beyond the correlation distance for a very large population.

The auto-correlation function determined from the Norman Wells and Landing Lake thaw settlement data is shown in Figure 4.17 The correlation is almost zero for 15 m and fluctuates about zero at greater spacings between boreholes. This suggests that thaw settlements are only weakly correlated at boreholes spaced 15 m apart. No data is available at spacings less than 15 m since the closest borehole spacing at these two ice variability test sites was 15 m. Field observations of disturbed areas in lacustrine silts and clays of the Mackenzie River Valley indicate that 15 m represents an upperbound for the distance at which ground ice content is correlated.

The thaw settlement data represents a one-dimensional integration of the ground ice conditions at a particular borehole over a given depth interval. The data derived from the MVPRL ice variability test sites at Norman Wells and Landing Lake suggest that for a uniform stratigraphic unit, the overall ground ice content of the soil mass can be described as a normally distributed variable. The ground ice content at a particular point is completely independent of neighboring points separated a distance of 15 m. Thus, the time-dependent deformation behavior of ice-rich frozen soil is most appropriately treated analytically by assuming homogeneity for the ice-rich permafrost until a better understanding of the lateral extent of individual ice lenses is obtained.

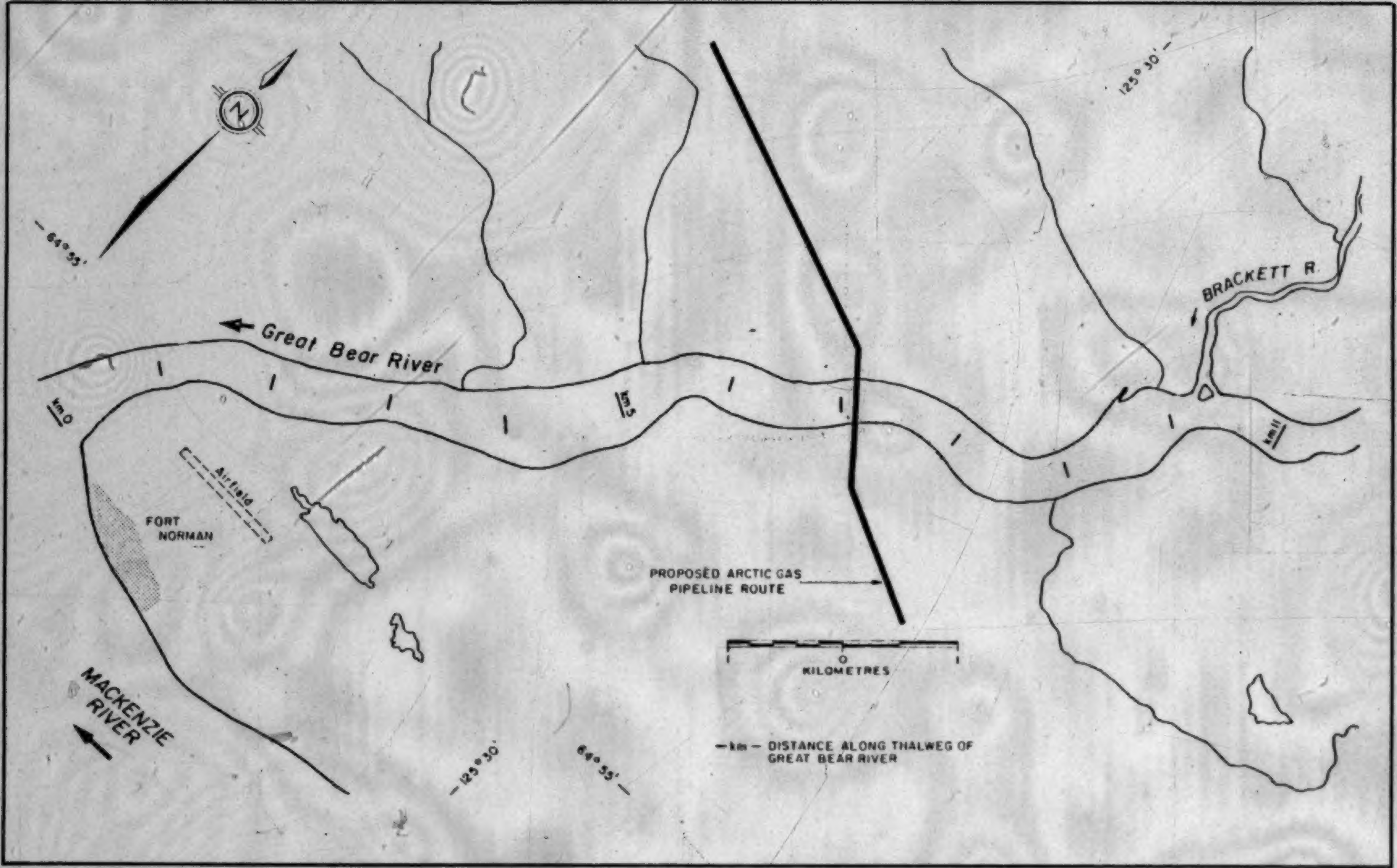
N
64° 55'
125° 30'
Great Bear River
BRACKETT R.
km 0
km 5
km 11
Airfield
FORT NORMAN
PROPOSED ARCTIC GAS PIPELINE ROUTE
0
KILOMETRES
— km — DISTANCE ALONG THALWEG OF GREAT BEAR RIVER
MACKENZIE RIVER
125° 30'
64° 55'

FIGURE 4.1 SITE PLAN OF PROPOSED ARCTIC GAS CROSSING OF GREY BEAR RIVER, N.W.T.
(Savigny, 1980)

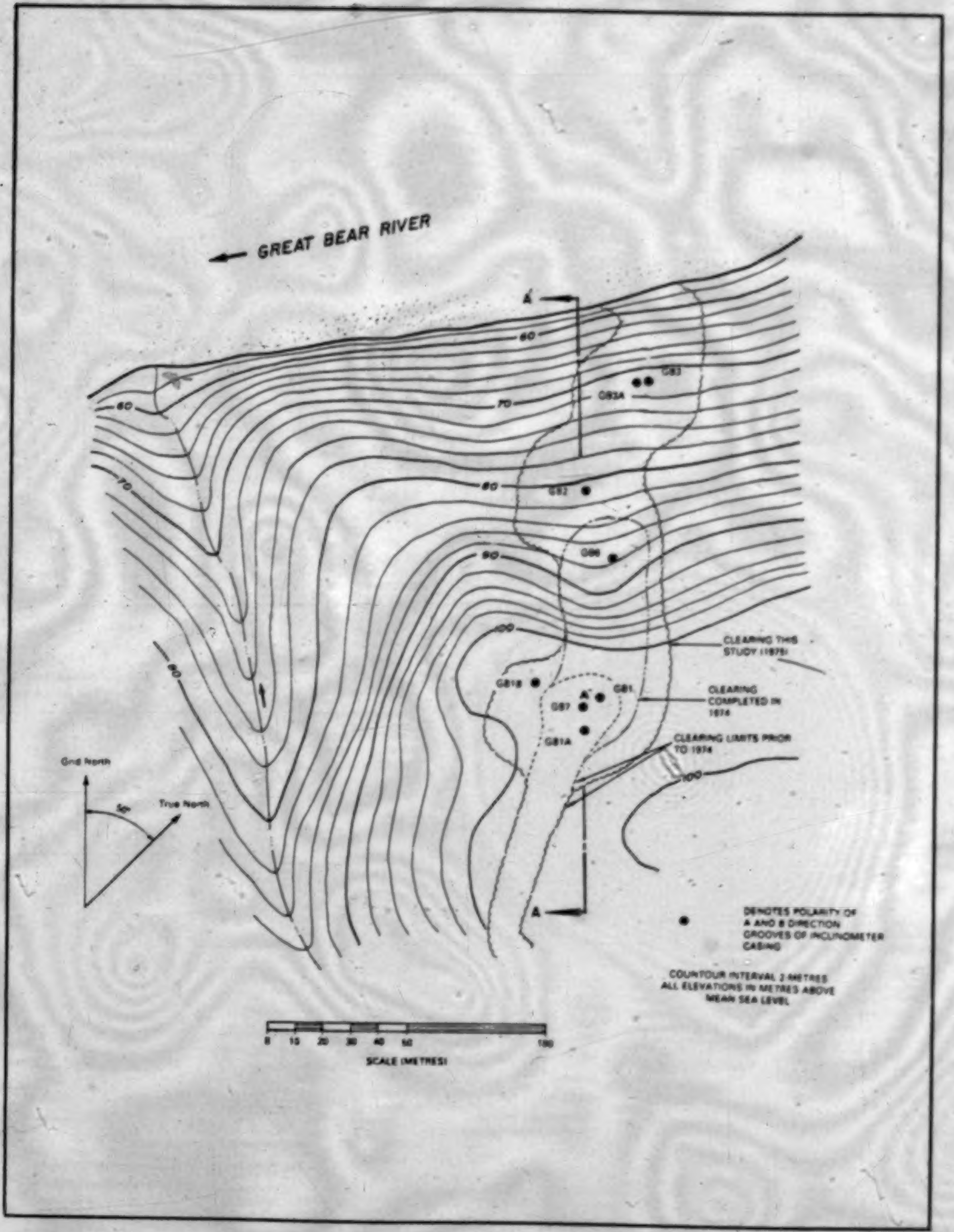
GREAT BEAR RIVER
A'
A
60
70
80
90
100
GB3
GB3A
GB2
GB6
GB1B
GB7
GB1
GB1A
CLEARING THIS STUDY (1979)
CLEARING COMPLETED IN 1974
CLEARING LIMITS PRIOR TO 1974
Grid North
True North
DENOTES POLARITY OF A AND B DIRECTION GROOVES OF INCLINOMETER CASING
COUNTOUR INTERVAL 2 METRES
ALL ELEVATIONS IN METRES ABOVE MEAN SEA LEVEL
0
10
20
30
40
50
100
SCALE (METRES)

FIGURE 4.2 SITE PLAN OF LEFT BANK OF GREAT BEAR RIVER AT PROPOSED ARCTIC GAS CROSSING (Savigny, 1980)

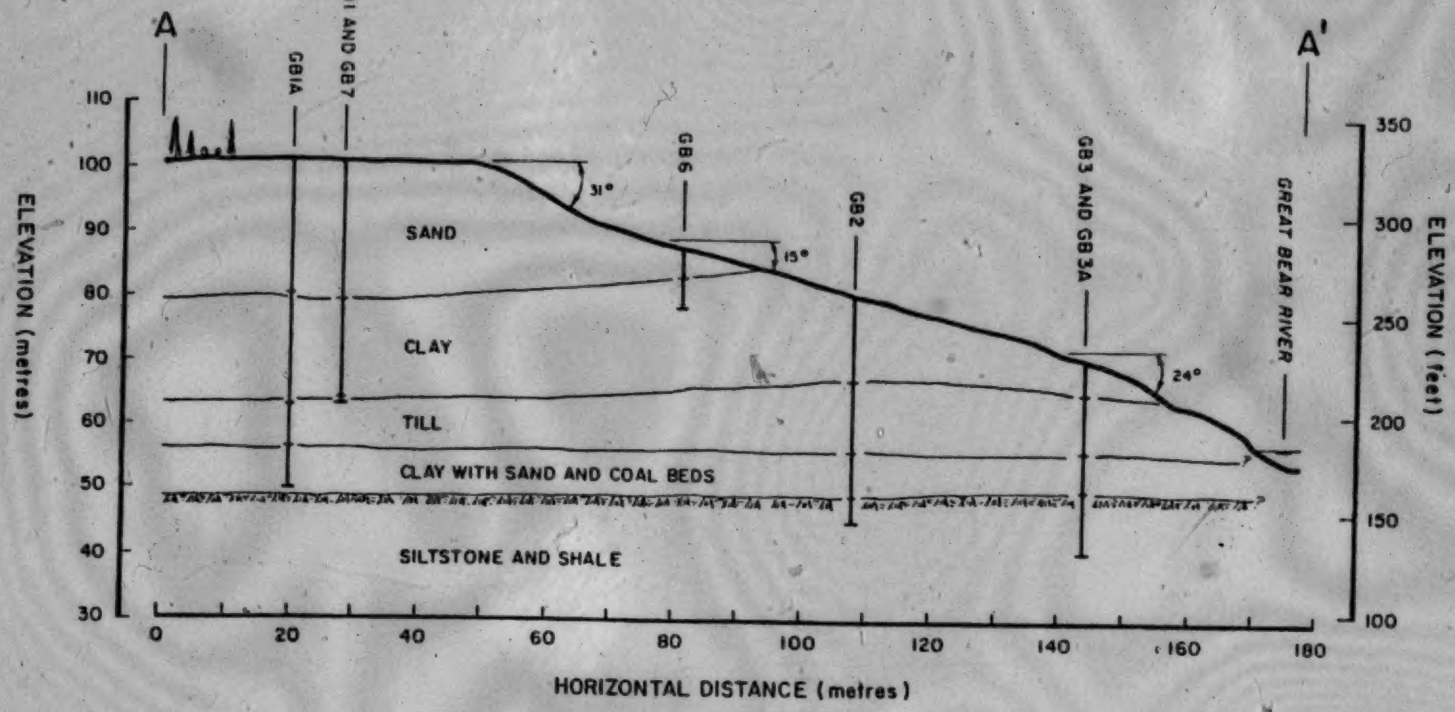

FIGURE 4.3 STRATIGRAPHIC CROSS SECTION; LEFT BANK OF GREAT BEAR RIVER AT PROPOSED ARCTIC GAS CROSSING (Savigny, 1980)

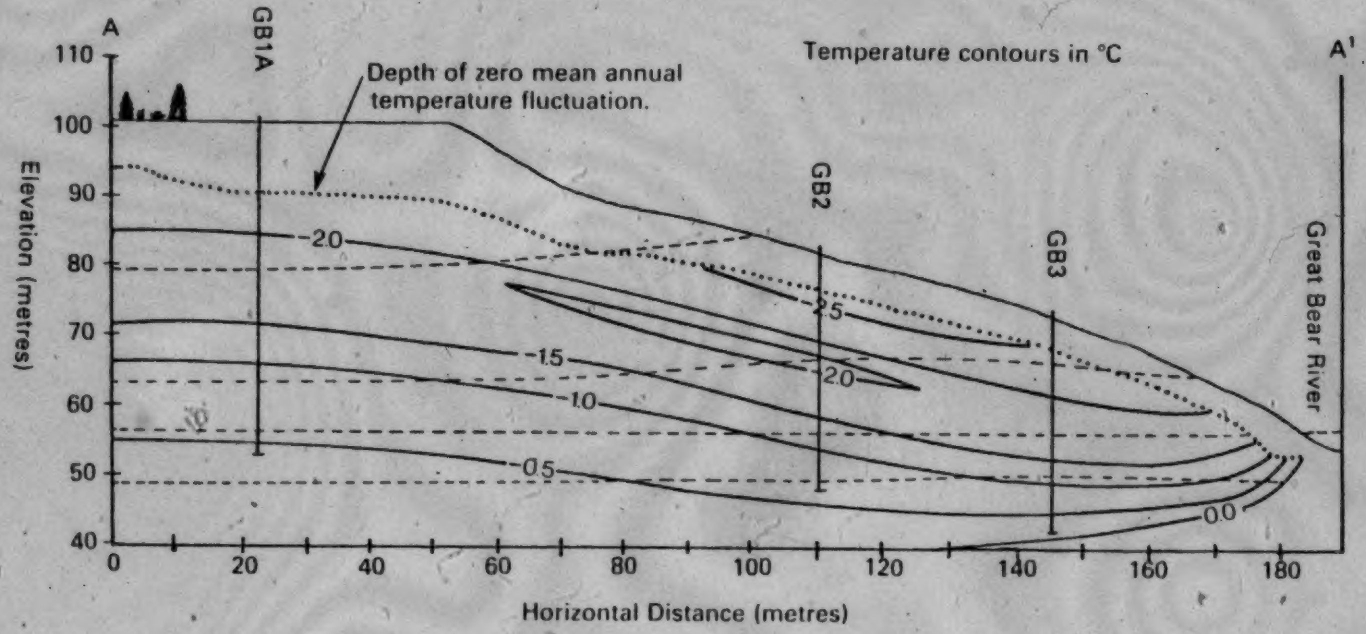

FIGURE 4.4 THERMAL CROSS SECTION; LEFT BANK OF GREAT BEAR RIVER AT PROPOSED ARCTIC GAS CROSSING
(Savigny, 1980)

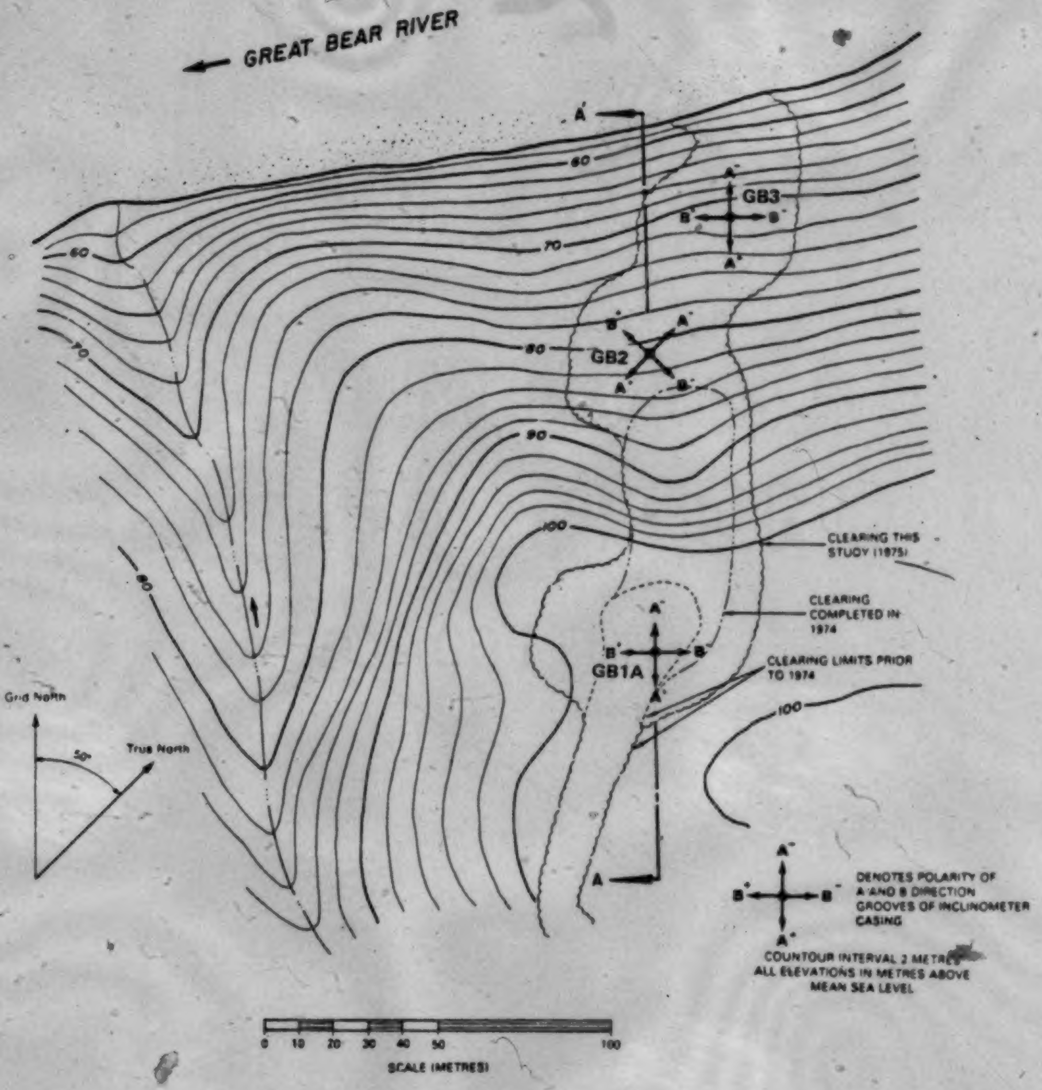
GREAT BEAR RIVER
A'
60
GB3
A⁻
B⁺
B⁻
A⁺
70
60
70
80
GB2
B⁺
A⁺
A⁻
B⁻
90
100
80
CLEARING THIS STUDY (1975)
CLEARING COMPLETED IN 1974
CLEARING LIMITS PRIOR TO 1974
GB1A
B⁺
B⁻
A⁻
A⁺
100
Grid North
50°
True North
A
A⁻
B⁺
B⁻
A⁺
DENOTES POLARITY OF A AND B DIRECTION GROOVES OF INCLINOMETER CASING
COUNTOUR INTERVAL 2 METRES
ALL ELEVATIONS IN METRES ABOVE MEAN SEA LEVEL
0 10 20 30 40 50 100
SCALE (METRES)

FIGURE 4.5 SITE PLAN OF INCLINOMETER LOCATIONS ON LEFT BANK OF GREAT BEAR RIVER AT PROPOSED ARCTIC GAS CROSSING (Savigny, 1980)

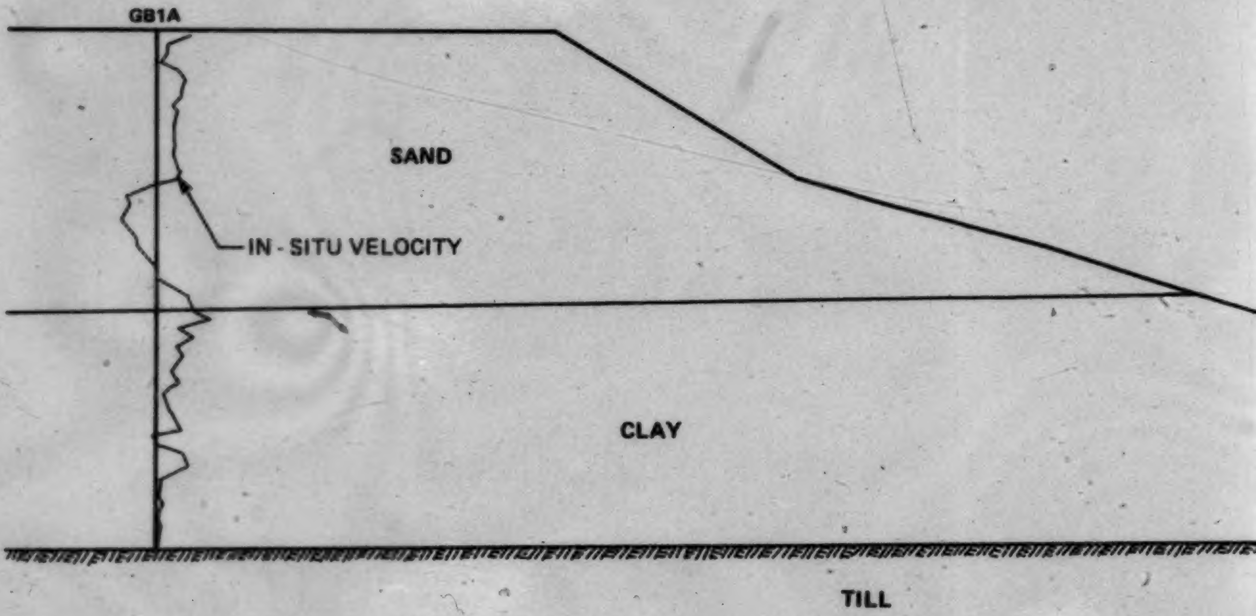
GB1A
SAND
IN - SITU VELOCITY
CLAY
TILL

FIGURE 4.6 VELOCITY VERSUS DEPTH PROFILES FOR GBI
INCLINOMETER LOCATIONS

1 of

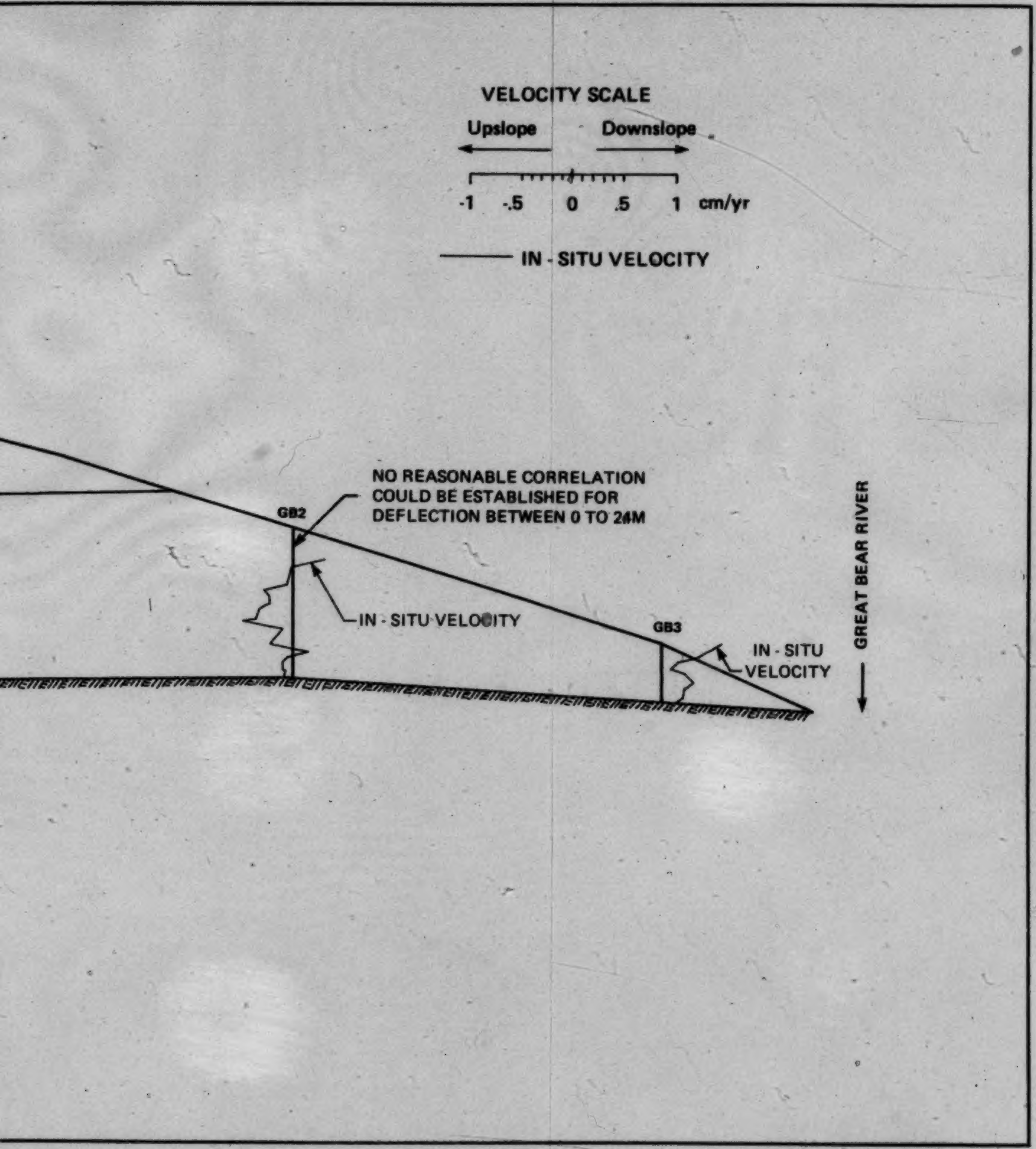
VELOCITY SCALE
Upslope
Downslope
-1
-.5
0
.5
1
cm/yr
IN - SITU VELOCITY
GB2
IN - SITU VELOCITY
GB3
IN - SITU VELOCITY
GREAT BEAR RIVER

NO REASONABLE CORRELATION COULD BE ESTABLISHED FOR DEFLECTION BETWEEN 0 TO 24M

TH PROFILES FOR GBIA, GB2, AND GB3
IONS

2 of 2

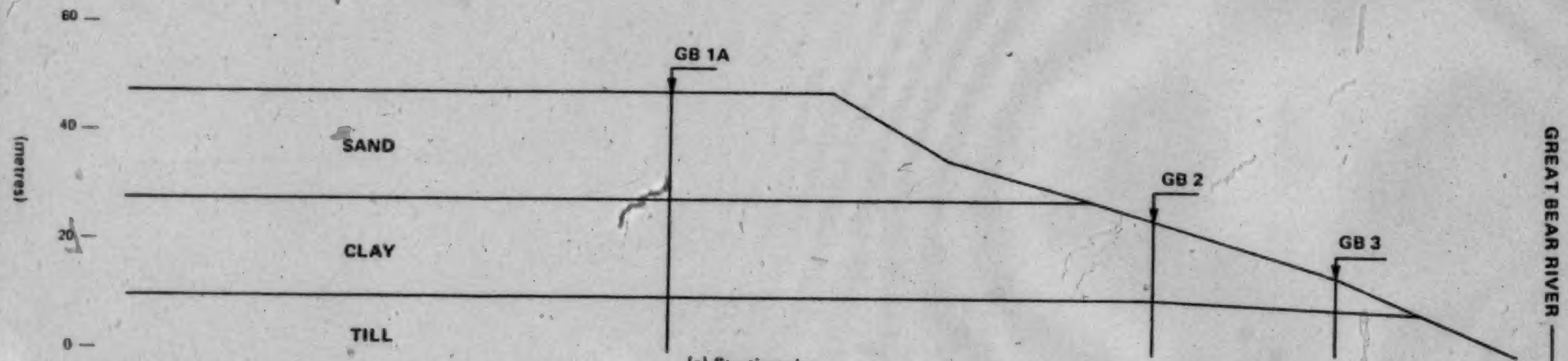
60
40
20
0
(metres)
SAND
CLAY
TILL
GB 1A
GB 2
GB 3
GREAT BEAR RIVER

(a) Stratigraphy

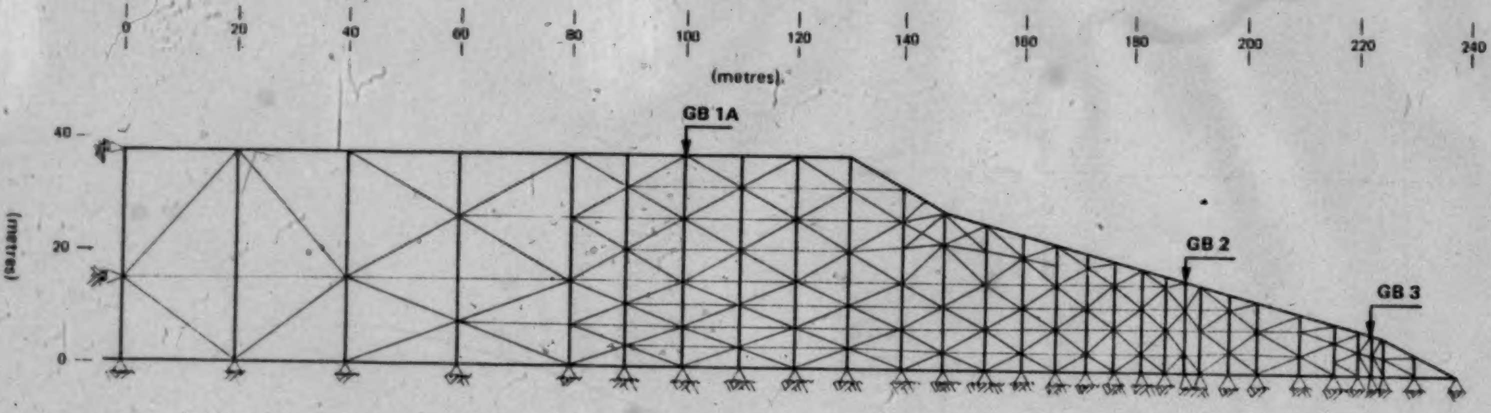
0
20
40
60
80
100
120
140
160
180
200
220
240
(metres)
40
20
0
(metres)
GB 1A
GB 2
GB 3

(b) Finite Element Discretization

FIGURE 4.7 FINITE ELEMENT DISCRETIZATION OF PROPOSED ARCTIC GAS CROSSING OF THE GREAT BEAR RIVER

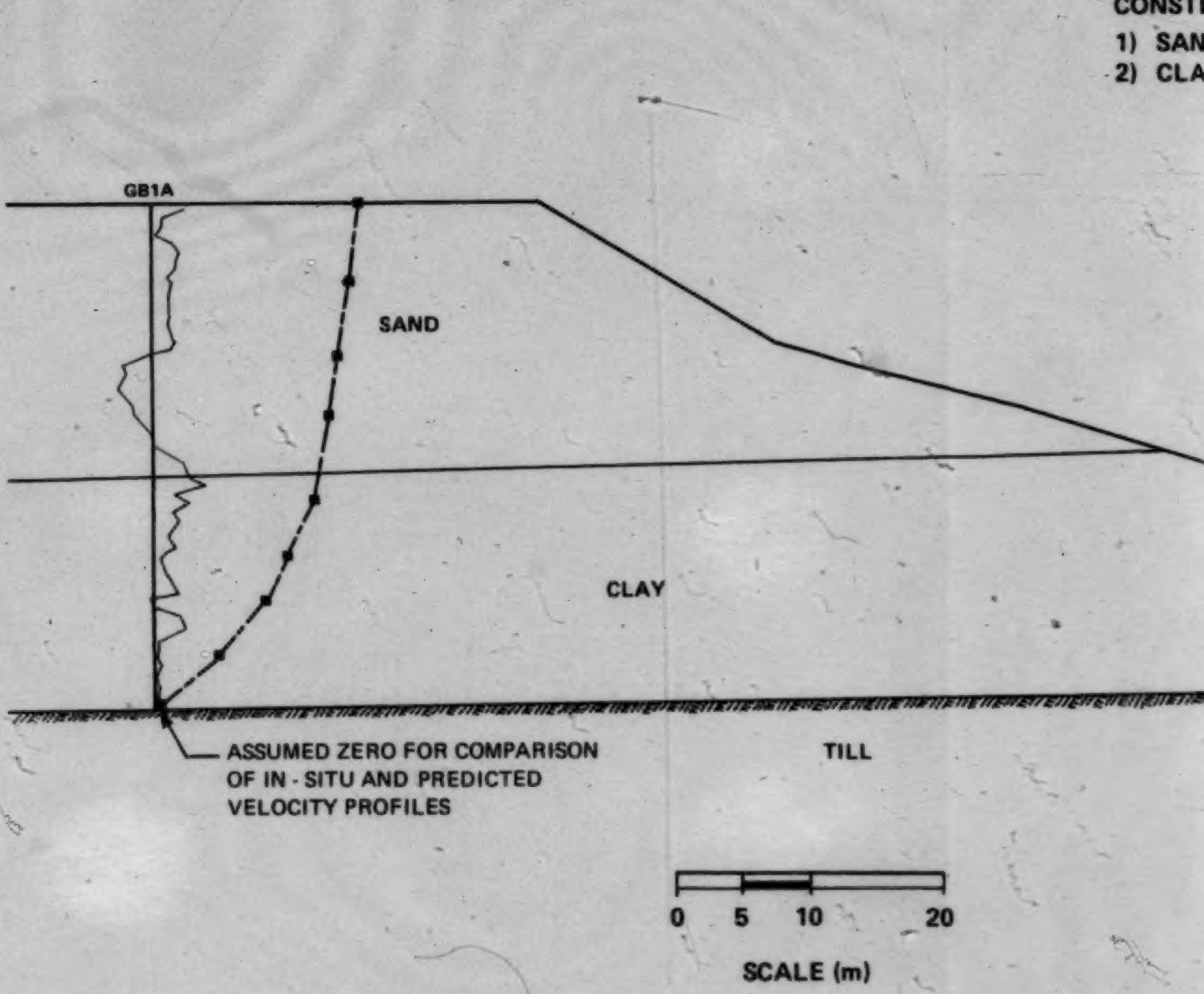
CONSTI
1) SAN
2) CLA
GB1A
SAND
CLAY
TILL
ASSUMED ZERO FOR COMPARISON OF IN - SITU AND PREDICTED VELOCITY PROFILES
0
5
10
20
SCALE (m)

FIGURE 4.8 PREDICTED STEADY STATE CREEP VELOC
FIRST CREEP ANALYSIS

1 of

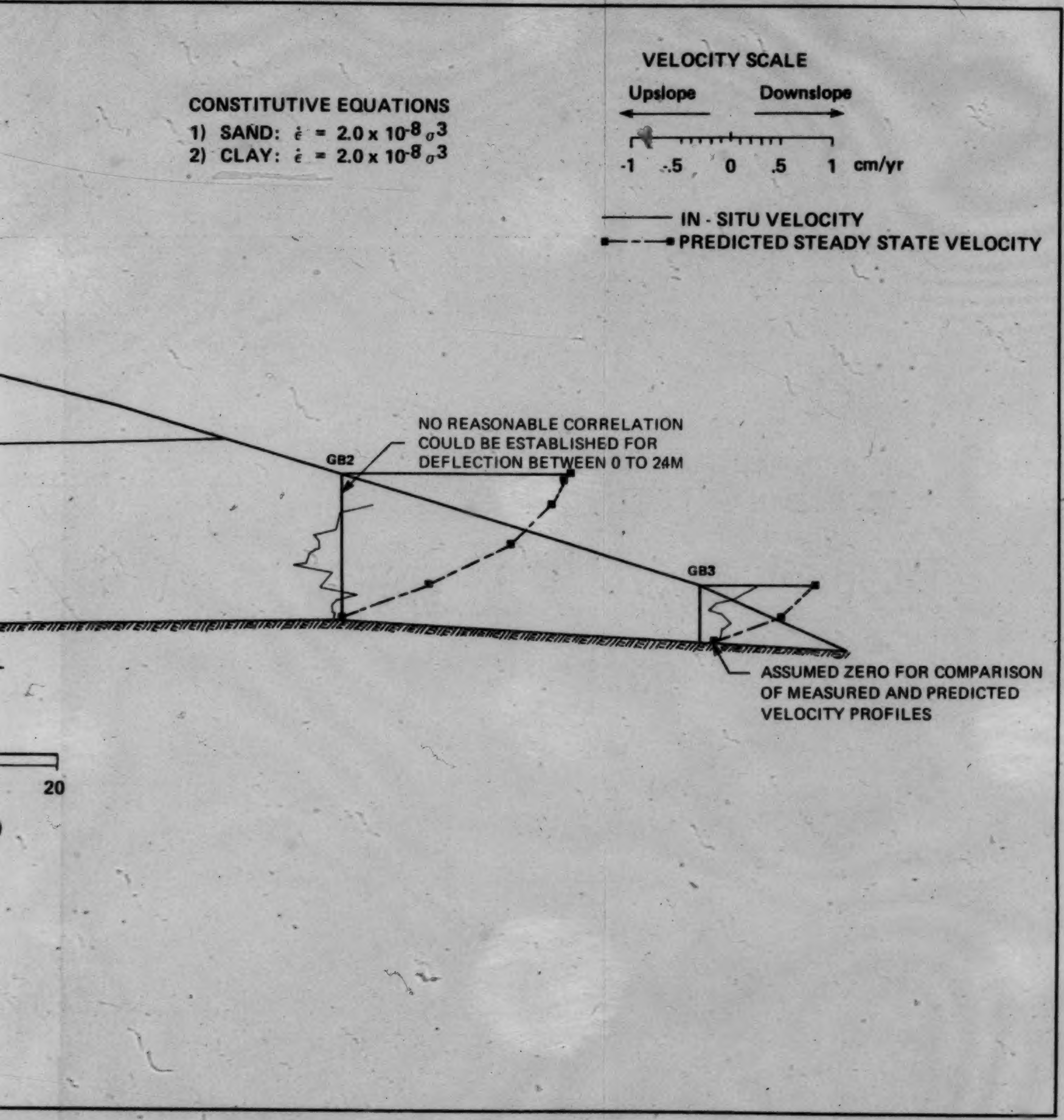
CONSTITUTIVE EQUATIONS
1) SAND: $\dot{\epsilon} = 2.0 \times 10^{-8} \sigma^3$
2) CLAY: $\dot{\epsilon} = 2.0 \times 10^{-8} \sigma^3$
VELOCITY SCALE
Upslope
Downslope
-1 -.5 0 .5 1 cm/yr
IN - SITU VELOCITY
PREDICTED STEADY STATE VELOCITY
NO REASONABLE CORRELATION COULD BE ESTABLISHED FOR DEFLECTION BETWEEN 0 TO 24M
GB2
GB3
ASSUMED ZERO FOR COMPARISON OF MEASURED AND PREDICTED VELOCITY PROFILES
20

EADY STATE CREEP VELOCITY PROFILES,
ANALYSIS

2 of 2

01

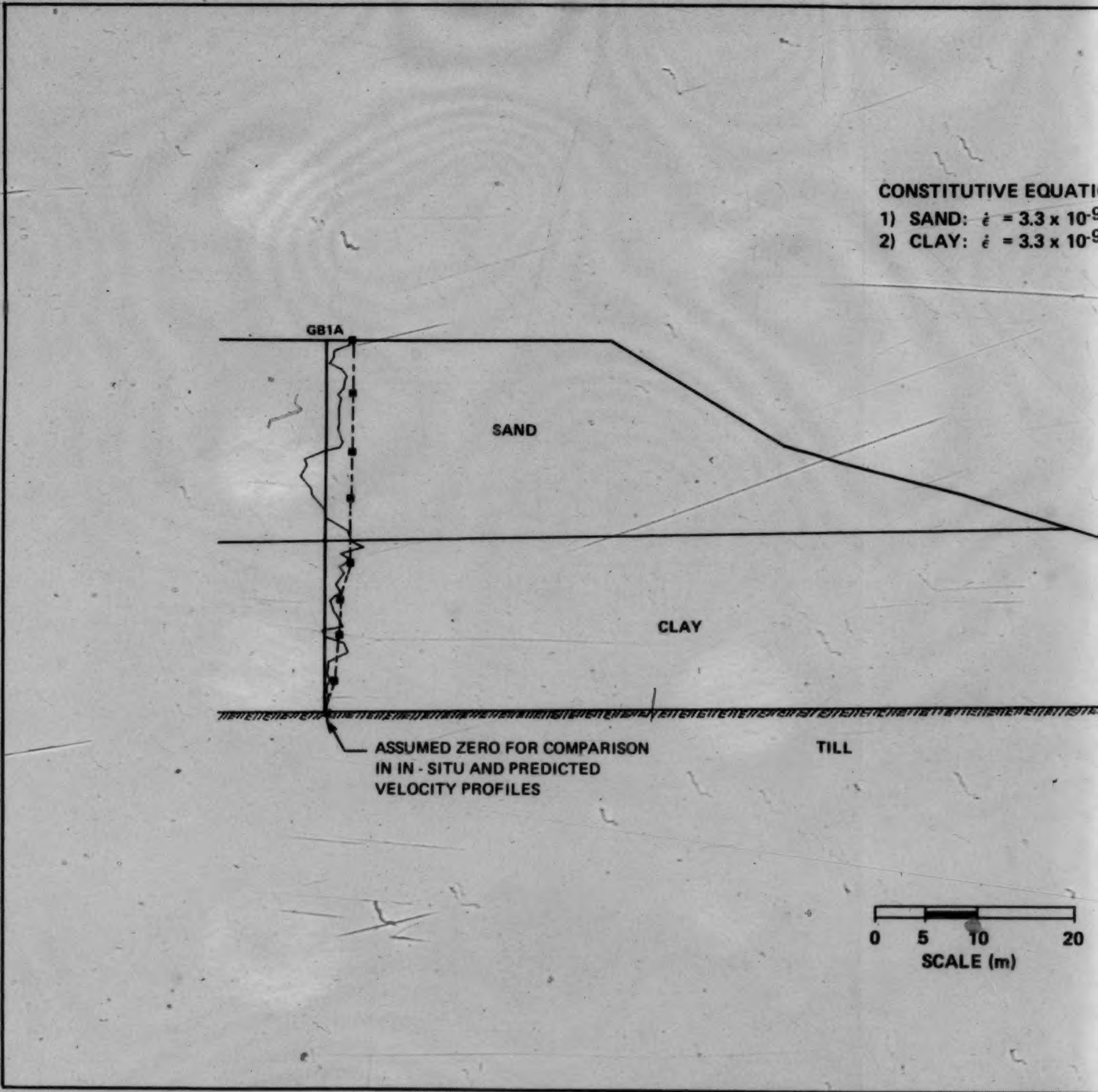
CONSTITUTIVE EQUATI
1) SAND: $\dot{\epsilon}$ = 3.3 x 10-9
2) CLAY: $\dot{\epsilon}$ = 3.3 x 10-9
GB1A
SAND
CLAY
TILL
ASSUMED ZERO FOR COMPARISON
IN IN - SITU AND PREDICTED
VELOCITY PROFILES
0
5
10
20
SCALE (m)

FIGURE 4.9 PREDICTED STEADY STATE VELOCITY PROFILE
VELOCITIES FROM FIRST CREEP ANALYSIS

1 of

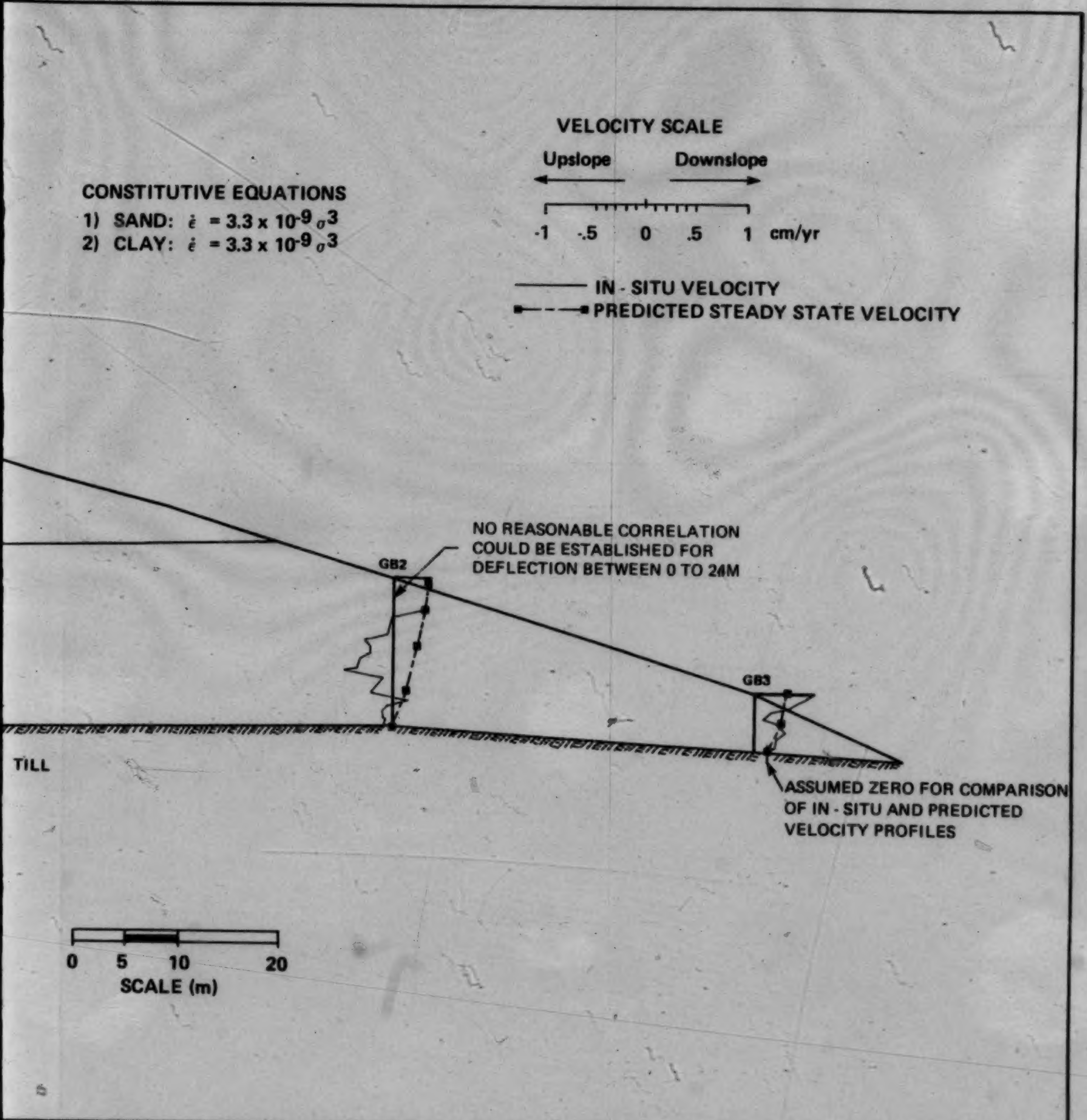
VELOCITY SCALE
Upslope
Downslope
-1 -.5 0 .5 1 cm/yr
CONSTITUTIVE EQUATIONS
1) SAND: ε̇ = 3.3 x 10-9 σ3
2) CLAY: ε̇ = 3.3 x 10-9 σ3
IN - SITU VELOCITY
PREDICTED STEADY STATE VELOCITY
NO REASONABLE CORRELATION
COULD BE ESTABLISHED FOR
DEFLECTION BETWEEN 0 TO 24M
GB2
GB3
TILL
ASSUMED ZERO FOR COMPARISON
OF IN - SITU AND PREDICTED
VELOCITY PROFILES
0 5 10 20
SCALE (m)

ADY STATE VELOCITY PROFILES, FACTORED
OM FIRST CREEP ANALYSIS

2 of 2

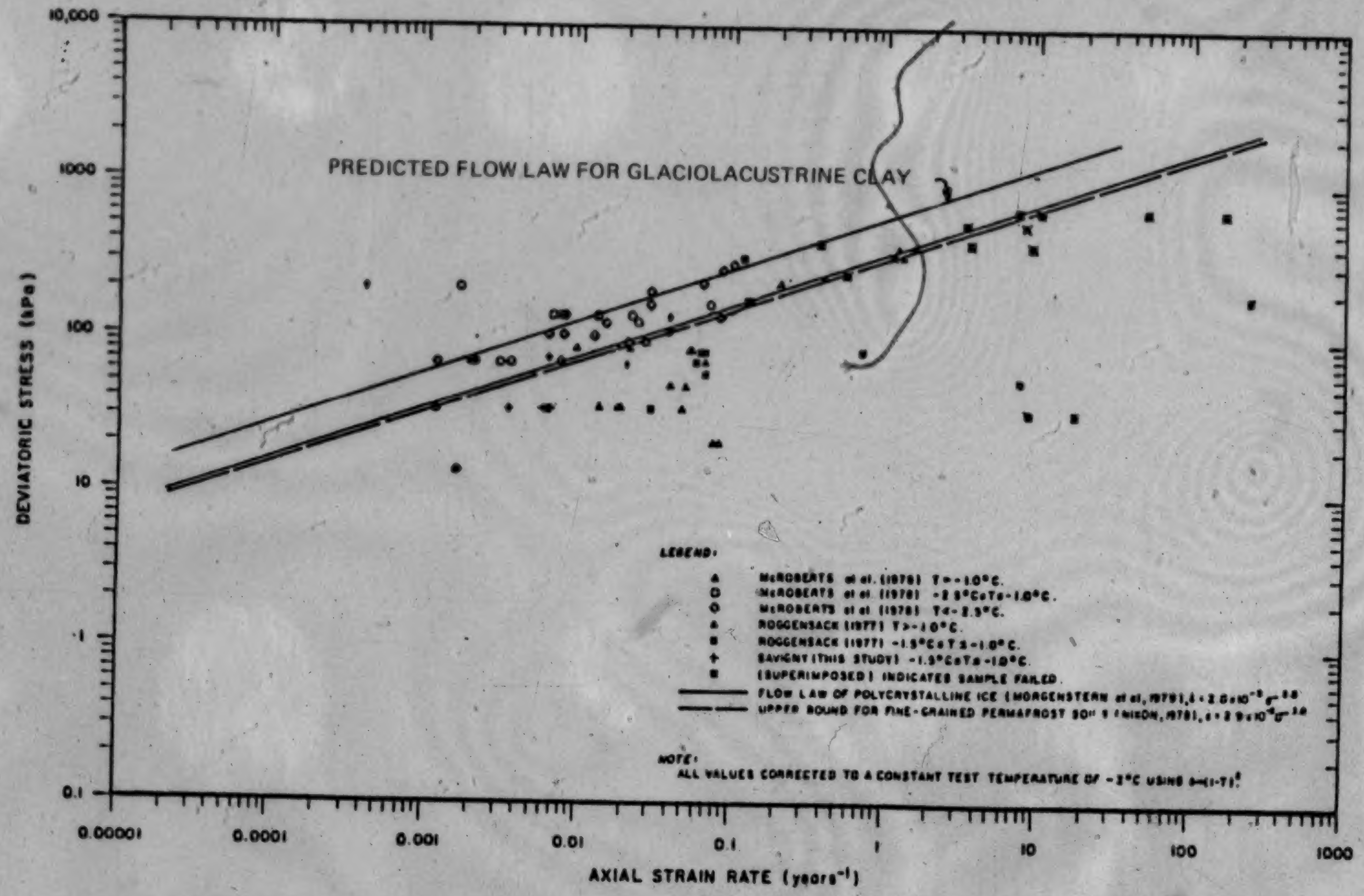

FIGURE 4.10 COMPARISON OF IN-SITU CREEP LAW AND STEADY-STATE CREEP DATA FOR ICE-RICH GLACIOLACUSTRINE CLAY FROM VARIOUS LOCATIONS IN THE MACKENZIE RIVER VALLEY, N.W.T.

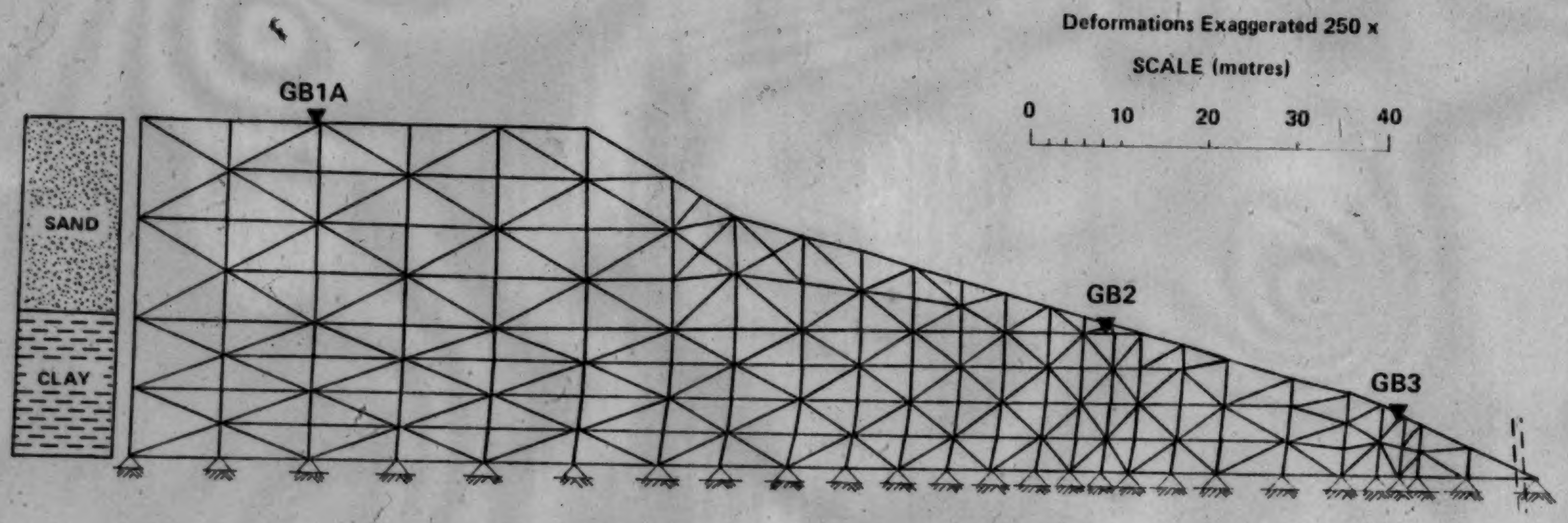
Deformations Exaggerated 250 x
SCALE (metres)
0
10
20
30
40
GB1A
GB2
GB3
SAND
CLAY

FIGURE 4.11 DEFORMED GRID FOR STEADY STATE CREEP IN SAND AND CLAY

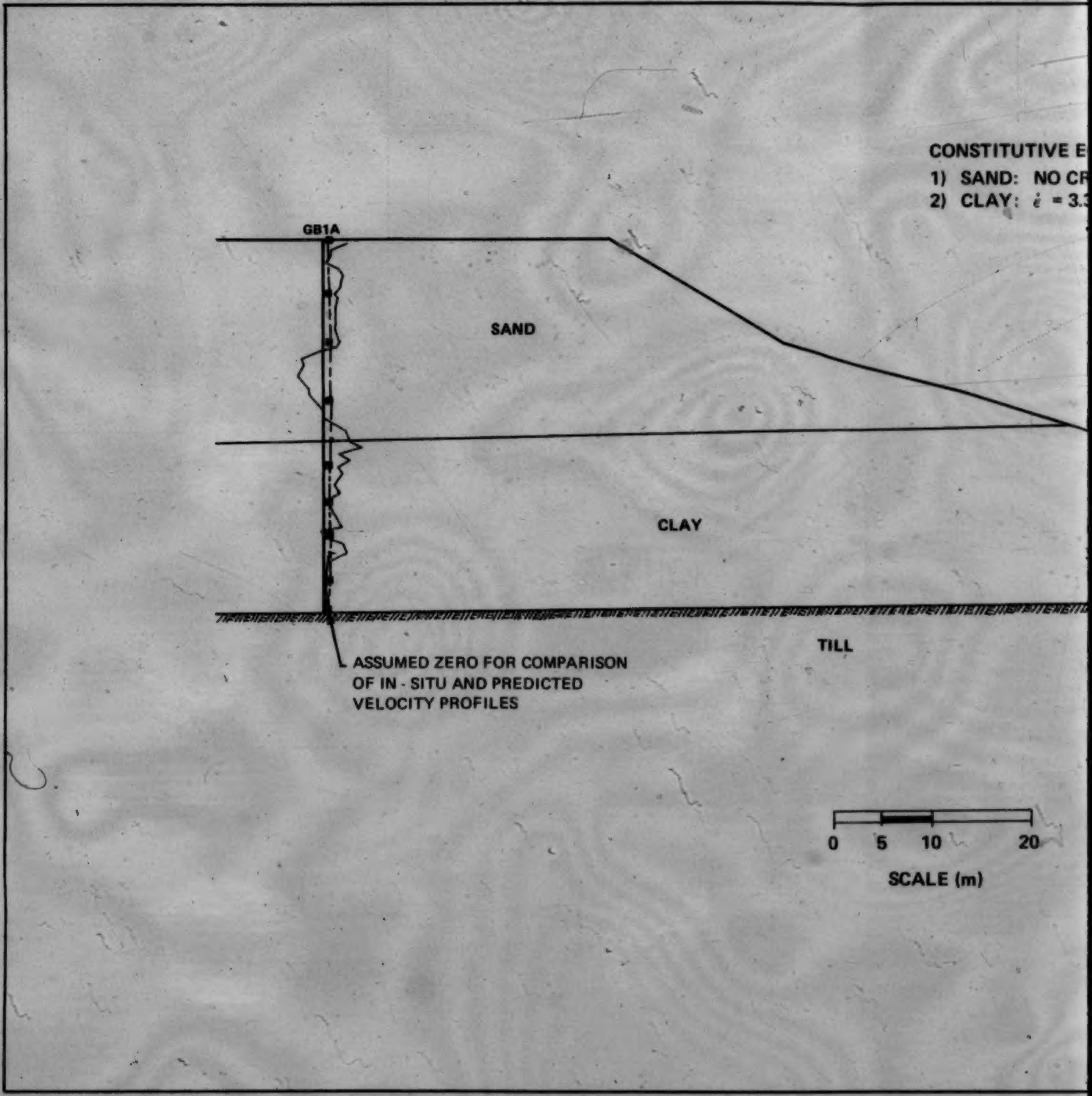
CONSTITUTIVE E
1) SAND: NO CR
2) CLAY: $\dot{\epsilon}$ = 3.3
GB1A
SAND
CLAY
TILL
ASSUMED ZERO FOR COMPARISON
OF IN - SITU AND PREDICTED
VELOCITY PROFILES
0 5 10 20
SCALE (m)

FIGURE 4.12 PREDICTED STEADY STATE VELO
CREEP IN GLACIOLACUSTRINE C

1 of

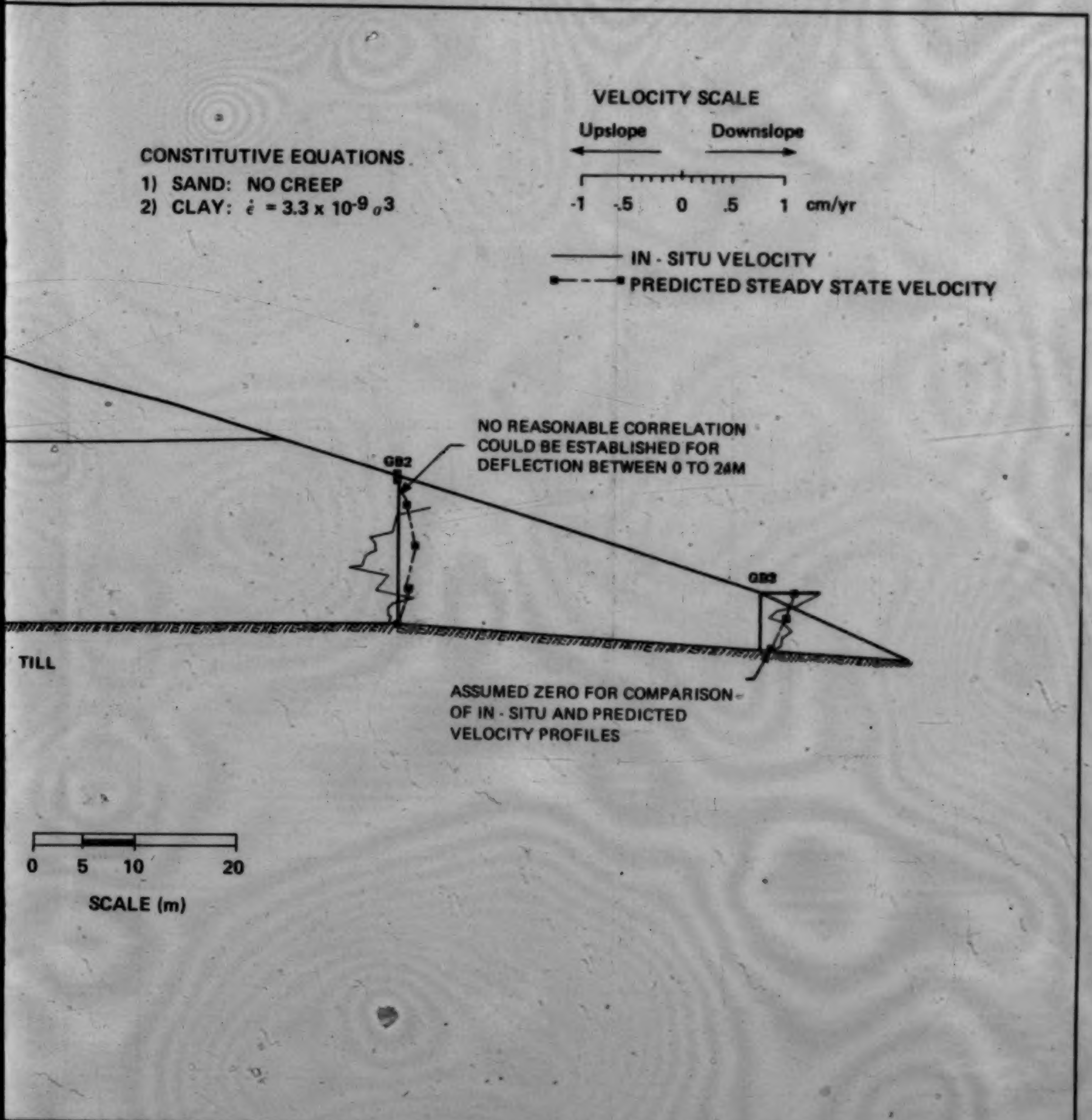
CONSTITUTIVE EQUATIONS
1) SAND: NO CREEP
2) CLAY: $\dot{\epsilon} = 3.3 \times 10^{-9} \sigma^3$
VELOCITY SCALE
Upslope
Downslope
-1
-.5
0
.5
1
cm/yr
IN - SITU VELOCITY
PREDICTED STEADY STATE VELOCITY
NO REASONABLE CORRELATION COULD BE ESTABLISHED FOR DEFLECTION BETWEEN 0 TO 24M
GB2
GB3
TILL
ASSUMED ZERO FOR COMPARISON OF IN - SITU AND PREDICTED VELOCITY PROFILES
0
5
10
20
SCALE (m)

EDICTED STEADY STATE VELOCITY PROFILES,
EEP IN GLACIOLACUSTRINE CLAY ONLY

2 of 2

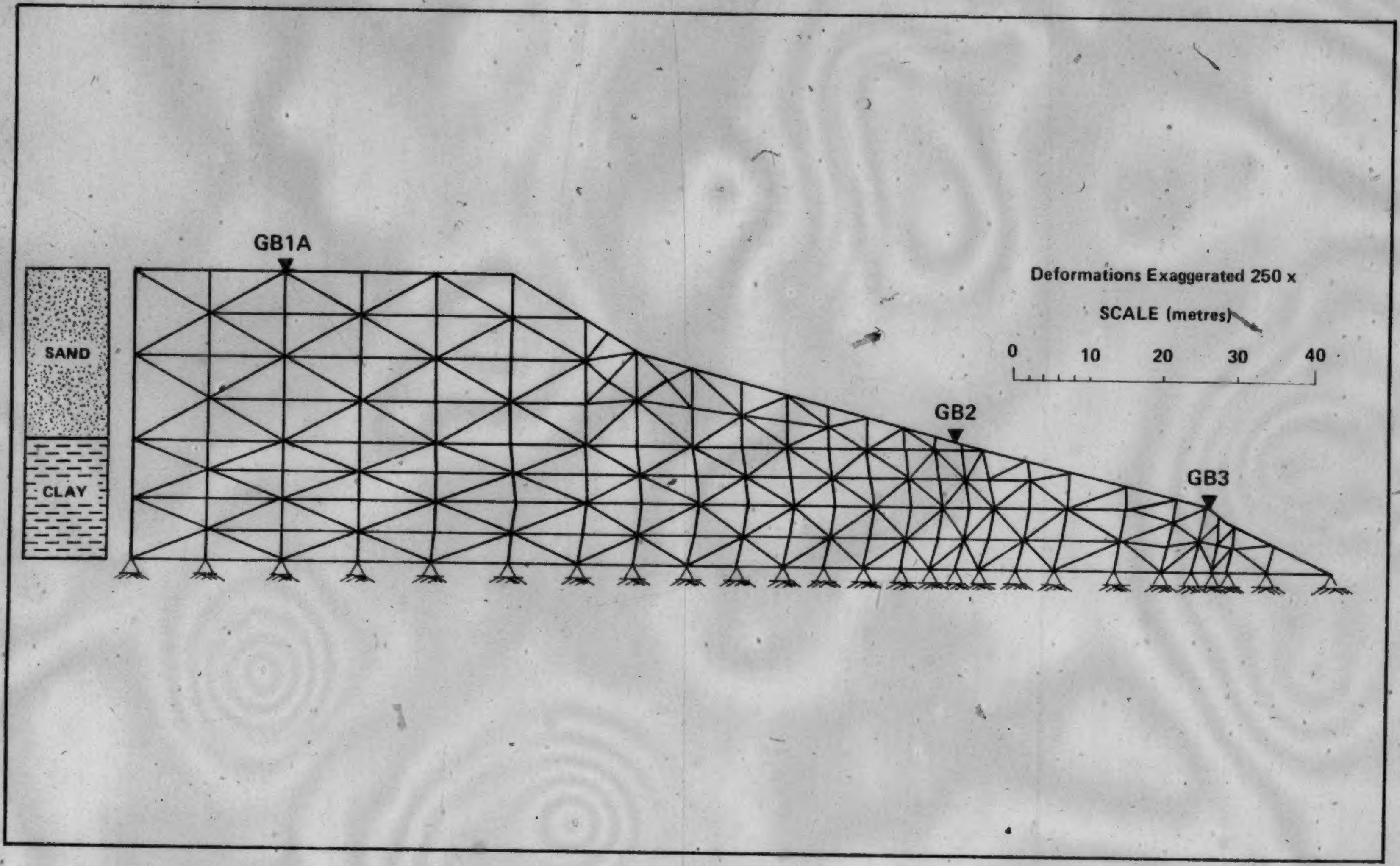
SAND
CLAY
GB1A
GB2
GB3
Deformations Exaggerated 250 x
SCALE (metres)
0
10
20
30
40

FIGURE 4.13 DEFORMED GRID FOR STEADY STATE CREEP IN CLAY ONLY

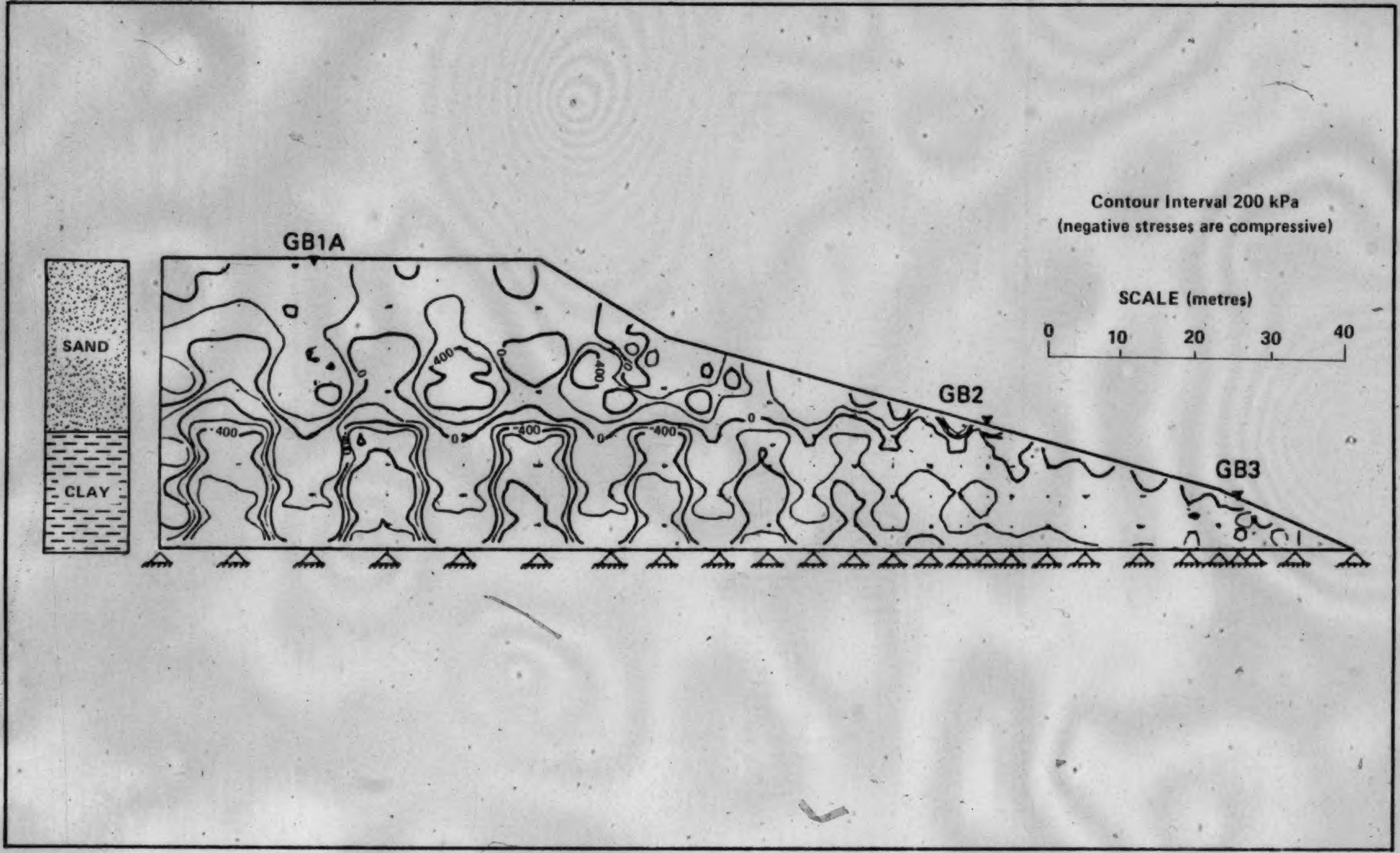
Contour Interval 200 kPa
(negative stresses are compressive)
SCALE (metres)
0
10
20
30
40
GB1A
GB2
GB3
SAND
CLAY
400
0
-400

FIGURE 4.14 HORIZONTAL STRESS CONTOURS FOR STEADY STATE CREEP IN CLAY ONLY

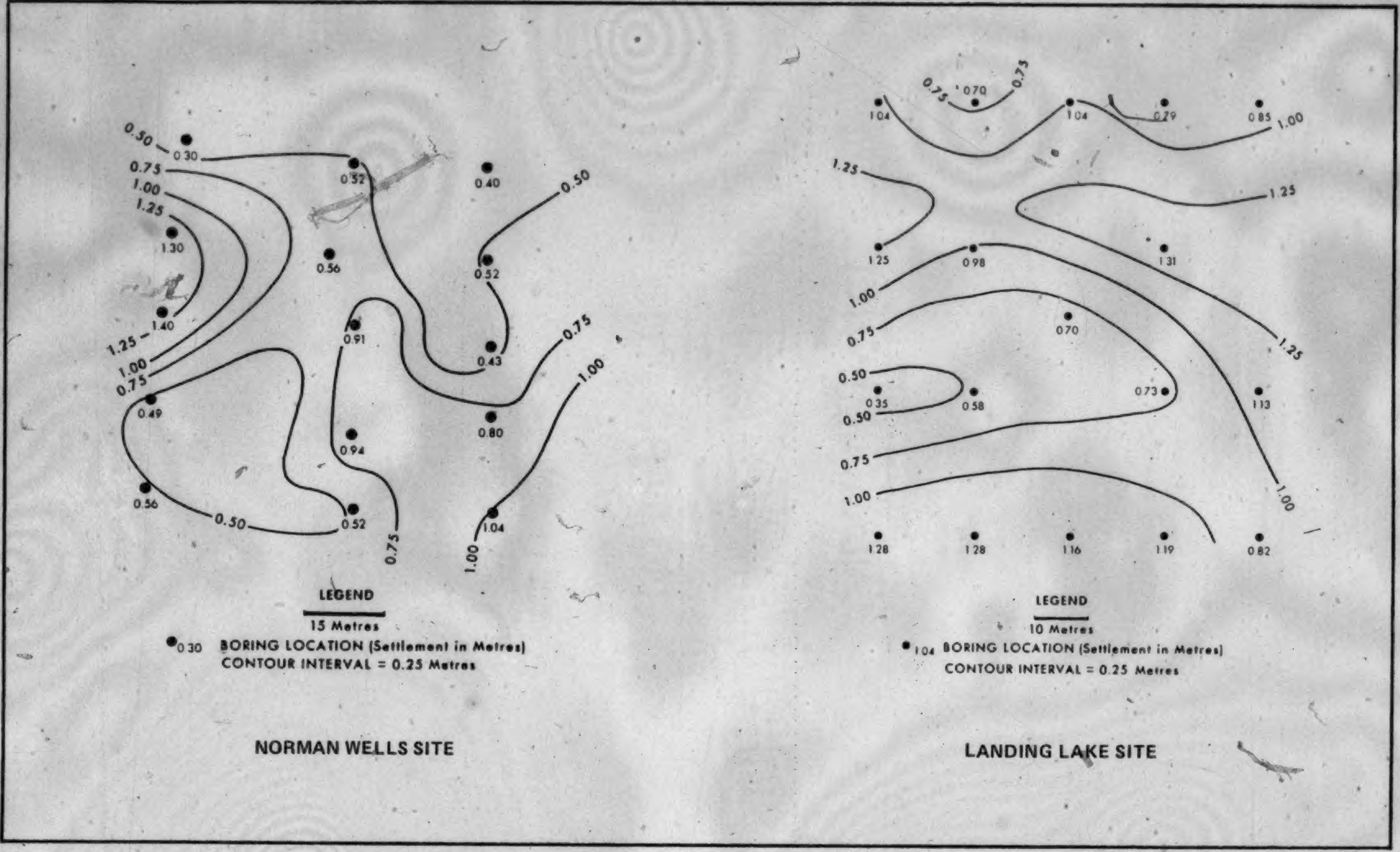
0.50
0.75
1.00
1.25
1.25
1.00
0.75
0.50
0.75
1.00
0.50
0.75
1.00
0.30
0.32
0.40
1.30
0.56
0.52
1.40
0.91
0.43
0.49
0.94
0.80
0.56
0.52
1.04
LEGEND
15 Metres
0.30 BORING LOCATION (Settlement in Metres)
CONTOUR INTERVAL = 0.25 Metres
NORMAN WELLS SITE
0.75
0.70
0.75
1.04
1.04
0.79
0.85
1.00
1.25
1.25
1.25
0.98
1.31
1.00
0.70
1.25
0.75
0.50
0.35
0.58
0.73
1.13
0.50
0.75
1.00
1.00
1.28
1.28
1.16
1.19
0.82
LEGEND
10 Metres
1.04 BORING LOCATION (Settlement in Metres)
CONTOUR INTERVAL = 0.25 Metres
LANDING LAKE SITE

FIGURE 4.15 THAW SETTLEMENT DATA FOR NORMAN WELLS AND LANDING LAKE ICE VARIABILITY TEST SITES (Speer et. al., 1973)

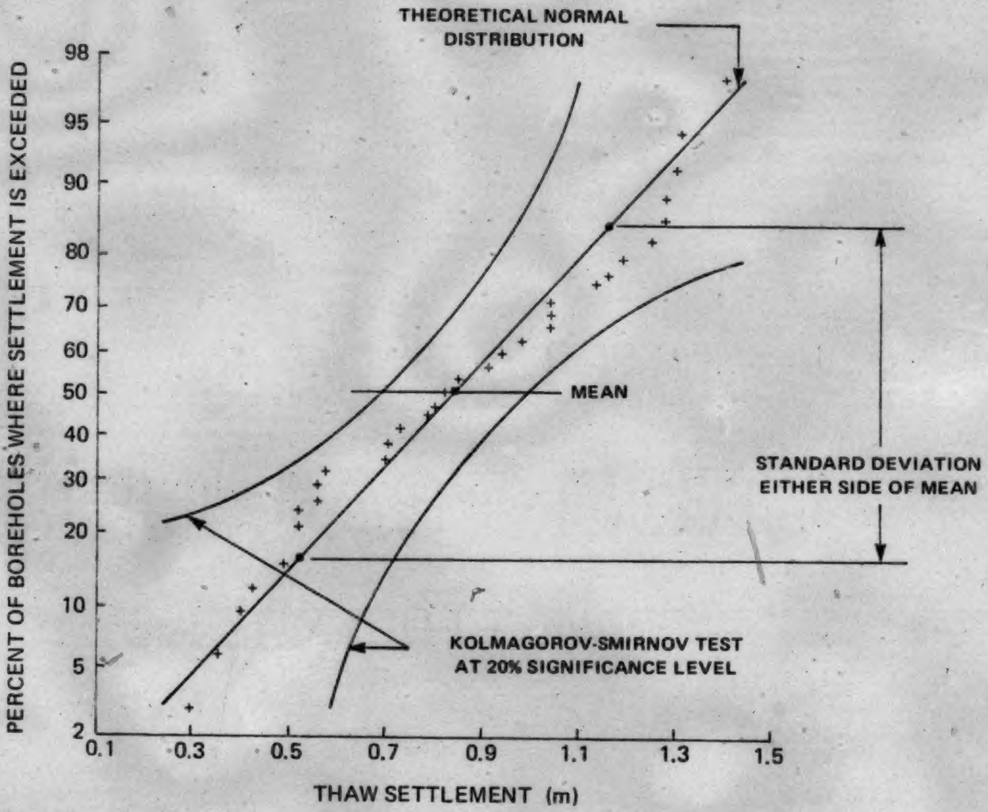

FIGURE 4.16 PROBABILITY RELATIONSHIP FOR THAW SETTLEMENT IN ICE-RICH LACUSTRINE SILT AND CLAY (Speer et. al., 1973)

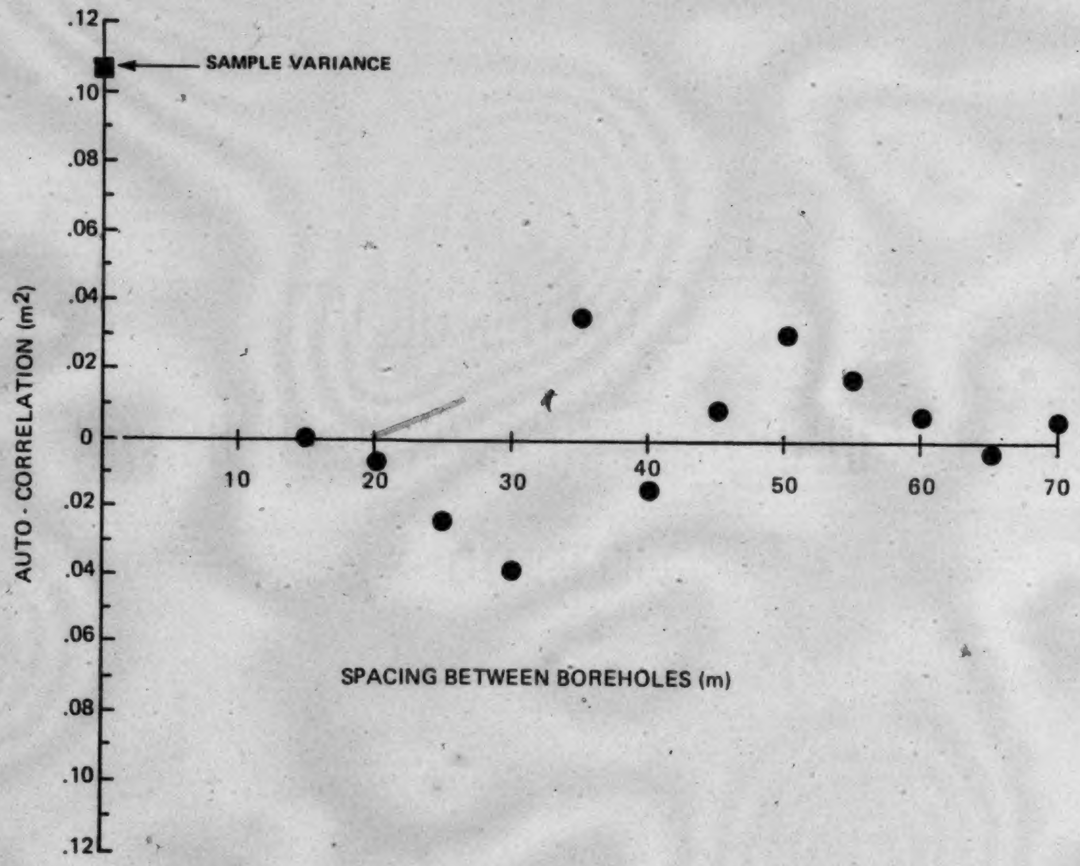

FIGURE 4.17 AUTO - CORRELATION FUNCTION FOR THAW SETTLEMENT IN ICE - RICH LACUSTRINE SILT AND CLAY

CHAPTER V

IN-SITU CREEP ANALYSIS OF FOX TUNNEL

5.1 General

The Fox Tunnel is located approximately 16 km north of Fairbanks, Alaska. The tunnel was excavated into perenially frozen silts. These silts have been of an economic interest in the Fairbanks area since the turn of the century because of the need to remove thick sections of the material to expose the underlying gold-bearing gravels. The old mining practice consisted of stripping the overburden of perenially frozen silt to expose the gravels which were subsequently worked with dredges. The Fox Tunnel excavations were part of two separate research programs from 1966 to 1969. The objectives of these research projects were to investigate methods of subsurface exploration in perenially frozen ground and evaluate subsurface openings as a shelter, storage space and site for military activities.

The first stage of this project was to excavate a tunnel 110 m long in the winters from 1963 to 1966 as shown in Figure 5.1. The excavation was carried out using a continuous mining machine and a modified blasting technique. The tunnel was excavated through ice-rich Fairbanks silt for its entire length. The tunnel portal was excavated into a near-vertical silt escarpment left from old placer mining operations. Closure measurements were undertaken following the mining operations. In November, 1966, a 1.22 m ventilation shaft was drilled from the surface and connected to the end of the tunnel. The ventilation shaft was left open the first winter to allow the heavier cold winter air to circulate through the tunnel by natural convection. The cooler air lowered the tunnel wall temperature from -1.0°C to -6.7°C (McAnerney, 1968). The lower ground temperature substantially decreased the closure rate of the tunnel. Deformations have been negligible since the ventilation stack was drilled.

The second stage of this project involved excavating a winze from the existing tunnel to provide access to the stratigraphically lower gold bearing gravels and bedrock. This phase of the project is shown as the shaded portions in Figure 5.2. This phase was a cooperative effort between the U.S. Bureau of Mines (USBM) and the U.S. Army Cold Regions Research and Engineering Laboratory (USA CRREL). The winze terminates in a room; designated as Room B by the USA CRREL. A second room USBM Room A, was excavated south of the inclined winze. The winze and two rooms were excavated using air and conventional blasting techniques. Slabbing of the gravel occurred in regions where the thickness of gravel separating the ceiling from the silt was thin. This necessitated that this material be scaled from the roof to ensure a safe working area. Extensive deformation studies were carried out in both rooms (Thompson and Sayles, 1972; Pettibone, 1973). These will be discussed in a subsequent section.

5.2 Site Geology

The sequence of geologic sediments encountered in the main tunnel and winze excavation exposures are shown in Figure 5.3. The disintegrated schist bedrock at the tunnel site is mantled by unconsolidated, ice-cemented silts and gravels. Immediately overlying the bedrock are the gold-bearing gravel deposits. The gravel is capped by a thick re-transported silt deposit.

The floor of both rooms excavated at the end of the winze consist of Birch Creek schist. The bedrock is perenially frozen and deeply weathered in these exposures. X-ray diffraction analyses performed on samples of the decomposed bedrock just below the gravel/bedrock interface showed a high montmorillonite peak (Sellman, 1972).

A stream deposited gravel layer lies unconformably on top of the bedrock. Stream deposition was inferred from the strong imbrication of the pebbles and cobbles. The average thickness of the gravel deposit in this region is approximately 4 m. Pockets of fine-grained materials are interbedded in the sand. The gravel is perenially frozen and bonded with ice. Pore ice is visible in the voids but the particles retain grain-to-grain contact.

A thick deposit of silt, the uppermost unit at this site, lies unconformably on top of the gravel. Although irregular, the silt-gravel contact is sharp. The silt deposit ranges in age from Illinoian to recent. The Illinoian deposits contain considerably less ground ice and organic matter than the younger units. The overlying silt of Wisconsin age is characterized by large ice wedges. Retransported silts of recent age mantle the top of the upland plain at the tunnel site. Generally, there are two types of ground ice present in the frozen silt; ice lenses and masses formed by ice segregation, and the massive ice structures of Aufeis (buried ice). Ice volumes range from 54 to 79%.

5.3 In-Situ Deformation Studies

The in-situ creep movements of the ice-rich Fairbanks silt were studied independently by Swinzow (1970), Thompson and Sayles (1972) and Pettibone (1973).

The closure rate of the main tunnel was measured by Swinzow (1970) immediately following the final excavation season. No details on the type of instrumentation or the exact time the measurements were recorded are given. Horizontal and vertical closure measurements were recorded at two different locations, Sta. 1+50 and Sta. 3+50 (45.7 m and 106.7 m, respectively, from the portal). The closure measurements recorded at the two tunnel sections are shown in Figures 5.4. The air temperature in the tunnel at the time the readings were recorded was very close to the melting point of ice (McAnerney, 1968). Measurements recorded over a 3200 hour time span showed that the deformation rate continued to attenuate with time. Very little difference was noted between horizontal and vertical closure of the tunnel at both locations. A closure of 14.6 cm was recorded at the instrumented section furthest removed from the tunnel portal. The difference in overburden between these two sections was only 2.1 m. The difference in closure between the two measuring stations is likely due to temperature since the end of the tunnel was consistently warmer during the observation period (Swinzow, 1970). The closure measurements clearly showed that artificial ventilation was inadequate to control the deformations within tolerable limits. In December, 1965 a vertical ventilation shaft was drilled at the end of the tunnel. Cold winter air created by the chimney effect lowered the temperature of the surrounding silt to -6.7°C and -10°C at distances of 0.61 m and 2.35 m from the tunnel wall. The colder tunnel wall temperature has subsequently reduced closure substantially.

McAnerney (1968) measured the vertical deformation of the tunnel at eight deformation points as shown in Figure 5.5(a). The readings plotted for one year commencing in April, 1966, are shown in Figure 5.5(b). The readings recorded by Swinzow in 1965 are superimposed on this plot. Note that the deformation is negligible after the ventilation shaft is opened and cold winter air enters the tunnel by natural convection.

Field observations of the USBM room were reported by Pettibone (1973). The USBM room was initially excavated 4.6 x 15.2 x 2.4 m high. In subsequent weeks 2.3 m was slabbed from each side to widen the room to approximately 9 m. The room was instrumented with vertical deformation points as excavation proceeded.

The instrumentation was designed to measure mass movement independent from parting. Floating points used to measure mass subsidence consisted of 1.8 m long steel rock bolts embedded in the roof in overbored holes. the parting was measured with a 152 mm wood dowel placed adjacent to the rock bolt. A 0.6 mm long rock bolt was permacreted into the bedrock floor directly underneath the rock bolt and wood dowel. Two thermocouple strings were installed in the roof and one in the wall.

The in-situ creep deformation versus time plot for one of the measuring points is shown in Figure 5.6. Deformation readings commenced in early February, 1969. Subsidence of the USBM room increased rapidly as the room was enlarged. Following excavation, the deformation rate dropped substantially. The room temperature up to mid-April was approximately -6.7°C. From mid-April to mid-July, 1969, the room temperature increased to about -3.3°C. The accompanying increase in deformation rate caused some thin slabbing near the back of the room. In early August, 1969, an insulated bulkhead was installed at Sta. 1+20. Following this the temperature increased rapidly and was maintained at approximately -2.2°C. The bulkhead was removed in early January, 1970. During the period the bulkhead was in place, the rate of floor to roof closure continually exceeded the closure between the floor and 1.8 m depth into the roof. Hydraulic props, installed as a safety precaution under portions of the roof that were scaling, continued to pick up load during this period indicating that they were picking up load from overall mass subsidence in addition to the dead load of the slab.

After the bulkhead was removed, the closure rate has decreased to approximately 1.5 cm/yr. This is consistent with the observations in the CRREL room. Colder average temperatures for the duration of observations in the USBM room resulted in less closure in this room than the CRREL room. In all, 30 cm of floor to roof deformation was recorded in 37 months with parting accounting for approximately 20% of total room closure. Several cracks were observed in the roof in April, 1970. Pettibone (1973) concludes that vertical separation and expansion of the formation account for the measured parting.

Thompson and Sayles (1972) reported the results of a finite element simulation of the closure of the USA CRREL room in the Fox Tunnel. Horizontal and vertical closure measurements were reported for one year. Laboratory samples were obtained from uniaxial creep testing.

The authors used the simple power law to predict the in-situ behavior of the room. They concluded that the form of the flow law predicted the in-situ behavior quite well. However, the back-calculated flow law predicted a creep rate 3.3 times faster than had been established in the laboratory on the same frozen silt. A few comments can be made regarding the analysis carried out by Thompson and Sayles (1972).

A two dimensional finite element analysis was used to model the room. The actual field configuration was three-dimensional. It is common practice to assume that sections within three tunnel diameters will be influenced by the end-restraint offered by the tunnel face. Both of the instrumented sections in this room are within this distance. The end effects of the room would delay the onset of in-situ steady-state creep.

There is a slight error involved in the boundary condition assumed along the gravel-bedrock interface. In their analysis, Thompson and Sayles (1972) assume the base of the gravel is free to translate in the horizontal direction due to a lean clay that is present immediately below the gravel-bedrock contact. The decomposed bedrock exposed at the base of the gravels in this room are perenially frozen and no excess segregated ice features were observed (Sellman, 1972). Thus, the clay would offer some frictional resistance which would decrease the predicted creep rate.

The form of the constitutive relationship of the placer gravels is questionable. The initial finite element simulations indicated that in-situ behavior of the room could not be predicted assuming constitutive models which exhibit continuously decreasing creep rate with time (Thompson and Sayles, 1972). The simple power law for the gravel was arrived at by a best fit to the actual field curves. The average density and moisture content of the gravel is 2.08 Mg/m^3 and 10%, respectively. Sellman (1972) described the gravel as retaining grain-to-grain contact with no massive ice forms present.

In light of the review of the constitutive behavior of frozen soils presented in Chapter 2, it would appear that the behavior of the frozen gravel will be governed by frictional response. Swinzow (1970) reported that a room excavated in cold, densly packed, permafrost till did not deform in excess of measurement error after 3 years of operation. Thus, depending on temperature, the in-situ deformation behavior of the gravel may be more accurately represented by elastic behavior or a creep law which is a function of confining pressure.

Examination of the laboratory creep data of the Fairbanks silt is necessary to establish whether a steady state condition did exist. Unconfined compression creep tests were performed on undisturbed samples of frozen Fairbanks silt obtained from the tunnel exposure. The test temperature was -1.7°C and the stress levels ranged from 245 kPa to 2100 kPa. A simple power law was fitted to the laboratory creep data with the following parameters:

$$\dot{\varepsilon} = 1.16 \times 10^{-9} \sigma^{-4} \qquad (5.1)$$

where the units for strain rate and stress are year^{-1} and kPa, respectively.

Thompson and Sayles (1972) reported strains in the laboratory typically in excess of 40% in 8 days. Tests performed by Savigny (1980) on ice-rich fine-grained glaciolacustrine clay showed that compatability at the soil-ice interface would not exist at strains of this magnitude. Thus, the minimum strain rates measured in the laboratory may well exceed the steady-state rate and the exponent of 4 is considered high.

A more detailed investigation of the U.S. Army CRREL Room was undertaken to gain further insight into the in-situ creep behavior of the frozen silt.

The horizontal and vertical closure of the USA CRREL room were monitored at two instrumented test sections, Sta. 1+83 and Sta. 2+02. The horizontal and vertical room deformations at each section were recorded between four closure points installed in the roof, walls and floor. Each point consisted of a 32 mm diameter wooden dowel embedded 0.3 m into the permafrost. A steel tape in conjunction with a steel ruler with an accuracy of 1.6 mm (1/16 inch) was used to measure the closure between opposing points in the walls, and roof and floor. In-situ ground temperatures were monitored by four strings of thermocouples installed at Sta. 1+96. The thermocouples were installed in the roof, floor and each side wall. The ground temperatures were recorded at 0.3 m intervals from the walls and roof to a total depth of 1.83 m.

The closure and temperature instrumentation could not be installed for three weeks after the room was excavated. An insulated bulkhead was installed at the entrance to the room (Sta. 1+81) approximately eight weeks after the initial closure and temperature readings were recorded. The purpose of this bulkhead was to maintain a constant room temperature thus minimizing the effect of seasonal fluctuations in air temperature on the permafrost temperature. Approximately 18 weeks later, a second bulkhead was installed by the USBM at Sta. 1+20 and subsequently removed five months after installation.

The vertical and horizontal closure measurement recorded at Sta. 1+83 and 2+02 in the USA CRREL room are shown in Figures 5.7 and 5.8, respectively. The in-situ ground temperatures measured in the roof and walls are also plotted in Figures 5.7 and 5.8. The vertical and horizontal closure rate determined from the closure versus time data (Figures 5.7 and 5.8) is shown in Figure 5.9. The closure observations were recorded for a period of 3.65 years.

The vertical and horizontal closure measurements increased rapidly during the first year of observations. This is probably due to the general warming trend in the surrounding permfrost as indicated by the temperature measurements. After removal of the USBM bulkhead at Sta. 1+20, the rate of closure decreased as a consequence of the cooler permafrost temperatures. The greatest vertical and horizontal movements were recorded at Sta. 2+02.

After 3 1/2 years of observations, 48 cm and 16.5 cm of vertical and horizontal movement, respectively, had taken place.

The temperature dependence on in-situ creep behavior is clearly illustrated by the vertical closure at Sta. 1+83. The first bulkhead was installed within .75 m of this instrumented section. The colder ambient air temperature just outside of the room would lower the permafrost temperature at Sta. 1+83. This would explain the slower vertical deformation rate at Sta. 1+83. From January, 1970 to October, 1972, the deformation readings indicate a steady-state closure rate at Sta. 1+83 at a velocity of 1 cm/yr. For the duration of this time interval the permafrost temperature has been maintained at an average value of -2.2°C.

The vertical closure at Sta. 2+02 shows much less sensitivity to changes in permafrost temperature brought about by installation and removal of the USBM bulkhead. At this section, the closure rate continued to attenuate with time for the entire period of time closure obsevations were recorded. During the final ten months of observations, the closure rate at Sta. 2+02 was 2.5 cm/yr.

The horizontal closure at Sta. 1+83 and 2+02 continued to accelerate for the first year movements were recorded. Following removal of the USBM bulkhead, the horizontal movements at Sta. 1+83 fluctuated seasonally with 1.3 cm of net closure being recorded for the final 2.5 years of observations. During the warm summer months and early fall, 1 to 2 cm of horizontal movement was recorded. Very little or negative closure was recorded during the cold winter months. Attenuation of the horizontal closure rate at Sta. 2+02 was observed for 1 year following removal of the USBM bulkhead. Seasonal fluctations have subsequently taken place. One centimetre of net horizontal closure was recorded during the final 1.7 years of obsevations.

A finite element simulation of the USA CRREL room was carried out using the programme CREEP. The purpose of this simulation was to assess the validity of the simple power low for ice as an upper bound solution for the in-situ creep deformations recorded in the frozen silt while the frozen placer gravels were treated as an elastic material.

The discretized continuum of the CRREL room used for this finite element simulation is shown in Figure 5.10. Only the Fairbanks silt and placer gravels were discretized. It was assumed that the competent bedrock floor would not contribute to vertical closure of the room. Only one half of the tunnel was analyzed due to symmetry. The thickness of overburden above the roof centerline was 16.9 m. The ground surface was assumed stress free. The two vertical boundaries were fixed by roller constraints which allowed movement in the vertical direction only. The base of the gravel was placed on roller constraints which allowed movement in the horizontal direction only as was done in finite element analysis carried out by Thompson and Sayles (1972). The elastic material properties of the frozen silt and gravel are given in Table 5.1.

The Young's Modulus values and unit weights were obtained from Thompson (1970). Creep properties of the silt and gravel were assigned the values of pure ice at -2°C (Morgenstern et al., 1980), i.e.:

$$\dot{\varepsilon} = 2.0 \times 10^{-8} \sigma^{3} \qquad (5.2)$$

where the units of stress and strain rate are kPa and yr^{-1}, respectively.

TABLE 5.1

ELASTIC MATERIAL PROPERTIES FOR FROZEN SILT AND GRAVEL FOX TUNNEL, ALASKA

PROPERTY	SILT	GRAVEL
Young's Modulus	346 MPa	718 MPa
Poissons' Ratio	.495	.450
Unit Weight	1.47 Mg/m^3	2.08 Mg/m^3

The nodal point labelled V in Figure 5.10 was chosen to represent the in-situ vertical closure points. The vertical displacement of node V was assumed to represent the total vertical closure since the closure point installed in the floor was fixed into bedrock.

The vertical steady-state velocity predicted by the programme CREEP using the simple power law given by equation 5.2 to model the creep behavior of the frozen silt was 1 mm/yr. The accummulated closure of the node point labelled H in Figure 5.10 after 2.5 years was 11 mm. The horizontal displacement of node H was assumed to be one half of the total hoizontal closure. The predicted results are at least one order of magnitude less than the in-situ measurements. The design of the instrumentation installed in the CRREL room was such that vertical separation in the ceiling could not be measured independently of total floor to ceiling closure. In the USBM room, 20% of the total room closure was due to parting in the ceiling. Thus, a portion of the total closure measured in the CRREL room is likely due to vertical separation in the ceiling.

In this case, the simple power law for ice does not represent a valid upper bound for the in-situ creep behavior of the frozen silt. However, examination of the closure rate versus time data presented in Figure 5.9 clearly shows that steady-state conditions did not exist during the first year of observations as assumed by Thompson and Sayles (1972). It is entirely possible that the overall closure measurements that were recorded consisted of both plastic and creep flow. Plastic flow in this sense refers to time-dependent failure of the frozen soil.

5.3 Assessment of In-Situ Deformation Behavior

The in-situ deformation studies of the Fox Tunnel reported by Swinzow (1970), Thompson and Sayles (1972) and Pettibone (1973) all showed that the deformations in the ice-rich Fairbanks silt became excessive when the room air temperature approached the ambient soil temperature of approximately -1.7°C. In each case, the room temperature was lowered to restrain the movements within tolerable limits.

The stress release in the ceiling of the USA CRREL room and the USBM room initiated by excavating the underlying frozen placer gravels is similar to that occurring in a soil mass located above a yielding trap door. In the past, it has been recognized that the behavior of a soil immediately above a flexible underground structure and that of a granular mass above a yielding bottom of a silo are equivalent for all practical purposes (Ladanyi and Hoyaux, 1969). This assumption allows arching or bin theory to be used to estimate the contact pressures between the ground and an underground structure.

The general expression for the pressure acting on the roof of a tunnel derived from arching theory is given by:

$$\sigma_v = \frac{B(\gamma - c/B)(1 - e^{-K\tan\phi D/B})}{K\tan\phi} \qquad (5.3)$$

where: σ_v = vertical contact pressure
B = half width of the zone of arching
(half width of the underground rooms in this case)
D = depth of the roof below the surface
γ = unit weight of soil above the roof
$c + \phi$ = shear strength parameters of the soil above the roof
K = ratio between vertical and horizontal stress

It is clear from the above expression that an underground opening located in a cohesionless material will not remain stable without additional ground support provided by a tunnel liner or timber lagging. For an unlined opening in a cohesive material, the following relationship must be satisfied:

$$c > B\gamma \qquad (5.4)$$

If the cohesion is less than $B\gamma$, the roof of the underground opening must be supported. For the USA CRREL room, values of $B = 2.44$ m and $\gamma = 1.47$ Mg/m^3 require a minimum cohesion of 35.1 kPa to ensure stability of the room.

Vialov (1962) proposed that the strength of a frozen soil can be represented by a series of Mohr-Coulomb failure envelopes, each one corresponding to a specific time to failure. The relationship between maximum shear and normal stress takes the form:

$$\tau(t) = c_t + \sigma_n \tan\phi_t \qquad (5.5)$$

where: $\tau(t)$ = shear strength at time = t
σ_n = maximum normal stress on shear plane
c_t, ϕ_t = cohesion and angle of internal friction, respectively (functions of time and temperature)

The time variation of the cohesion intercept, c_t, can be described by

$$c_t = \beta / \ln(t_f / B) \qquad (5.6)$$

where: β, B = experimentally determined material parameters
t_f = time to failure

Time and temperature have very little influence on the angle of internal friction.

The laboratory studies carried out to date indicate that the long term strength of frozen soil is frictional. The angle of internal friction can well be approximated by the effective friction angle for the same soil in an unfrozen state. For coarse-grained soils, the friction angle is relatively independent of temperature and strain rate. Frictional resistance is hindered by the presence of ice in ice-rich frozen soils. In very ice-rich soils which have very little grain-to-grain contact, the strength will be that of the ice and in the long term will approach zero.

The general nature of the failure envelopes for frozen soils is nonlinear. The time variation of the cohesion and angle of internal friction is reflected by the mutual distribution of each envelope. The inclination of each envelope represents the time variation of the angle of internal friction. The loss of cohesion with time is represented by the cohesion intercept of each envelope.

In predicting the time-dependent settlements for foundations in frozen soils, Ladanyi (1981) recognized that creep and consolidation can occur simultaneously in frozen soils containing large amounts of unfrozen water. Although the treatment of creep and consolidation as two distinct phenomena would seem appropriate for predicting delayed settlements in frozen soils, experimental limitations necessitate that these two phenomena be lumped together. Thus, frozen soil is treated as a quasi-single-phase medium with an empirically derived creep relationship. Recognizing that under certain conditions consolidation volume change may have a significant impact on the delayed settlement of a footing, Ladanyi (1981) studied the frozen soil's response to a stress increment with the aid of the Rendulic plot. These plots conveniently enable any given stress increment in a triaxial test to be separated into its hydrostatic and deviatoric components.

Interaction between strength and deformation is illustrated by considering a triaxial test on a normally consolidated sample of frozen soil containing three phases: mineral particles, ice and unfrozen water. The sample is initially in equilibrium at point O', Figure 5.11. A significant difference between frozen and unfrozen soil is that a total stress increment, $\Delta\sigma$, (O'A), can be applied to a frozen soil exceeding its long term strength. As the soil is allowed to deform under closed system conditions, the stresses are internally shared by the mineral particles and the pore filling. The unfrozen water can only support hydrostatic pressure. The shear stresses are supported by the mineral phase and temporarily by the ice. Since the ice phase supports a portion of the shear stress, the effective strength is mobilized only to point B'. The hydrostatic pressure generated by this straining, assumed to be equal in the ice and unfrozen water, is given by:

$$\Delta u_i = \Delta\sigma_{oct} - \Delta\sigma'_{oct} \qquad (5.7)$$

This is somewhat less than for the same soil in an unfrozen state. Similarly, the shear stress, $\Delta\tau_{oct,i}$, acting in the ice phase is given by:

$$\Delta\tau_{oct,i} = \Delta\tau_{oct} - \Delta\tau'_{oct} \qquad (5.8)$$

where: $\Delta\tau_{oct}$ and $\Delta\tau'_{oct}$ are the total applied shear stress increment and effective shear stress assumed by the soil, respectively.

Maintaining closed system conditions, the frozen soil will creep and the ice will gradually transfer its applied shear stress to the soil skeleton. The point B' will move along the effective stress path to mobilize full soil strength at B. Creep brings the ice closer to failure producing a loss of strength with time. The failure surface shrinks from its initial position at t=0 until failure occurs at point A at $t = t_A$. Since point A lies beyond the long term strength, creep failure will inevitably occur. The stresses at failure will be $\Delta\tau'_{oct}$ and $\Delta\sigma'_{oct}$ in the soil skeleton, Δu_i in the ice and unfrozen water and $\Delta\tau_{oct,i}$ in the ice.

Opening the system at point B' will initiate consolidation following the stress path B'A'. The total deformation of the soil will consist of consolidation and creep, occurring simultaneously. Full soil strength mobilization at point A' will depend on the rate of consolidation relative to the steady state creep rate.

The foregoing example of a triaxial specimen clearly showed that at least for short term conditions, the strength of the ice matrix can be relied on to support stress increments that exceed the soil's long term strength. However, the shape and position of the long term strength envelope must be known to clearly define the long term response of a frozen soil to an arbitrary stress increment.

In using the quasi-single phase approach, it is important that the stress paths followed in the laboratory to develop the constitutive equation coincide with those expected under field conditions. The stress paths shown in Figure 5.11 are for an axially symmetric stress state which would be suitable for calculating the time dependent response of the frozen soil underneath a circular footing. Under conditions of plane strain, such as the stress state in the soil mass surrounding an underground opening, the use of a simple stress space in which the coordinates are the vertical and horizontal principal stresses would be more appropriate. This arises from the fact that the intermediate principal stress is generally unknown.

The stress paths shown in the Rendulic plot, Figure 5.11, have been replotted in a vertical and horizontal stress space as shown in Figure 5.12. In this plot, the stress paths for undrained extension tests are also shown. The deviatoric stress is given by either the vertical or horizontal distance between the point characterizing the stress state and the hydrostatic pressure line, $\sigma'_V = \sigma'_H$.

Although a clear understanding of effective stress changes in a frozen soil during shear has not been developed to date, Ladanyi's (1981) conceptualization provides a useful framework to study the response of a frozen soil to a stress increment. The interaction between strength and deformation will shed some light on the in-situ deformation behavior of the CRREL room in the Fox Tunnel.

Excavation of an underground opening will initiate deformation in the soil mass surrounding the opening. Considering the CRREL room at the Fox Tunnel, the ice-rich silt comprising the roof will deform much more readily than the frozen dense gravel forming the walls. Downward movement of the unsupported ceiling must now be resisted by shear stresses that develop at the interface between the yielding and stationary soil mass.

Before excavation of the USA CRREL room, the vertical stress along the ice-rich silt/gravel contact was equal to the overburden pressure. After excavation, the vertical stress along the ceiling of the room is zero. This stress release is accompanied by a corresponding increase in stress in the adjoining soil mass above the frozen gravel. Considering the two elements shown in Figure 5.13(a), the stress in element A will be a small fraction of what it was before excavation commenced. The vertical pressure in element B will have to increase by the same amount to maintain equilibrium. The horizontal stress these two elements exert upon each other must remain equal and opposite. The induced shear stress at the interface between elements A and B will cause a rotation of the principal stresses above the tunnel supports.

Although the actual stress paths followed by the soil elements surrounding a rectangular opening are quite complicated, some insight into the interaction between strength and deformation of frozen soil may be gained by studying the simple stress paths shown in Figure 5.13(b). The stress release in element A is given by the stress path O'A while an equal but opposite stress increment is applied to element B, ie. path O'B. As shown in the figure, the stress release in element A exceeds the long term $\sigma_H > \sigma_V$ failure line. However, an equal stress increase in element B lies below the long term $\sigma_V > \sigma_H$ failure line.

This simplified stress path description clearly shows the importance of considering the stress path in selecting an appropriate constitutive relationship for predicting the initial time dependent response of the frozen soil surrounding an underground opening. Since the stress increase in the soil above the gravel does not exceed the soil's long term strength, the creep behavior may well continue to attenuate with time. On the other hand, the soil above the roof of the Tunnel that experiences a stress release that exceeds the soil's long term strength will creep at either a steady state or decreasing rate. The creep rate will depend on the relative position of the stress point A with respect to the service life strength, envelope for the frozen soil under consideration. Failure will inevitably occur for the purely frictional long term strength shown in Figure 5.13(b).

Evidence of the frozen silt approaching failure can be inferred from the vertical closure rate versus time plot at Sta 1+ 83. Installation of the USBM bulkhead at Sta 1 + 20 increased the permafrost temperature at Sta.

1+83. The warmer soil temperatures resulted in a 50% increase in vertical closure rate at Sta. 1+83 over a period of three months. A portion of the increase is due to the temperature dependence of creep. However, the warmer soil temperatures will increase the unfrozen water content of the frozen silt. Increasing a frozen soils unfrozen moisture content will shrink the delayed failure surface from its original position (ie. instantaneous or short term strength) towards the long term failure line. The soil temperature becomes cooler following removal of the USBM bulkhead at Sta. 1+20. As the soil temperature decreases, its failure surface expands towards the instantaneous strength. Thus, a numerical prediction of the insitu deformation behavior of the CRREL room would have to account for temperature dependent creep properties and a temperature and time dependent failure criterion governing the strength of the frozen soil.

The vertical deformation instrumentation installed in the CRREL and USBM rooms at the Fox Tunnel was not able to measure vertical deformations in the gravel walls independently of the overall vertical closure of the room. The arching support provided by the overlying silt (due to the stress release above the roof) will increase the vertical stress in the frozen gravel walls in the vicinity of the room. The increase in vertical stress coupled with a horizontal stress release brought about by excavating the room will significantly increase the shear stress in the frozen gravel. The build up of shear stress in the frozen gravel walls will lead to time dependent deformations occurring in the gravel that may eventually lead to delayed failure.

Thompson and Sayles (1972) incorporated a yield criterion in their finite element program to account for plastic yield of the material. In their analysis, the effective stress as defined by Odqvist (1966) was used as the yield criterion. After each creep increment, the effective stress for each element was checked to determine whether it had exceeded a given stress level. Plastic deformations were allowed to take place in all elements that exceeded the given yield stress. It is interesting to note that when the in situ creep behavior of the frozen silt and gravel was governed by primary creep, plastic yielding was initiated in the gravel walls. The elastic-plastic analysis carried out by Thompson and Sayles (1972) indicate that a catastrophic failure would occur which lead the authors to conclude that the long term strength of the frozen silt and gravel was zero and that the in situ creep behavior was more accurately represented by a steady-state creep relationship.

The use of effective stress for a failure criterion is over-simplified. Numerous studies have shown that the strength of frozen soil is governed by a Mohr-Coulomb failure law where the shape of the failure envelope depends on soil type, density, ice saturation, temperature and strain rate. The strength of the gravel will most certainly be governed by a Mohr-Coulomb failure envelope.

It is possible that the frozen gravel was approaching the failure envelope and experiencing large vertical strains during the period of time the soil temperatures increased while USBM bulkhead was in place at Sta 1+20. Thus, vertical displacements in the gravel walls may be superimposed on to vertical creep displacement in the frozen silt to give the total room closure as recorded by Thompson and Sayles (1972). The strain rate measured in the laboratory is independent of the vertical deformations, in the gravel walls. This is very likely why the creep equation which gave the best fit to the observed room closured yielded a strain rate 3.3 times greater than the strain rate measured in the laboratory.

5.5 Underground Circular Cavities in Permafrost

Major design considerations of tunnels in frozen ground are stand-up time, change in diameter of the unlined opening with time and the change in pressure on the tunnel liner with time. The first two factors will influence the decision on whether or not to support the underground opening with a tunnel liner. The third factor will provide guidelines for dimensioning the tunnel liner. A small parametric study of shallow circular tunnels in frozen ground was carried out to study closure phenomena and the stress changes in the frozen soil surrounding the opening.

The first part of this study deals with the closure behavior of an unlined circular opening excavated at various depths in warm ice-rich permafrost. The warm ice-rich permafrost was chosen as the host soil medium as it would present an upper bound for the closure rates. A circular opening was chosen since it is more amenable to simpler analysis under certain conditions.

The height to diameter (H/D) ratios of the circular openings varied from 1.5 to 4.0. The finite element mesh for H/D=2.0 is shown in Figure 5.14. A homogeneous soil profile was assumed for all analysis. Material properties were assigned on the basis of data reported in the literature.

The flow law for frozen soil used in this study was:

$$\dot{\varepsilon} = 2.0 \times 10^{-8} \sigma^{3} \qquad (5.9)$$

This flow law is identical to the flow law for ice at -2°C (Morgenstern et al., 1980) and represents a valid upper bound to the in-situ creep behavior of fine-grained, ice-rich frozen soils of the Mackenzie River Valley, N.W.T.

A plot of the closure velocity versus depth of overburden for the crown, springline and invert of the tunnel is shown in Figure 5.15. The depth of overburden in this figure is expressed non-dimensionally as the H/D ratio. For all three points considered, the closure rate increases with the depth of overburden. Also, the downward movement of the crown is greater than the upward movement of the invert creating a sag in the roof. Thus, for shallow tunnels, the initial circular cross section undergoes a transition to an oval shape as the frozen soil creeps inward. At greater depths, this transition will be less pronounced because the relative change in overburden stress from crown to invert will be smaller. Based on these preliminary results, it would appear that a circular opening located 9 to 10 diameters below the surface would behave axisymmetrically. This is somewhat deeper than a circular opening in an elastic soil or rock.

Velocity vectors depicting magnitude and direction throughout the region analyzed for H/D=2.0 and H/D=3.0 are shownin Figures 5.16 and 5.17, respectively. The relative magnitude in these figures is given by the length of the line segment. For both tunnel depths, the frozen soil flows in towards the opening. The transformed cross section is shown on a grossly exaggerated scale by the dashed line joining the velocity vectors around the periphery of the opening.

Contours of effective strain rate for H/D=2.0 and H/D=3.0 are shown in Figures 5.18 and 5.19, respectively. Although the magnitude of individual strain rate components are not given by the effective strain rate, the contours serve the purpose of indicating where the high strain rate gradients exist. The greatest effective strain rate gradients directly above the crown of the opening and diminish as one sweeps around from the crown to the invert. Higher gradients exist for the tunnel located at H/D=3.0 (see Figure 5.19) indicating that the disturbing influence of the ground surfaces decreases with deeper tunnels. Both Figures 5.18 and 5.19 show the high strain rate gradients extend only 1.5 to 2 tunnel diameters above the crown of the opening. This zone of influence will decrease with deeper tunnels.

It was clear from the foregoing analyses that shallow circular cavities located in warm ice-rich permafrost would become unstable unless some measures were undertaken to arrest the deformations. The second part of this study dealt with the closure of a lined circular opening in permafrost. Only one opening located 2 diameters below the surface was analyzed. The same finite element mesh as shown in Figure 5.14 was used except that a narrow ring of elements was added to the periphery of the opening to simulate a 100 mm thick concrete liner. The geometry is shown in Figure 5.20.

This analysis was carried out by calculating the elastic gravity stress field surrounding the circular opening without the liner elements present. After this step, the elements representing the tunnel liner were added to the geometry and the creep solution was initiated. It was felt that this sequence would be more representative of actual construction operations.

The velocity vector diagram for the lined tunnel placed 2 diameters below the ground surface is shown in Figure 5.21. As shown in the figure, the tunnel liner plays a significant role in altering the velocity distribution in the frozen soil surrounding the opening. The overall movement of the soil mass and tunnel opening is downward due to gravity stress. In the vicinity of the tunnel, the creeping frozen soil is deflected around the tunnel since its stiffness is much greater than that of the frozen soil. The velocity profile is a function of the stiffness properties of the tunnel liner. The tunnel liner also serves to drastically reduce the downward velocity of the crown of the tunnel. In this case, the crown velocity is reduced by 3 orders of magnitude for a tunnel at the same depth with no liner present.

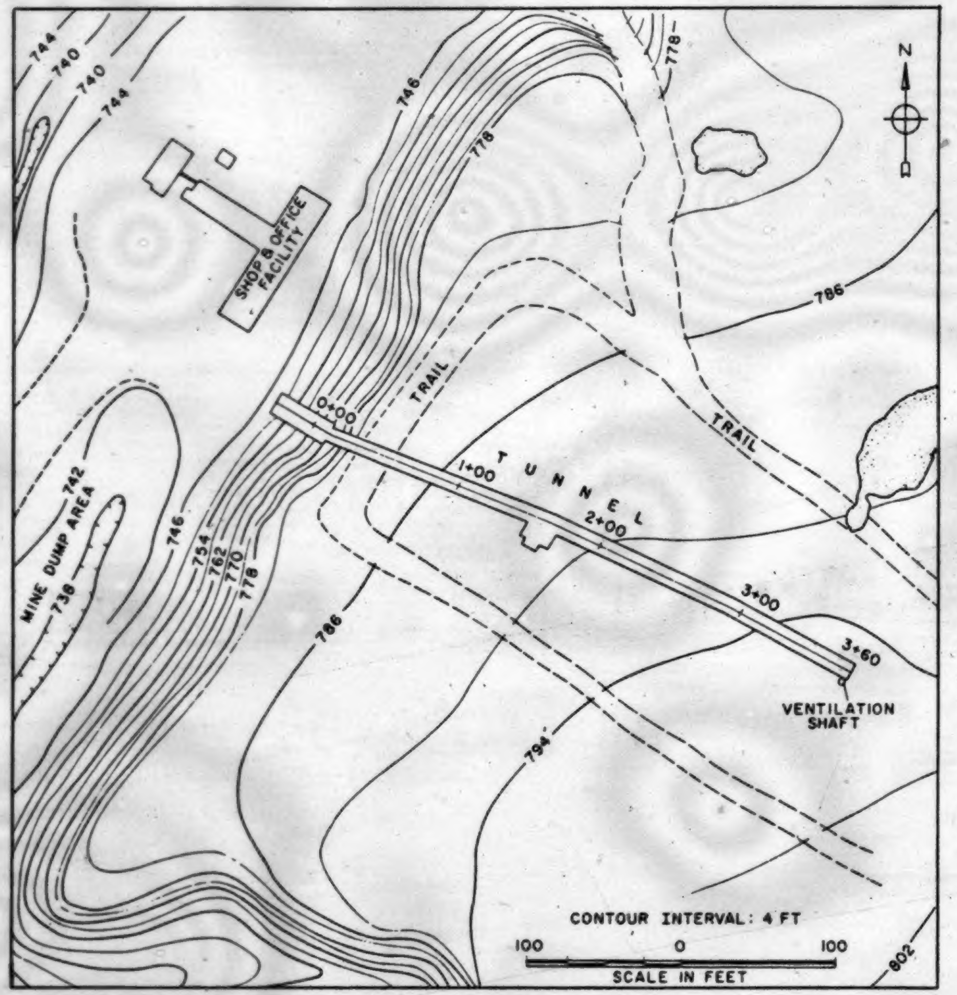
744
740
740
744
SHOP & OFFICE FACILITY
746
778
778
786
TRAIL
0+00
TRAIL
1+00
TUNNEL
2+00
3+00
3+60
VENTILATION SHAFT
742
MINE DUMP AREA
738
746
754
762
770
778
786
794
802
N
CONTOUR INTERVAL: 4 FT
100
0
100
SCALE IN FEET

FIGURE 5.1 SITE PLAN OF FOX TUNNEL SITE, ALASKA (Sellman, 1967)

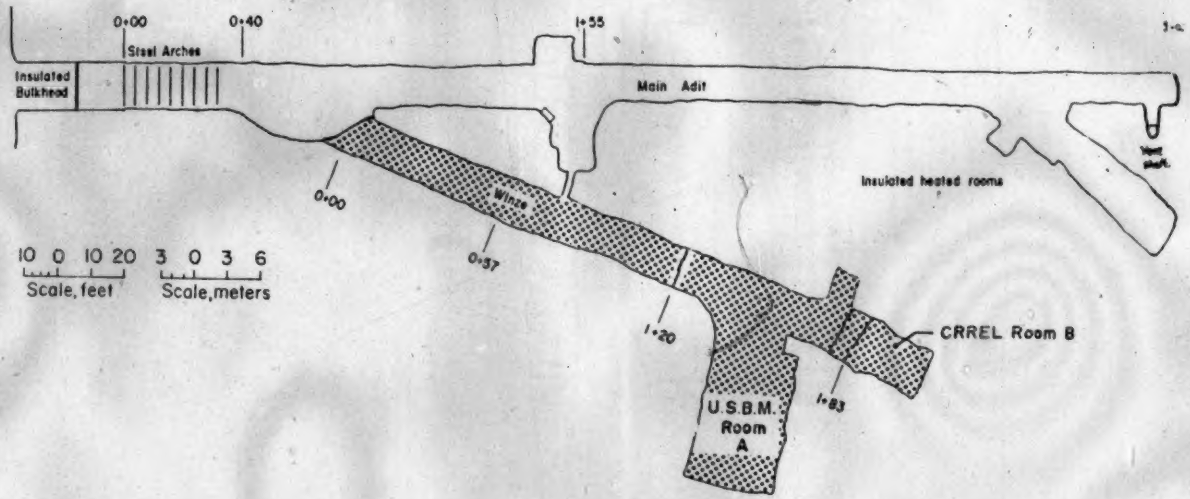
0+00
0+40
1+55
Steel Arches
Insulated Bulkhead
Main Adit
Vent shaft
Insulated heated rooms
0+00
Winze
0+37
1+20
1+83
CRREL Room B
U.S.B.M. Room A
10 0 10 20
Scale, feet
3 0 3 6
Scale, meters

FIGURE 5.2 PLAN FOF FOX TUNNEL SHOWING SECOND STAGE OF EXCAVATION (Pettibone, 1973)

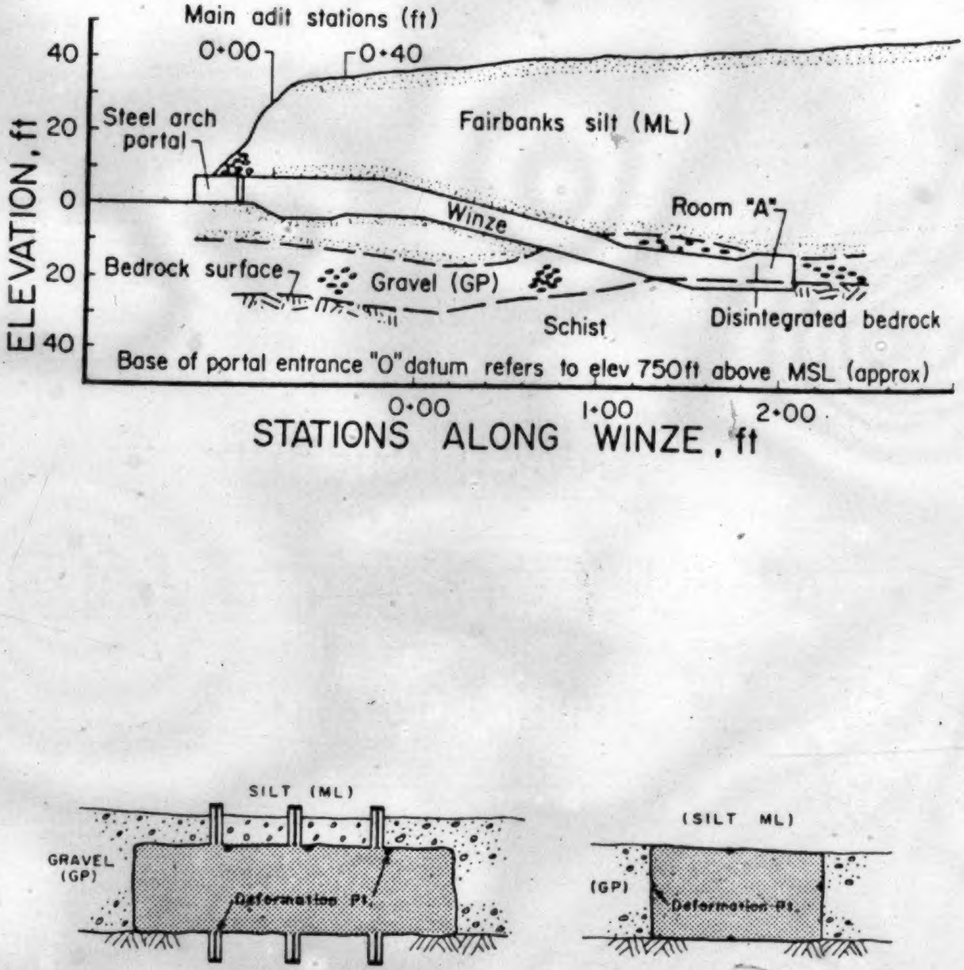
Main adit stations (ft)
0+00
0+40
Steel arch portal
Fairbanks silt (ML)
Room "A"
Winze
Bedrock surface
Gravel (GP)
Schist
Disintegrated bedrock
Base of portal entrance "0" datum refers to elev 750ft above MSL (approx)
ELEVATION, ft
40
20
0
20
40
0+00
1+00
2+00
STATIONS ALONG WINZE, ft
SILT (ML)
GRAVEL (GP)
Deformation Pt.
(SILT ML)
(GP)
Deformation Pt.

TYPE. SECT. USBM ROOM
(Looking east)

TYP. SECT. USA CREEL ROOM

FIGURE 5.3 GEOLOGIC CROSS SECTION, FOX TUNNEL SITE (Pettibone, 1973)

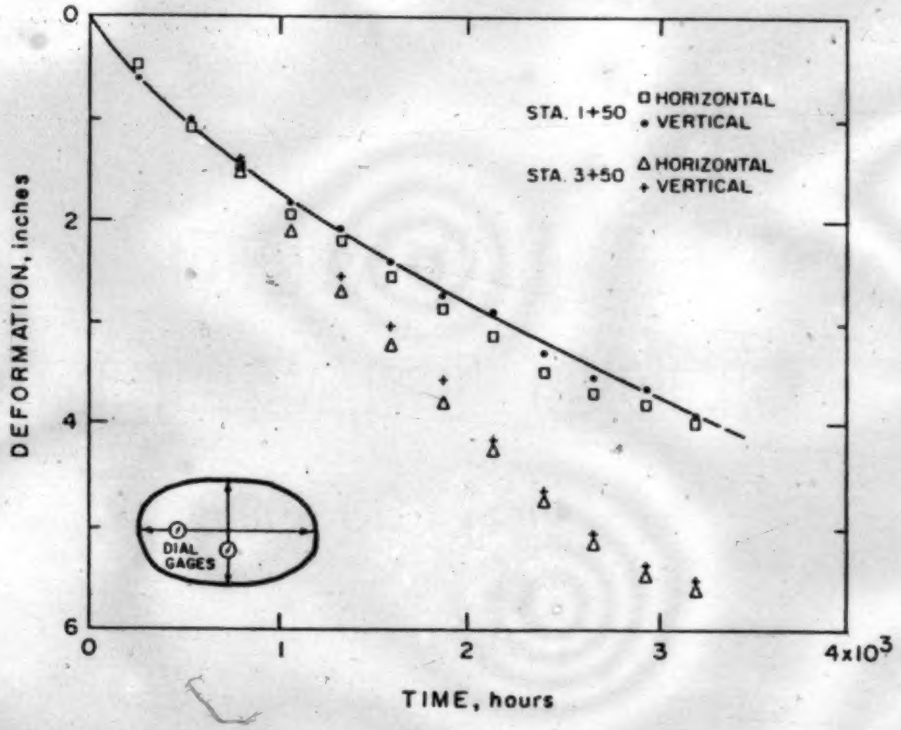

FIGURE 5.4 CLOSURE MEASUREMENTS OF MAIN TUNNEL FOLLOWING 1965 CONSTRUCTION SEASON (Swinzow, 1970)

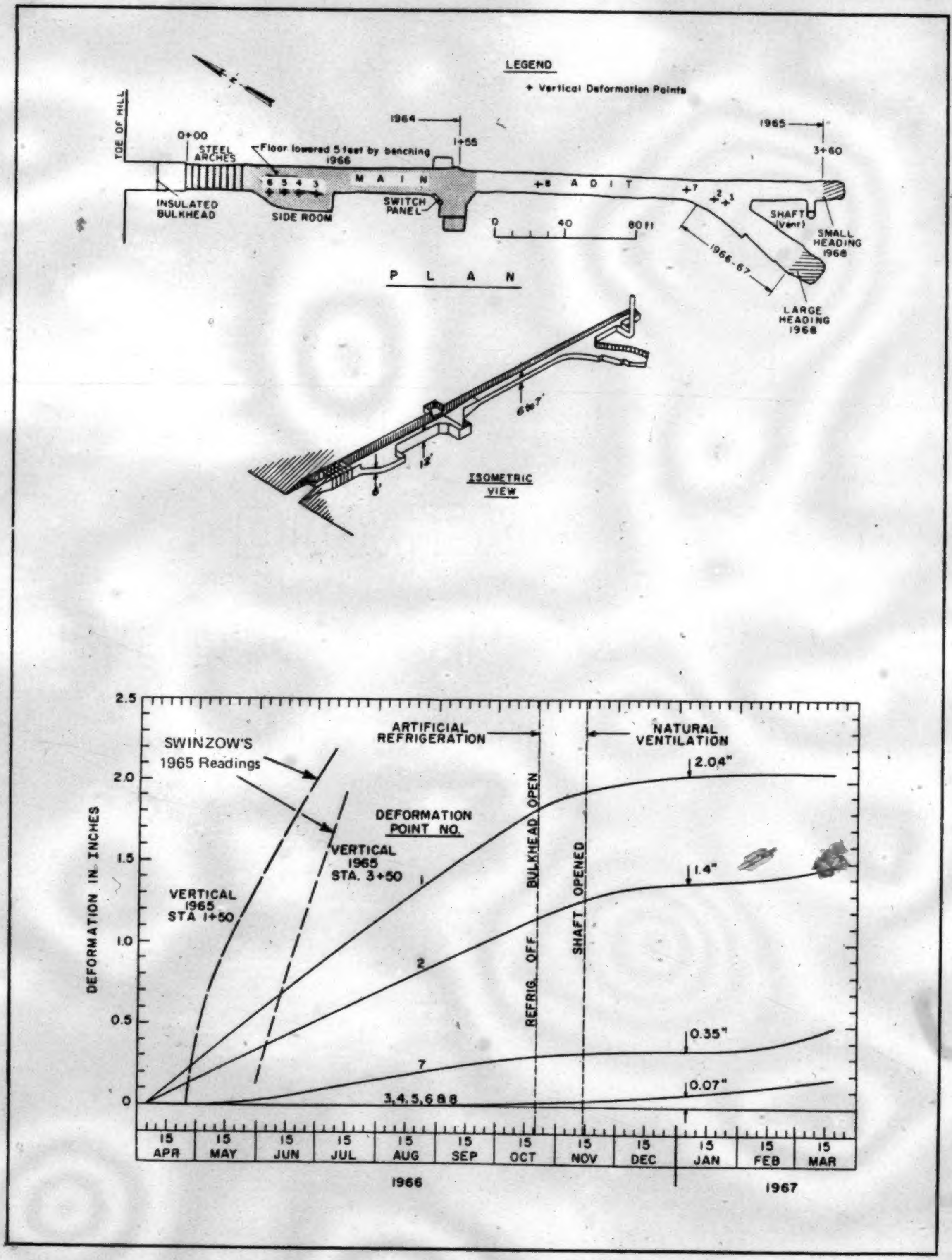

FIGURE 5.5 CLOSURE MEASUREMENTS OF MAIN TUNNEL FOLLOWING 1965 CONSTRUCTION SEASON (McAnerney, 1968)

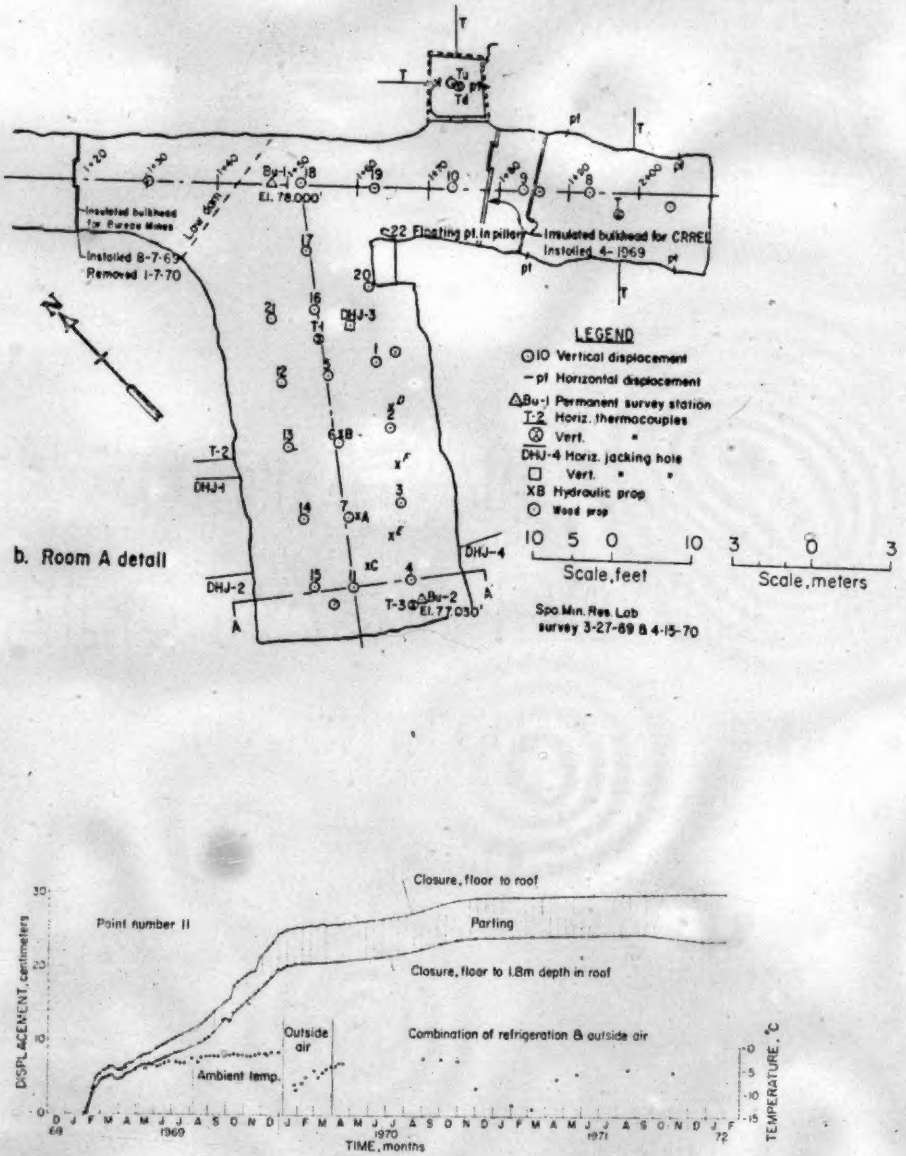
T
Tu
Td
pt
Bu-1
El. 78.000'
Low dam
Insulated bulkhead for Bureau Mines
Installed 8-7-69
Removed 1-7-70
22 Floating pt. in pillar
Insulated bulkhead for CRREL
Installed 4-1969
N
DHJ-3
T-1
T-2
DHJ-1
DHJ-2
DHJ-4
T-3
Bu-2
El. 77.030'
A
A'
xA
xB
xC
xD
xE
xF
LEGEND
10 Vertical displacement
pt Horizontal displacement
Bu-1 Permanent survey station
T-2 Horiz. thermocouples
Vert.
DHJ-4 Horiz. jacking hole
Vert.
XB Hydraulic prop
Wood prop
10 5 0 10
Scale, feet
3 0 3
Scale, meters
Spo. Min. Res. Lab survey 3-27-69 & 4-15-70
Point number 11
Closure, floor to roof
Parting
Closure, floor to 1.8m depth in roof
Outside air
Combination of refrigeration & outside air
Ambient temp.
DISPLACEMENT, centimeters
TEMPERATURE, °C
0
10
20
30
-0
-5
-10
-15
D J F M A M J J A S O N D J F M A M J J A S O N D J F M A M J J A S O N D J F
68
1969
1970
1971
72
TIME, months

b. Room A detail

FIGURE 5.6 VERTICAL CLOSURE OF USBM ROOM IN THE FOX TUNNEL (Pettibone, 1973)

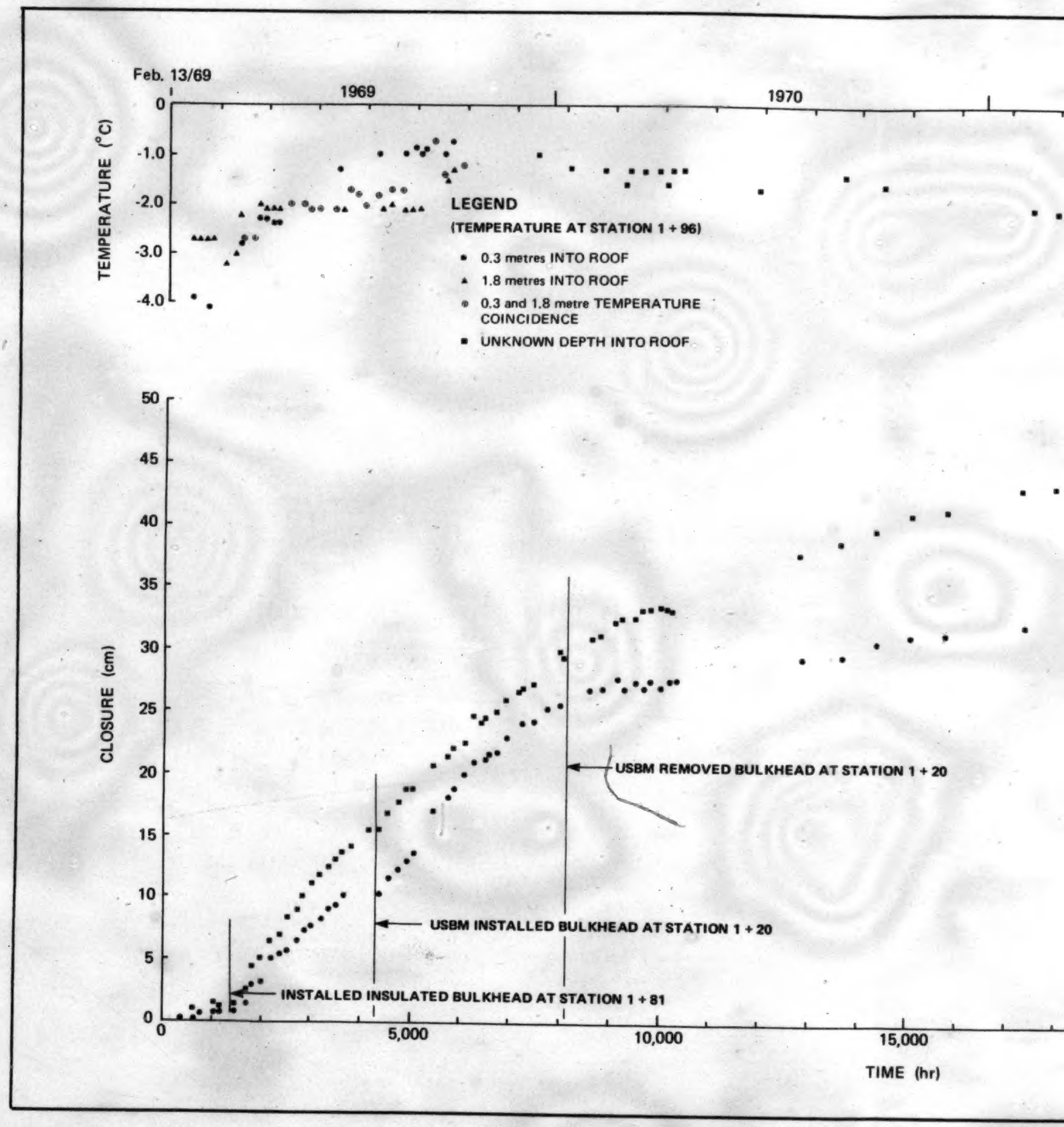

1 OF

FIGURE 5.7 VERTICAL CLOSURE OF USA CRREL ROOM

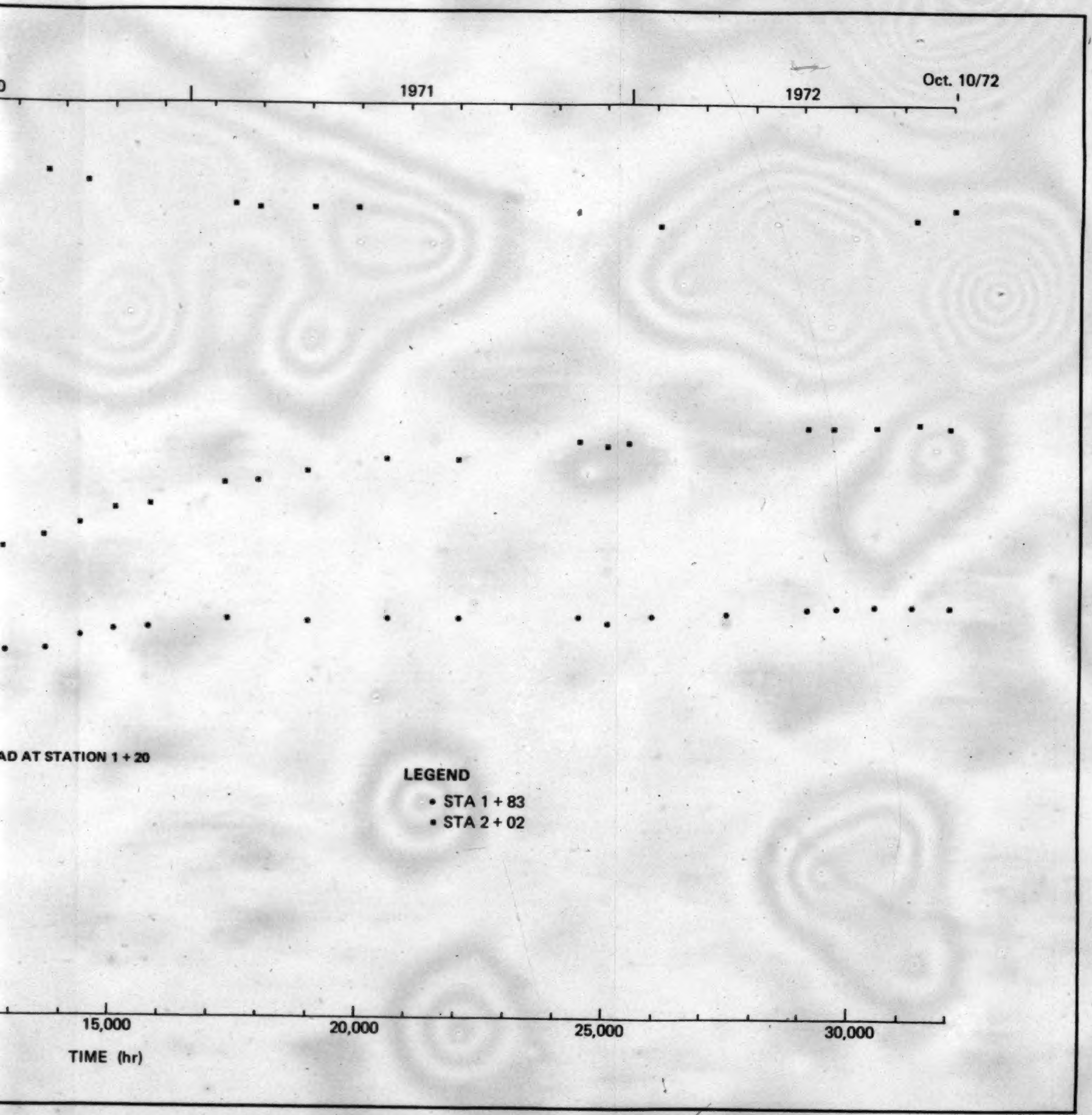

OSURE OF USA CRREL ROOM IN THE FOX TUNNEL

2 OF 2

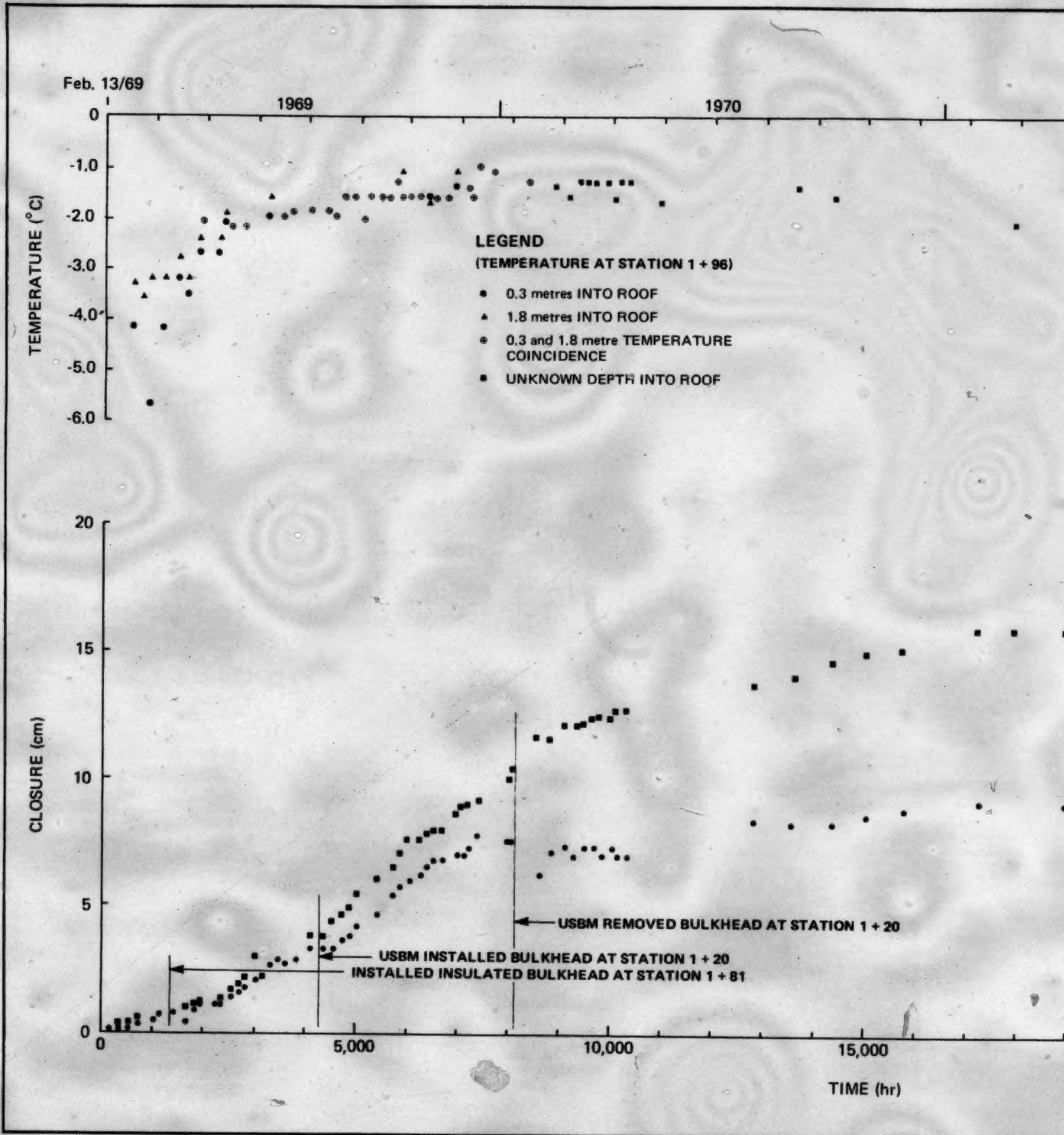

FIGURE 5.8 HORIZONTAL CLOSURE OF USA CRRE
FOX TUNNEL, ALASKA

1 OF

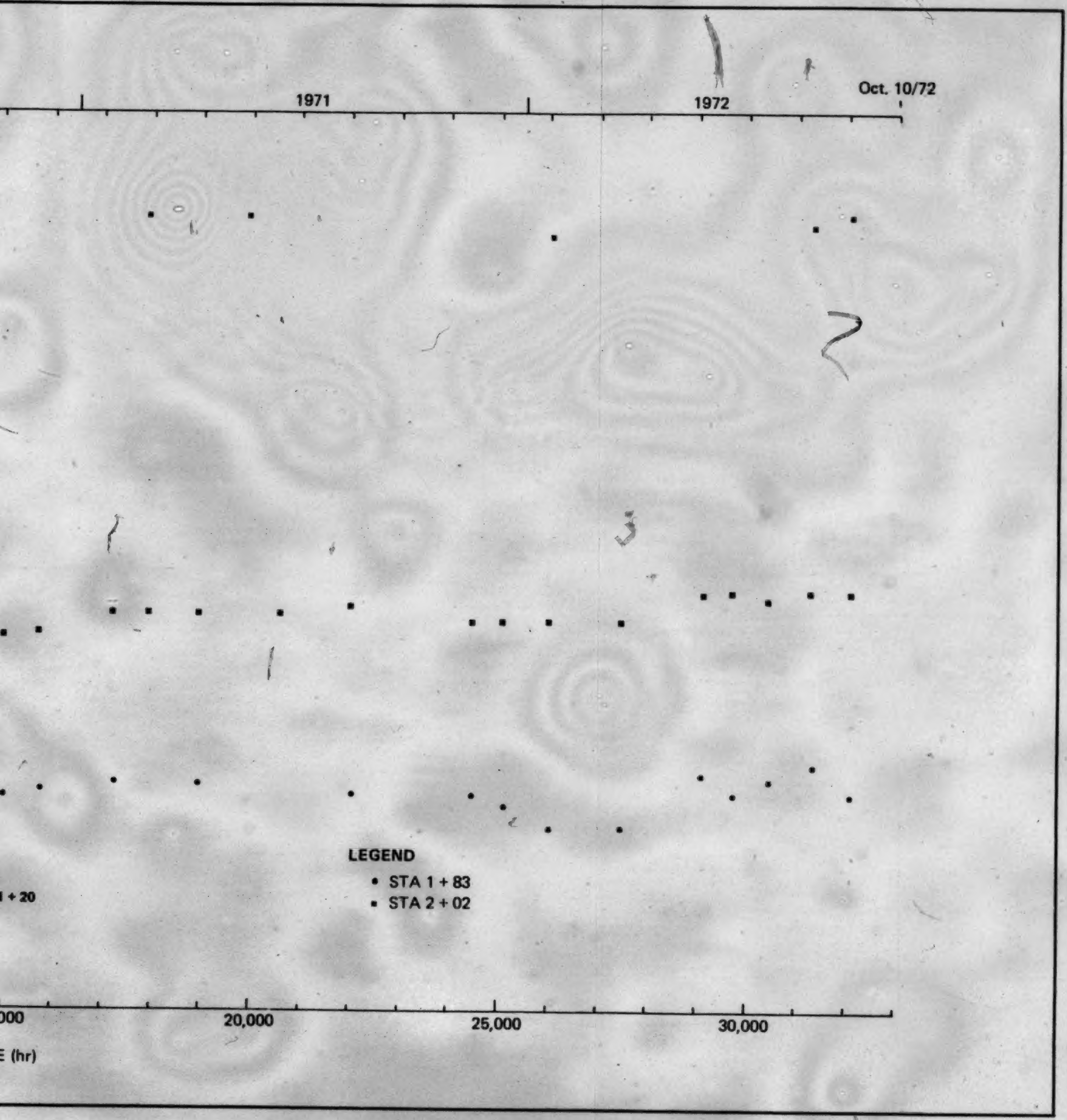

OSURE OF USA CRREL ROOM IN THE
LASKA

2 OF 2

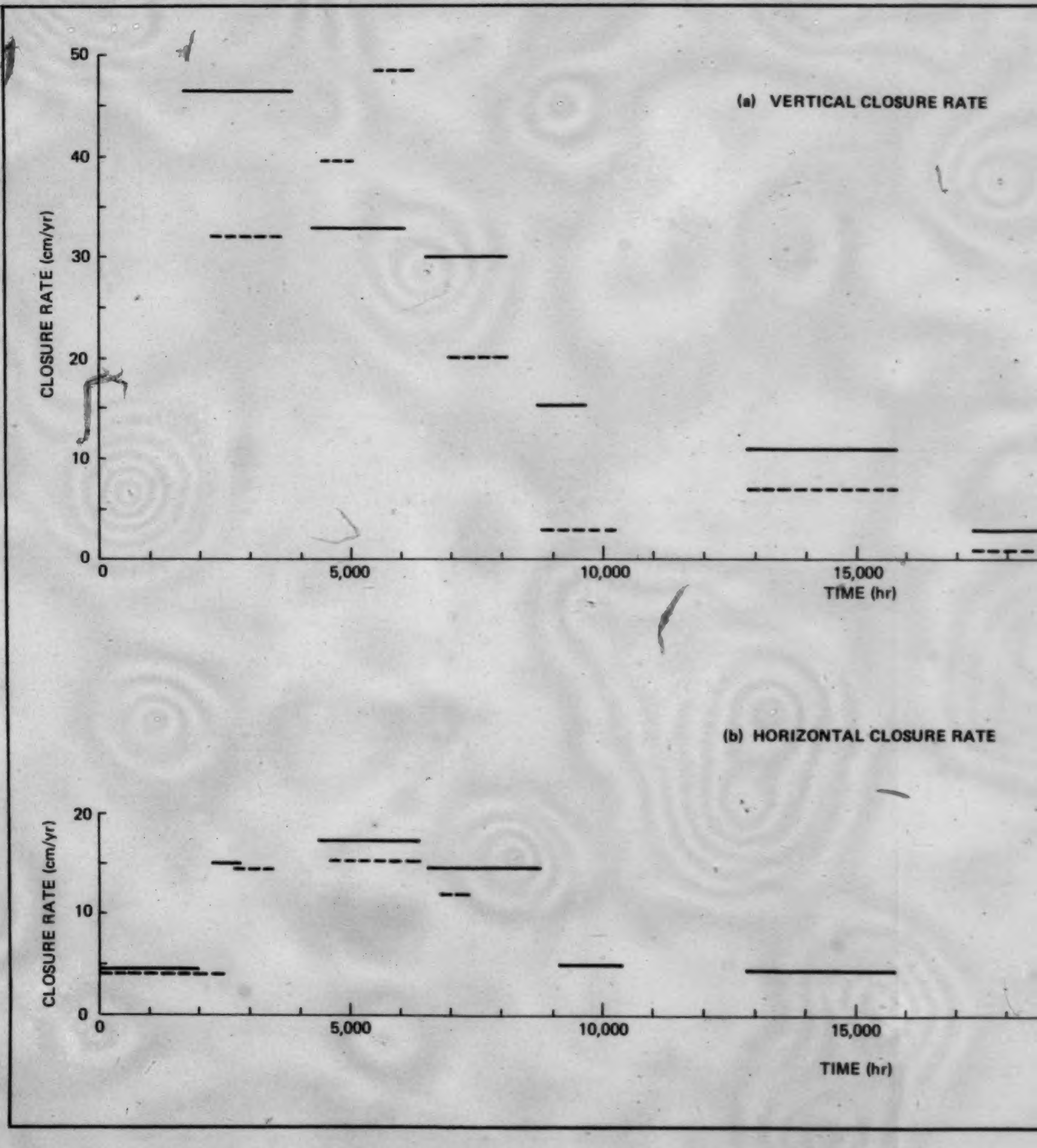

FIGURE 5.9 VERTICAL AND HORIZONTAL CLOSURE RAT
IN THE FOX TUNNEL, ALASKA

1 OF

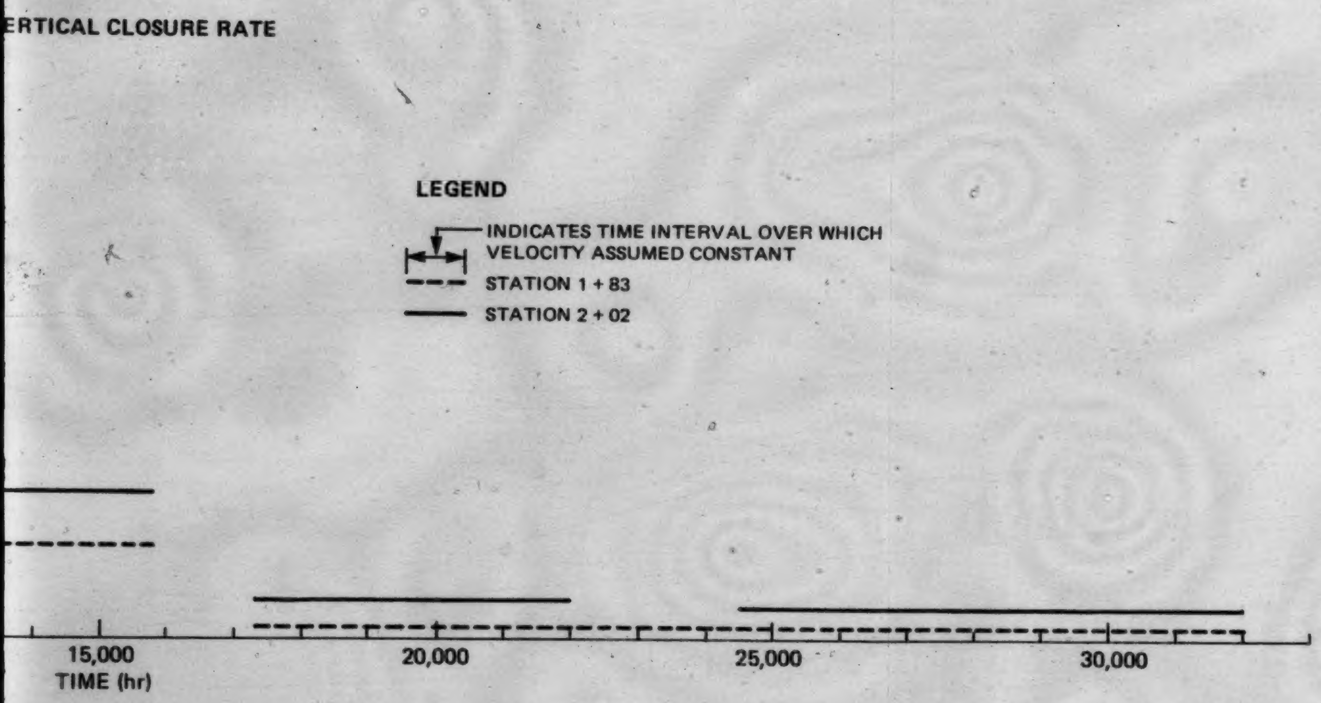

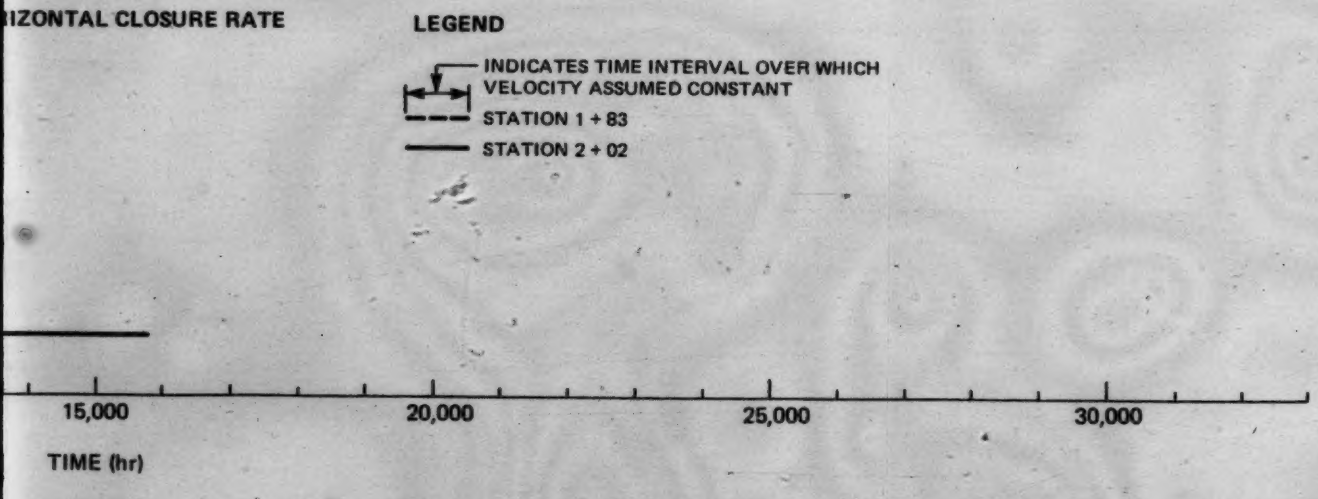

RIZONTAL CLOSURE RATE OF USA CRREL ROOM
EL, ALASKA

2 OF 2

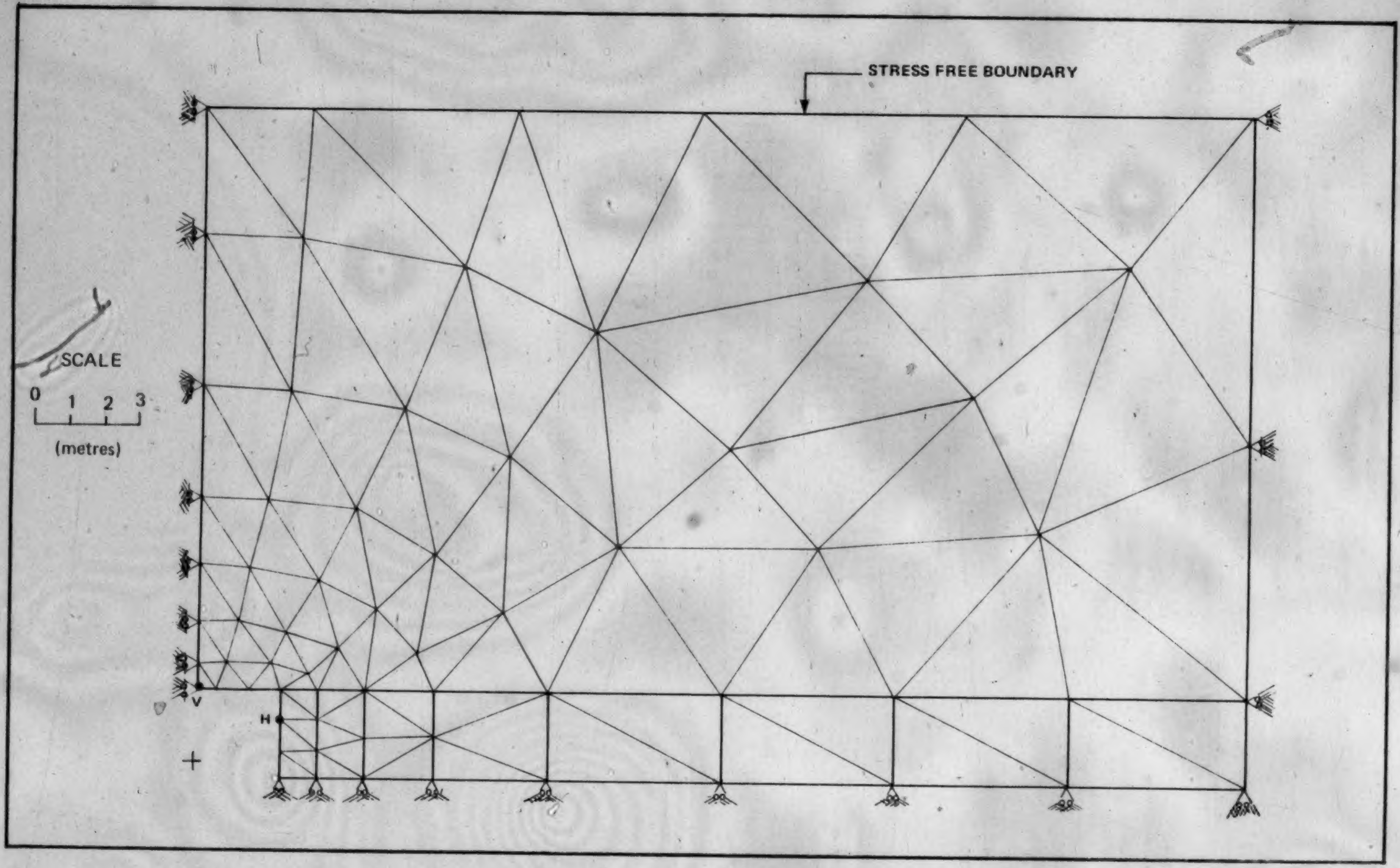
STRESS FREE BOUNDARY
SCALE
0 1 2 3
(metres)
V
H
+

FIGURE 5.10 FINITE ELEMENT DISCRETIZATION OF USA CRREL ROOM IN THE FOX TUNNEL

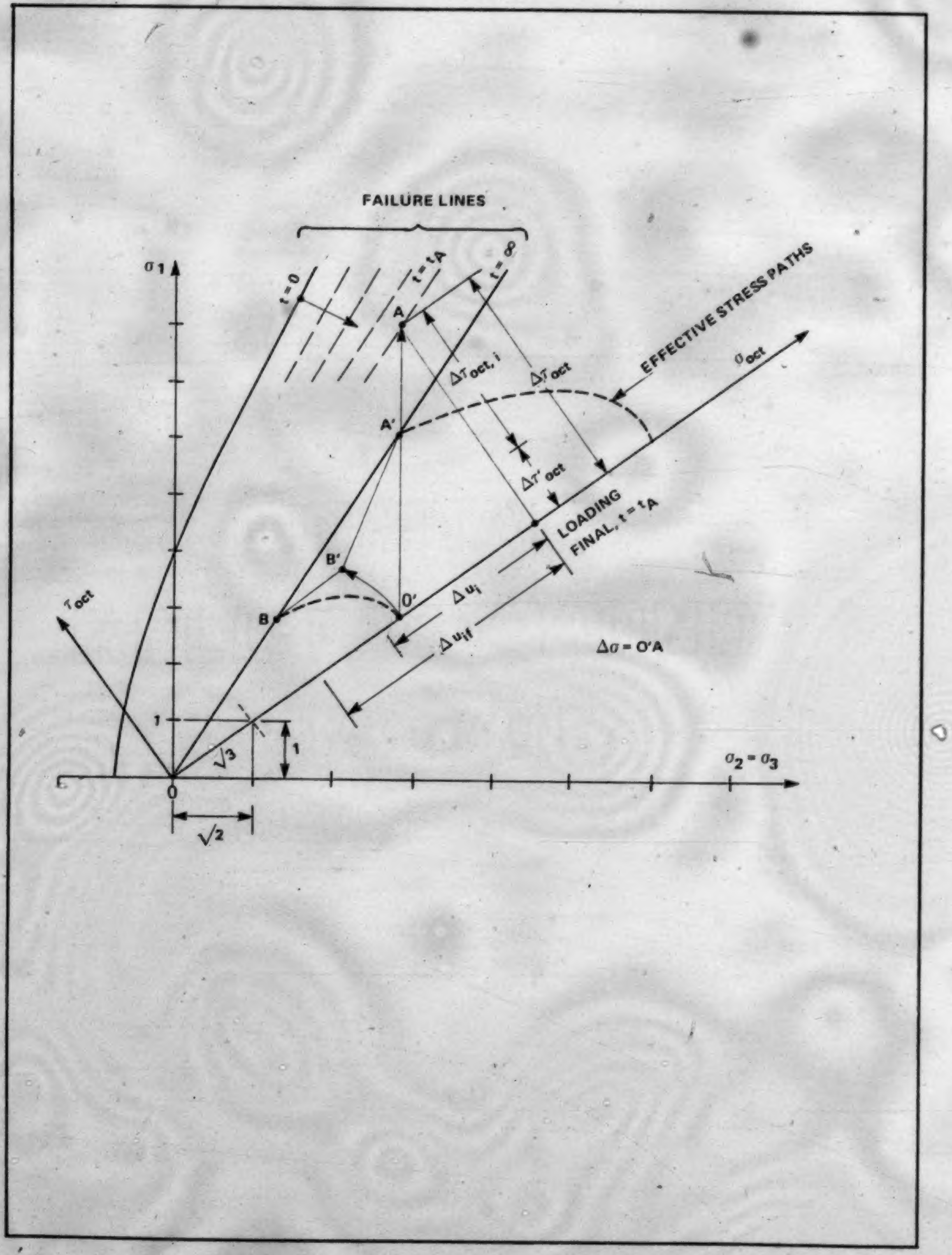
FAILURE LINES
t = 0
t = t_A
t = ∞
σ1
A
A'
B'
B
O'
EFFECTIVE STRESS PATHS
σoct
Δτoct, i
Δτoct
Δτ'oct
LOADING
FINAL, t = t_A
Δui
Δuif
Δσ = O'A
τoct
1
√3
1
0
√2
σ2 = σ3

FIGURE 5.11 RENDULIC PLOT OF NORMALLY CONSOLIDATED PLASTIC FROZEN SOIL STRESSED BEYOND ITS LONG TERM STRENGTH (Ladanyi, 1981)

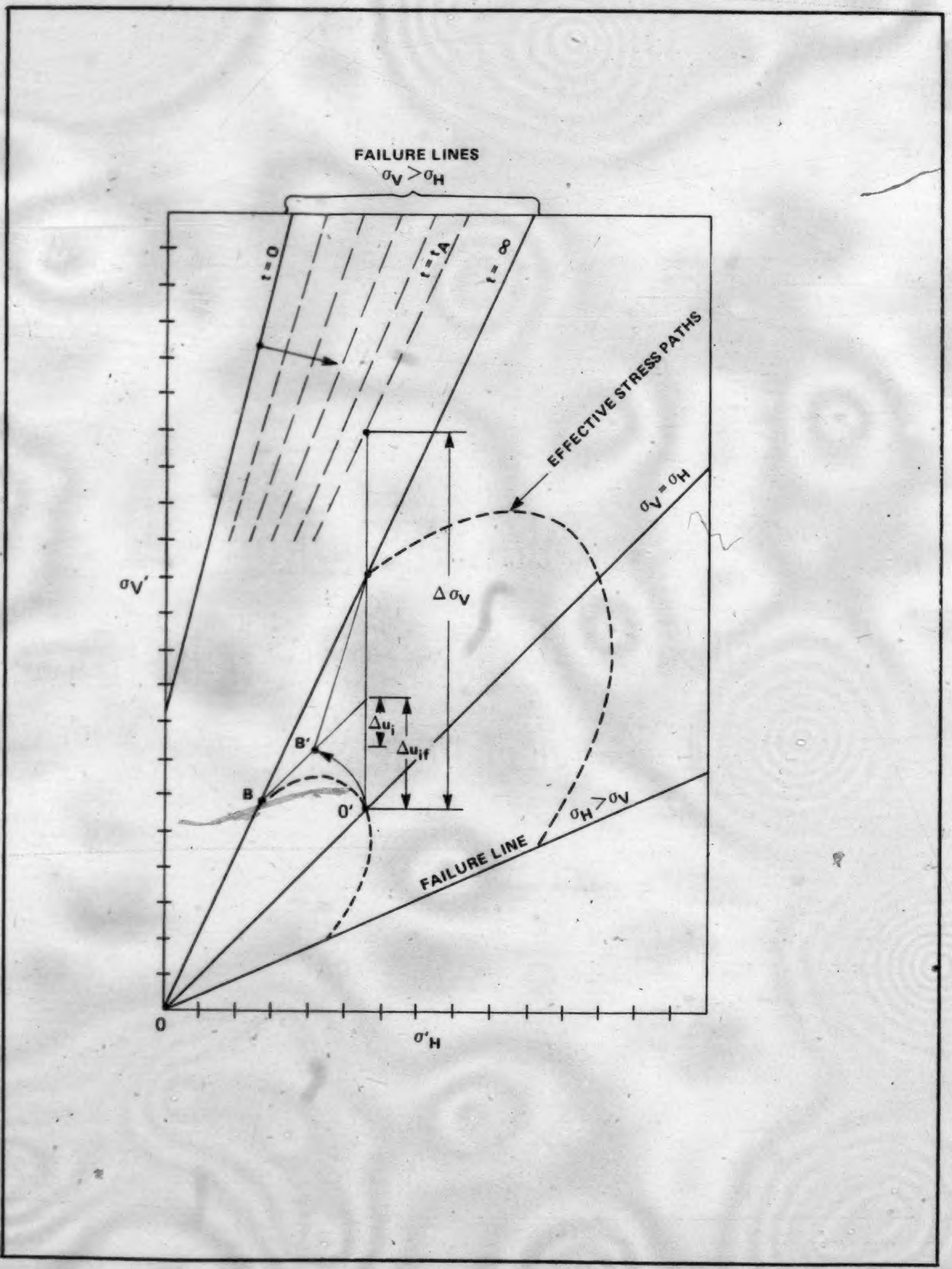
FAILURE LINES
σV > σH
t = 0
t = tA
t = ∞
EFFECTIVE STRESS PATHS
σV = σH
σV'
Δ σV
Δui
Δuif
B
B'
O'
σH > σV
FAILURE LINE
0
σ'H

FIGURE 5.12 STRESS PATHS FOR NORMALLY CONSOLIDATED PLASTIC FROZEN SOIL STRESSED BEYOND ITS LONG TERM STRENGTH

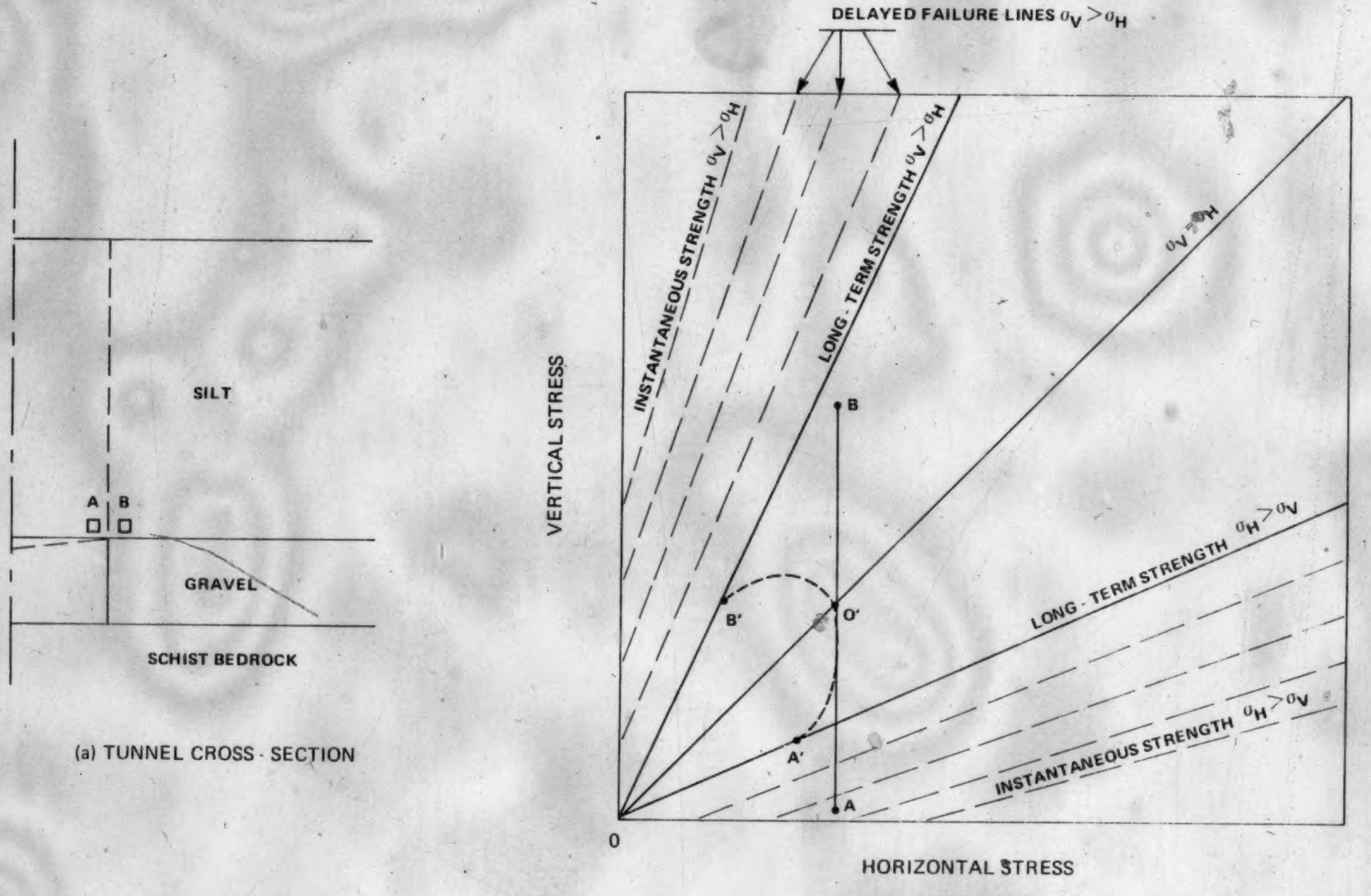
SILT
A
B
GRAVEL
SCHIST BEDROCK
DELAYED FAILURE LINES $\sigma_V > \sigma_H$
INSTANTANEOUS STRENGTH $\sigma_V > \sigma_H$
LONG - TERM STRENGTH $\sigma_V > \sigma_H$
$\sigma_V = \sigma_H$
VERTICAL STRESS
B
B'
O'
A'
A
0
LONG - TERM STRENGTH $\sigma_H > \sigma_V$
INSTANTANEOUS STRENGTH $\sigma_H > \sigma_V$
HORIZONTAL STRESS

(a) TUNNEL CROSS - SECTION

(b) STRESS PATHS

FIGURE 5.13 STRESS PATHS FOR SOIL ELEMENTS ABOVE AN UNDERGROUND OPENING

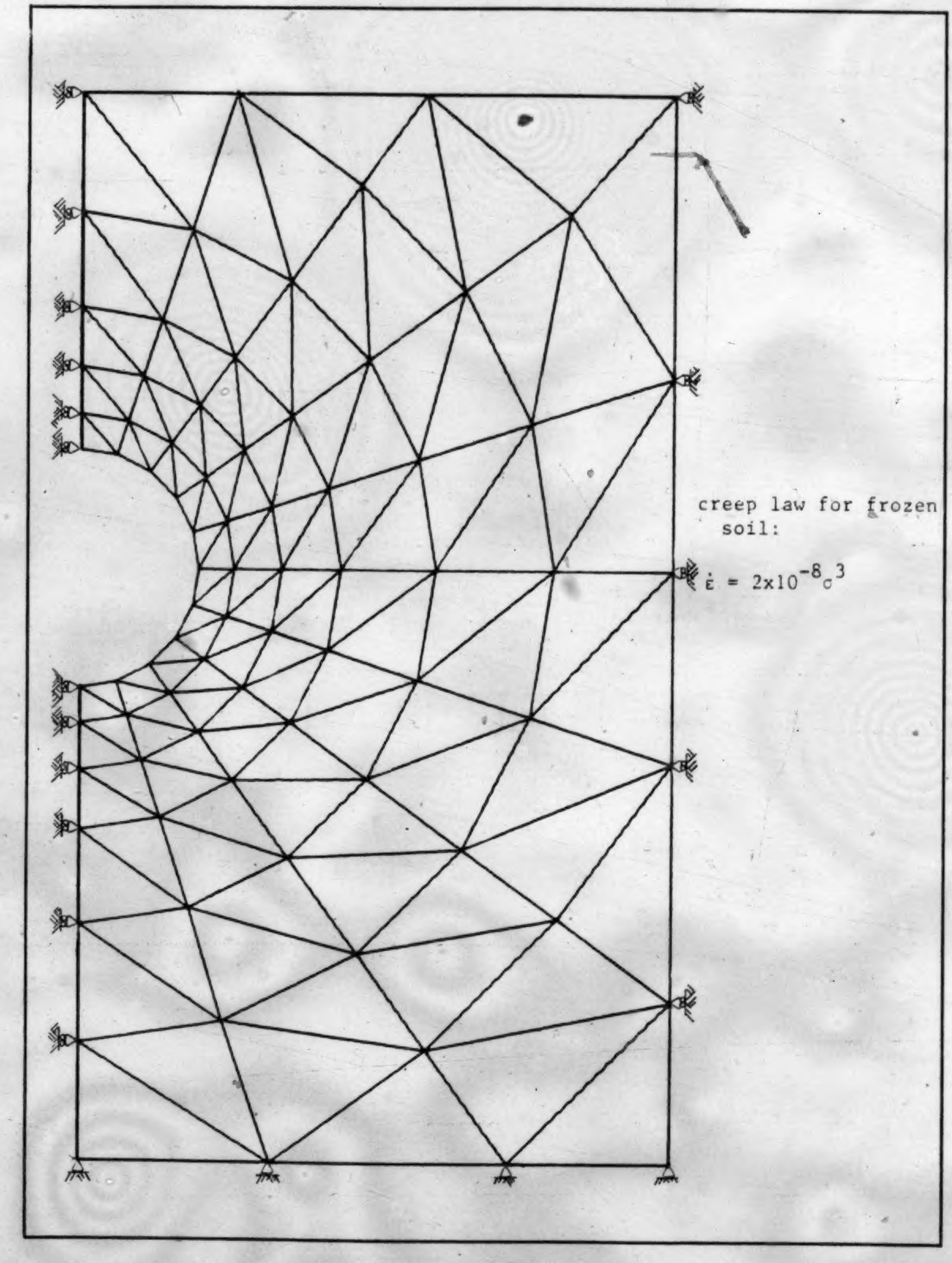

creep law for frozen soil:

$\dot{\varepsilon} = 2\times10^{-8}\sigma^3$

FIGURE 5.14 FINITE ELEMENT MESH FOR TUNNEL AT H/D = 2.0

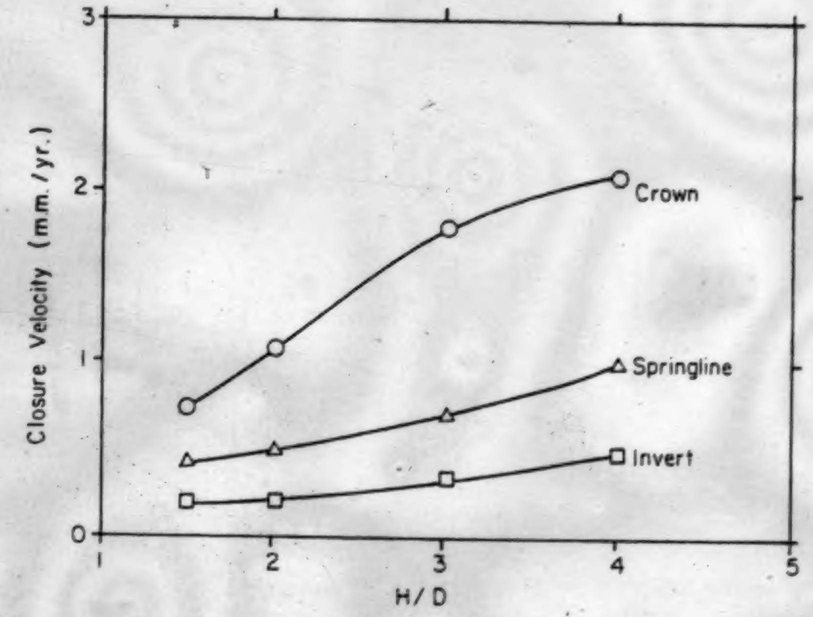

FIGURE 5.15 TUNNEL CLOSURE VELOCITY VERSUS DEPTH OF OVERBURDEN

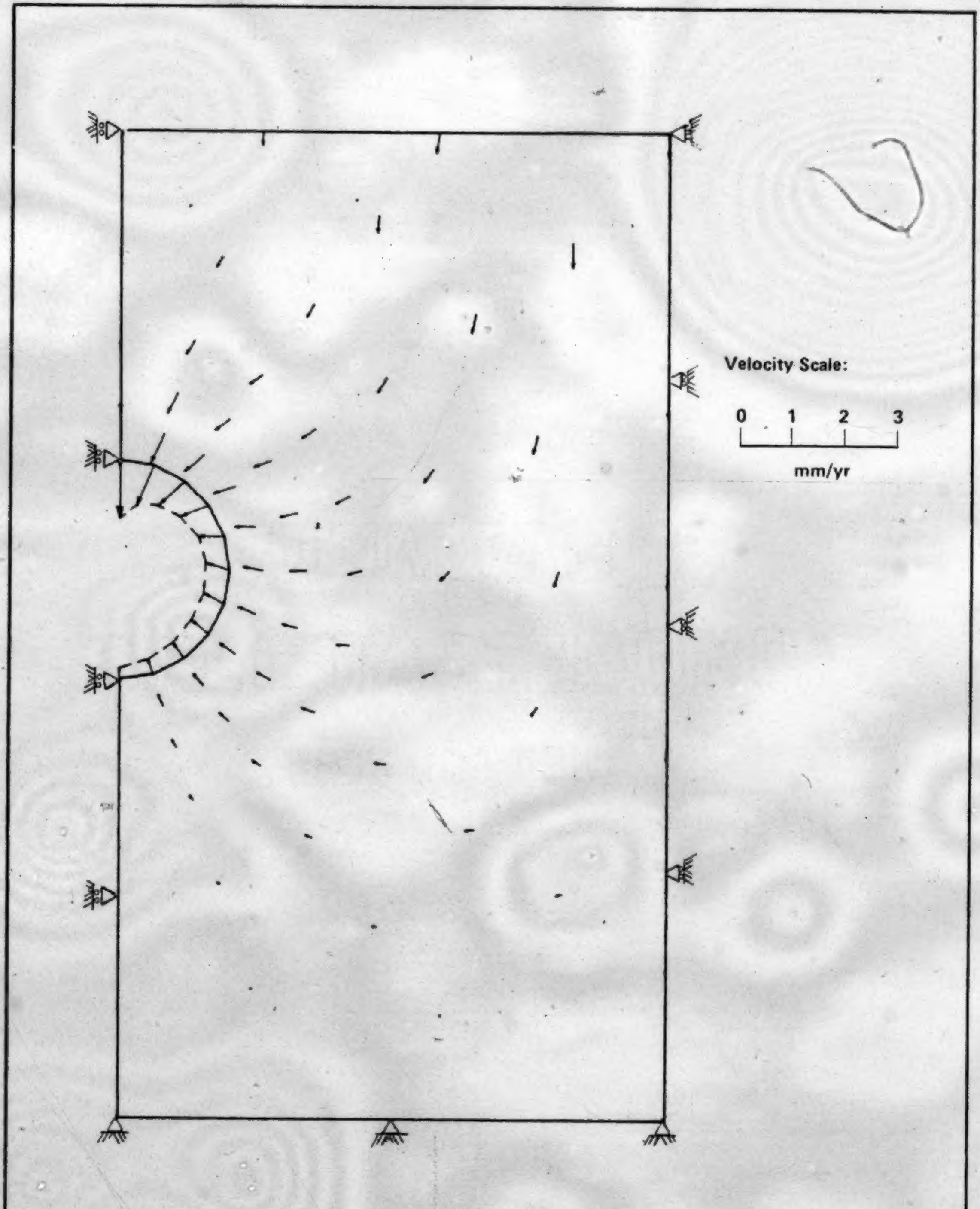
Velocity Scale:
0
1
2
3
mm/yr

FIGURE 5.16 VELOCITY VECTOR PLOT FOR TUNNEL AT H/D = 2.0

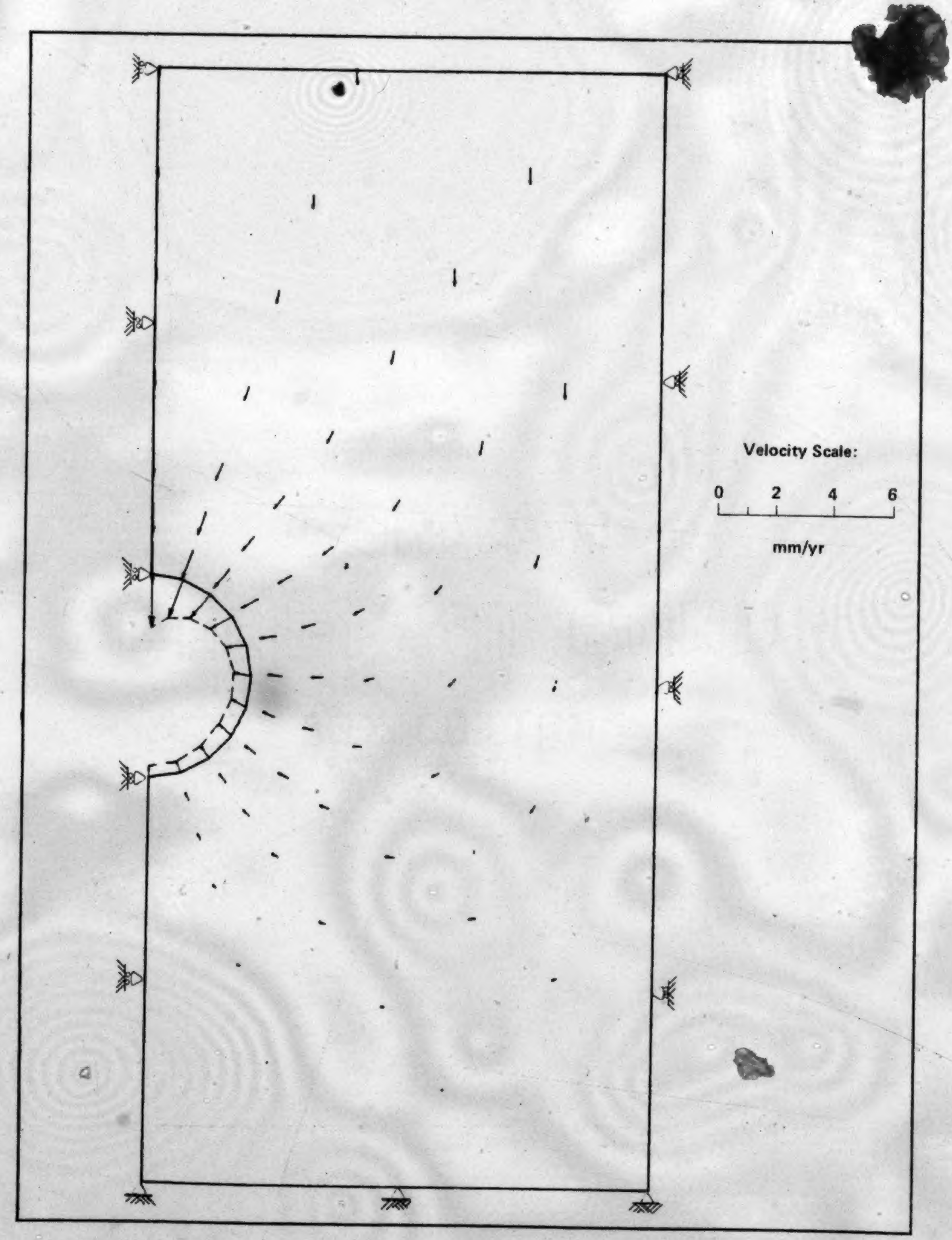
Velocity Scale:
0
2
4
6
mm/yr

FIGURE 5.17 VELOCITY VECTOR PLOT FOR TUNNEL AT H/D = 3.0

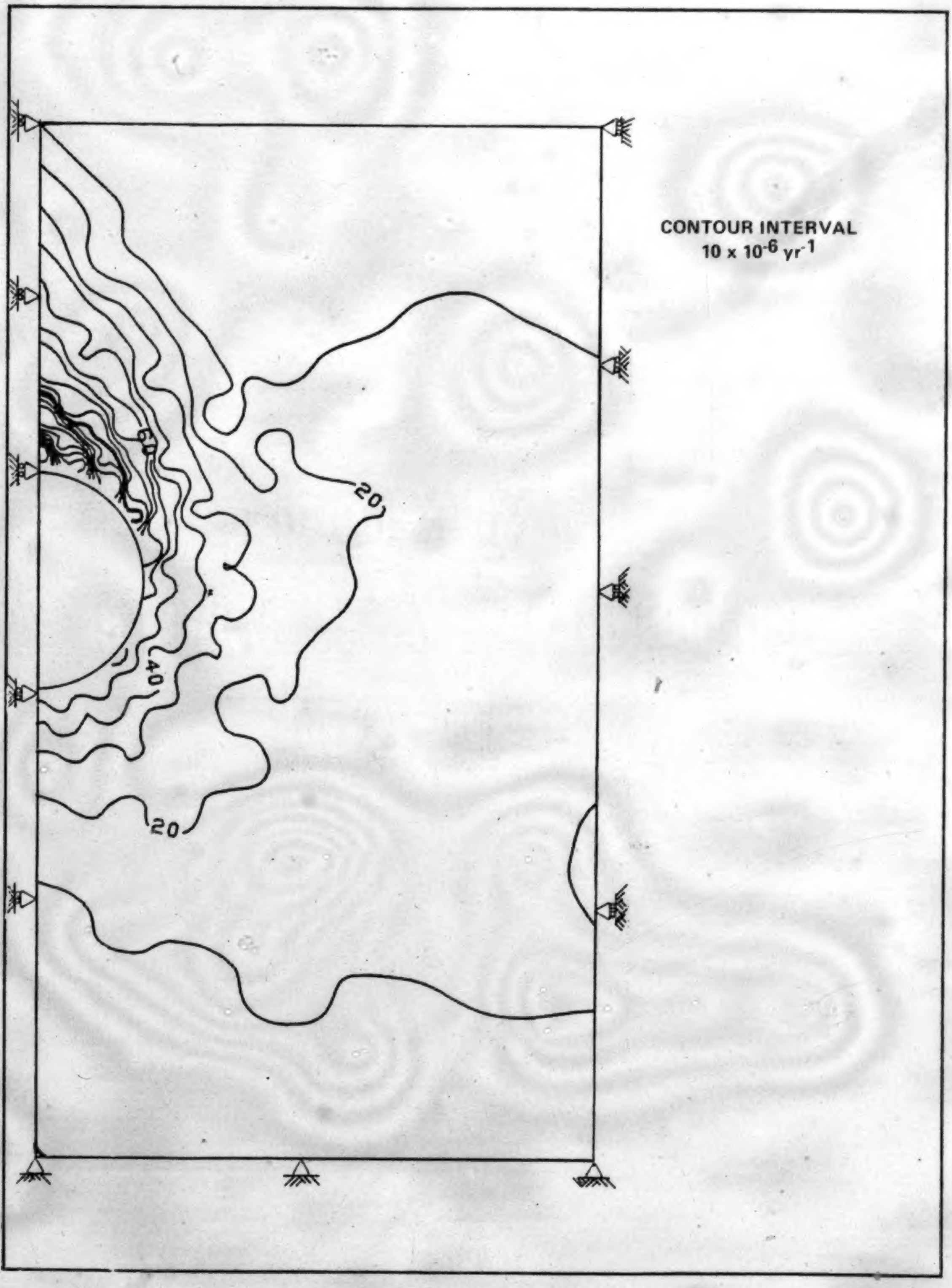

FIGURE 5.18 EFFECTIVE STRAIN RATE CONTOURS FOR TUNNEL AT H/D = 2.0

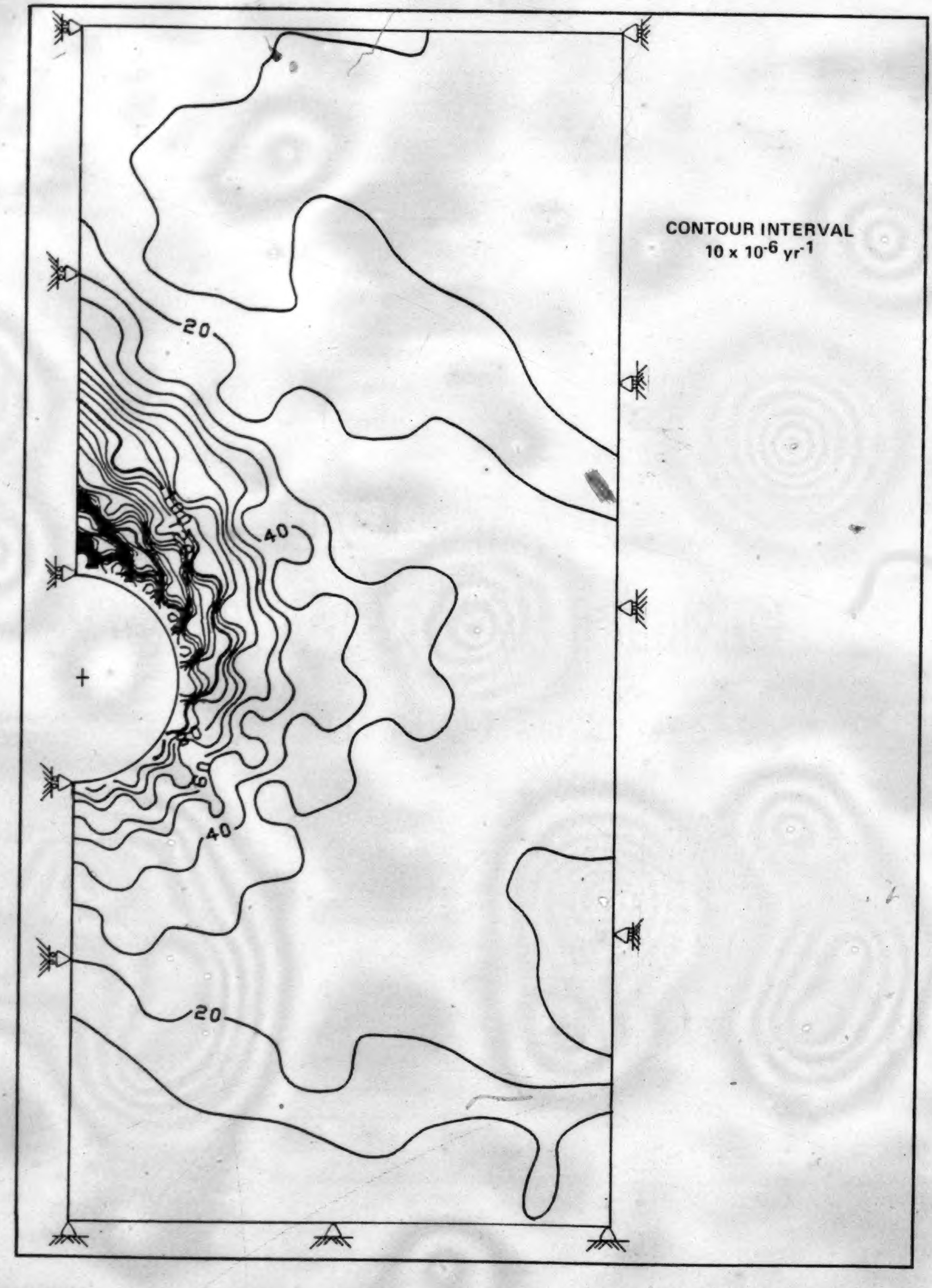

FIGURE 5.19 EFFECTIVE STRAIN RATE CONTOURS FOR TUNNEL AT H/D = 3.0

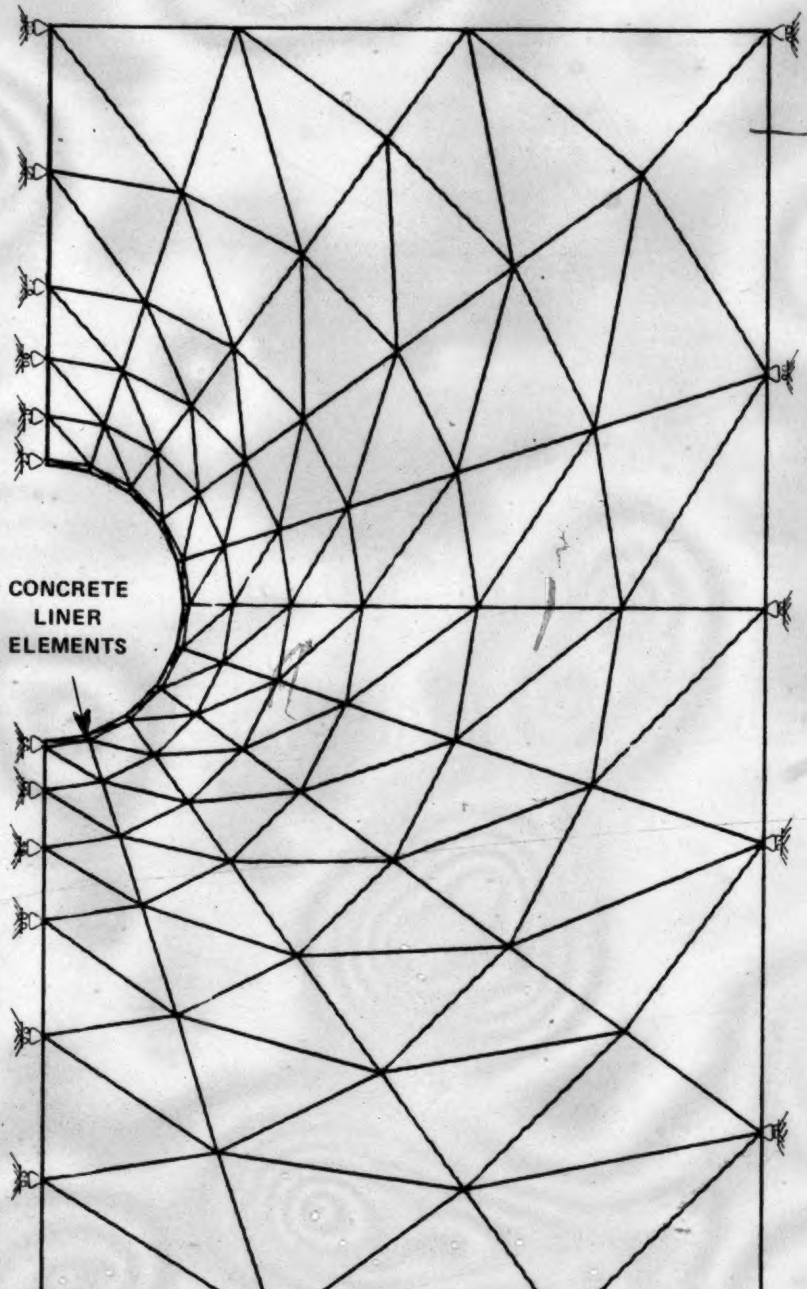
CONCRETE
LINER
ELEMENTS

creep law for
frozen soil:
$\dot{\varepsilon} = 2 \times 10^{-8}\,\sigma^{3}$

FIGURE 5.20 FINITE ELEMENT MESH FOR LINED TUNNEL AT H/D = 2.0

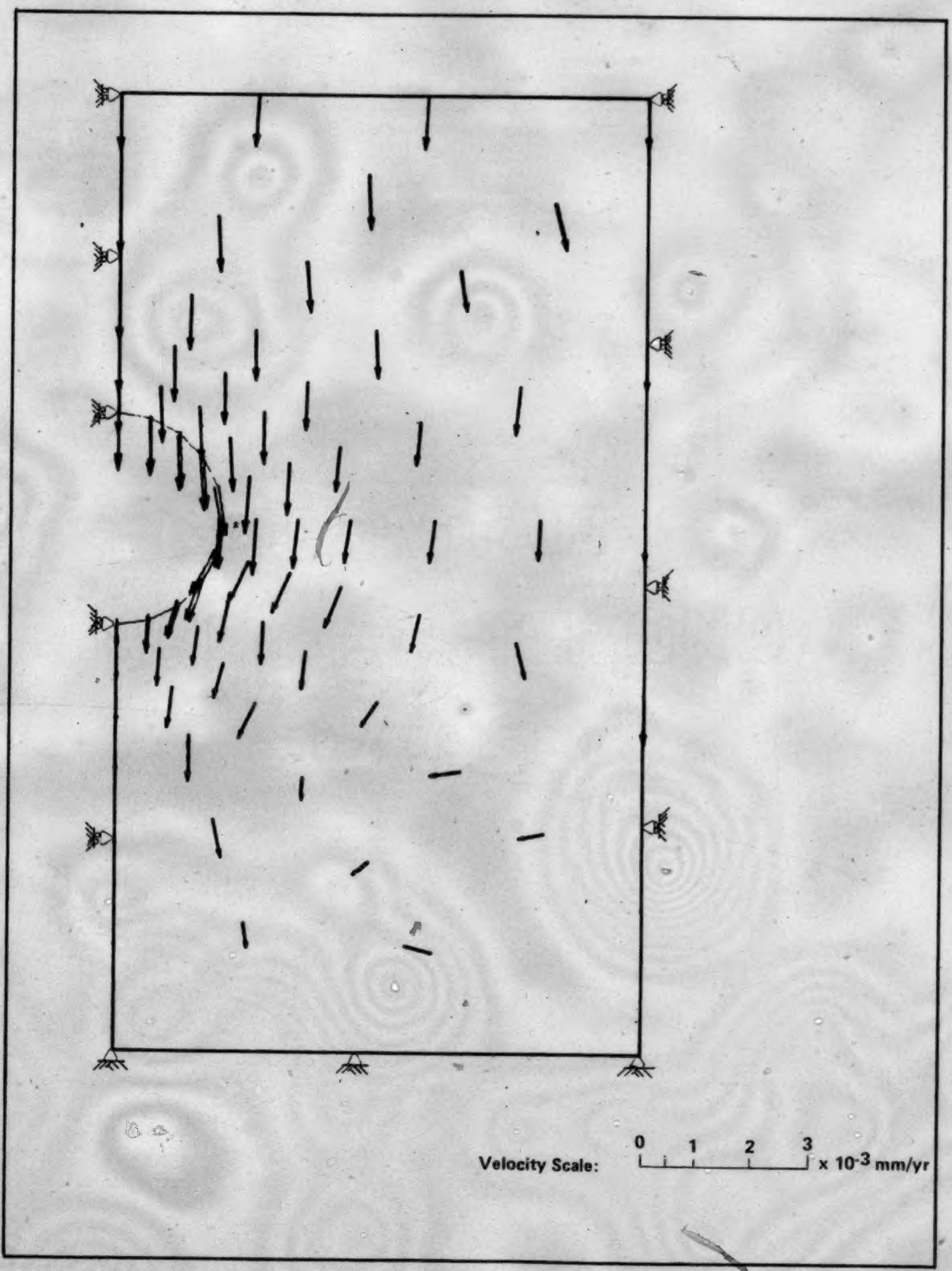
Velocity Scale:
0
1
2
3
x 10^{-3} mm/yr

FIGURE 5.21 VELOCITY VECTOR PLOT FOR LINED TUNNEL AT H/D = 2.0

CHAPTER VI

CONCLUDING REMARKS

6.1 GENERAL

An analytical study of the in-situ creep behavior in ice-rich frozen soil has been reported herein. A review of the deformation behavior of frozen soil has lead to the conclusion that the steady state creep of ice-rich frozen soil is adequately described by an empirically derived simple power law which relates strain rate to stress. The flow law for steady state creep in polycrystalline ice (Morgenstern et al., 1980) represents a valid upper bound for the constitutive behavior of frozen soil under equivalent loading conditions. The importance of testing natural permafrost samples with representative segregated ice features was also noted.

The incremental initial strain finite element procedure was applied to two case histories of naturally occurring creep in ice-rich permafrost. The in-situ creep behavior of a relatively steep slope on the left bank of the Great Bear River at the proposed Arctic Gas crossing was studied by Savigny (1980). Naturally occurring creep in ice-rich Fairbanks silt at the Fox Tunnel near Fairbanks, Alaska was studied by Swinzow (1970), Thompson and Sayles (1972) and Pettibone (1973). The following sections summarize the major conclusions of the analytical creep studies at these two sites.

6.2 Conclusions

6.2.1 Great Bear River

The finite element creep analysis of the left bank of the Great Bear River at the proposed Arctic Gas crossing has shown that the in-situ creep behavior of the glaciolacustrine clay can be accurately represented by the simple power law. The flow law which gave the best fit between observed and predicted velocities had an exponent of 3.0 and a coefficient of 3.33×10^{-9}. This strain rate is six times slower than the value for polycrystalline ice at -2°C (Morgenstern et al., 1980).

The exact form of the constitutive relationship for the glaciodeltaic sand remains inconclusive. In the first creep analysis, the creep behavior of the sand was assumed to be given by the simple power law with the same parameters as those in the glaciolacustrine clay. The velocities predicted by the simple power law were much greater than the observed values. A second analysis was carried out in which the sand was treated as an elastic material. This proved to be much too serious a restriction on the creep movements in the sand and the glaciolacustrine clay where it was overlain by sand. This analysis did predict the build up of horizontal tensile stress in the sand much greater than the sand would be able to sustain under in-situ conditions.

The creep movements recorded at the GB1A and GB3 inclinometer locations at the Great Bear River showed that more movement was associated with large ice lenses when they are widely separated (Savigny, 1980). Numerical modelling of permafrost as composite soil-ice medium would require an accurate mapping of the lateral continuity of these large ice lenses. Statistical analysis of the data derived from the MVPRL ice variability test sites at Norman Wells N.W.T. and Landing Lake N.W.T. suggest that for a uniform stratigraphic unit, the overall ground ice content of permafrost can be described as a normally distributed variable. Thus, for practical purposes, the assumption of homogeneity is valid for predicting overall time-dependent ground movements in ice-rich frozen soil.

A general conclusion derived from the study of the left bank of the Great Bank River at the proposed Arctic Gas crossing that the time-dependent deformation behavior of homogeneous slopes consisting of ice-rich fine-grained permafrost can be modelled by a simple power law. Using the creep parameters for polycrystalline ice will provide an upper bound to the creep velocities.

6.2.2 Fox Tunnel

The in-situ deformation studies of the Fox Tunnel reported by Swinzow (1970), Thompson and Sayles (1972), and Pettibone (1973) showed that underground openings excavated in warm ice-rich permafrost can become unstable when the ambient air temperature is near the soil temperature. In each case, primary creep behavior contributed substantially to the overall room closure.

The closure data of the USA CRREL room recorded over a 3 year period clearly showed attenuating creep for well over one year. The closure versus time data for the USA CRREL room and the USBM room in the Fox Tunnel both have the same general form for the first 3 years of operation. Thus, Thompson and Sayles (1972) were premature in concluding that steady state creep dominated the closure of the USA CRREL room during the first year of operation.

A finite element creep analysis of the USA CRREL room showed that the simple power law for polycrystalline ice does not represent a valid upper bound for the in-situ creep behavior of the frozen Fairbanks silt. However, analyzing the stress changes above a rectangular underground opening in terms of arching theory clearly shows that the stress paths followed by soil elements above the roof of the opening are entirely different from that normally used in constant stress or constant strain rate creep tests. The strain rate predicted by finite element computations was 3.3 times faster than the laboratory measured value (Thompson and Sayles, 1972) because the vertical room closure measurements could not distinguish between vertical compression in the gravel walls and downward creep movement of the overlying ice-rich silt. For this particular case it was not possible to isolate in-situ creep deformations by measuring the closure between opposing points in the roof, floor and walls.

6.3 Recommendations for Further Study

The analytical study of naturally occurring creep in a slope and underground cavity located in ice-rich permafrost has shown that the simple power law can be used to predict in-situ deformations provided that the stress does not approach failure.

The largest discrepancies between predicted and observed behavior appear to coincide with regions where the stresses experienced by the soil mass are unlike the stress paths used in laboratory constant stress or constant strain rate creep tests. This was illustrated at the GB2 inclinometer location at the Great Bear River. The stresses at this location are altered from the simple shear condition because the downslope creep movement in the glaciolacustrine clay is impeded by the overlying sand just upslope of this location. Downslope of the GB2 inclinometer, the glaciolacustrine clay creeps at a faster rate since there is no overlying sand to restrict movement. Thus, the clay in the vicinity of the GB2 inclinometer would experience an unloading in the horizontal direction.

The frozen silt above the roof in the USA CRREL room in the Fox Tunnel experiences an unloading due to excavation of the room. Arching behavior will transfer the vertical stress release in the roof to the frozen silt above the walls and to the frozen gravel walls. Thus, while the soil which experiences greater compressive stress may still lie below the compression failure envelope, the soil above the roof of the tunnel may experience tensile failure at some time after the room is excavated. The stress state can become quite complicated whenever two or more frozen materials are present with different creep properties. Thus, it is important to obtain an accurate assessment of the creep behavior of the materials relative to each other.

Future numerical modelling of ice-rich permafrost under complex stress conditions should be directed towards studying the stress changes experienced by the soil as deformations develop and to incorporate the concept of a limiting long term strength into the analysis. Toward this end, laboratory studies should be carried out to study the creep behavior of frozen soils under stress conditions that simulate unloading. Also, future field programs should have carefully designed and installed instrumentation to ensure that the in-situ creep deformations can be isolated from other deformation processes which may be occurring simultaneously.

REFERENCES

ABEL, J.F., 1961. Ice Tunnel Closure Phenomena. U.S. Army Snow Ice and Permafrost Research Establishment, Technical Report 74, 37 p.

ALKIRE, B.D., and ANDERSLAND, O.B., 1973. The Effect of Confining Pressure on the Mechanical Properties of Sand-Ice Materials. Journal of Glaciology. Vol. 12 (66), pp. 469-481.

ANDERSLAND, O.B. and ALNOURI, I., 1970. Time-Dependent Strength Behavior of Frozen Soils. A.S.C.E. Journal of Soil Mechanics and Foundations Division. Vol. 90 (SM4) pp. 1249-1265.

ANDERSLAND, O.B. and ANDERSON, D.M., 1978. Geotechnical Engineering for Cold Regions. McGraw-Hill Book Company, New York, 566p.

ANDERSON, D.M. and MORGENSTERN, N.R., 1973. Physics, Chemistry and Mechanics of Frozen Ground. A Review. Proceedings, North American Contribution, 2nd International Permafrost Conference, Yakutsk, USSR, pp. 257-258.

ATKINSON, J.H., and POTTS, D.M., 1977. Stability of a Shallow Circular Tunnel in Cohesionless Soil. Geotechnique, Vol. 27(2), pp. 203-215.

BARNES, P., TABOR, D., and WALKER, J.C.F., 1971. The Friction and Creep of Polycrystalline Ice. Proceedings of the Royal Society, London, Vol. 324A, pp. 127-155.

BENJAMIN, J.R., and CORNEL, C.A., 1970. Probability, Statistics and Decision For Civil Engineers. McGraw-Hill Book Campany, New York, 652p.

CHANG, C-Y, NAIR, K., and SINGH, R.D., 1974. Finite Element Methods for the Nonlinear and Time-Dependent Analysis of Geotechnical Problems. Proceedings, Conference on Analysis and Design in Geotechnical Engineering, Austin, Texas, pp. 269-302.

DAVIS, E.H., GUN, M.J., and SENEVIRATINE, H.N., 1980. The Stability of Shallow Tunnels and Underground Openings in Cohesive Soil. Geotechnique, Vol. 30(4), pp. 397-416.

REFERENCES (cont'd)

DAWSON, P.R., and TILLERSON, J.R., 1978. Salt Motion Following Nuclear Waste Disposal. Proceedings, Conference on Evaluation and Prediction of Subsidence, Pensacola Beach, Florida, pp. 459-478.

DESAI, C.S., and ABEL, J.F., 1972. Introduction to the Finite Element Method: A Numerical Method for Engineering Analysis. Van Nostrand Reinhold Co., New York, 477p.

DESAI, C.S., and CHRISTIAN, J.L., 1977. Numerical Methods in Geotechnical Engineering. McGraw-Hill Book Company, New York, 748p.

DORN, J.E., 1961. Mechanical Behavior of Metals at Elevated Temperatures. McGraw-Hill Book Company, New York, 529p.

EMERY, J.J, 1971. Finite Element Analysis of Creep Problems in Soil Mechanics. Unpublished Ph.D. Thesis, University of British Columbia, Vancouver, B.C. 155 p.

EMERY, J.J., and FINN, W.D.L., 1972. Creep Problems in Soil Mechanics. Proceedings, Symposium on Solid Mechanics, University of Waterloo, Waterloo, Ontario, pp. 417-437.

EMERY, J.J., and NGUYEN, T.Q., 1974. Simulation of Ice Flow Problems. Proceedings, 2nd Symposium on Applications of Solid Mechanics, McMaster University, Hamilton, Ontario, pp. 25-40.

EMERY, J.J., 1978. Simulation of Slope Creep. In: Rockslides and Avalances. Vol. 1. Natural Phenomena, Edited by B. Voight, Recent Developments in Geotechnical Engineering, pp. 669-691.

FINNIE, I., and HELLER, W.R., 1959. Creep of Engineering Materials. McGraw-Hill Book Company, New York, 341p.

GERSTENKORN, G.F., and KOBAYASKI, A.S., 1966. Application of the Direct Stiffness Method to Plane Problems Involving Large, Time - Dependent Deformations. Transactions of A.S.M.E., Journal of Basic Engineering.

REFERENCES (cont'd)

GHABOUSSI, J., WILSON, E.L., and ISENBERG, J., 1973. Finite Element for Rock Joints and Interfaces. Journal of Soil Mechanics and Foundations Division, A.S.C.E. Vol. 99 (SM10), pp. 833-848.

GLEN, J.W., 1975. The Mechanics of Ice. U.S. Army Cold Regions Research and Engineering Laboratory, Monograph 11-2cb, 47p.

GREENHAUM, G.A., and RUBINSTIEN, M.F., 1968. Creep Analysis of Axisymmetric Bodies Using Finite Elements. Nuclear Engineering and Design, Vol. 7, pp. 379-397.

GOODMAND, R.E., TAYLOR, R.L., and BREKKE, T.L., 1968. A Model for the Mechanics of Jointed Rock. Journal of Soil Mechanics and Foundations Division, A.S.C.E., Vol. 94 (SM3), pp. 637-659.

GUDEHUS, G., 1977. Finite Elements in Geomechanics. John Wiley and Sons, Inc., London, 573p.

HAWKES, I. and MELLOR, M., 1972. Deformation and Fracture of Ice Under Uniaxial Stress. Journal of Claciology, Vol. II (61), pp. 103-131.

HAYNES, F.D., 1973. Tensile Strength of Ice Under Triaxial Stresses. U.S. Army Cold Regions Research and Engineering Laboratory, Research Report 312, 15p.

HAYNES, F.D., 1978. Strength and Deformation of Frozen Silt. Proceedings, 3rd International Permafrost Conference, Edmonton, Alberta, pp. 656-661.

HAYNES, F.D., and KARALIUS, J.A., 1977. Effect of Temperature on the Strength of Frozen Silt. U.S. Army Cold Regions Research and Engineering Laboratory, Report 77-3, 27 p.

HAYNES, F.D., KARALIUS, J.A., and KAFUT, J., 1975. Strain-Rate Effect on the Strength of Frozen Silt. U.S. Army Cold Regions Research and Engineering Laboratory, Research Report 350, 27p.

REFERENCES (cont'd)

HENKEL, D.J., 1960. Relationship Between the Effective Stress and Water Content in Saturated Clays. Geotechnique, Vol. 10(2), pp. 41-54.

HENKEL, D.J., 1970. Geotechnical Considerations of Lateral Stress. Proceedigns, Conference on Lateral Stresses in the Ground and the Design of Earth Retaining Structures, Cornell University, Ithaca, New York, pp 1-49.

HOFF, N.J., 1954. Approximate Analysis of Structures in the Presence of Moderately Large Creep Deformations. Quarterly of Applied Mathematics, Vol. 12(1), pp. 49-55.

HOTZ, R.P., and KRIZEK, R.J., 1971. Statistical Evaluation of Soils Test Data. Proceedings, 1st International Conference on Applications of Statistics and Probability to Soil and Structural Engineering, Hong Kong, pp. 229-266.

HULT, S.A.H., 1966. Creep in Engineering Structures. Blaisdell Publishing Company, Waltham, Massachusets, 115 p.

KAY, J.N., and KRIZEK, R.J., 1971. Estimation of the Mean for Soil Properties. Proceedings, 1st International Conference on Applications of Statistics and Probability to Soil and Structural Engineering, Hong Kong, pp. 279-286.

KIM, H.D., and KUHLEMEYER, R.L., 1977. A Finite Element Formulation for Creep Analysis. International Journal for Numerical Methods in Engineering, Vol. 11, pp. 1865-1877.

KRUMBEIN, W.C., and GRAYBILL, F.A., 1965. An Introduction to Statistical Models in Geology. McGraw-Hill Company, New York.

LADANYI, B., 1972. An Engineering Theory of Creep in Frozen Soils. Canadian Geotechnical Journal, Vol. 9(1), pp. 63-80.

LADANYI, B., 1974(a). Bearing Capacity of Frozen Soils. Preprints, 27th Canadian Geotechnical Conference, Edmonton, pp. 97-107.

REFERENCES (cont'd)

LADANYI, B., 1974(b). Use of Long Term Strength Concept in the Determination of Ground Pressure on Tunnel Linings. Proceedings, 3rd Congress of International Society for Rock Mechanics, Denver, Vol. 2B, pp. 1150-1156.

LADANYI, B., 1975. Bearing Capacity of Strip Footings in Frozen Soils. Canadian Geotechnical Journal, Vol. 12(3), pp. 393-407.

LADANYI, B., 1981. Mechanical Behavior of Frozen Soils. Proceedings, International Symposium on the Mechanical Behavior of Structured Media, Carleton University, Ottawa, pp. 205-245.

LADANYI, B., and HOYAUX, B., 1969. A Study of Trap-door Problem in a Granular Mass. Canadian Geotechnical Journal. Vol. 6(1), pp. 1-14.

LADANYI, B., and JOHNSTON, G.H., 1973. Evaluation of In-situ Creep Properties of Frozen Soils with the Pressuremeter. Proceedings, North American Contribution, and International Permafrost Conference, Yakutsk, pp. 310-319.

LAMBE, T.W., 1967. Stress Path Method. Journal of Soil Mechanics and Foundations Division, A.S.C.E., Vol. 93 (SM6), pp. 309-331.

LIN, T.H., 1962. Bending of a Plate with Non-linear Strain Hardening Creep. In: Creep in Structures, edited by N.J. Hoff, Academic Press Inc., New York, pp. 215-228.

LUBAHN, J.D., and FELGER, R.P., 1961. Plasticity and Creep of Metals, John Wiley and Sons, Inc., New York.

McANERNEY, J.A., 1968. Tunnelling in a Subfreezing Environment. Proceedings, Tunnel and Shaft Conference, Minnesota, Edited by D.H. Yardley, pp. 378-394.

McROBERTS, E.C., LAW, T.C. and MURRAY, T.K., 1978. Creep Tests on Undisturbed Ice-Rich Silt. Proceedings, 3rd International Permafrost Conference, Edmonton, Vol. 1, pp. 539-545.

REFERENCES (cont'd)

MEIER, M.F., 1960. Mode of Flow of the Saskatchewan Glacier, Alberta, Canada. U.S. Geological Survey Professional Paper 351.

MENDELSON, A., HERSCHBERG, M.H., and MANSON, S.S., 1959. A General Approach to Practical Solution of Creep Problems. Transactions of A.S.M.E., Journal of Basic Engineering, Vol. 81(2), pp. 585-598.

MICHEL, B., 1978. A Mechanical Model of Creep of Polycrystalline Ice. Canadian Geotechnical Journal, Vol. 15(2), pp. 155-170.

MORGENSTERN, N.R., and SEGO, D., 1978. Utilization of Cavities in Frozen Ground for Military Purposes. Report prepared for Department of National Defence, DRES, Ralston, Alberta, 53p.

MORGENSTERN, N.R., ROGGENSACK, W.D., and WEAVER, J.S., 1980. The behavior of Friction Piles in Ice and Ice-Rich Soils. Canadian Geotechnical Journal, Vol. 17 (3), pp. 405-415.

NADAI, A., 1963. Theory of Fracture and Flow of Solids. McGraw-Hill Book Company. New York.

NAIR, K., and BORESI, A.P., 1970. Stress Analysis for Time-Dependant Problems in Rock Mechanics, Proceedings, 2nd Congress of International Society of Rock Mechanics, Belgrade, Vol. 2, pp. 531-536.

NYE, J.F., 1951. The Flow of Glaciers and Ice Sheets as a Problem in Plasticity. Proceedings of the Royal Society, London, Vol. 207A, pp. 554-572.

NYE, J.F., 1952. The Mechanics of Glacier Flow. Journal of Glaciology, Vol. 2, pp. 82-93.

NYE, J.F., 1953. The Flow Law of Ice From Measurements in Glacier Ice Tunnels, Laboratory Experiments and the Jungafraufin Borehole Experiment. Proceedings of Royal Society London, Vol. 219A, pp. 477-489.

REFERENCES (cont'd)

NYE, J.F., 1957. The Distribution of Stress and Velocity in Glaciers and Ice-Sheets. Proceedings of Royal Society, London, Vol. 239A, pp. 113-133.

NIXON, J.F., 1978. Foundation Design Approaches in Permafrost Areas. Canadian Geotechnical Journal, Vol. 15(1), pp. 96-112.

ODQVIST, F.K.G., 1966. Mathematical Theory of Creep and Creep Rupture. Oxford Mathematical Monograph, Clarendon Press, Oxford, 168p.

PALMER, A.C., 1972. Settlement of Pipeline on Thawing Permafrost. Transportation Engineering Journal, A.S.C.E., Vol. 98 (TE3), pp. 477-491.

PATERSON, W.S.B., 1969. The Physics of Glaciers. Pergammon Press, Oxford, 250 p.

PETTIBONE, H.C., 1973. Stability of an Underground Room in Frozen Gravel. Proceedings, North American Contribution, 2nd International Permafrost Conference, Yakutsk, USSR, pp. 669-706.

RAUSCH, D.D., 1958. Ice Tunnel, Tuto Area, Greenland, 1950. U.S. Army Snow Ice and Permafrost Research Establishment, Technical Report 44, 34p.

ROGGENSACK, W.D., 1977. Geotechnical Properties of Permafrost Soils. Unpublished Ph.D. Thesis, University of Alberta, 494p.

RUSSELL, F., 1961. An Under-Ice Camp in the Arctic. U.S. Army Cold Regions Research and Engineering Laboratory, Special Report 44, 14p.

SAVIGNY, K.W., 1980. In-Situ Analysis of Naturally Occurring Creep in Ice-Rich Permafrost Soil. Unpublished Ph.D. Thesis, University of Alberta.

SAYLES, F.H., 1968. Creep of Frozen Sands. US Army Cold Regions Research and Engineering Laboratory, Technical Report 190, 54p.

REFERENCES (cont'd)

SAYLES, F.H., 1973. Triaxial and Creep Tests on Frozen Ottawa Sand. Proceedings, North American Contribution, 2nd International Permafrost Conference, Yakutsk, USSR, pp. 384-391.

SEGO, D.C.C., 1980. Deformation of Ice Under Low Stresses. Unpublished Ph.D. Thesis, University of Alberta.

SELLMAN, P.V., 1967. Geology of the USA CRREL Permafrost Tunnel, Fairbanks, Alaska. U.S. Army Cold Regions Research and Engineering Laboratory, Technical Report 199, 22p.

SELLMAN, P.V., 1972. Geology and Properties of Materials Exposed in the USA CRREL Permafrost Tunnel. U.S. Army Cold Regions Research and Engineering Laboratory, Special Report 177.

SIMMONS, J.V., 1981. Shearband Yielding and Strain Weakening. Unpublished Ph.D. Thesis, University of Alberta, Edmonton, Alberta, 387 p.

SPEER, T.L., WATSON, G.H., and ROWLEY, R.K., 1973. Effects of Ground Ice Variability and Resulting Thaw Settlement on a Buried Warm Oil Pipeline. Proceedings, North American Contribution, 2nd International Permafrost Conference, Yakutsk, pp. 746-752.

SUTHERLAND, W.H., 1970. AXICRP-Finite Element Computer Code for Creep Analysis of Plane Stress, Plane Strain and Axisymmetric Bodies. Nuclear Engineering and Design, Vol. II, pp. 269-285.

SWINZOW, G.K., 1964. Tunnelling in Permafrost. U.S. Army Cold Regions Research and Engineering Laboratory, Technical Report 91, 19p.

SWINZOW, G.K., 1970. Permafrost Tunnelling by a Continuous Mechanical Method. U.S. Army Cold Regions Research and Engineering Laboratory, Technical Report 221, 36p.

REFERENCES (cont'd)

TERZAGHI, K., 1943. Theoretical Soil Mechanics. John Wiley and Sons, Inc., New York, 479p.

THOMPSON, E.G., 1969. A Finite Element Program for Creep of Ice and Frozen Soil. Report prepared for U.S. Army Terrestrial Sciences Centre.

THOMPSON, E.G., 1970. A Finite Element Analysis of the Creep Closure of an Underground Room in Permafrost. Report prepared for U.S. Army Cold Regions Research and Engineering Laboratory.

THOMPSON, E.G., and SAYLES, F.H., 1972. In-Situ Creep Analysis of Room in Frozen Soil. Journal of the Soil Mechanics and Foundation Division, A.S.C.E., Vol. 98, pp. 899-915.

TSYTOVICH, N.A., 1975. The Mechanics of Frozen Ground. McGraw-Hill Book Company, New York, 426p.

VAN WINKEL, B., GERSTLE, K.H, and KO, H.Y., 1972. Analysis of Time-Dependant Deformations of Openings in Salt Media. International Journal of Rock Mechanics and Mining Science, Vol. 9, pp. 249-260.

VIALOV, S.S., 1959. Rheological Properties and Bearing Capacity of Frozen Soils. U.S. Army Cold Regions Research and Engineering Laboratory, Technical Translation 74, 1965.

VIALOV, S.S., 1962. Strength and Creep of Frozen Soils and Calculations of Ice-Soil Retaining Structures. U.S. Army Cold Regions Research and Engineering Laboratory, Technical Translation 76, 1965.

VIALOV, S.S., 1963. Rheology of Frozen Soils, Proceedings, 1st International Conference on Permafrost, Lafayette, Indianna. pp. 332-337.

WEAVER, J.S., 1979. Pile Foundations in Permafrost. Unpublished Ph.D. Thesis, Univeristy of Alberta, 225p.

REFERENCES (cont'd)

WEERDENBURG, P.C., 1979. Study of Geotechnical Military Engineering in the Arctic, Part 2 - Utilization of Underground Space in Frozen Ground. Report prepared for Department of National Defence, DRES, Ralston, Alberta, 27p.

WEERDENBURG, P.C., 1980a. Study of Geotechnical Military Engineering in the Arctic, Part I - Analytical Load - Deformation and Heat Transfer Analysis in Frozen Ground. Report prepared for Department of National Defense, DRES, Ralston, Alberta.

WEERDENBURG, P.C., 1980b. Study of Geotechnical Military Engineering in the Arctic, Part II - Finite Element Time-Dependent Load-Deformation Analysis. Report prepared for Department of National Defence, DRES, Ralston, Alberta.

WEERDENBURG, P.C., and THOMPSON, S., 1981. Study of Geotechnical Military Engineering in the Arctic, Part 2 - Cavities in Frozen Ground. Report prepared for Department of National Defense, DRES, Ralston, Alberta.

ZIENKIEWICZ, O.C., 1971. The Finite Element Method in Engineering Science, McGraw-Hill Book Company, London, 521p.

ZIENKIEWICZ, O.D., BEST, B., DULLAGE, C., and STAGG, K.G., 1970. Analysis of Nonlinear Problems in Rock Mechanics with Particular Reference to Jointed Rock Systems. Proceedings, 2nd Congress of the International Society of Rock Mechanics, Belgrade, pp. 501-509.

APPENDIX A

FORMULATION OF FINITE ELEMENT EQUATIONS FOR THE INCREMENTAL INITIAL STRAIN PROCEDURE

APPENDIX A

FORMULATION OF FINITE ELEMENT EQUATIONS FOR INCREMENTAL INITIAL STRAIN PROCEDURE

This appendix presents a brief review of how the incremental theory of creep is introduced into the finite element method using the initial strain procedure.

In the incremental theory of creep, the increment of creep strain is treated as an initial strain for any one time interval and is assumed to be constant for that time interval.

The increment of total strain, $\Delta\varepsilon^T$, for any time interval can be assumed to consist of an increment of elastic strain, $\Delta\varepsilon^E$, and an increment increment of creep strain, $\Delta\varepsilon^C$. This can be expressed as:

$$\{\Delta\varepsilon^T\} = \{\Delta\varepsilon^E\} + \{\Delta\varepsilon^C\} \tag{A1}$$

Solving equation A1 for the elastic strain gives:

$$\{\Delta\varepsilon^E\} = \{\Delta\varepsilon^T\} - \{\Delta\varepsilon^C\} \tag{A2}$$

and applying Hooke's law:

$$\{\Delta\sigma\} = [D]\{\Delta\varepsilon^T - \Delta\varepsilon^C\} \tag{A3}$$

where: $[D]$ = matrix of elastic constants

For the linear elastic case, an increment of strain energy density of a body is given by:

$$\Delta U(x,y,z) = \frac{1}{2}\{\Delta\varepsilon^{E}\}^{T}\{\Delta\sigma\} \qquad (A4)$$

Substitution of equation A2 and A3 into A8 gives:

$$\Delta U(x,y,z) = \frac{1}{2}\{\Delta\varepsilon^{T} - \Delta\varepsilon^{C}\}^{T}[D]\{\Delta\varepsilon^{T} - \Delta\varepsilon^{C}\} \qquad (A5)$$

An increment of potential energy of a body is expressed mathematically as:

$$\Delta\pi_{p} = \int_{V}\Delta U(x,y,z)\,dV - \int_{V}(\overline{X}\Delta u + \overline{Y}\Delta v + \overline{Z}\Delta w)\,dV$$

$$- \int_{S_{T}}(\overline{T}_{x}\,\Delta u + \overline{T}_{y}\Delta V + \overline{T}_{z}\Delta w)\,dS_{T} \qquad (A6)$$

where V represents the volume of the body and S_T is the surface on which surface tractions are prescribed. The last two integrals in equation A6 represent the work done by the external forces; i.e. the body forces $\overline{X}$, $\overline{Y}$, $\overline{Z}$, and the surface tractions, $\overline{T}_x$, $\overline{T}_y$, and $\overline{T}_z$. The bar denotes quantities that are prescribed. Substituting equation A5 into A6 yields:

$$\Delta\pi_p = \frac{1}{2}\int_V \{\Delta\varepsilon^T\}^T [D]\{\Delta\varepsilon^T\}\,dV - \frac{1}{2}\int_V \{\Delta\varepsilon^T\}^T [D]\{\Delta\varepsilon^C\}\,dV$$

$$- \frac{1}{2}\int_V \{\Delta\varepsilon^C\}^T [D]\{\Delta\varepsilon^T\}\,dV + \frac{1}{2}\int_V \{\Delta\varepsilon^C\}^T [D]\{\Delta\varepsilon^C\}\,dV \qquad (A7)$$

$$- \frac{1}{2}\int_V \{\Delta\psi(x,y)\}^T \{F\}\,dV - \int_{S_T} \{\Delta\psi(x,y)^T \{T\}\,dS_T$$

where: $\{\Delta\psi(x,y,z)\}^T = \lfloor\, \Delta u \quad \Delta y \quad \Delta z \,\rfloor$

$$\{F\} = \begin{Bmatrix} \bar{X} \\ \bar{Y} \\ \bar{Z} \end{Bmatrix} \qquad \{T\} = \begin{Bmatrix} \bar{T}_x \\ \bar{T}_y \\ \bar{T}_z \end{Bmatrix}$$

Using standard finite element calculations, one can write:

$$\{\Delta\varepsilon\} = [B]\,\{\Delta q\} \qquad (A8)$$

$$\{\Delta\psi(x,y,z)\} = [N]\,\{\Delta q\} \qquad (A9)$$

where [B] = matrix relating element strains to the values of the displacement at its nodes.

[N] = coefficient matrix for displacement interpolation model.

Substituting equation A8 and A9 into equation A7 yields:

$$\Delta\pi_p = \frac{1}{2}\int_V \{\Delta q\}^T [B]^T [D][B]\{\Delta q\}\,dV - \int_V \{\Delta q\}^T [B]^T [D]\{\Delta\varepsilon^C\}\,dV$$

$$+\frac{1}{2}\int_V \{\Delta\varepsilon^C\}^T [D]\{\Delta\varepsilon^C\}\,dV - \int_V \{\Delta q\}^T [N]^T \{F\}\,dV$$

$$- \int_{S_T} \{\Delta q\}^T [N]^T \{T\}\,dS_T \qquad \text{(A10)}$$

The Theorem of Minimum Potential Energy states:

> "Of all possible displacement configurations a body can assume which satisfy compatability on the constraints or kinematic boundary conditions, the configuration satisfying equilibrium makes the potential energy assume a minimum value".

Mathematically, this is expressed as:

$$\delta(\Delta\pi_p) = 0 \qquad \text{(A11)}$$

Taking the first variation of equation A10 with respect to the incremental displacements, $\{\Delta q\}$, and setting it equal to zero gives:

$$\{\delta(\Delta q)\}^T [\int_V [B]^T [D][B]\,dV\{\Delta q\} - \int_V [B]^T [D]\{\Delta\varepsilon^C\}\,dV$$

$$- \int_V [N]^T \{F\}\,dV - \int_{S_T} [N]^T \{T\}\,dS_T = 0 \qquad \text{(A12)}$$

Since the variation of the displacements are arbitrary, the quantity enclosed in the brackets must vanish. The variation of the third integral in equation A10 is zero because it is not a function of the nodal displacements. The set of equilibrium equations for each time interval is:

$$[K]_s\{\Delta q\}_s = \{P\}_s + \{\Delta F_c\}_s \qquad \text{(A13)}$$

where:

$$[K]_s = \sum_{m=1}^{M}[K]^{el}_m = \sum_{m=1}^{M}\left(\int_V [B]^T[D][B]\,dV\right)_m$$

$$\{P\}_s = \sum_{m=1}^{M}\{P\}^{el}_m = \sum_{m=1}^{M}\left(\int_V [N]^T\{F\}\,dV + \int_{S_T}[N]^T\{T\}\,dS_T\right)_m$$

$$\{\Delta F_c\}_s = \sum_{m=1}^{M}\{\Delta F_c\}^{el}_m = \sum_{m=1}^{M}\left(\int_V [B]^T[D]\{\Delta\varepsilon^C\}\,dV\right)_m$$

The summation sign is carried over the total number of elements, M, to obtain the equilibrium equations for the entire assemblage.

The vector $\{F_c\}_s$ represents the creep strain nodal load vector. Thus, it can be seen that for each interval of time, creep strains are allowed to take place. Equivalent nodal forces are then calculated which would be necessary to cause elastic strains of the same magnitude. These fictitious nodal forces are then added to the load vector and new set of nodal displacements are calculated during that time interval with equation A13.

APPENDIX B

CALCULATION OF FICTITIOUS NODAL FORCES

APPENDIX B

CALCULATION OF FICTITIOUS NODAL FORCES

This appendix presents the derivation of the fictitious nodal creep forces used in the initial strain approach to solving creep problems.

In each time interval, the increment of creep strain is given by the stress-strain-rate law, i.e.:

$$\Delta\dot{\varepsilon}_{ij} = \frac{3}{2}(\Delta\dot{\varepsilon}_e/\sigma_e)\, s_{ij} \tag{B1}$$

Using Hooke's law, the increments of creep strain are converted to incremental creep stresses:

$$\{\sigma^C\} = [D]\{\varepsilon^C\} \tag{B2}$$

The constant stress state for the constant strain triangular finite element is represented by Figure B-1(a).

The stresses can be replaced by a set of statically equivalent forces acting at the node points of the constant strain triangle. Elements with higher order displacement interpolation functions require that the nodal forces be work-equivalent loads. However, for the constant strain triangle, work-equivalent and statically-equivalent loads are equal.

The incremental stresses are related to the nodal forces for each element as follows:

$$\begin{Bmatrix} F_{xi} \\ F_{xj} \\ F_{xk} \\ F_{yi} \\ F_{yj} \\ F_{yk} \end{Bmatrix} = \frac{1}{2}\begin{bmatrix} y_k-y_i & 0 & x_j-x_k \\ y_i-y_j & 0 & x_k-x_i \\ y_j-y_k & 0 & x_i-x_j \\ 0 & x_j-x_k & y_k-y_i \\ 0 & x_k-x_i & y_i-y_j \\ 0 & x_i-x_j & y_j-y_k \end{bmatrix} \begin{Bmatrix} \sigma_x^c \\ \sigma_y^c \\ \tau_{xy}^c \end{Bmatrix}_{el} \tag{B3}$$

The fictitious nodal load vector is computed for each element in turn and then summed to obtain the incremental load vector for the entire assemblage. The incremental load vector is then used to calculate a new set of incremental displacements for the current time step.

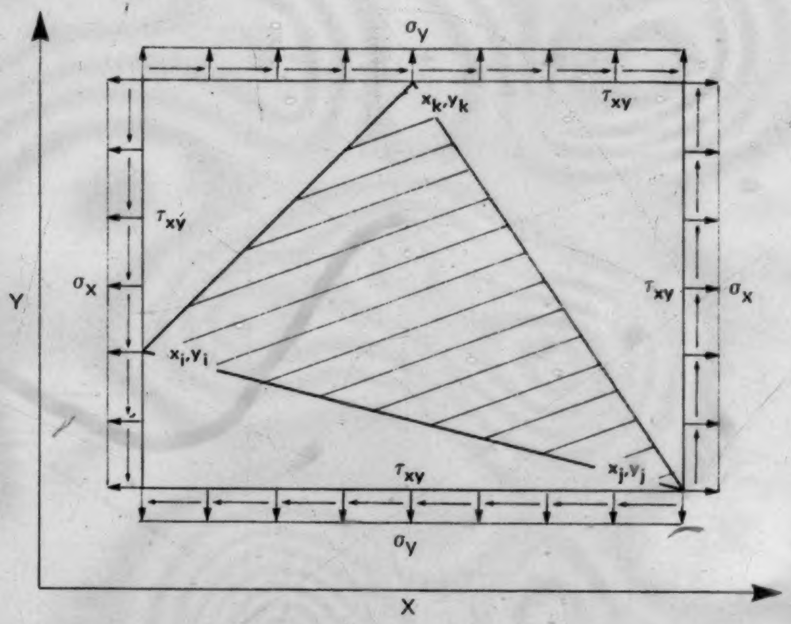
σy
xk,yk
τxy
τxy
σx
Y
τxy
σx
xi,yi
τxy
xj,yj
σy
X

a) CONSTANT STRESS DISTRIBUTION

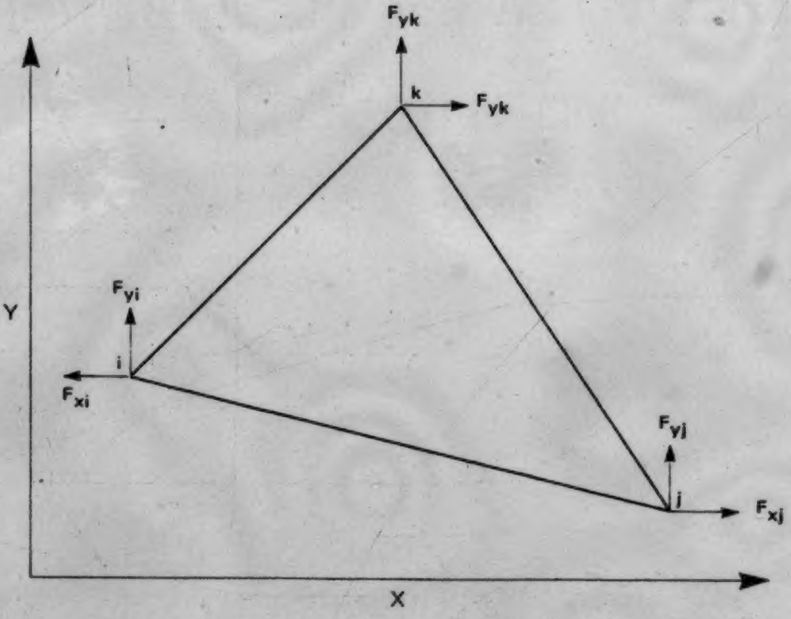
Fyk
k
Fyk
Y
Fyi
i
Fxi
Fyj
j
Fxj
X

b) STATICALLY-EQUIVALENT NODAL FORCES

FIGURE B.1 STATICALLY EQUIVALENT NODAL FORCES FOR CONSTANT STRAIN TRIANGLE

APPENDIX C

USER'S MANUAL FOR CREEP

INPUT DATA FORMAT FOR PROGRAM: CREEP

****

CARD TYPE NO. 1 - TITLE OF THE PROBLEM [Format(20A4)]

****

Columns	Variable	Entry
1-80	TITLE	Enter the heading information that is to be printed with the output

****

-any alphanumeric characters can be entered

****

CARD TYPE NO. 2 - PROBLEM SOLUTION CONTROL [Format(2A8)]

****

Columns	Variable	Entry
*******	********	*****
1-8	CODE1	START - For an initial run of the program, all data is input on cards RSTART - For a continuation of a previous problem, that was terminated early
9-16	CODE2	RUN - For a normal run of the program CONTIN - Write the results of the final time step on to tape for restarting the problem at a future date

****

- if CODE1 = RSTART, card sets 1, 2, 3, 11, 12, 14 and 15 are required

- to restart a previous problem, the results of the last increment of the terminated run are read from unit ITAPE

****

CARD TYPE NO. 3 - INPUT AND OUTPUT DESIGNATION [Format(2I6)]

****

Columns	Variable	Entry
*******	********	*****
1-6	ITAPE	Unit number from which the results of a terminated run will be read
7-12	JTAPE	Unit number onto which the results for the final time step will be written for a run that will be terminated early

****

-for an initial run of the program, all the input data is assumed to be read from cards

-to continue a problem at a future date, a unit number for JTAPE must be specified; otherwise solution of the problem will terminate

****

CARD TYPE NO. 4 - MASTER CONTROL CARD [Format(7I6)]

****

Columns	Variable	Entry
*******	********	*****
1-6	NN	Total number of nodes (maximum of 200)
7-12	NE	Total number of elements (maximum of 300)
13-18	NUE	Total number of materials for the elastic solution (maximum of 20)
19-24	NUC	Total number of materials for the creep solution (maximum of 20)
25-30	NGI	Gravity loading condition NGI=0 no gravity load NGI=1 gravity load considered
31-36	NLC	External load condition NLC=0 no external loads NLC=1 external loads considered
37-42	KV	Creep condition KV=0 only an elastic solution is performed KV=1 creep solution is required

****

CARD TYPE NO. 5 - NODAL POINT DATA [Format(3I5,2F10.3)]

Columns	Variable	Entry
1-5	I	Node
6-10	ND(I,1)	X-direction boundary condition code for node I ND(I,1)=0 fixed in X-direction ND(I,1)=1 free
11-15	ND(I,2)	Y-direction boundary condition code for node I ND(I,2)=0 fixed in Y-direction ND(I,2)=1 free
16-25	X(I)	X coordinate for node number I
26-35	Y(I)	Y coordinate for node number I

-one node per card

CARD TYPE NO. 6 - ELASTIC MATERIAL PROPERTIES [Format(F12.0,2F6.3)]

Columns	Variable	Entry
1-12	EI(I)	Young's Modulus of material number I
13-18	UI(I)	Poisson's Ratio of material number I
19-24	UNI(I)	Unit weight of material number I

-there should be one card for each material up to a maximum of 20

CARD TYPE NO. 7 - ELEMENT INCIDENCES [Format(6X,5I6)]

Columns	Variable	Entry
7-12	NI	Corner node number I
13-18	NJ	Corner node number J
19-24	NK	Corner node number K
25-30	MET	Elastic material number indicator for each element
31-36	MMET(I)	Creep material indicator for each element

-one element per card

-node numbers I, J, K are entered in a counter-clockwise direction; the starting node is arbitrary.

****

CARD TYPE NO. 8 - EXTERNAL LOADING [Format(I6)]

****

Columns	Variable	Entry
*******	********	*****
1-6	NNL	Number of noads loaded

****

-if NLC=0, card type no. 7 as well as card type no. 8 must not appear.

****

CARD TYPE NO. 9 - EXTERNAL LOADS [Format(I6,2F12.3)]

****

Columns	Variable	Entry
*******	********	*****
1-6	JNU	Node number of loaded node
7-18	FF(1)	Load in X-direction
19-30	FF(2)	Load in Y-direction

****

-one node per card

-this card set must not appear if NLC=0

****

CARD TYPE NO. 10 - NODAL PRINT OUT CONTROL [Format(12I6)]

****

Columns	Variable	Entry
*******	********	*****
1-6	NNPR(I)	Nodal print out control indicator for node number I NNPR(I)= 0 print out and no rotation NNPR(I)=-1 do not print NNPR(I)= k print out and rotate an angle of k degrees. (k=an integer)
7-12	NNPR(I+1)	Nodal print out control indicator for node number I+1
13-18	NNPR(I+2)	Nodal print out control indicator for node number I+2
. . . . .	. . . . .	. . . . .
67-72	NNPR(I+5)	Nodal print out control indicator for node number I+5

****

-twelve nodes per card

****

CARD TYPE NO. 11 - ELEMENT PRINT OUT CONTROL [(Format (12I6)]

****

Columns	Variable	Entry
1-6	NEPR(I)	Element print out control indicator for element number I NEPR(I)= 0 Print out and no rotation NEPR(I)=-1 do not print NEPR(I)= k print out and rotate an angle of k degrees (k=an integer)
7-12	NEPR(I+1)	Element print out control indicator for element number I+1
13-18	NEPR(I+2)	Element print out control indicator for element number I+2
.	.	.
.	.	.
.	.	.
.	.	.
.	.	.
67-72	NEPR(I+5)	Element print out control indicator for element number I+5

****

-twelve elements per card

-if KV = 0 (i.e., an elastic solution only) no more data is required

-if a creep solution is desired, the following card sets must be included.

****

CARD TYPE NO. 12 - CREEP SOLUION CONTROL CARD [Format(F12.0,3I6)]

****

Columns	Variable	Entry
*******	********	*****
1-12	TDM	Maximum time allowed for creep solution
13-18	MNI	Maximum number of creep increments
19-24	NCPR	Creep solution print control NCPR=0 print all output NCPR=1 print selective output
25-30	NSPO	Total number ofcreep increments to be printed

****

****

CARD TYPE NO. 13 - CREEP SOLUTION PRINT CONTROL [Format (12I6)]

****

Columns	Variable	Entry
*******	********	*****
1-6	IPRIN(1)	The increment number for which the first set of creep results are to be printed
.	.	.
.	.	.
.	.	.
.	.	.
.	.	.
.	.	
.	IPRIN(IMAX)	The increment number for which the Ith set of creep results are to be printed (IMAX = NSPO)

****

****

CARD TYPE NO. 14 - CREEP MATERIAL PROPERTIES
[Format(2(E15.4,F5.2),F5.2)]

****

Columns *******	Variable ********	Entry *****
1-15	COEF1(I)	Coefficient in the creep law
16-20	EXP1(I)	Stress exponent in the creep law
21-35	COEF2(I)	Coefficient in the creep law
36-40	EXP2(I)	Stress exponent in the creep law
41-45	EXP3(I)	Time exponent in the creep law

****

-one card for each material

-the general form of the power law creep relationship is:

$$\dot{\varepsilon}_e = [A_1\sigma_e^{n_1} + A_2\sigma_e^{n_2}]\, t^m$$

where $\dot{\varepsilon}_e$ = effective strain rate

σ_e = effective strain

t = time

A_1, A_2 = coefficients

n_1, n_2 = creep exponents

m = time exponent

****

CARD TYPE NO. 15 - CREEP SOLUTION CONVERGENCE PARAMETERS
[Format(3f10.3)]

****

Columns *******	Variable ********	Entry *****
1-10	ETA0	Maximum ratio of effective elastic strain to increment of effective creep strain for first time interval
11-20	ETA1	Maximum ratio of effective elastic strain to increment of effective creep strain for succeeding time intervals
21-30	OMEGA	Maximum fractional change in effective stress allowed per creep increment

****

-to ensure convergence, ETA0, ETA1 and OMEGA should lie within the following ranges:

$$10 \le \text{ETA0} \le 25$$
$$1 \le \text{ETA1} \le 10$$
$$0.03 \le \text{OMEGA} \le 0.10$$

-default values have been set equal to:

ETA0 = 25
ETA1 = 10
OMEGA = 0.03

-these default values will produce the minimum time increment

****

CARD TYPE NO. 16 - NODE PRINT OUT CONTROL (CREEP SOLUTION ONLY) [Format(12I6)]

****

Columns	Variable	Entry
*******	********	*****
1-6	NNPR(I)	Node print out control indicator for node number I NNPR(I)= 0 print out and no rotation NNPR(I)=-1 do not print NNPR(I)= k print out and rotate an angle of k degrees (k=an integer)
7-12	NNPR(I+1)	Node print out control indicator for node number I+1
13-18	NNPR(I+2)	Node print out control indicator for node number I+2
.	.	.
.	.	.
.	.	.
.	.	.
.	.	.
67-72	NNPR(I+5)	Node print out control indicator for node number I+5

****

-twelve nodes per card

****

CARD TYPE NO. 17 - ELEMENT PRINT OUT CONTROL (CREEP SOLUTION ONLY) [Format (12I6)]

****

Columns	Variable	Entry
1-6	NEPR(I)	Element print out control indicator for element number I NEPR(I)= 0 Print out and no rotation NEPR(I)=-1 do not print NEPR(I)= k print out and rotate an angle of k degrees (k=an integer)
7-12	NEPR(I+1)	Element print out control indicator for element number I+1
13-18	NEPR(I+2)	Element print out control indicator for element number I+2
.	.	.
67-72	NEPR(I+5)	Element print out control indicator for element number I+5

****

-twelve elements per card

APPENDIX D

PROGRAMME LISTING FOR CREEP

C

```
MTS  FORTRAN IV G COMPILER(21.8) WITH SDS SUPPORT        MAIN        04-21-80     11:35:29          PAGE 0001
     1.000              C
     2.000              C
     3.000              C     *************************************************************
     4.000              C     *                                                           *
     5.000              C     * TITLE-- CREEP                                             *
     6.000              C     *                                                           *
     7.000              C     *         PURPOSE OF THIS PROGRAM IS TO CALCULATE ELASTIC   *
     8.000              C     *         DEFORMATIONS, ELASTIC STRESSES AND STRAINS, CREEP *
     9.000              C     *         DEFORMATIONS AND CREEP STRESSES AND STRAINS OF PLANE *
    10.000              C     *         STRAIN TYPE EARTH STRUCTURES                      *
    11.000              C     *                                                           *
    12.000              C     *         PROGRAM WAS ORIGINALLY WRITTEN BY J. EMERY AND    *
    13.000              C     *         T. NGUYEN AT MC MASTER UNIVERSITY, HAMILTON, ONTARIO *
    14.000              C     *         1976                                              *
    15.000              C     *         MINOR REVISIONS MADE BY P. WEERDENBURG AT THE     *
    16.000              C     *         UNIVERSITY OF ALBERTA, EDMONTON, ALBERTA          *
    17.000              C     *                                                           *
    18.000              C     *         CAPACITY OF PROGRAM:  MAX. # OF NODES     = 200   *
    19.000              C     *                               MAX. # OF ELEMENTS  = 300   *
    20.000              C     *                               MAX. # OF MATERIALS =  20   *
    21.000              C     *                                                           *
    22.000              C     *************************************************************
    23.000              C
    24.000              C
    25.000              C
    26.000              C-----COMMON AND DIMENSION STATEMENTS
    27.000              C
    28.000    0001            INTEGER*2 ND,NNPR,NEPR,MET,MMET,NP,NODES,IPRIN(200)
    29.000    0002            INTEGER*4 TITLE(20)
    30.000    0003            REAL*8 START/'   START'/,RSTART/'  RSTART'/,RUN/'     RUN'/,
    31.000                   &       STOP/'    STOP'/,PLOT/'    PLOT'/,CONTIN/'  CONTIN'/,
    32.000                   &       CODE1,CODE2
    33.000    0004            REAL*8 EI,UI,UNI,FN,F,FG,COEF1,COEF2,EXP1,EXP2,EXP3,
    34.000                   &       SM,PT,S,TAV,ARR,ARW
    35.000              C
    36.000    0005            COMMON /BLK1/ ND(200,2),X(200),Y(200)
    37.000              C
    38.000    0006            COMMON /BLK2/ MET(300),EI(20),UI(20),UNI(20)
    39.000              C
    40.000    0007            COMMON /BLK3/ FN(400),F(400),FG(400)
    41.000              C
    42.000    0008            COMMON /BLK5/ NNPR(200),NEPR(300)
    43.000              C
    44.000    0009            COMMON /BLK9/ PT(9),S(6,6),NP(6)
    45.000              C
    46.000    0010            COMMON /BLK10/ J,NI,NJ,NK,ARR,ARW
    47.000              C
    48.000    0011            COMMON /BLK11/ NN,NE,NUE,NOC,NGI,NLC,KV,NU,NB,NB1
    49.000              C
    50.000    0012            COMMON /BLK12/ JC,TIM,TAV,IPP,ITAPE,JTAPE
    51.000              C
    52.000    0013            COMMON /BLK13/ SM(5000)
    53.000              C
    54.000    0014            COMMON /BLK14/ NODES(300,3)
    55.000              C
```

```
MTS  FORTRAN IV G COMPILER(21.8) WITH SDS SUPPORT        MAIN        04-21-80     11:35:29          PAGE 0002
    56.000    0015            COMMON /BLK15/ ETAO,ETA1,OMEGA,RHO,BETA
    57.000              C
    58.000    0016            COMMON /BLK16/ MMET(300),COEF1(20),COEF2(20),EXP1(20),EXP2(20),
    59.000                   &             EXP3(20)
    60.000              C
    61.000    0017            COMMON /BLK17/ CODE1,CODE2
    62.000              C
    63.000              C
    64.000              C-----READ INPUT DATA
    65.000              C
    66.000    0018            READ(5,50)(TITLE(I),I=1,20)
    67.000    0019            WRITE(6,51)(TITLE(I),I=1,20)
    68.000    0020            READ(5,49)CODE1,CODE2
    69.000    0021            READ(5,3)ITAPE,JTAPE
    70.000    0022            IF(CODE1.EQ.RSTART)GOTO 68
    71.000    0023            READ(5,3)NN,NE,NUE,NUC,NGI,NLC,KV
    72.000    0024            WRITE(6,4)NN,NE,NUE,NUC
    73.000    0025            WRITE(6,12)
    74.000    0026            IF(NGI.EQ.0.AND.NLC.EQ.1)WRITE(6,13)
    75.000    0027            IF(NGI.EQ.1.AND.NLC.EQ.0)WRITE(6,14)
    76.000    0028            IF(NGI.EQ.1.AND.NLC.EQ.1)WRITE(6,15)
    77.000              C
    78.000              C-----NN = NUMBER OF NODES
    79.000              C-----NE = NUMBER OF ELEMENTS
    80.000              C-----NUE = NUMBER OF DIFFERENT MATERIALS FOR THE ELASTIC
    81.000              C           SOLUTION (MAXIMUM OF 20)
    82.000              C-----NUC = NUMBER OF DIFFERENT MATERIALS FOR THE CREEP
    83.000              C           SOLUTION (MAXIMUM OF 20)
    84.000              C-----NGI = GRAVITY LOADING CONDITION
    85.000              C                   NGI = 0  NO GRAVITY LOAD
    86.000              C                   NGI = 1  GRAVITY LOAD CONSIDERED
    87.000              C-----NLC = EXTERNAL LOAD CONDITION
    88.000              C                   NLC = 0  NO EXTERNAL LOADS APPLIED
    89.000              C                   NLC = 1  EXTERNAL LOADS CONSIDERED
    90.000              C-----KV = CREEP CONDITION
    91.000              C                   KV = 0  ONLY AN ELASTIC SOLUTION IS PERFORMED
    92.000              C                   KV = 1  CREEP CONSIDERED
    93.000              C
    94.000    0029            READ(5,5)((ND(I,J),J=1,2),X(I),Y(I),I=1,NN)
    95.000              C
    96.000              C-----ND(I,J).    FIXITY FACTORS FOR EACH NODE
    97.000              C                 ND(I,J) = 0  FIXED
    98.000              C                 ND(I,J) = 1  FREE
    99.000              C-----X(I) = X-COORDINATE FOR NODE I
   100.000              C-----Y(I) = Y-COORDINATE FOR NODE I
   101.000              C
   102.000    0030            WRITE(6,35)
   103.000    0031            WRITE(6,37)(I,(ND(I,J),J=1,2),X(I),Y(I),I=1,NN)
   104.000              C
   105.000    0032            REWIND 1
   106.000    0033            REWIND 2
   107.000    0034            NN2=2*NN
   108.000    0035            NU=1
   109.000    0036            DO 1 II=1,NN
   110.000    0037            DO 1 JJ=1,2
```

FINE PRINT

```
MTS  FORTRAN IV G COMPILER(21.8) WITH SDS SUPPORT          MAIN         04-21-80     11:35:29          PAGE 0003
   111.000     0038                IF(NO(II,JJ).EQ.0) GO TO 1
   112.000     0039                ND(II,JJ)=NU
   113.000     0040                NU=NU+1
   114.000     0041          1     CONTINUE
   115.000     0042                NU=NU-1
   116.000               C
   117.000     0043                DO 102 I=1,NUE
   118.000     0044                READ(5,6)EI(I),UI(I),UNI(I)
   119.000     0045          102   CONTINUE
   120.000               C
   121.000               C-----EI = ELASTIC MODULUS
   122.000               C-----UI = POISSON'S RATIO
   123.000               C-----UNI = UNIT WEIGHT
   124.000               C
   125.000     0046                SARR=0.0
   126.000     0047                IKK=0
   127.000     0048                IPP=0
   128.000     0049                NB=0
   129.000     0050                JC=0
   130.000               C
   131.000     0051                WRITE(6,23)
   132.000     0052                DO 104 I=1,NE
   133.000     0053                READ(5,8)(NODES(I,J),J=1,3),MET(I),MMET(I)
   134.000     0054                IF(MET(I).EQ.0)MET(I)=1
   135.000     0055                IF(MMET(I).EQ.0)MMET(I)=1
   136.000               C
   137.000               C-----NODES(I,J) = ELEMENT CORNER NODES (ENTERED COUNTERCLOCKWISE)
   138.000               C-----MET(I) = ELASTIC  MATERIAL NUMBER INDICATOR (UP TO 20)
   139.000               C-----MMET(I) = CREEP MATERIAL NUMBER INDICATOR (UP TO 20)
   140.000               C
   141.000     0056                WRITE(6,36)I,(NODES(I,J),J=1,3),MET(I),MMET(I)
   142.000     0057          104   CONTINUE
   143.000               C
   144.000     0058                DO 105 J=1,NE
   145.000     0059                NI=NODES(J,1)
   146.000     0060                NJ=NODES(J,2)
   147.000     0061                NK=NODES(J,3)
   148.000               C
   149.000               C-----DETERMINE THE ELEMENT AREA AND THE TRANSPOSE MATRIX P
   150.000               C
   151.000     0062                CALL GEOM
   152.000               C
   153.000     0063                MNE=MET(J)
   154.000     0064                UN=UNI(MNE)
   155.000     0065                ARW=(UN*ARR)/3.
   156.000     0066                SARR=SARR+ARR
   157.000               C
   158.000               C-----DETERMINE THE CODE NUMBERS, BAND WIDTH, AND THE NODAL
   159.000               C     GRAVITY LOADING FOR EACH ELEMENT
   160.000               C
   161.000     0067                CALL CNODE
   162.000               C
   163.000               C-----CALCULATE THE ELEMENT STIFFNESS MATRIX S
   164.000               C
   165.000     0068                CALL FSM
```

```
MTS  FORTRAN IV G COMPILER(21.8) WITH SDS SUPPORT        MAIN        04-21-80     11:35:29        PAGE 0004
  166.000              C
  167.000              C-----WRITE ELEMENT DATA ON TAPE
  168.000              C
  169.000    0069            WRITE(1)(NP(I),I=1,6),(PT(K),K=1,9),ARR
  170.000    0070            WRITE(2)(NP(I),I=1,6),((S(MM,MN),MN=1,6),MM=1,6)
  171.000              C
  172.000    0071      105   CONTINUE
  173.000              C
  174.000    0072            REWIND 1
  175.000    0073            REWIND 2
  176.000              C
  177.000              C-----CHECK TO ENSURE THE PROBLEM DOES NOT EXCEED THE PROGRAM
  178.000              C     CAPACITY
  179.000              C
  180.000    0074            NB1=NB+1
  181.000    0075            NV=NB1*NU
  182.000    0076            WRITE(6,999)NB
  183.000    0077            IF(NV.LE.5000)GOTO 122
  184.000    0078            WRITE(6,17)NV
  185.000    0079            STOP
  186.000    0080      122   CONTINUE
  187.000              C
  188.000              C-----ASSEMBLE STRUCTURE STIFFNESS MATRIX
  189.000              C
  190.000    0081            DO 40 JL=1,NV
  191.000    0082            SM(JL)=0.0
  192.000    0083      40    CONTINUE
  193.000    0084            DO 20 KJJ=1,NE
  194.000    0085            READ(2)(NP(I),I=1,6),((S(MM,MN),MN=1,6),MM=1,6)
  195.000    0086            DO 7 JJ=1,6
  196.000    0087            IF(NP(JJ).EQ.0)GOTO 7
  197.000    0088            DO 11 II=JJ,6
  198.000    0089            IF(NP(II).EQ.0)GOTO 11
  199.000    0090            IF(NP(JJ)-NP(II))9,10,10
  200.000    0091      10    K=(NP(II)-1)*NB+NP(JJ)
  201.000    0092            SM(K)=SM(K)+S(JJ,II)
  202.000    0093            GOTO 11
  203.000    0094      9     K=(NP(JJ)-1)*NB+NP(II)
  204.000    0095            SM(K)=SM(K)+S(JJ,II)
  205.000    0096      11    CONTINUE
  206.000    0097      7     CONTINUE
  207.000    0098      20    CONTINUE
  208.000    0099            REWIND 2
  209.000              C
  210.000              C     ******************************
  211.000              C     *                            *
  212.000              C     *   START ELASTIC SOLUTION   *
  213.000              C     *                            *
  214.000              C     ******************************
  215.000              C
  216.000              C
  217.000              C-----READ IN EXTERNAL LOADS AND SET UP NODAL LOAD VECTOR
  218.000              C
  219.000    0100            IF(NGI.EQ.1.AND.NLC.EQ.0)GOTO 22
  220.000              C
```

```
MTS  FORTRAN IV G COMPILER(21.8) WITH SDS SUPPORT          MAIN          04-21-80    11:35:29          PAGE 0005
  221.000    0101               CALL NLOAD
  222.000               C
  223.000    0102       22      CONTINUE
  224.000    0103               DO 124 JJ=1,NU
  225.000    0104               F(JJ)=0.0
  226.000    0105               F(JJ)=F(JJ)+FG(JJ)
  227.000    0106               FN(JJ)=FG(JJ)
  228.000    0107       124     CONTINUE
  229.000               C
  230.000               C-----PRINT OUT NODAL LOADS
  231.000               C
  232.000    0108               WRITE(6,28)
  233.000    0109               WRITE(6,18)
  234.000    0110               DO 16 I=1,NUE
  235.000    0111       16      WRITE(6,19)I,EI(I),UI(I),UNI(I)
  236.000    0112               WRITE(6,80)
  237.000               C
  238.000    0113               CALL CNLP
  239.000               C
  240.000               C-----SOLVE FOR THE ELASTIC DISPLACEMENTS
  241.000               C
  242.000    0114               CALL BAND(1)
  243.000               C
  244.000               C-----PRINT OUT THE ELASTIC DISPLACEMENTS
  245.000               C
  246.000    0115               WRITE(6,30)
  247.000               C
  248.000    0116               CALL CNDI
  249.000               C
  250.000               C-----READ IN THE NODAL AND ELEMENT PRINT OUT CONTROL VECTORS
  251.000               C
  252.000    0117               READ(5,3)(NNPR(II),II=1,NN)
  253.000               C
  254.000               C-----NNPR(II) = NODAL PRINT OUT CONTROL
  255.000               C                   NNPR(II) =  0  PRINT OUT AND NO ROTATION
  256.000               C                   NNPR(II) = -1  DO NOT PRINT
  257.000               C                   NNPR(II) =  K  PRINT OUT AND ROTATE AN ANGLE OF K
  258.000               C                                  DEGREES
  259.000               C
  260.000    0118               READ(5,3)(NEPR(II),II=1,NE)
  261.000               C
  262.000               C-----NEPR(II) = ELEMENT PRINT OUT CONTROL
  263.000               C                   NEPR(II) =  0  PRINT OUT AND NO ROTATION
  264.000               C                   NEPR(II) = -1  DO NOT PRINT
  265.000               C                   NEPR(II) =  K  PRINT OUT AND ROTATE AN ANGLE OF K
  266.000               C                                  DEGREES
  267.000               C
  268.000               C-----PRINT OUT THE ELASTIC ELEMENT STRAINS AND STRESSES
  269.000               C
  270.000    0119               WRITE(6,33)
  271.000    0120               WRITE(6,46)
  272.000               C
  273.000    0121               CALL CESS
  274.000               C
  275.000               C-----CALCULATE AND PRINT OUT THE AVERAGE NODAL STRESSES
```

```
MTS  FORTRAN IV G COMPILER(21.8) WITH SDS SUPPORT        MAIN        04-21-80     11:35:29         PAGE 0006

  276.000                 C
  277.000     0122              WRITE(6,34)
  278.000     0123              WRITE(6,47)
  279.000                 C
  280.000     0124              CALL CNAVE
  281.000                 C
  282.000     0125              IF(KV.EQ.O) STOP
  283.000                 C
  284.000                 C     ***************************
  285.000                 C     *                         *
  286.000                 C     *   START CREEP SOLUTION  *
  287.000                 C     *                         *
  288.000                 C     ***************************
  289.000                 C
  290.000     0126              WRITE(6,900)
  291.000     0127              WRITE(6,42)
  292.000                 C
  293.000                 C-----READ ALL THE NECESSARY DATA OFF OF TAPE IF THE CURRENT RUN
  294.000                 C     IS A CONTINUATION OF A PREVIOUS PROBLEM THAT WAS TERMINATED
  295.000                 C     EARLY
  296.000                 C
  297.000     0128        68    IF(CODE1.EQ.RSTART)CALL INPUT
  298.000                 C
  299.000                 C-----CONTROL AND TYPE OF CREEP SOLUTION REQUIRED.
  300.000                 C
  301.000     0129              READ(5,57)TDM,MNI,NCPR,NSPO
  302.000                 C
  303.000                 C-----TDM = MAXIMUM TIME ALLOWED FOR CREEP SOLUTION
  304.000                 C-----MNI = MAXIMUM NUMBER OF CREEP INCREMENTS
  305.000                 C-----NCPR = PRINT CONTROL
  306.000                 C                NCPR = O  PRINT ALL OUTPUT
  307.000                 C                NCPR = 1  PRINT SELECTIVE OUTPUT
  308.000                 C-----NSPO = TOTAL NUMBER OF CREEP INCREMENTS TO BE PRINTED
  309.000                 C
  310.000     0130              READ(5,3)(IPRIN(I),I=1,NSPO)
  311.000                 C
  312.000                 C-----IPRIN(I) = VECTOR CONTAINING THE INCREMENT NUMBERS FOR WHICH
  313.000                 C                THE CREEP RESULTS ARE TO BE PRINTED
  314.000                 C
  315.000     0131              IF(CODE1.EQ.RSTART)GOTO 70
  316.000                 C
  317.000                 C-----READ CREEP MATERIAL PROPERTIES
  318.000                 C
  319.000     0132              WRITE(6,65)
  320.000     0133              DO 69 I=1,NUC
  321.000     0134              READ(5,62)COEF1(I),EXP1(I),COEF2(I),EXP2(I),EXP3(I)
  322.000     0135              IF(EXP3(I).EQ.O.O)EXP3(I)=1.O
  323.000                 C
  324.000                 C-----COEF1(I),COEF2(I) = COEFFICIENTS IN THE CREEP LAW
  325.000                 C-----EXP1(I),EXP2(I) = STRESS EXPONENTS IN THE CREEP LAW
  326.000                 C-----EXP3(I) = TIME EXPONENT IN THE CREEP LAW
  327.000                 C
  328.000     0136              WRITE(6,66)I,COEF1(I),COEF2(I),EXP1(I),EXP2(I),EXP3(I)
  329.000     0137        69    CONTINUE
  330.000                 C
```

```
MTS  FORTRAN IV G COMPILER(21.8) WITH SDS SUPPORT        MAIN        04-21-80     11:35:28        PAGE 0007
   331.000     0138              READ(5,21)ETAO,ETA1,OMEGA
   332.000               C
   333.000               C-----ETAO,ETA1,OMEGA = CREEP SOLUTION CONVERGENCE PARAMETERS
   334.000               C
   335.000     0139              IF(ETAO.EQ.0.0)ETAO=25.
   336.000     0140              IF(ETA1.EQ.0.0)ETA1=1.
   337.000     0141              IF(OMEGA.EQ.0.0)OMEGA=0.1
   338.000     0142              WRITE(6,24)ETAO,ETA1,OMEGA
   339.000               C
   340.000     0143      70      IF(NCPR.EQ.0)GOTO 71
   341.000     0144              READ(5,3)(NNPR(II),II=1,NN)
   342.000     0145              READ(5,3)(NEPR(II),II=1,NE)
   343.000     0146              GOTO 74
   344.000     0147      71      CONTINUE
   345.000     0148              DO 72 II=1,NN
   346.000     0149      72      NNPR(II)=0
   347.000     0150              DO 73 II=1,NE
   348.000     0151      73      NEPR(II)=0
   349.000               C
   350.000     0152      74      IPR=1
   351.000     0153              IF(CODE1.EQ.START)TIM=0.0
   352.000               C
   353.000               C-----THIS SECTION PROVIDES THE NON-LINEAR CREEP SOLUTION.
   354.000               C
   355.000     0154      501     JC=JC+1
   356.000     0155              IKK=IKK+1
   357.000     0156              IPP=1
   358.000     0157              IF(JC.EQ.IPRIN(IPR))IPP=0
   359.000     0158              IF(IPP.EQ.0)IPR=IPR+1
   360.000               C
   361.000               C-----GENERATE THE TIME INTERVAL FOR THE INCREMENT OF CREEP
   362.000               C
   363.000     0159              CALL TIMGEN
   364.000               C
   365.000     0160              TIM=TIM+TAV
   366.000     0161              IF(IPP.EQ.0)GOTO 480
   367.000     0162              WRITE(6,53)JC,TAV,TIM
   368.000     0163              GO TO 1544
   369.000     0164      480     IF(JC.GT.1)WRITE(6,900)
   370.000     0165              WRITE(6,53)JC,TAV,TIM
   371.000     0166      1544    CONTINUE
   372.000               C
   373.000               C-----COMPUTE THE CREEP STRAIN INCREMENTS AND THE INCREMENTAL
   374.000               C     FICTICOUS LOAD VECTOR
   375.000               C
   376.000     0167              CALL TSME
   377.000               C
   378.000               C-----SUM THE FORCES TO OBTAIN TOTAL APPLIED LOAD
   379.000               C
   380.000     0168              DO 505 JJ=1,NU
   381.000     0169              F(JJ)=F(JJ)+FN(JJ)
   382.000     0170      505     CONTINUE
   383.000               C
   384.000               C-----PRINT THE INCREMENTAL AND TOTAL NODAL LOADS
   385.000               C
```

```
MTS  FORTRAN IV G COMPILER(21.8) WITH SDS SUPPORT          MAIN        04-21-80     11:35:29          PAGE 0008
   386.000     0171               IF(IPP.EQ.1)GOTO 81
   387.000     0172               WRITE(6,54)JC
   388.000              C
   389.000     0173               CALL CNLP
   390.000              C
   391.000              C-----SOLVE FOR THE NEW INCREMENTAL NODAL DISPLACEMENTS
   392.000              C
   393.000     0174     81        CALL BAND(2)
   394.000              C
   395.000              C-----PRINT THE INCREMENTAL AND TOTAL NODAL DISPLACEMENTS
   396.000              C
   397.000     0175               IF(IPP.EQ.1)GOTO 1545
   398.000     0176               WRITE(6,55)JC
   399.000     0177     1545      CONTINUE
   400.000              C
   401.000     0178               CALL CNDI
   402.000              C
   403.000              C-----PRINT OUT THE TOTAL AND INCREMENTAL ELEMENT STRAINS AND
   404.000              C     STRESSES
   405.000              C
   406.000     0179               IF(IPP.EQ.1)GOTO 1546
   407.000     0180               WRITE(6,56)JC
   408.000     0181               WRITE(6,46)
   409.000     0182     1546      CONTINUE
   410.000              C
   411.000     0183               CALL CESS
   412.000              C
   413.000              C-----COMPUTE AND PRINT OUT THE TOTAL AND INCREMENTAL AVERAGE
   414.000              C     NODAL STRESSES
   415.000              C
   416.000     0184               IF(IPP.EQ.1)GOTO 1547
   417.000     0185               WRITE(6,58)JC
   418.000     0186               WRITE(6,47)
   419.000     0187     1547      CONTINUE
   420.000              C
   421.000     0188               CALL CNAVE
   422.000              C
   423.000              C-----CHECK TO SEE IF A STEADY STATE CONDITION HAS BEEN ACHIEVED
   424.000              C
   425.000     0189               CALL STEADY
   426.000              C
   427.000              C-----CHECK TO SEE IF THE MAXIMUM TIME OR MAXIMUM NUMBER OF
   428.000              C     INCREMENTS HAVE BEEN EXCEEDED
   429.000              C
   430.000     0190               IF(TIM.LT.TDM.AND.JC.LT.MNI)GOTO 501
   431.000     0191               IF(TIM.GE.TDM) WRITE(6,60)TIM,TDM
   432.000     0192               IF(JC.GE.MNI)WRITE(6,61)JC,MNI
   433.000              C
   434.000              C-----WRITE THE COMPLETE SET OF RESULTS FOR THE FINAL CREEP
   435.000              C     INCREMENT AND WRITE THE NECESSARY DATA ON TAPE IF A
   436.000              C     CONTINUATION IS DESIRED AT A LATER DATE
   437.000              C
   438.000     0193               CALL FINAL
   439.000              C
   440.000              C-----FORMAT STATEMENTS
```

```
MTS  FORTRAN IV G COMPILER(21.8) WITH SDS SUPPORT        MAIN        04-21-80     11:35:29          PAGE 0009

  441.000                   C
  442.000     0194          3    FORMAT(12I6)
  443.000     0195          4    FORMAT(/////2X,45('*')/2X,'*',43X,'*'/2X,'* INPUT DATA ',
  444.000                      &       'DESCRIBING THE FINITE ELEMENTS *'/2X,'*',43X,'*'/2X,
  445.000                      &       45('*'),///5X,'NUMBER OF NODES     =',I5,/5X,'NUMBER OF ',
  446.000                      &       'ELEMENTS =',I5,/5X,'NUMBER OF MATERIALS FOR ELASTIC ',
  447.000                      &       'SOLUTION =',I5,/5X,'NUMBER OF MATERIALS FOR CREEP ',
  448.000                      &       'SOLUTION    =',I5/)
  449.000     0196          5    FORMAT(3(4X,2I3,2F7.3))
  450.000     0197          6    FORMAT(F12.0,2F6.3)
  451.000     0198          8    FORMAT(6X,5I6)
  452.000     0199         12    FORMAT(//5X,'LOADING CASES CONSIDERED:')
  453.000     0200         13    FORMAT('+',31X,'EXTERNAL LOADING ONLY')
  454.000     0201         14    FORMAT('+',31X,'GRAVITY LOADING ONLY')
  455.000     0202         15    FORMAT('+',31X,'EXTERNAL + GRAVITY LOADING')
  456.000     0203         17    FORMAT(1X,'SIZE OF THE PROBLEM IS. ',I6,'  PROGRAM CAPACITY ',
  457.000                      &       'EXCEEDED.')
  458.000     0204         18    FORMAT(///5X,'MATERIAL PROPERTIES:')
  459.000     0205         19    FORMAT(/5X,'MATERIAL NO.',I3,3X,'YOUNGS MODULUS = ',1PE15.4,/23X,
  460.000                      &       'POISSONS RATIO = ',0PF15.3,/23X,'UNIT WEIGHT      = ',
  461.000                      &       1PE15.4)
  462.000     0206         21    FORMAT(3F10.3)
  463.000     0207         23    FORMAT(///5X,'ELEMENT INCIDENCE LIST (NODES ENTERED COUNTER-',
  464.000                      &       'CLOCKWISE)'//5X,'ELEMENT     I-NODE     J-NODE     K-NODE',
  465.000                      &       '      MATERIAL NUMBER     CREEP LAW INDICATOR'/)
  466.000     0208         24    FORMAT(//5X,'CREEP SOLUTION CONVERGENCE PARAMETERS:  ETAO  = ',
  467.000                      &       F6.2/45X,'ETA1  = ',F6.2/45X,'OMEGA = ',F6.2)
  468.000     0209         28    FORMAT('1'///2X,28('*')/2X,'*',26X,'*'/2X;'* ELASTIC SOLUTION',
  469.000                      &       ' RESULTS *'/2X,'*',26X,'*'/2X,28('*'))
  470.000     0210         30    FORMAT(///5X,'NODAL DISPLACEMENTS',//5X,'NODE     X-DISPLACEMENT',
  471.000                      &       '     Y-DISPLACEMENT',/)
  472.000     0211         33    FORMAT(///5X,'ELEMENT STRAINS AND STRESSES')
  473.000     0212         34    FORMAT(///5X,'AVERAGE NODAL STRESSES')
  474.000     0213         35    FORMAT(///5X,'NODAL POINT DATA'//2(5X,'NODE       FIXITY CODE',
  475.000                      &       '       NODAL POINT COORDINATES',5X)/2(5X,'NUMBER',7X,
  476.000                      &       'X   Y',12X,'X-COORD      Y-COORD',5X)/)
  477.000     0214         36    FORMAT(5X,I5,1X,3I10,11X,I2,18X,I2)
  478.000     0215         37    FORMAT(2(5X,I4,6X,2I4,7X,2F12.3,5X))
  479.000     0216         42    FORMAT(///2X,26('*')/2X,'*',24X,'*'/2X,'* CREEP SOLUTION RESULTS *
  480.000                      &       '/2X,'*',24X,'*'/2X,26('*')/)
  481.000     0217         46    FORMAT(/5X,'ELEMENT    X-STRAIN    Y-STRAIN   XY-STRAIN    X-STRESS',
  482.000                      &       '   Y-STRESS  XY-STRESS  MAXSTRESS  MINSTRESS    MAXSHEAR',
  483.000                      &       '  DIRECTION'/)
  484.000     0218         47    FORMAT(/5X,'NODE     X-STRESS     Y-STRESS     XY-STRESS  MAX STRESS',
  485.000                      &       '  MIN STRESS   MAX SHEAR    DIRECTION'/)
  486.000     0219         49    FORMAT(2A8)
  487.000     0220         50    FORMAT(20A4)
  488.000     0221         51    FORMAT('1',//2X,'TITLE OF PROBLEM :   ',20A4)
  489.000     0222         53    FORMAT(//2X,'CREEP INCREMENT NUMBER',I5,5X,'INCREMENT OF TIME  =',
  490.000                      &       1PE13.3/2X,27('*'),5X,'TOTAL ELAPSED TIME =',1PE13.3)
  491.000     0223         54    FORMAT(///5X,'NODAL LOADS DUE TO CREEP INCREMENT',I4//14X,
  492.000                      &       'INCREMENT OF LOAD    TOTAL APPLIED LOAD'/5X,'NODE',
  493.000                      &       2('      X-LOAD      Y-LOAD')/)
  494.000     0224         55    FORMAT(///5X,'NODAL DISPLACEMENTS AND DISPLACEMENT RATE DUE TO ',
  495.000                      &       'CREEP INCREMENT',I5//18X,'INCREMENT OF DISPLACEMENT',8X,
```

FINE PRINT

```
          &        'TOTAL ACCUMULATED DISPLACEMENT',14X,'DISPLACEMENT RATE'/
          &        5X,'NODE',1X,2('    X-DISPLACEMENT     Y-DISPLACEMENT'),
          &        8X,'X-VELOCITY',8X,'Y-VELOCITY'/)
   56     FORMAT(///5X,'ELEMENT STRAINS AND STRESSES DUE TO CREEP ',
          &        'INCREMENT',I4/7X,'(FIRST LINE GIVES TOTAL, SECOND LINE ',
          &        'GIVES INCREMENT)')
   57     FORMAT(F12.0,5I6)
   58     FORMAT(///5X,'AVERAGE NODAL STRESSES FOR CREEP INCREMENT',I4/7X,
          &        '(FIRST LINE GIVES TOTAL, SECOND LINE GIVES INCREMENT)')
   60     FORMAT(//1X,F12.0,' MINUTES EXCEEDS OR EQUALS THE MAXIMUM TIME ',
          &        'OF',1F12.0,'  MINUTES REQUESTED, SOLUTION TERMINATED')
   61     FORMAT(//2X,'CREEP INCREMENT #',I5,' EXCEEDS THE MAXIMUM OF',I5,
          &        ' REQUESTED, SOLUTION TERMINATED'/)
   62     FORMAT(2(E15.4,F5.2),F5.2)
   65     FORMAT(///5X,'CREEP LAW PARAMETERS:')
   66     FORMAT(/5X,'CREEP LAW NO.',I3,3X,2('COEFFICIENT = ',1PE11.3,5X),
          &        /24X,2('EXPONENT     = ',0PF11.3,5X)/35X,'TIME EXPONENT = ',
          &        1PE10.3)
   78     FORMAT(18I4)
   80     FORMAT(///5X,'NODAL LOADS'//5X,'NODE      X-LOAD      Y-LOAD'/)
  900     FORMAT('1')
  999     FORMAT(///2X,'HALF BANDWIDTH = ',I5)
          STOP
          END
```

```
MTS   FORTRAN IV G COMPILER(21.8) WITH SDS SUPPORT        MAIN        04-21-80     11:35:34        PAGE 0001
   520.000                C
   521.000                C      ***********************************************************
   522.000                C      *                                                         *
   523.000                C      *                            GEOM                         *
   524.000                C      *                                                         *
   525.000                C      ***********************************************************
   526.000                C
   527.000                C
   528.000     0001             SUBROUTINE GEOM
   529.000                C
   530.000                C
   531.000                CCCCCCCCCCCCCCCCCCCCCCCCCCCCCCCCCCCCCCCCCCCCCCCCCCCCCCCCCCCCCCCCCCCCCCCC
   532.000                C
   533.000                C     SUBROUTINE GEOM - DETERMINES THE ELEMENT AREA AND THE TRANSPOSE  C
   534.000                C                       MATRIX FOR EACH ELEMENT                         C
   535.000                C                                                                      C
   536.000                C     DATA REQIURED FROM COMMON BLOCKS                                 C
   537.000                C                                                                      C
   538.000                C     J          = ELEMENT NUMBER                                      C
   539.000                C     XI, XJ, XK = X-COORDINATES OF CORNER NODES I, J, AND K,          C
   540.000                C                  RESPECTIVELY                                        C
   541.000                C     YI, YJ, YK = Y-COORDINATES OF CORNER NODES I, J, AND K,          C
   542.000                C                  RESPECTIVELY                                        C
   543.000                C                                                                      C
   544.000                C     OUTPUT PLACED IN BLK9 AND BLK10                                  C
   545.000                C                                                                      C
   546.000                C     PT  = MATRIX CONTAINING THE COEFFICIENTS OF THE SHAPE            C
   547.000                C           FUNCTIONS                                                  C
   548.000                C     ARR = AREA OF ELEMENT #J                                         C
   549.000                C                                                                      C
   550.000                CCCCCCCCCCCCCCCCCCCCCCCCCCCCCCCCCCCCCCCCCCCCCCCCCCCCCCCCCCCCCCCCCCCCCCCC
   551.000                C
   552.000                C
   553.000                C-----COMMON AND DIMENSION STATEMENTS
   554.000                C
   555.000     0002             REAL*8  PT,ARR
   556.000     0003             INTEGER*2 ND,NP
   557.000                C
   558.000     0004             COMMON /BLK1/ ND(200,2),X(200),Y(200)
   559.000                C
   560.000     0005             COMMON /BLK9/ PT(9)
   561.000                C
   562.000     0006             COMMON /BLK10/ J,NI,NJ,NK,ARR
   563.000                C
   564.000                C-----SELECT X AND Y COORDINATES FOR ELEMENT
   565.000                C
   566.000     0007             XI=X(NI)
   567.000     0008             YI=Y(NI)
   568.000     0009             XJ=X(NJ)
   569.000     0010             YJ=Y(NJ)
   570.000     0011             XK=X(NK)
   571.000     0012             YK=Y(NK)
   572.000                C
   573.000                C-----CALCULATE AREA OF ELEMENT
   574.000                C
```

```
MTS  FORTRAN IV G COMPILER(21.8) WITH SDS SUPPORT        GEOM        04-21-80     11:35:34          PAGE 0002
   575.000    0013                 ARR=((XI-XJ)*(YI-YK)-(XI-XK)*(YI-YJ))/2.
   576.000    0014                 IF(ARR.GT.0.0)GOTO 1
   577.000    0015                 WRITE(6,10)J
   578.000    0016                 STOP
   579.000               C
   580.000               C-----COMPUTE COEFFICIENTS OF THE SHAPE FUNCTIONS
   581.000               C
   582.000    0017       1         PT(1)=XJ*YK-XK*YJ
   583.000    0018                 PT(2)=XK*YI-XI*YK
   584.000    0019                 PT(3)=XI*YJ-XJ*YI
   585.000    0020                 PT(4)=YJ-YK
   586.000    0021                 PT(5)=YK-YI
   587.000    0022                 PT(6)=YI-YJ
   588.000    0023                 PT(7)=XK-XJ
   589.000    0024                 PT(8)=XI-XK
   590.000    0025                 PT(9)=XJ-XI
   591.000               C
   592.000               C-----FORMAT STATEMENTS
   593.000               C
   594.000    0026       10        FORMAT(//5X,'ERROR: ELEMENT NUMBER',I4,' HAS A NEGATIVE AREA, ',
   595.000                        &'SOLUTION TERMINATED')
   596.000    0027                 RETURN
   597.000    0028                 END
```

FINE PRINT

```
MTS  FORTRAN IV G COMPILER(21.8) WITH SDS SUPPORT        MAIN        04-21-80     11:35:34          PAGE 0001
    598.000                 C
    599.000                 C     ****************************************************************
    600.000                 C     *                                                              *
    601.000                 C     *                            CNODE                             *
    602.000                 C     *                                                              *
    603.000                 C     ****************************************************************
    604.000                 C
    605.000                 C
    606.000     0001              SUBROUTINE CNODE
    607.000                 C
    608.000                 C
    609.000                 CCCCCCCCCCCCCCCCCCCCCCCCCCCCCCCCCCCCCCCCCCCCCCCCCCCCCCCCCCCCCCCCCCCCCCCC
    610.000                 C                                                                      C
    611.000                 C     SUBROUTINE CNODE - DETERMINES THE CODE NUMBERS, THE BAND WIDTH   C
    612.000                 C                        AND THE NODAL GRAVITY LOADS FOR EACH          C
    613.000                 C                        ELEMENT                                       C
    614.000                 C                                                                      C
    615.000                 C     DATA REQIURED FROM COMMON BLOCKS                                 C
    616.000                 C                                                                      C
    617.000                 C     J   = ELEMENT NUMBER                                             C
    618.000                 C     NU  = TOTAL NUMBER OF UNKNOWNS IN CURRENT PROBLEM                C
    619.000                 C     ND  = RESTRAINED CODE MATRIX                                     C
    620.000                 C     NI  = CORNER NODE I                                              C
    621.000                 C     NJ  = CORNER NODE J                                              C
    622.000                 C     NK  = CORNER NODE K                                              C
    623.000                 C     ARW = PORTION(1/3) OF WEIGHT OF ELEMENT #J TO BE ADDED TO        C
    624.000                 C           EACH CORNER NODE                                           C
    625.000                 C                                                                      C
    626.000                 C     OUTPUT PLACED IN BLK3, BLK9 AND BLK11                            C
    627.000                 C                                                                      C
    628.000                 C     NB = MAXIMUM HALF BAND WIDTH OF CURRENT PROBLEM                  C
    629.000                 C     NP = DEGREE OF FREEDOM CODE MATRIX.                              C
    630.000                 C     FG = GRAVITY LOAD VECTOR                                         C
    631.000                 C                                                                      C
    632.000                 CCCCCCCCCCCCCCCCCCCCCCCCCCCCCCCCCCCCCCCCCCCCCCCCCCCCCCCCCCCCCCCCCCCCCCCC
    633.000                 C
    634.000                 C
    635.000                 C-----DIMENSION STATEMENTS
    636.000                 C
    637.000     0002              REAL*8 FN,F,FG,ARR,ARW,PT,S
    638.000     0003              INTEGER*2 ND,NP
    639.000                 C
    640.000     0004              COMMON /BLK1/ ND(200,2)
    641.000                 C
    642.000     0005              COMMON /BLK3/ FN(400),F(400),FG(400)
    643.000                 C
    644.000     0006              COMMON /BLK9/ PT(9),S(6,6),NP(6)
    645.000                 C
    646.000     0007              COMMON /BLK10/ J,NI,NJ,NK,ARR,ARW
    647.000                 C
    648.000     0008              COMMON /BLK11/ NN,NE,NUE,NUC,NGI,NLC,KV,NU,NB,NB1
    649.000                 C
    650.000                 C-----INITIALIZATION
    651.000                 C
    652.000     0009              IF(J.NE.1)GOTO 13
```

```
MTS  FORTRAN IV G COMPILER(21.8) WITH SDS SUPPORT        CNODE        04-21-80     11:35:34          PAGE 0002
   653.000     0010                 NB=0
   654.000     0011                 DO 12 IJ=1,NJ
   655.000     0012                 FG(IJ)=0.0
   656.000     0013          12     CONTINUE
   657.000     0014          13     CONTINUE
   658.000                  C
   659.000                  C-----SET UP DEGREE OF FREEDOM CODE MATRIX
   660.000                  C
   661.000     0015                 NP(1)=ND(NI,1)
   662.000     0016                 NP(2)=ND(NJ,1)
   663.000     0017                 NP(3)=ND(NK,1)
   664.000     0018                 NP(4)=ND(NI,2)
   665.000     0019                 NP(5)=ND(NJ,2)
   666.000     0020                 NP(6)=ND(NK,2)
   667.000                  C
   668.000                  C-----COMPUTE NODAL LOADS DUE TO GRAVITY.
   669.000                  C
   670.000     0021                 IF(ND(NI,2).EQ.0)GOTO 10
   671.000     0022                 IK=ND(NI,2)
   672.000     0023                 FG(IK)=FG(IK)-ARW
   673.000     0024          10     CONTINUE
   674.000     0025                 IF(ND(NJ,2).EQ.0)GOTO 11
   675.000     0026                 IK=ND(NJ,2)
   676.000     0027                 FG(IK)=FG(IK)-ARW
   677.000     0028          11     CONTINUE
   678.000     0029                 IF(ND(NK,2).EQ.0)GOTO 25
   679.000     0030                 IK=ND(NK,2)
   680.000     0031                 FG(IK)=FG(IK)-ARW
   681.000     0032          25     CONTINUE
   682.000                  C
   683.000                  C-----COMPUTE THE MAXIMUM HALF BAND WIDTH OF CURRENT PROBLEM
   684.000                  C
   685.000     0033                 MAX=0
   686.000     0034                 MIN=3000
   687.000     0035                 DO 5 KK=1,6
   688.000     0036                 IF(NP(KK).EQ.0)GOTO 5
   689.000     0037                 IF(NP(KK)-MAX)6,6,7
   690.000     0038           7     MAX=NP(KK)
   691.000     0039           6     IF(NP(KK)-MIN)8.5,5
   692.000     0040           8     MIN=NP(KK)
   693.000     0041           5     CONTINUE
   694.000     0042                 NB1=MAX-MIN
   695.000     0043                 IF(NB1.GT.NB) NB=NB1
   696.000     0044                 RETURN
   687.000     0045                 END
```

```
MTS  FORTRAN IV G COMPILER(21.8) WITH SDS SUPPORT        MAIN        04-21-80     11:35:35        PAGE 0001
   698.000                 C
   699.000                 C    *************************************************************
   700.000                 C    *                                                           *
   701.000                 C    *                             FSM                           *
   702.000                 C    *                                                           *
   703.000                 C    *************************************************************
   704.000                 C
   705.000                 C
   706.000    0001               SUBROUTINE FSM
   707.000                 C
   708.000                 C
   709.000                 CCCCCCCCCCCCCCCCCCCCCCCCCCCCCCCCCCCCCCCCCCCCCCCCCCCCCCCCCCCCCCCCC
   710.000                 C                                                                C
   711.000                 C     SUBROUTINE FSM - DETERMINES THE INDIVIDUAL ELEMENT STIFFNESS C
   712.000                 C                      MATRICIES                                 C
   713.000                 C                                                                C
   714.000                 C     DATA REQIURED FROM COMMON BLOCKS                           C
   715.000                 C                                                                C
   716.000                 C     PT  = MATRIX CONTAINING THE COEFFICIENTS OF THE SHAPE FUNCTIONS C
   717.000                 C     E   = YOUNG'S MODULUS                                      C
   718.000                 C     U   = POISSON'S RATIO                                      C
   719.000                 C     ARR = AREA OF ELEMENT                                      C
   720.000                 C                                                                C
   721.000                 C     OUTPUT PLACED IN BLK9                                      C
   722.000                 C                                                                C
   723.000                 C     S = ELEMENT STIFFNESS MATRIX                               C
   724.000                 C                                                                C
   725.000                 CCCCCCCCCCCCCCCCCCCCCCCCCCCCCCCCCCCCCCCCCCCCCCCCCCCCCCCCCCCCCCCCCC
   726.000                 C
   727.000                 C
   728.000                 C-----COMMON AND DIMENSION STATEMENTS
   729.000                 C
   730.000                 C
   731.000    0002               REAL*8 PT,S,ARR,EI,UI,E,U,EU,R(6,6),P(6,6)
   732.000    0003               INTEGER*2 MET,NP
   733.000                 C
   734.000    0004               COMMON /BLK2/ MET(300),EI(20),UI(20)
   735.000                 C
   736.000    0005               COMMON /BLK8/ PT(9),S(6,6),NP(6)
   737.000                 C
   738.000    0006               COMMON /BLK10/ J,NI,NJ,NK,ARR
   739.000                 C
   740.000                 C-----INITIALIZATION
   741.000                 C
   742.000    0007               DO 1 II=1,6
   743.000    0008               DO 1 JJ=1,6
   744.000    0009               S(II,JJ)=0.0
   745.000    0010               P(II,JJ)=0.0
   746.000    0011           1   CONTINUE
   747.000                 C
   748.000                 C-----SELECT THE COEFFICIENTS OF THE STRAIN-DISPLACEMENT MATRIX
   749.000                 C
   750.000    0012               DO 110 II=1,3
   751.000    0013               DO 110 JJ=1,3
   752.000    0014               KK=3*(II-1)+JJ
```

FINE PRINT

```
MTS  FORTRAN IV G COMPILER(21.8) WITH SDS SUPPORT        FSM        04-21-80     11:35:35        PAGE 0002

   753.000     0015               P(II,JJ)=PT(KK)
   754.000     0016               MJJ=II+3
   755.000     0017               NJJ=JJ+3
   756.000     0018               P(MJJ,NJJ)=P(II,JJ)
   757.000     0019        110    CONTINUE
   758.000                 C
   759.000                 C-----SET UP CONSTITUTIVE MATRIX
   760.000                 C
   761.000     0020               MNE=MET(J)
   762.000     0021               E=EI(MNE)
   763.000     0022               U=UI(MNE)
   764.000     0023               EU = E/((1.+U)*(1.-2.*U))
   765.000     0024               S(2,2)=EU*(1.-U)
   766.000     0025               S(2,6)=EU*U
   767.000     0026               S(3,3)=EU*(1.-2.*U)/2.
   768.000     0027               S(3,5)=S(3,3)
   769.000     0028               S(5,3)=S(3,3)
   770.000     0029               S(5,5)=S(3,3)
   771.000     0030               S(6,2)=S(2,6)
   772.000     0031               S(6,6)=S(2,2)
   773.000                 C
   774.000                 C-----CALCULATE ELEMENT STIFFNESS MATRIX
   775.000                 C
   776.000     0032               DO 4 JJ=1,6
   777.000     0033               DO 4 II=1,6
   778.000     0034               R(JJ,II)=0.0
   779.000     0035               DO 4 KK=1,6
   780.000     0036               R(JJ,II)=R(JJ,II)+S(JJ,KK)*P(KK,II)
   781.000     0037        4      CONTINUE
   782.000     0038               DO 5 JJ=1,6
   783.000     0039               DO 5 II=1,6
   784.000     0040               S(JJ,II)=0.0
   785.000     0041               DO 5 KK=1,6
   786.000     0042               S(JJ,II)=S(JJ,II)+P(KK,JJ)*R(KK,II)/(4.*ARR)
   787.000     0043        5      CONTINUE
   788.000     0044               RETURN
   789.000     0045               END
```

```
MTS  FORTRAN IV G COMPILER(21.8) WITH SDS SUPPORT        MAIN        04-21-80    11:35:36        PAGE 0001
 790.000               C
 791.000               C    ************************************************************
 792.000               C    *                                                          *
 793.000               C    *                                                          *
 794.000               C    *                        NLOAD                             *
 795.000               C    *                                                          *
 796.000               C    ************************************************************
 797.000               C
 798.000    0001             SUBROUTINE NLOAD
 799.000               C
 800.000               C
 801.000               CCCCCCCCCCCCCCCCCCCCCCCCCCCCCCCCCCCCCCCCCCCCCCCCCCCCCCCCCCCCCCCCCCCC
 802.000               C                                                                  C
 803.000               C     SUBROUTINE NLOAD - READS THE EXTERNALLY APPLIED LOADS AND    C
 804.000               C                        SETS UP THE INITIAL LOAD VECTOR           C
 805.000               C                                                                  C
 806.000               C     DATA REQIURED FROM COMMON BLOCKS                             C
 807.000               C                                                                  C
 808.000               C     NU  = TOTAL NUMBER OF UNKNOWNS OF CURRENT PROBLEM            C
 809.000               C     ND  = RESTRAINED DEGREE OF FREEDOM CODE MATRIX               C
 810.000               C     NGI = GRAVITY LOAD INDICATOR                                 C
 811.000               C     FG  = GRAVITY LOAD VECTOR                                    C
 812.000               C                                                                  C
 813.000               C     OUTPUT PLACED IN BLK3                                        C
 814.000               C                                                                  C
 815.000               C     FG = LOAD VECTOR (EXTERNAL AND/OR GRAVITY LOADS)             C
 816.000               C                                                                  C
 817.000               CCCCCCCCCCCCCCCCCCCCCCCCCCCCCCCCCCCCCCCCCCCCCCCCCCCCCCCCCCCCCCCCCCCC
 818.000               C
 819.000               C
 820.000               C-----DIMENSION STATEMENTS
 821.000               C
 822.000    0002             REAL*8 FN,F,FG,FF(2)
 823.000    0003             INTEGER*2 ND
 824.000               C
 825.000    0004             COMMON /BLK1/ ND(200,2)
 826.000               C
 827.000    0005             COMMON /BLK3/ FN(400),F(400),FG(400)
 828.000               C
 829.000    0006             COMMON /BLK11/ NN,NE,NUE,NUC,NGI,NLC,KV,NU,NB,NB1
 830.000               C
 831.000               C-----INITIALIZATION
 832.000               C
 833.000    0007             IF(NGI.EQ.1)GOTO 21
 834.000    0008             DO 20 KK=1,NU
 835.000    0009             FG(KK)=0.0
 836.000    0010        20   CONTINUE
 837.000    0011        21   CONTINUE
 838.000               C
 839.000               C-----READ EXTERNALLY APPLIED NODAL LOADS
 840.000               C
 841.000    0012             READ(5,3)NNL
 842.000               C
 843.000               C-----NNL = NUMBER OF NODES LOADED
 844.000               C
```

```
MTS  FORTRAN IV G COMPILER(21.8) WITH SDS SUPPORT         NLOAD        04-21-80     11:35:36          PAGE 0002

   845.000     0013                  DO 2 II=1,NNL
   846.000     0014                  READ(5,3)JNU,FF(1),FF(2)
   847.000               C
   848.000               C-----JNU = NODE NUMBER OF LOADED NODE
   849.000               C-----FF(1) = X-LOAD
   850.000               C-----FF(2) = Y-LOAD
   851.000               C
   852.000               C
   853.000               C-----SET UP THE LOAD VECTOR
   854.000               C
   855.000     0015                  DO 6 JJ=1,2
   856.000     0016                  IF(ND(JNU,JJ).EQ.0)GOTO 6
   857.000     0017                  IK=ND(JNU,JJ)
   858.000     0018                  FG(IK)=FG(IK)+FF(JJ)
   859.000     0019      6           CONTINUE
   860.000     0020      2           CONTINUE
   861.000               C
   862.000               C-----FORMAT STATEMENTS
   863.000               C
   864.000     0021      3           FORMAT(I6,2F12.3)
   865.000     0022                  RETURN
   866.000     0023                  END
```

```
MTS  FORTRAN IV G COMPILER(21.8) WITH SDS SUPPORT        MAIN        04-21-80     11:35:37         PAGE 0001
   867.000             C
   868.000             C     ****************************************************************
   869.000             C     *                                                              *
   870.000             C     *                            CNLP                              *
   871.000             C     *                                                              *
   872.000             C     ****************************************************************
   873.000             C
   874.000             C
   875.000    0001           SUBROUTINE CNLP
   876.000             C
   877.000             C
   878.000             CCCCCCCCCCCCCCCCCCCCCCCCCCCCCCCCCCCCCCCCCCCCCCCCCCCCCCCCCCCCCCCCCCCCCCCC
   879.000             C                                                                      C
   880.000             C     SUBROUTINE CNLP - PRINTS OUT INCREMENTAL AND TOTAL NODAL         C
   881.000             C                       LOADS                                          C
   882.000             C                                                                      C
   883.000             C     DATA REQIURED FROM COMMON BLOCKS                                 C
   884.000             C                                                                      C
   885.000             C     JC = CREEP INCREMENT NUMBER                                      C
   886.000             C     NN = TOTAL NUMBER OF NODES                                       C
   887.000             C     ND = RESTRAINED DEGREE OF FREEDOM CODE MATRIX                    C
   888.000             C     F  = ACCUMULATED TOTAL LOAD VECTOR                               C
   889.000             C     FN = INCREMENTAL FICTICOUS LOAD VECTOR                           C
   890.000             C                                                                      C
   891.000             CCCCCCCCCCCCCCCCCCCCCCCCCCCCCCCCCCCCCCCCCCCCCCCCCCCCCCCCCCCCCCCCCCCCCCCC
   892.000             C
   893.000             C
   894.000             C-----DIMENSION STATEMENTS
   895.000             C
   896.000    0002           REAL*8 FN,F,TAV
   897.000    0003           INTEGER*2 ND
   898.000             C
   899.000    0004           COMMON /BLK1/ ND(200,2)
   900.000             C
   901.000    0005           COMMON /BLK3/ FN(400),F(400)
   902.000             C
   903.000    0006           COMMON /BLK11/ NN,NE,NUE,NUC,NGI,NLC,KV,NU,NB,NB1
   904.000             C
   905.000    0007           COMMON /BLK12/ JC,TIM,TAV,IPP
   906.000             C
   907.000             C-----INIALIZATION
   908.000             C
   909.000    0008           SUMX1=0.0
   910.000    0009           SUMY1=0.0
   911.000    0010           SUMX2=0.0
   912.000    0011           SUMY2=0.0
   913.000    0012           DO 1 JJ=1,NN
   914.000             C
   915.000             C-----SELECT INCREMENTAL AND TOTAL X-FORCES FROM FN AND F
   916.000             C
   917.000    0013           IF(ND(JJ,1).NE.0)GOTO 4
   918.000    0014           FX1=0.0
   919.000    0015           FX2=0.0
   920.000    0016           GOTO 5
   921.000    0017         4 IK=ND(JJ,1)
```

FINE PRINT

```
MTS  FORTRAN IV G COMPILER(21.8) WITH SDS SUPPORT       CNLP        04-21-80    11:35:37          PAGE 0002
   922.000     0018                FX1=FN(IK)
   923.000     0019                FX2=F(IK)
   924.000     0020          5     CONTINUE
   925.000                   C
   926.000                   C-----SELECT INCREMENTAL AND TOTAL Y-FORCES FROM FN AND F
   927.000                   C
   928.000     0021                IF(ND(JJ,2).NE.0)GOTO 6
   929.000     0022                FY1=0.0
   930.000     0023                FY2=0.0
   931.000     0024                GOTO 7
   932.000     0025          6     IK=ND(JJ,2)
   933.000     0026                FY1=FN(IK)
   934.000     0027                FY2=F(IK)
   935.000     0028          7     CONTINUE
   936.000                   C
   937.000                   C-----SUM FORCES TO OBTAIN TOTAL APPLIED LOAD
   938.000                   C
   939.000     0029                SUMX1=SUMX1+FX1
   940.000     0030                SUMY1=SUMY1+FY1
   941.000     0031                SUMX2=SUMX2+FX2
   942.000     0032                SUMY2=SUMY2+FY2
   943.000                   C
   944.000                   C-----PRINT OUT INCREMENTAL AND TOTAL LOADS
   945.000                   C
   946.000     0033                IF(JC.EQ.0)GOTO 10
   947.000     0034                WRITE(6,8) JJ,FX1,FY1,FX2,FY2
   948.000     0035                GOTO 1
   949.000     0036         10     WRITE(6,9)JJ,FX1,FY1
   950.000     0037          1     CONTINUE
   951.000     0038                IF(JC.EQ.0)GOTO 15
   952.000     0039                WRITE(6,11)SUMX1,SUMY1,SUMX2,SUMY2
   953.000     0040                GOTO 20
   954.000     0041         15     WRITE(6,12)SUMX1,SUMY1
   955.000                   C
   956.000                   C-----FORMAT STATEMENTS
   957.000                   C
   958.000     0042          8     FORMAT(5X,I3,1X,4F11.2)
   959.000     0043          9     FORMAT(5X,I3,1X,2F11.2)
   960.000     0044         11     FORMAT(//T7,'SUM OF INCREMENTAL FORCES:  X-DIRECTION = ',E10.4,
   961.000                        &      /T35,'Y-DIRECTION = ',E10.4,//T7,'SUM OF TOTAL FORCES:  ',
   962.000                        &      'X-DIRECTION = ',E10.4,/T29,'Y-DIRECTION = ',E10.4,/)
   963.000     0045         12     FORMAT(//T7,'SUM OF APPLIED LOADING:  X-DIRECTION = ',E10.4,
   964.000                        &      /T32,'Y-DIRECTION = ',E10.4/)
   965.000     0046         20     RETURN
   966.000     0047                END
```

```
MTS   FORTRAN IV G COMPILER(21.8) WITH SDS SUPPORT        MAIN        04-21-80     11:35:38          PAGE 0001
   967.000          C
   968.000          C     .................................................................
   969.000          C     .                                                               .
   970.000          C     .                              BAND                             .
   971.000          C     .                                                               .
   972.000          C     .................................................................
   973.000          C
   974.000          C
   975.000   0001         SUBROUTINE BAND(LT)
   976.000          C
   977.000          C
   978.000          CCCCCCCCCCCCCCCCCCCCCCCCCCCCCCCCCCCCCCCCCCCCCCCCCCCCCCCCCCCCCCCCCCCCCCCCC
   979.000          C                                                                       C
   980.000          C     SUBROUTINE BAND - DETERMINES THE NODAL DISPLACEMENTS USING THE    C
   981.000          C                       CHOLESKI SQUARE ROOT METHOD                     C
   982.000          C                                                                       C
   983.000          C     INPUT                                                             C
   984.000          C                                                                       C
   985.000          C     LT  = EXECUTION PARAMETER                                         C
   986.000          C             LT=1: DECOMPOSE STIFFNESS MATRIX AND BACK SUBSTITUTE      C
   987.000          C             LT=2: BACK SUBSTITUTE ONLY                                C
   988.000          C                                                                       C
   989.000          C     DATA REQIURED FROM COMMON BLOCKS                                  C
   990.000          C                                                                       C
   991.000          C     A   = ASSEMBLED STRUCTURE STIFFNESS MATRIX                        C
   992.000          C     B   = LOAD VECTOR                                                 C
   993.000          C     N   = TOTAL NUMBER OF UNKNOWNS                                    C
   994.000          C     M   = MAXIMUM HALF BAND WIDTH                                     C
   995.000          C                                                                       C
   996.000          C     OUTPUT PLACED IN BLK3                                             C
   997.000          C                                                                       C
   998.000          C     B = NODAL X AND Y DISPLACEMENTS                                   C
   999.000          C                                                                       C
  1000.000          CCCCCCCCCCCCCCCCCCCCCCCCCCCCCCCCCCCCCCCCCCCCCCCCCCCCCCCCCCCCCCCCCCCCCCCCC
  1001.000          C
  1002.000          C
  1003.000          C-----COMMON AND DIMENSION STATEMENTS
  1004.000          C
  1005.000   0002         REAL*8 A,B,BIGL,SML,ASUM1,ASUM2,BSUM1,BSUM2,DET,FAC,S
  1006.000          C
  1007.000   0003         COMMON /BLK3/ B(400)
  1008.000          C
  1009.000   0004         COMMON /BLK11/ NP,NE,NUE,NUC,NGI,NLC,KV,N,NB,M
  1010.000          C
  1011.000   0005         COMMON /BLK13/ A(5000)
  1012.000          C
  1013.000   0006         DET=1.E-8
  1014.000   0007         MM=M-1
  1015.000   0008         NM=N*M
  1016.000   0009         NM1=NM-MM
  1017.000   0010         IF (LT.NE.1) GO TO 55
  1018.000   0011         MP=M+1
  1019.000   0012         KK=2
  1020.000   0013         FAC=DET
  1021.000   0014         A(1)=1./DSQRT(A(1))
```

```
MTS   FORTRAN IV G COMPILER(21.8) WITH SDS SUPPORT          BAND          04-21-80     11:35:38          PAGE 0002

  1022.000     0015            BIGL=A(1)
  1023.000     0016            SML=A(1)
  1024.000     0017            A(2)=A(2)*A(1)
  1025.000     0018            A(MP)=1./DSQRT(A(MP)-A(2)*A(2))
  1026.000     0019            IF(A(MP).GT.BIGL)BIGL=A(MP)
  1027.000     0020            IF(A(MP).LT.SML)SML=A(MP)
  1028.000     0021            MP=MP+M
  1029.000     0022            DO 62 J=MP,NM1,M
  1030.000     0023            JP=J-MM
  1031.000     0024            MZC=0
  1032.000     0025            IF(KK.GE,M) GO TO 1
  1033.000     0026            KK=KK+1
  1034.000     0027            II=1
  1035.000     0028            JC=1
  1036.000     0029            GO TO 2
  1037.000     0030      1     KK=KK+M
  1038.000     0031            II=KK-MM
  1039.000     0032            JC=KK-MM
  1040.000     0033      2     DO 65 I=KK,JP,MM
  1041.000     0034            IF(A(I).EQ.0.)GO TO 64
  1042.000     0035            GO TO 66
  1043.000     0036      64    JC=JC+M
  1044.000     0037      65    MZC=MZC+1
  1045.000     0038            ASUM1=0.
  1046.000     0039            GO TO 61
  1047.000     0040      66    MMZC=MM*MZC
  1048.000     0041            II=II+MZC
  1049.000     0042            KM=KK+MMZC
  1050.000     0043            A(KM)=A(KM)*A(JC)
  1051.000     0044            IF(KM.GE.JP)GO TO 6
  1052.000     0045            KJ=KM+MM
  1053.000     0046            DO 5 I=KJ,JP,MM
  1054.000     0047            ASUM2=0.
  1055.000     0048            IM=I-MM
  1056.000     0049            II=II+1
  1057.000     0050            KI=II+MMZC
  1058.000     0051            DO 7 K=KM,IM,MM
  1059.000     0052            ASUM2=ASUM2+A(KI)*A(K)
  1060.000     0053      7     KI=KI+MM
  1061.000     0054      5     A(I)=(A(I)-ASUM2)*A(KI)
  1062.000     0055      6     CONTINUE
  1063.000     0056            ASUM1=0.
  1064.000     0057            DO 4 K=KM,JP,MM
  1065.000     0058      4     ASUM1=ASUM1+A(K)*A(K)
  1066.000     0059      61    S=A(J)-ASUM1
  1067.000     0060            IF(S.LT.0.)DET=S
  1068.000     0061            IF(S.EQ.0.)DET=0.
  1069.000     0062            IF(S.GT.0.)GO TO 63
  1070.000     0063            NROW=(J+MM)/M
  1071.000     0064            WRITE(6,99) NROW
  1072.000     0065      99    FORMAT(35H0ERROR CONDITION ENCOUNTERED IN ROW,I6)
  1073.000     0066            GOTO 56
  1074.000     0067      63    A(J)=1./DSQRT(S)
  1075.000     0068            IF(A(J).GT.BIGL)BIGL=A(J)
  1076.000     0069            IF(A(J).LT.SML)SML=A(J)
```

```
MTS  FORTRAN IV G COMPILER(21.8) WITH SDS SUPPORT        BAND        04-21-80    11:35:38          PAGE 0003
  1077.000     0070         62    CONTINUE
  1078.000     0071               IF(SML.LE.FAC*BIGL)GO TO 54
  1079.000     0072               GO TO 53
  1080.000     0073         54    DET=0.
  1081.000     0074         56    IF(DET)70,71,72
  1082.000     0075         70    WRITE(6,73)DET
  1083.000     0076         73    FORMAT(1X,'MATRIX SM IS NOT POSITIVE DEFINITE.  DET=',E15.7)
  1084.000     0077               STOP
  1085.000     0078         71    WRITE(6,74)DET
  1086.000     0079         74    FORMAT(1X,'DETERMINANT IS ZERO.  DET=',E15.7)
  1087.000     0080               STOP
  1088.000     0081         72    CONTINUE
  1089.000     0082         53    DET=SML/BIGL
  1090.000     0083         55    B(1)=B(1)*A(1)
  1091.000     0084               KK=1
  1092.000     0085               K1=1
  1093.000     0086               J=1
  1094.000     0087               DO 8 L=2,N
  1095.000     0088               BSUM1=0.
  1096.000     0089               LM=L-1
  1097.000     0090               J=J+M
  1098.000     0091               IF(KK.GE.M)GO TO 12
  1099.000     0092               KK=KK+1
  1100.000     0093               GO TO 13
  1101.000     0094         12    KK=KK+M
  1102.000     0095               K1=K1+1
  1103.000     0096         13    JK=KK
  1104.000     0097               DO 9 K=K1,LM
  1105.000     0098               BSUM1=BSUM1+A(JK)*B(K)
  1106.000     0099               JK=JK+MM
  1107.000     0100          9    CONTINUE
  1108.000     0101          8    B(L)=(B(L)-BSUM1)*A(J)
  1109.000     0102               B(N)=B(N)*A(NM1)
  1110.000     0103               NMM=NM1
  1111.000     0104               NN=N-1.
  1112.000     0105               ND=N
  1113.000     0106               DO 10 L=1,NN
  1114.000     0107               BSUM2=0.
  1115.000     0108               NL=N-L
  1116.000     0109               NL1=N-L+1
  1117.000     0110               NMM=NMM-M
  1118.000     0111               NJ1=NMM
  1119.000     0112               IF(L.GE.M)ND=ND-1
  1120.000     0113               DO 11 K=NL1,ND
  1121.000     0114               NJ1=NJ1+1
  1122.000     0115               BSUM2=BSUM2+A(NJ1)*B(K)
  1123.000     0116         11    CONTINUE
  1124.000     0117         10    B(NL)=(B(NL)-BSUM2)*A(NMM)
  1125.000     0118               RETURN
  1126.000     0119               END
```

FINE PRINT

```
MTS  FORTRAN IV G COMPILER(21.8) WITH SDS SUPPORT        MAIN        04-21-80     11:35:41        PAGE 0001
  1127.000               C
  1128.000               C     ***************************************************************
  1129.000               C     *                                                             *
  1130.000               C     *                            CNDI                             *
  1131.000               C     *                                                             *
  1132.000               C     ***************************************************************
  1133.000               C
  1134.000               C
  1135.000      0001           SUBROUTINE CNDI
  1136.000               C
  1137.000               C
  1138.000               CCCCCCCCCCCCCCCCCCCCCCCCCCCCCCCCCCCCCCCCCCCCCCCCCCCCCCCCCCCCCCCCCCCCCCC
  1139.000               C                                                                     C
  1140.000               C     SUBROUTINE CNDI - PRINTS OUT INCREMENTAL AND TOTAL              C
  1141.000               C                        DISPLACEMENTS                                C
  1142.000               C                                                                     C
  1143.000               C     DATA REQIURED FROM COMMON BLOCKS                                C
  1144.000               C                                                                     C
  1145.000               C     NN  = TOTAL NUMBER OF NODES                                     C
  1146.000               C     ND  = RESTRAINED DEGREE OF FREEDOM CODE MATRIX                  C
  1147.000               C     FN  = NODAL X AND Y DISPLACEMENTS                               C
  1148.000               C     IPP = INCREMENT PRINT OUT CONTROL FLAG                          C
  1149.000               C     JC  = CREEP INCREMENT NUMBER                                    C
  1150.000               C                                                                     C
  1151.000               C     OUTPUT PLACED IN BLK4                                           C
  1152.000               C                                                                     C
  1153.000               C     DX   = TOTAL NODAL X-DISPLACEMENTS                              C
  1154.000               C     DY   = TOTAL NODAL Y-DISPLACEMENTS                              C
  1155.000               C     DXI  = INCREMENTAL X-DISPLACEMENT                               C
  1156.000               C     DYI  = INCREMENTAL Y-DISPLACEMENT                               C
  1157.000               C     VELX = CREEP VELOCITY IN X-DIRECTION FOR CURRENT INCREMENT      C
  1158.000               C     VELY = CREEP VELOCITY IN Y-DIRECTION FOR CURRENT INCREMENT      C
  1159.000               C                                                                     C
  1160.000               CCCCCCCCCCCCCCCCCCCCCCCCCCCCCCCCCCCCCCCCCCCCCCCCCCCCCCCCCCCCCCCCCCCCCCC
  1161.000               C
  1162.000               C
  1163.000               C-----COMMON AND DIMENSION STATEMENTS
  1164.000               C
  1165.000      0002           REAL*8 FN,TAV
  1166.000      0003           INTEGER*2 ND
  1167.000               C
  1168.000      0004           COMMON /BLK1/ ND(200,2)
  1169.000               C
  1170.000      0005           COMMON /BLK3/ FN(400)
  1171.000               C
  1172.000      0006           COMMON /BLK4/ DX(200),DY(200),DXI(200),DYI(200),
  1173.000                   &               VELX(200),VELY(200)
  1174.000               C
  1175.000      0007           COMMON /BLK11/ NN,NE,NUE,NUC,NGI,NLC,KV,NU,NB,NB1
  1176.000               C
  1177.000      0008           COMMON /BLK12/ JC,TIM,TAV,IPP
  1178.000               C
  1179.000      0009           IF(JC.NE.0)GOTO 3
  1180.000      0010           DO 2 I=1,NN
  1181.000      0011           DX(I)=0.0
```

```
MTS  FORTRAN IV G COMPILER(21.8) WITH SDS SUPPORT        CNDI        04-21-80     11:35:41         PAGE 0002
  1182.000     0012                 DY(I)=0.0
  1183.000     0013          2      CONTINUE
  1184.000     0014          3      CONTINUE
  1185.000     0015                 DO 1 JJ=1,NN
  1186.000                   C
  1187.000                   C-----SELECT X-DISPLACEMENT FROM FN
  1188.000                   C
  1189.000     0016                 IF(ND(JJ,1).NE.0)GOTO 5
  1190.000     0017                 DXI(JJ)=0.0
  1191.000     0018                 GOTO 4
  1192.000     0019          5      IK=ND(JJ,1)
  1193.000     0020                 DXI(JJ)=FN(IK)
  1194.000     0021          4      CONTINUE
  1195.000                   C
  1196.000                   C-----SELECT Y-DISPLACEMENT FROM FN
  1197.000                   C
  1198.000     0022                 IF(ND(JJ,2).NE.0)GOTO 6
  1199.000     0023                 DYI(JJ)=0.0
  1200.000     0024                 GOTO 9
  1201.000     0025          6      IK=ND(JJ,2)
  1202.000     0026                 DYI(JJ)=FN(IK)
  1203.000     0027          9      CONTINUE
  1204.000                   C
  1205.000                   C-----CALCULATE TOTAL DISPLACEMENTS
  1206.000                   C
  1207.000     0028                 DX(JJ)=DX(JJ)+DXI(JJ)
  1208.000     0029                 DY(JJ)=DY(JJ)+DYI(JJ)
  1209.000                   C
  1210.000                   C-----CALCULATE CREEP VELOCITY
  1211.000                   C
  1212.000     0030                 IF(JC.EQ.0)GOTO 10
  1213.000     0031                 VELX(JJ)=DXI(JJ)/TAV
  1214.000     0032                 VELY(JJ)=DYI(JJ)/TAV
  1215.000                   C
  1216.000                   C-----PRINT OUT INCREMENTAL AND TOTAL DISPLACEMENTS
  1217.000                   C
  1218.000     0033                 IF(IPP.EQ.1)GOTO 1
  1219.000     0034                 IF(JC.EQ.0)GOTO 10
  1220.000     0035                 WRITE(6,8)JJ,DXI(JJ),DYI(JJ),DX(JJ),DY(JJ),VELX(JJ),VELY(JJ)
  1221.000     0036                 GOTO 1
  1222.000     0037          10     WRITE(6,11)JJ,DXI(JJ),DYI(JJ)
  1223.000     0038          1      CONTINUE
  1224.000                   C
  1225.000                   C-----FORMAT STATEMENTS
  1226.000                   C
  1227.000     0039          8      FORMAT(5X,I4,1X,6(1PE18.4))
  1228.000     0040          11     FORMAT(5X,I3,2(1PE18.4))
  1229.000     0041                 RETURN
  1230.000     0042                 END
```

```
MTS  FORTRAN IV G COMPILER(21.8) WITH SDS SUPPORT        MAIN        04-21-80     11:35:42          PAGE 0001
         C
         C     *********************************************************
         C     *                                                       *
         C     *                         CESS                          *
         C     *                                                       *
         C     *********************************************************
         C
         C
         C
   000             SUBROUTINE CESS
         C
         C
         CCCCCCCCCCCCCCCCCCCCCCCCCCCCCCCCCCCCCCCCCCCCCCCCCCCCCCCCCCCCCCCCCCCCCCCC
         C                                                                      C
         C     SUBROUTINE CESS - CALCULATES AND PRINTS OUT THE ELEMENT STRAINS  C
         C                       AND STRESSES FOR THE ELASTIC SOLUTION AND THE  C
         C                       INCREMENTAL AND TOTAL ELEMENT STRAINS AND      C
         C                       STRESSES FOR THE CREEP SOLUTION                C
         C                                                                      C
         C     DATA REQIURED FROM COMMON BLOCKS                                 C
         C                                                                      C
         C     NN    = NUMBER OF NODES                                          C
         C     NE    = NUMBER OF ELEMENTS                                       C
         C     KV    = CREEP CONDITION INDICATOR                                C
         C     JC    = CREEP INCREMENT NUMBER                                   C
         C     FN    = NODAL X AND Y DISPLACEMENTS                              C
         C     EXL   = INCREMENT OF CREEP STRAIN IN X-DIRECTION                 C
         C     EYL   = INCREMENT OF CREEP STRAIN IN Y-DIRECTION                 C
         C     EZL   = INCREMENT OF CREEP STRAIN IN Z-DIRECTION                 C
         C     EXYL  = INCREMENT OF CREEP SHEAR STRAIN                          C
         C     UI    = POISSON'S RATIO FOR EACH MATERIAL                        C
         C     EI    = ELASTIC MODULUS FOR EACH MATERIAL                        C
         C     MET   = ELASTIC MATERIAL NUMBER INDICATOR                        C
         C     NODES = ARRAY CONTAINING THE ELEMENT INCIDENCE LIST              C
         C     NEPR  = PRINT OUT CONTROL INDICATOR FOR EACH ELEMENT             C
         C     IPP   = INCREMENT PRINT OUT CONTROL FLAG                         C
         C                                                                      C
         C     OUTPUT PLACED IN BLK6, BLK7 AND BLK8                             C
         C                                                                      C
         C     EX    = ACCUMULATED TOTAL ELEMENT STRAINS IN X-DIRECTION         C
         C     EY    = ACCUMULATED TOTAL ELEMENT STRAINS IN Y-DIRECTION         C
         C     EXY   = ACCUMULATED TOTAL ELEMENT SHEAR STRAINS                  C
         C     SEX   = ACCUMULATED ELASTIC ELEMENT SIGMA-X STRESSES             C
         C     SEY   = ACCUMULATED ELASTIC ELEMENT SIGMA-Y STRESSES             C
         C     SEZ   = ACCUMULATED ELASTIC ELEMENT SIGMA-Z STRESSES             C
         C     SEXY  = ACCUMULATED ELASTIC ELEMENT SHEAR STRESSES               C
         C     SEXYL = CHANGE IN ELASTIC EFFECTIVE STRESS FOR INCREMENT #JC     C
         C     SEYL  = ELASTIC EFFECTIVE STRESSES FOR INCREMENT #JC             C
         C     FS1   = ACCUMULATED ELASTIC ELEMENT STRAINS IN X-DIRECTION       C
         C     FS2   = ACCUMULATED ELASTIC ELEMENT-STRAINS IN Y-DIRECTION       C
         C     FS3   = ACCUMULATED ELASTIC ELEMENT SHEAR STRAINS                C
         C     EEFFC = EFFECTIVE CREEP STRAIN                                   C
         C     CXI   = SUM OF ADJOINING ELEMENT SIGMA-X STRESSES FOR EACH       C
         C             NODE                                                     C
         C     CYI   = SUM OF ADJOINING ELEMENT SIGMA-Y STRESSES FOR EACH       C
```

```
MTS  FORTRAN IV G COMPILER(21.8) WITH SDS SUPPORT        MAIN        04-21-80     11:35:42          PAGE 0002
  1286.000               C              NODE                                                  C
  1287.000               C      CXYI   = SUM OF ADJOINING ELEMENT SHEAR STRESSES FOR EACH NODE    C
  1288.000               C      CNC    = TOTAL NUMBER OF ELEMENTS CONNECTED TO EACH NODE          C
  1289.000               C                                                                    C
  1290.000               CCCCCCCCCCCCCCCCCCCCCCCCCCCCCCCCCCCCCCCCCCCCCCCCCCCCCCCCCCCCCCCCCCCCCCCC
  1291.000               C
  1292.000               C
  1293.000               C-----DIMENSION STATEMENTS
  1294.000               C
  1295.000     0002            REAL*8 FN,EX,EY,EXY,SEX,SEY,SEZ,SEXY,EXL,EYL,EZL,EXYL,
  1296.000                    &       SEXYL,SEYL,XS,YS,XYS,FS1E,FS2E,FS3E,DISP(6),TAV,PT(9),
  1297.000                    &       SIX,SIY,SIZ,SIXY,EI,UI,E,U,COMM,EXC,EYC,EZC,EXYC,EEFFC
  1298.000     0003            INTEGER*2 NNPR,NEPR,NP(6),MET,NODES
  1299.000               C
  1300.000     0004            COMMON /BLK2/ MET(300),EI(20),UI(20)
  1301.000               C
  1302.000     0005            COMMON /BLK3/ FN(400)
  1303.000               C
  1304.000     0006            COMMON /BLK5/ NNPR(200),NEPR(300)
  1305.000               C
  1306.000     0007            COMMON /BLK6/ EX(300),EY(300),EXY(300),
  1307.000                    &              EXL(300),EYL(300),EZL(300),EXYL(300),
  1308.000                    &              EXC(300),EYC(300),EZC(300),EXYC(300),
  1309.000                    &              FS1(300),FS2(300),FS3(300)
  1310.000               C
  1311.000     0008            COMMON /BLK7/ SEX(300),SEY(300),SEZ(300),SEXY(300),
  1312.000                    &              CXI(200),CYI(200),CXYI(200),CNC(200),
  1313.000                    &              SNX(200),SNY(200),SNXY(200)
  1314.000               C
  1315.000     0009            COMMON /BLK8/ SEYL(300),SEXYL(300),EEFFC(300)
  1316.000               C
  1317.000     0010            COMMON /BLK11/ NN,NE,NUE,NUC,NGI,NLC,KV,NU,NB,NB1
  1318.000               C
  1319.000     0011            COMMON /BLK12/ JC,TIM,TAV,IPP
  1320.000               C
  1321.000     0012            COMMON /BLK14/ NODES(300,3)
  1322.000               C
  1323.000               C
  1324.000               C-----INITIALIZATION
  1325.000               C
  1326.000     0013            DO 128 JJ=1,NN
  1327.000     0014            CXI(JJ)=0.0
  1328.000     0015            CYI(JJ)=0.0
  1329.000     0016            CXYI(JJ)=0.0
  1330.000     0017            CNC(JJ)=0.0
  1331.000     0018      128   CONTINUE
  1332.000     0019            SIGMAX=0.0
  1333.000     0020            IF(JC.NE.0)GOTO 140
  1334.000     0021            DO 130 J=1,NE
  1335.000     0022            EX(J)=0.0
  1336.000     0023            EY(J)=0.0
  1337.000     0024            EXY(J)=0.0
  1338.000     0025            FS1(J)=0.0
  1339.000     0026            FS2(J)=0.0
  1340.000     0027            FS3(J)=0.0
```

FINE PRINT

```
MTS  FORTRAN IV G COMPILER(21.8) WITH SDS SUPPORT         CESS         04-21-80     11:35:42         PAGE 0003

 1341.000     0028                 SEX(J)=0.0
 1342.000     0029                 SEY(J)=0.0
 1343.000     0030                 SEZ(J)=0.0
 1344.000     0031                 SEXY(J)=0.0
 1345.000     0032                 EXL(J)=0.0
 1346.000     0033                 EYL(J)=0.0
 1347.000     0034                 EZL(J)=0.0
 1348.000     0035                 EXYL(J)=0.0
 1349.000     0036                 EXC(J)=0.0
 1350.000     0037                 EYC(J)=0.0
 1351.000     0038                 EZC(J)=0.0
 1352.000     0039                 EXYC(J)=0.0
 1353.000     0040          130    CONTINUE
 1354.000     0041          140    CONTINUE
 1355.000                   C
 1356.000                   C-----CALCULATE STRAIN AND STRESS FOR EACH ELEMENT
 1357.000                   C
 1358.000     0042                 DO 1 J=1,NE
 1359.000     0043                 MNE=MET(J)
 1360.000     0044                 E=EI(MNE)
 1361.000     0045                 U=UI(MNE)
 1362.000                   C
 1363.000                   C-----READ ELEMENT DATA
 1364.000                   C
 1365.000     0046                 READ(1)(NP(I),I=1,6),(PT(K),K=1,9),ARR
 1366.000                   C
 1367.000                   C-----SELECT X AND Y DISPLACEMENTS OF EACH NODE IN ELEMENT #J
 1368.000                   C
 1369.000     0047                 DO 2 K=1,6
 1370.000     0048                 DISP(K)=0.0
 1371.000     0049                 LL=NP(K)
 1372.000     0050                 IF(LL.EQ.0) GO TO 2
 1373.000     0051                 DISP(K)=FN(LL)
 1374.000     0052          2      CONTINUE
 1375.000                   C
 1376.000                   C-----CALCULATE INCREMENTAL TOTAL ELEMENT STRAIN
 1377.000                   C
 1378.000     0053                 XS=(DISP(1)*PT(4)+DISP(2)*PT(5)+DISP(3)*PT(6))/(2.*ARR)
 1379.000     0054                 XYS=(DISP(1)*PT(7)+DISP(2)*PT(8)+DISP(3)*PT(9)+DISP(4)*PT(4)
 1380.000                        &     +DISP(5)*PT(5)+DISP(6)*PT(6))/(2.*ARR)
 1381.000     0055                 YS=(DISP(4)*PT(7)+DISP(5)*PT(8)+DISP(6)*PT(9))/(2.*ARR)
 1382.000                   C
 1383.000                   C-----ACCUMULATE TOTAL ELEMENT STRAIN
 1384.000                   C
 1385.000     0056                 EX(J)=EX(J)+XS
 1386.000     0057                 EY(J)=EY(J)+YS
 1387.000     0058                 EXY(J)=EXY(J)+XYS
 1388.000                   C
 1389.000                   C-----CALCULATE INCREMENTAL ELASTIC ELEMENT STRAIN
 1390.000                   C
 1391.000     0059                 FS1E=XS-EXL(J)
 1392.000     0060                 FS2E=YS-EYL(J)
 1393.000     0061                 FS3E=XYS-EXYL(J)
 1394.000                   C
 1395.000                   C-----ACCUMULATE ELASTIC ELEMENT STRAIN
```

```
MTS  FORTRAN IV G COMPILER(21.8) WITH SDS SUPPORT        CESS        04-21-80    11:35:42        PAGE 0004

  1396.000                  C
  1397.000     0062              FS1(J)=FS1(J)+FS1E
  1398.000     0063              FS2(J)=FS2(J)+FS2E
  1399.000     0064              FS3(J)=FS3(J)+FS3E
  1400.000                  C
  1401.000                  C-----CALCULATE INCREMENTAL ELASTIC ELEMENT STRESS
  1402.000                  C
  1403.000     0065              COMM=E/((1.+U)*(1.-2.*U))
  1404.000     0066              SIX=COMM*((1.-U)*FS1E+U*FS2E)-COMM*U*EZL(J)
  1405.000     0067              SIY=COMM*(U*FS1E+(1.-U)*FS2E)-COMM*U*EZL(J)
  1406.000     0068              SIZ=U*(SIX+SIY)-E*EZL(J)
  1407.000     0069              SIXY=COMM*((1.-2.*U)/2.)*FS3E
  1408.000     0070              SEXYL(J)=DSQRT(.5*((SIX-SIY)**2+(SIY-SIZ)**2+(SIZ-SIX)**2
  1409.000                      &            +6.*SIXY**2))
  1410.000                  C
  1411.000                  C-----ACCUMULATE ELASTIC ELEMENT STRESS
  1412.000                  C
  1413.000     0071              SEX(J)=SEX(J)+SIX
  1414.000     0072              SEY(J)=SEY(J)+SIY
  1415.000     0073              SEXY(J)=SEXY(J)+SIXY
  1416.000     0074              SEZ(J)=U*(SEX(J)+SEY(J))-E*EZL(J)
  1417.000     0075              SEYL(J)=DSQRT(.5*((SEX(J)-SEY(J))**2+(SEY(J)-SEZ(J))**2
  1418.000                      &          +(SEZ(J)-SEX(J))**2+6.*(SEXY(J)**2)))
  1419.000     0076              IF(SEYL(J).LT.SIGMAX)GOTO 108
  1420.000     0077              SIGMAX=SEYL(J)
  1421.000     0078              IELM=J
  1422.000     0079         108   IF(JC.EQ.0)GOTO 109
  1423.000                  C
  1424.000                  C-----CALCULATE TOTAL ACCUMULATED CREEP STRAIN
  1425.000                  C
  1426.000     0080              EXC(J)=EXC(J)+EXL(J)
  1427.000     0081              EYC(J)=EYC(J)+EYL(J)
  1428.000     0082              EZC(J)=EZC(J)+EZL(J)
  1429.000     0083              EXYC(J)=EXYC(J)+EXYL(J)
  1430.000     0084              EEFFC(J)=DSQRT((4./3.)*(EXC(J)**2+EXC(J)*EYC(J)
  1431.000                      &          +EYC(J)**2+(EXYC(J)**2)/4.))
  1432.000                  C
  1433.000                  C-----PRINT OUT THE TOTAL ELEMENT STRAINS AND STRESSES
  1434.000                  C
  1435.000     0085         109   IF(IPP.EQ.1.OR.NEPR(J).LT.0)GOTO 112
  1436.000     0086              CALL SMAX(SEX(J),SEY(J),SEXY(J),XM1,XM2,XM3,XM4)
  1437.000     0087              WRITE(6,5)J,EX(J),EY(J),EXY(J),SEX(J),SEY(J),SEXY(J),
  1438.000                      &         XM1,XM2,XM3,XM4
  1439.000     0088              IF(NEPR(J).EQ.0)GOTO 110
  1440.000     0089              CALL ROTATE(EX(J),EY(J),EXY(J),NEPR(J),C1,C2,C3)
  1441.000     0090              CALL ROTATE(SEX(J),SEY(J),SEXY(J),NEPR(J),D1,D2,D3)
  1442.000     0091              WRITE(6,7)C1,C2,C3,D1,D2,D3
  1443.000     0092         110   CONTINUE
  1444.000                  C
  1445.000                  C-----PRINT OUT THE INCREMENTAL ELEMENT STRAINS AND STRESSES
  1446.000                  C
  1447.000     0093              IF(JC.EQ.0)GOTO 112
  1448.000     0094              WRITE(6,6)XS,YS,XYS,SIX,SIY,SIXY
  1449.000     0095              WRITE(6,605)FS1E,FS2E,FS3E
  1450.000     0096              WRITE(6,606)FS1(J),FS2(J),FS3(J)
```

FINE PRINT

```
MTS  FORTRAN IV G COMPILER(21.8) WITH SDS SUPPORT        CESS        04-21-80   11:35:42         PAGE 0005
  1451.000     0097              WRITE(6,609)EXL(J),EYL(J),EZL(J),EXYL(J)
  1452.000     0098              WRITE(6,608)EXC(J),EYC(J),EZC(J),EXYC(J)
  1453.000     0099              WRITE(6,607)SEYL(J),SEZ(J)
  1454.000     0100        112   CONTINUE
  1455.000                 C
  1456.000                 C-----SUM THE ELEMENT STRESSES THAT ARE CONNECTED TO EACH NODE
  1457.000                 C
  1458.000     0101              DO 77 K=1,3
  1459.000     0102              L=NODES(J,K)
  1460.000     0103              CXI(L)=CXI(L)+SIX
  1461.000     0104              CYI(L)=CYI(L)+SIY
  1462.000     0105              CXYI(L)=CXYI(L)+SIXY
  1463.000     0106              CNC(L)=CNC(L)+1.
  1464.000                 C
  1465.000     0107        77    CONTINUE
  1466.000     0108        1     CONTINUE
  1467.000                 C
  1468.000     0109              WRITE(6,610)SIGMAX,IELM
  1469.000                 C
  1470.000                 C-----FORMAT STATEMENTS
  1471.000                 C
  1472.000     0110        5     FORMAT(5X,I5,2X,9(1PE11.3),0PF10.2)
  1473.000     0111        6     FORMAT(12X,6(1PE11.3))
  1474.000     0112        7     FORMAT(12X,6(1PE11.3),'  (ROTATED STRAINS AND STRESSES)')
  1475.000     0113        605   FORMAT(12X,3(1PE11.3),'  (ELASTIC STRAIN INCREMENTS)')
  1476.000     0114        606   FORMAT(12X,3(1PE11.3),'  (TOTAL ELASTIC STRAIN)')
  1477.000     0115        607   FORMAT(14X,'EFFECTIVE STRESS = ',1PE11.3,14X,'SIGMA-Z = ',
  1478.000                     &        1PE11.3/)
  1479.000     0116        608   FORMAT(12X,4(1PE11.3),'  (TOTAL ACCUMULATED CREEP STRAIN, ',
  1480.000                     &        'X, Y, Z & XY COMPONENTS)')
  1481.000     0117        609   FORMAT(12X,4(1PE11.3),'  (CREEP STRAIN INCREMENTS, ',
  1482.000                     &        'X, Y, Z & XY COMPONENTS)')
  1483.000     0118        610   FORMAT(/5X,'MAXIMUM EFFECTIVE STRESS = ',1PE12.3,' OCCURS IN ',
  1484.000                     &        'ELEMENT ',I5)
  1485.000     0119              REWIND 1
  1486.000     0120              RETURN
  1487.000     0121              END
```

```
MTS  FORTRAN IV G COMPILER(21.8) WITH SDS SUPPORT        MAIN        04-21-80     11:35:47         PAGE 0001
  1488.000                 C
  1489.000                 C    ************************************************************
  1490.000                 C    *                                                          *
  1491.000                 C    *                          CNAVE                           *
  1492.000                 C    *                                                          *
  1493.000                 C    ************************************************************
  1494.000                 C
  1495.000                 C
  1496.000     0001              SUBROUTINE CNAVE
  1497.000                 C
  1498.000                 C
  1499.000                 CCCCCCCCCCCCCCCCCCCCCCCCCCCCCCCCCCCCCCCCCCCCCCCCCCCCCCCCCCCCCCCCC C
  1500.000                 C                                                                   C
  1501.000                 C     SUBROUTINE CNAVE - DETERMINES AND PRINTS OUT THE AVERAGE NODAL  C
  1502.000                 C                        STRESSES                                    C
  1503.000                 C                                                                   C
  1504.000                 C     DATA REQIURED FROM COMMON BLOCKS                               C
  1505.000                 C                                                                   C
  1506.000                 C     NN   = TOTAL NUMBER OF NODES                                  C
  1507.000                 C     CXI  = SUM OF ADJOINING ELEMENT SIGMA-X STRESSES FOR EACH     C
  1508.000                 C            NODE                                                   C
  1509.000                 C     CYI  = SUM OF ADJOINING ELEMENT SIGMA-Y STRESSES FOR EACH     C
  1510.000                 C            NODE                                                   C
  1511.000                 C     CXYI = SUM OF ADJOINING ELEMENT SHEAR STRESS FOR EACH NODE    C
  1512.000                 C     CNC  = TOTAL NUMBER OF ELEMENTS CONNECTED TO EACH NODE        C
  1513.000                 C     NNPR = PRINT OUT CONTROL INDICATOR FOR EACH NODE              C
  1514.000                 C     IPP  = INCREMENT PRINT OUT CONTROL FLAG                       C
  1515.000                 C     JC   = CREEP INCREMENT NUMBER                                 C
  1516.000                 C                                                                   C
  1517.000                 C     OUTPUT PLACED IN BLK7                                         C
  1518.000                 C                                                                   C
  1519.000                 C     SNX  = ACCUMULATED AVERAGE NODAL SIGMA-X STRESSES             C
  1520.000                 C     SNY  = ACCUMULATED AVERAGE NODAL SIGMA-Y STRESSES             C
  1521.000                 C     SNXY = ACCUMULATED AVERAGE NODAL SHEAR STRESSES               C
  1522.000                 C                                                                   C
  1523.000                 CCCCCCCCCCCCCCCCCCCCCCCCCCCCCCCCCCCCCCCCCCCCCCCCCCCCCCCCCCCCCCCCCCC
  1524.000                 C
  1525.000                 C
  1526.000                 C-----DIMENSION STATEMENTS
  1527.000                 C
  1528.000     0002              REAL*8 SEX,SEY,SEZ,SEXY,TAV
  1529.000     0003              INTEGER*2 NNPR
  1530.000                 C
  1531.000     0004              COMMON /BLK5/ NNPR(200)
  1532.000                 C
  1533.000     0005              COMMON /BLK7/ SEX(300),SEY(300),SEZ(300),SEXY(300),
  1534.000                      &               CXI(200),CYI(200),CXYI(200),CNC(200),
  1535.000                      &               SNX(200),SNY(200),SNXY(200)
  1536.000                 C
  1537.000     0006              COMMON /BLK11/ NN,NE,NUE,NUC,NGI,NLC,KV,NU,NB,NB1
  1538.000                 C
  1539.000     0007              COMMON /BLK12/ JC,TIM,TAV,IPP
  1540.000                 C
  1541.000                 C-----CALCULATE INCREMENTAL AVERAGE NODAL STRESSES
  1542.000                 C
```

```
MTS  FORTRAN IV G COMPILER(21.8) WITH SDS SUPPORT        CNAVE       04-21-80    11:35:47        PAGE 0002
            DO 1 J=1,NN
            CXI(J)=CXI(J)/CNC(J)
            CYI(J)=CYI(J)/CNC(J)
            CXYI(J)=CXYI(J)/CNC(J)
      C
      C-----ACCUMULATE AVERAGE NODAL STRESSES
      C
            SNX(J)=SNX(J)+CXI(J)
            SNY(J)=SNY(J)+CYI(J)
            SNXY(J)=SNXY(J)+CXYI(J)
      C
      C-----PRINT OUT ACCUMULATED AVERAGE NODAL STRESSES
      C
            IF(IPP.EQ.1.OR.NNPR(J).LT.O)GOTO 1
            CALL SMAX(SNX(J),SNY(J),SNXY(J),XM1,XM2,XM3,XM4)
            WRITE(6,4)J,SNX(J),SNY(J),SNXY(J),XM1,XM2,XM3,XM4
            IF(NNPR(J).EQ.O)GOTO 112
            CALL ROTATE(SNX(J),SNY(J),SNXY(J),NNPR(J),S1,S2,S3)
            WRITE(6,7) S1,S2,S3
      112   CONTINUE
      C
      C-----PRINT OUT INCREMENTAL AVERAGE NODAL STRESSES
      C
            IF(JC.EQ.O)GOTO 1
            WRITE(6,5)CXI(J),CYI(J),CXYI(J)
      1     CONTINUE
      C
      C-----FORMAT STATEMENTS
      C
      4     FORMAT(5X,I4,6(1PE12.3),OPF11.2)
      5     FORMAT(9X,3(1PE12.3))
      7     FORMAT(9X,3(1PE12.3),'    (ROTATED STRESSES)')
            RETURN
            END
```

```
MTS  FORTRAN IV G COMPILER(21.8) WITH SDS SUPPORT         MAIN        04-21-80   11:35:48        PAGE 0001
   1577.000                 C
   1578.000                 C     *****************************************************************
   1579.000                 C     *                                                               *
   1580.000                 C     *                              SMAX                             *
   1581.000                 C     *                                                               *
   1582.000                 C     *****************************************************************
   1583.000                 C
   1584.000                 C
   1585.000     0001              SUBROUTINE SMAX(X,Y,XY,PM1,PM2,TV3,THETA)
   1586.000                 C
   1587.000                 C
   1588.000                 CCCCCCCCCCCCCCCCCCCCCCCCCCCCCCCCCCCCCCCCCCCCCCCCCCCCCCCCCCCCCCCCCCCCCCC
   1589.000                 C                                                                     C
   1590.000                 C     SUBROUTINE SMAX - DETERMINES THE PRINCIPAL STRESSES AND         C
   1591.000                 C                       THEIR DIRECTIONS                              C
   1592.000                 C                                                                     C
   1593.000                 C     INPUT                                                           C
   1594.000                 C                                                                     C
   1595.000                 C     X  = SIGMA-X STRESS                                             C
   1596.000                 C     Y  = SIGMA-Y STRESS                                             C
   1597.000                 C     XY = SHEAR STRESS                                               C
   1598.000                 C                                                                     C
   1599.000                 C     OUTPUT                                                          C
   1600.000                 C                                                                     C
   1601.000                 C     PM1   = MAJOR PRINCIPAL STRESS                                  C
   1602.000                 C     PM2   = MINOR PRINCIPAL STRESS                                  C
   1603.000                 C     TV3   = MAXIMUM SHEAR STRESS                                    C
   1604.000                 C     THETA = DIRECTION OF MAJOR PRINCIPAL STRESS                     C
   1605.000                 C                                                                     C
   1606.000                 CCCCCCCCCCCCCCCCCCCCCCCCCCCCCCCCCCCCCCCCCCCCCCCCCCCCCCCCCCCCCCCCCCCCCCC
   1607.000                 C
   1608.000                 C
   1609.000                 C-----CALCULATE PRINCIPAL STRESSES
   1610.000                 C
   1611.000     0002              TV1=0.5*(X+Y)
   1612.000     0003              TV2=0.5*(X-Y)
   1613.000     0004              TV3=SQRT(TV2**2+XY**2)
   1614.000     0005              PM1=TV1+TV3
   1615.000     0006              PM2=TV1-TV3
   1616.000                 C
   1617.000                 C-----CALCULATE DIRECTION OF PRINCIPAL STRESSES
   1618.000                 C
   1619.000     0007              IF(TV3) 1,2,1
   1620.000     0008          2   THETA=0.785398
   1621.000     0009              GO TO 3
   1622.000     0010          1   TV1=TV2/TV3
   1623.000     0011              IF((1.0-ABS(TV1)).GT.0.0001)GOTO 6
   1624.000     0012              IF(TV1.GT.0.0) THETA=0.0
   1625.000     0013              IF(TV1.LT.0.0) THETA=1.570796
   1626.000     0014              GO TO 3
   1627.000     0015          6   THETA=ARCOS(TV1)*0.5
   1628.000     0016          3   IF(XY.LT.0.0) THETA=-THETA
   1629.000     0017              TV1=PM1
   1630.000     0018              IF(ABS(PM1).GE.ABS(PM2))GOTO 5
   1631.000     0019              PM1=PM2
```

FINE PRINT

```
MTS  FORTRAN IV G COMPILER(21.8) WITH SDS SUPPORT        SMAX        04-21-80     11:35:48        PAGE 0002

 1632.000     0020                 PM2=TV1
 1633.000     0021                 THETA=THETA+1.570796
 1634.000     0022          5      THETA=THETA*(180./3.141593)
 1635.000     0023                 RETURN
 1636.000     0024                 END
```

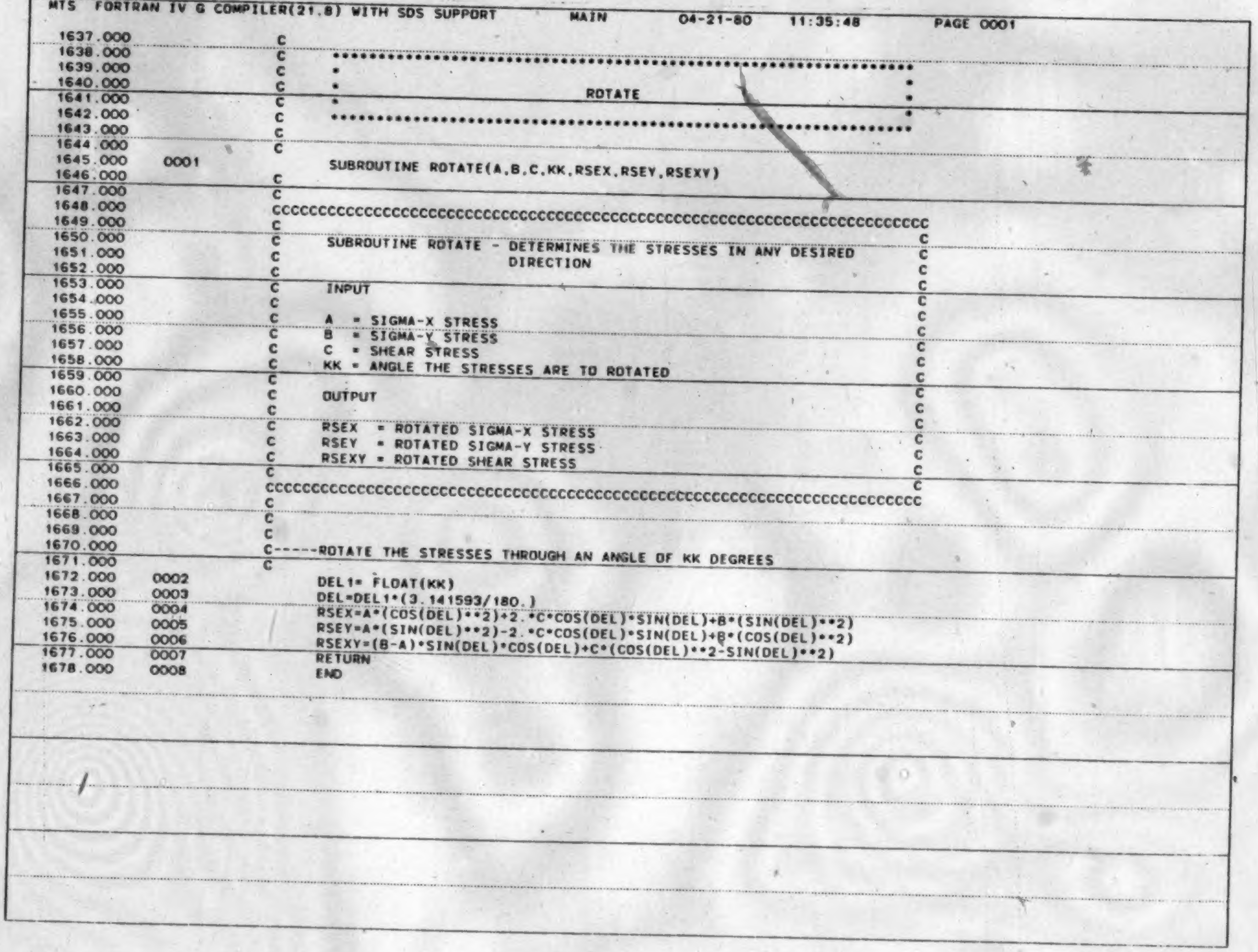

```
MTS  FORTRAN IV G COMPILER(21.8) WITH SDS SUPPORT        MAIN        04-21-80    11:35:48        PAGE 0001
   1637.000              C
   1638.000              C    *********************************************************
   1639.000              C    *                                                       *
   1640.000              C    *                       ROTATE                          *
   1641.000              C    *                                                       *
   1642.000              C    *********************************************************
   1643.000              C
   1644.000              C
   1645.000     0001           SUBROUTINE ROTATE(A,B,C,KK,RSEX,RSEY,RSEXY)
   1646.000              C
   1647.000              C
   1648.000              CCCCCCCCCCCCCCCCCCCCCCCCCCCCCCCCCCCCCCCCCCCCCCCCCCCCCCCCCCCCCCCCCCCC
   1649.000              C                                                                  C
   1650.000              C     SUBROUTINE ROTATE - DETERMINES THE STRESSES IN ANY DESIRED   C
   1651.000              C                         DIRECTION                                C
   1652.000              C                                                                  C
   1653.000              C     INPUT                                                        C
   1654.000              C                                                                  C
   1655.000              C     A  = SIGMA-X STRESS                                          C
   1656.000              C     B  = SIGMA-Y STRESS                                          C
   1657.000              C     C  = SHEAR STRESS                                            C
   1658.000              C     KK = ANGLE THE STRESSES ARE TO ROTATED                       C
   1659.000              C                                                                  C
   1660.000              C     OUTPUT                                                       C
   1661.000              C                                                                  C
   1662.000              C     RSEX  = ROTATED SIGMA-X STRESS                               C
   1663.000              C     RSEY  = ROTATED SIGMA-Y STRESS                               C
   1664.000              C     RSEXY = ROTATED SHEAR STRESS                                 C
   1665.000              C                                                                  C
   1666.000              CCCCCCCCCCCCCCCCCCCCCCCCCCCCCCCCCCCCCCCCCCCCCCCCCCCCCCCCCCCCCCCCCCCC
   1667.000              C
   1668.000              C
   1669.000              C
   1670.000              C-----ROTATE THE STRESSES THROUGH AN ANGLE OF KK DEGREES
   1671.000              C
   1672.000     0002           DEL1= FLOAT(KK)
   1673.000     0003           DEL=DEL1*(3.141593/180.)
   1674.000     0004           RSEX=A*(COS(DEL)**2)+2.*C*COS(DEL)*SIN(DEL)+B*(SIN(DEL)**2)
   1675.000     0005           RSEY=A*(SIN(DEL)**2)-2.*C*COS(DEL)*SIN(DEL)+B*(COS(DEL)**2)
   1676.000     0006           RSEXY=(B-A)*SIN(DEL)*COS(DEL)+C*(COS(DEL)**2-SIN(DEL)**2)
   1677.000     0007           RETURN
   1678.000     0008           END
```

FINE PRINT

```
MTS  FORTRAN IV G COMPILER(21.8) WITH SDS SUPPORT        MAIN        04-21-80    11:35:49        PAGE 0001

1679.000              C
1680.000              C     ****************************************************************
1681.000              C     *                                                              *
1682.000              C     *                            TIMGEN                            *
1683.000              C     *                                                              *
1684.000              C     ****************************************************************
1685.000              C
1686.000              C
1687.000   0001             SUBROUTINE TIMGEN
1688.000              C
1689.000              C
1690.000              CCCCCCCCCCCCCCCCCCCCCCCCCCCCCCCCCCCCCCCCCCCCCCCCCCCCCCCCCCCCCCCCCCCCCCC
1691.000              C                                                                     C
1692.000              C     SUBROUTINE TIMGEN - GENERATES THE AVERAGE TIME INTERVAL FOR     C
1693.000              C                         EACH INCREMENT OF CREEP                     C
1694.000              C                                                                     C
1695.000              C     DATA REQUIRED FROM COMMON BLOCKS                                C
1696.000              C                                                                     C
1697.000              C     JC    = CURRENT CREEP INCREMENT NUMBER                          C
1698.000              C     NE    = NUMBER OF ELEMENTS                                      C
1699.000              C     MET   = ELASTIC MATERIAL NUMBER INDICATOR FOR EACH ELEMENT      C
1700.000              C     MMET  = CREEP MATERIAL NUMBER INDICATOR FOR EACH ELEMENT        C
1701.000              C     EI    = ELASTIC MODULUS FOR EACH MATERIAL                       C
1702.000              C     COEF1 = STRESS COEFFICIENT IN THE CREEP LAW                     C
1703.000              C     COEF2 = STRESS COEFFICIENT IN THE CREEP LAW                     C
1704.000              C     EXP1  = STRESS EXPONENT IN THE CREEP LAW                        C
1705.000              C     EXP2  = STRESS EXPONENT IN THE CREEP LAW                        C
1706.000              C     EXP3  = TIME EXPONENT IN THE CREEP LAW                          C
1707.000              C     SEYL  = EFFECTIVE ELASTIC STRESS FOR EACH ELEMENT               C
1708.000              C     SEXYL = CHANGE IN EFFECTIVE ELASTIC STRESS FOR EACH ELEMENT     C
1709.000              C                                                                     C
1710.000              C     OUTPUT PLACED IN BLK12                                          C
1711.000              C                                                                     C
1712.000              C     TAV = TIME INTERVAL FOR CREEP INCREMENT #JC                     C
1713.000              C                                                                     C
1714.000              CCCCCCCCCCCCCCCCCCCCCCCCCCCCCCCCCCCCCCCCCCCCCCCCCCCCCCCCCCCCCCCCCCCCCCC
1715.000              C
1716.000              C
1717.000              C-----COMMON AND DIMENSION STATEMENTS
1718.000              C
1719.000   0002             REAL*8 SEYL,SEXYL,DT,TF,TIV,TAV,EI,UI,COEF1,COEF2,EXP1,EXP2,EXP3,
1720.000                   &       E,A1,A2,B1,B2,CN1,CN2,CM,CMI,EEFFC
1721.000   0003             INTEGER*2 MET,MMET
1722.000              C
1723.000   0004             COMMON /BLK2/ MET(300),EI(20),UI(20)
1724.000              C
1725.000   0005             COMMON /BLK8/ SEYL(300),SEXYL(300),EEFFC(300)
1726.000              C
1727.000   0006             COMMON /BLK11/ NN,NE,NUE,NUC,NGI,NLC,KV,NU,NB,NB1
1728.000              C
1729.000   0007             COMMON /BLK12/ JC,TIM,TAV,IPP
1730.000              C
1731.000   0008             COMMON /BLK15/ ETAO,ETA1,OMEGA,BETA,RHO
1732.000              C
1733.000   0009             COMMON /BLK16/ MMET(300),COEF1(20),COEF2(20),EXP1(20),EXP2(20),
MTS  FORTRAN IV G COMPILER(21.8) WITH SDS SUPPORT        TIMGEN      04-21-80     11:35:49            PAGE 0002
  1734.000                         &                EXP3(20)
  1735.000                    C
  1736.000                    C-----INTIALIZATION
  1737.000                    C
  1738.000      0010                 TIV=1000000.
  1739.000                    C
  1740.000                    C-----CALCULATE TIME INTERVAL
  1741.000                    C
  1742.000      0011                 DO 10 I=1,NE
  1743.000      0012                 MNE=MET(I)
  1744.000      0013                 MNC=MMET(I)
  1745.000      0014                 E=EI(MNE)
  1746.000      0015                 B1=COEF1(MNC)
  1747.000      0016                 B2=COEF2(MNC)
  1748.000      0017                 CN1=EXP1(MNC)
  1749.000      0018                 CN2=EXP2(MNC)
  1750.000      0019                 CM=EXP3(MNC)
  1751.000      0020                 CMI=1./CM
  1752.000      0021                 A1=B1*SEYL(I)**CN1
  1753.000      0022                 A2=B2*SEYL(I)**CN2
  1754.000      0023                 IF(JC-1)9,7,8
  1755.000                    C
  1756.000      0024          7      DT=(SEYL(I)/(ETAO*E*(A1+A2)))**CMI
  1757.000      0025                 GOTO 9
  1758.000                    C
  1759.000      0026          8      TF=(EEFFC(I)/(A1+A2))**CMI
  1760.000      0027                 DT=(((SEYL(I)/(ETA1*E*(A1+A2)))+(TF**CM))**CMI)-TF
  1761.000      0028                 GOTO 9
  1762.000                    C
  1763.000      0029          9      IF(DT.LT.TIV)TIV=DT
  1764.000      0030          10     CONTINUE
  1765.000      0031                 IF(JC.EQ.1)GOTO 30
  1766.000                    C
  1767.000                    C-----CHECK MAGNITUDE OF TIME INTERVAL
  1768.000                    C
  1769.000      0032                 SRMAX=0.0
  1770.000      0033                 DO 20 I=1,NE
  1771.000      0034                 SR=SEXYL(I)/SEYL(I)
  1772.000      0035                 SRMAX=AMAX1(SR,SRMAX)
  1773.000      0036          20     CONTINUE
  1774.000      0037                 D=OMEGA/SRMAX
  1775.000      0038                 IF(D.GT.1.2)D=1.2
  1776.000      0039                 DT=D*TAV
  1777.000      0040                 IF(DT.LT.TIV)TIV=DT
  1778.000                    C
  1779.000      0041          30     TAV=TIV
  1780.000                    C
  1781.000      0042                 RETURN
  1782.000      0043                 END
```

FINE PRINT

```
MTS  FORTRAN IV G COMPILER(21.8) WITH SDS SUPPORT        MAIN        04-21-80    11:35:51        PAGE 0001

            C
            C     ***********************************************************
            C     *                                                         *
            C     *                         TSME                            *
            C     *                                                         *
            C     ***********************************************************
            C
            C
    0001          SUBROUTINE TSME
            C
            C
            CCCCCCCCCCCCCCCCCCCCCCCCCCCCCCCCCCCCCCCCCCCCCCCCCCCCCCCCCCCCCCCCCCCCCCCC
            C                                                                      C
            C     SUBROUTINE TSME - CALCULATES THE INCREMENTS OF CREEP STRAIN      C
            C                       AND THE FICTICOUS CREEP FORCES FOR EACH        C
            C                       INCREMENT OF CREEP                             C
            C                                                                      C
            C     DATA REQIURED FROM COMMON BLOCKS                                 C
            C                                                                      C
            C     JC   = CURRENT INCREMENT NUMBER                                  C
            C     NE   = NUMBER OF ELEMENTS                                        C
            C     NU   = TOTAL NUMBER OF UNKNOWNS IN CURRENT PROBLEM               C
            C     SEX  = ELASTIC ELEMENT SIGMA-X STRESSES                          C
            C     SEY  = ELASTIC ELEMENT SIGMA-Y STRESSES                          C
            C     SEZ  = ELASTIC ELEMENT SIGMA-Z STRESSES                          C
            C     SEXY = ELASTIC ELEMENT SHEAR STRESSES                            C
            C     SEYL = EFFECTIVE ELASTIC STRESS FOR EACH ELEMENT                 C
            C     TAV  = TIME INTERVAL FOR INCREMENT #JC                           C
            C     EI   = ELASTIC MODULUS FOR EACH ELEMENT                          C
            C     UI   = POISSON'S RATIO FOR EACH ELEMENT                          C
            C     COEF1 = STRESS COEFFICIENT IN THE CREEP LAW                      C
            C     COEF2 = STRESS COEFFICIENT IN THE CREEP LAW                      C
            C     EXP1  = STRESS EXPONENT IN THE CREEP LAW                         C
            C     EXP2  = STRESS EXPONENT IN THE CREEP LAW                         C
            C     EXP3  = TIME EXPONENT IN THE CREEP LAW                           C
            C     MET  = ELASTIC MATERIAL INDICATOR FOR EACH ELEMENT               C
            C     MMET = CREEP MATERIAL INDICATOR FOR EACH ELEMENT                 C
            C                                                                      C
            C     OUTPUT PLACED IN BLK3 AND BLK6                                   C
            C                                                                      C
            C     EXL  = INCREMENT OF CREEP STRAIN IN X-DIRECTION                  C
            C     EYL  = INCREMENT OF CREEP STRAIN IN Y-DIRECTION                  C
            C     EZL  = INCREMENT OF CREEP STRAIN IN Z-DIRECTION                  C
            C     EXYL = INCREMENT OF CREEP SHEAR STRAIN                           C
            C     FN   = FICTICOUS LOAD VECTOR FOR CREEP INCREMENT #JC             C
            C                                                                      C
            CCCCCCCCCCCCCCCCCCCCCCCCCCCCCCCCCCCCCCCCCCCCCCCCCCCCCCCCCCCCCCCCCCCCCCCC
            C
            C
            C-----DIMENSION STATEMENTS
            C
    0002          REAL*8 SEX,SEY,SEZ,SEXY,SEYL,SEXYL,EXL,EYL,EZL,EXYL,FL(6),FN,
                 &       PT(9),FCX,FCY,FCXY,TAV,EI,COEF1,COEF2,EXP1,EXP2,EXP3,
                 &       A1,A2,B1,B2,CN1,CN2,CM,CMI,TF,CRE,EX,EY,EXY,EEFFC
            C
```

```
MTS  FORTRAN IV G COMPILER(21.8) WITH SDS SUPPORT          TSME          04-21-80     11:35:51          PAGE 0002

  1838.000     0003                INTEGER*2 MET,MMET,NP(6)
  1839.000               C
  1840.000     0004                COMMON /BLK2/ MET(300),EI(20)
  1841.000               C
  1842.000     0005                COMMON /BLK3/ FN(400)
  1843.000               C
  1844.000     0006                COMMON /BLK6/ EX(300),EY(300),EXY(300),
  1845.000                    &                  EXL(300),EYL(300),EZL(300),EXYL(300)
  1846.000               C
  1847.000     0007                COMMON /BLK7/ SEX(300),SEY(300),SEZ(300),SEXY(300)
  1848.000               C
  1849.000     0008                COMMON /BLK8/ SEYL(300),SEXYL(300),EEFFC(300)
  1850.000               C
  1851.000     0009                COMMON /BLK11/ NN,NE,NUE,NUC,NGI,NLC,KV,NU,NB,NB1
  1852.000               C
  1853.000     0010                COMMON /BLK12/ JC,TIM,TAV,IPP
  1854.000               C
  1855.000     0011                COMMON /BLK16/ MMET(300),COEF1(20),COEF2(20),EXP1(20),EXP2(20),
  1856.000                    &                   EXP3(20)
  1857.000               C
  1858.000               C-----INTIALIZATION
  1859.000               C
  1860.000     0012                DO 10 I=1,NU
  1861.000     0013                FN(I)=0.0
  1862.000     0014          10    CONTINUE
  1863.000               C
  1864.000     0015                DO 4 I=1,NE
  1865.000     0016                MNE=MET(I)
  1866.000     0017                MNC=MMET(I)
  1867.000     0018                E=EI(MNE)
  1868.000     0019                B1=COEF1(MNC)
  1869.000     0020                B2=COEF2(MNC)
  1870.000     0021                CN1=EXP1(MNC)
  1871.000     0022                CN2=EXP2(MNC)
  1872.000     0023                CM=EXP3(MNC)
  1873.000     0024                CMI=1./CM
  1874.000     0025                A1=B1*(SEYL(I)**CN1)
  1875.000     0026                A2=B2*(SEYL(I)**CN2)
  1876.000               C
  1877.000     0027                IF(JC.EQ.1)GOTO 8
  1878.000     0028                TF=(EEFFC(I)/(A1+A2))**CMI
  1879.000     0029                GOTO 9
  1880.000     0030          8     TF=0.0
  1881.000               C
  1882.000               C-----CALCULATE THE INCREMENTS OF CREEP STRAIN IN EACH DIRECTION
  1883.000               C
  1884.000     0031          9     CRE=(A1+A2)*((TF+TAV)**CM-TF**CM)
  1885.000     0032                EXL(I)=(CRE*(2.*SEX(I)-SEY(I)-SEZ(I)))/(2.*SEYL(I))
  1886.000     0033                EYL(I)=(CRE*(2.*SEY(I)-SEZ(I)-SEX(I)))/(2.*SEYL(I))
  1887.000     0034                EZL(I)=(CRE*(2.*SEZ(I)-SEX(I)-SEY(I)))/(2.*SEYL(I))
  1888.000     0035                EXYL(I)=(3.*CRE*SEXY(I))/SEYL(I)
  1889.000               C
  1890.000               C-----READ ELEMENT DATA
  1891.000               C
  1892.000     0036                READ(1)(NP(K),K=1,6),(PT(K),K=1,9),ARR
```

```
MTS  FORTRAN IV G COMPILER(21.8) WITH SDS SUPPORT        TSME        04-21-80    11:35:51        PAGE 0003

  1893.000                  C
  1894.000                  C-----CALCULATE THE FICTICOUS CREEP FORCES
  1895.000                  C
  1896.000      0037              COMM=E/(1+.5)
  1897.000      0038              FCX=COMM*EXL(I)
  1898.000      0039              FCY=COMM*EYL(I)
  1899.000      0040              FCXY=COMM*EXYL(I)/2.
  1900.000      0041              FL(1)=(PT(4)*FCX+PT(7)*FCXY)/2.
  1901.000      0042              FL(2)=(PT(5)*FCX+PT(8)*FCXY)/2.
  1902.000      0043              FL(3)=(PT(6)*FCX+PT(9)*FCXY)/2.
  1903.000      0044              FL(4)=(PT(4)*FCXY+PT(7)*FCY)/2.
  1904.000      0045              FL(5)=(PT(5)*FCXY+PT(8)*FCY)/2.
  1905.000      0046              FL(6)=(PT(6)*FCXY+PT(9)*FCY)/2.
  1906.000                  C
  1907.000                  C-----ADD THE FICTICOUS CREEP FORCES INTO THE LOAD VECTOR
  1908.000                  C
  1909.000      0047              DO 7 J=1,6
  1910.000      0048              IF(NP(J).EQ.0)GOTO 7
  1911.000      0049              IJ=NP(J)
  1912.000      0050              FN(IJ)=FN(IJ)+FL(J)
  1913.000      0051        7     CONTINUE
  1914.000      0052        4     CONTINUE
  1915.000      0053              REWIND 1
  1916.000      0054              RETURN
  1917.000      0055              END
```

```
MTS  FORTRAN IV G COMPILER(21.8) WITH SDS SUPPORT        MAIN        04-21-80    11:35:53        PAGE 0001
  1918.000              C
  1919.000              C
  1920.000              C    ******************************************************
  1921.000              C    *
  1922.000              C    *                                                    *
  1923.000              C    *                        STEADY                      *
  1924.000              C    ******************************************************
  1925.000              C
  1926.000              C
  1927.000     0001          SUBROUTINE STEADY
  1928.000              C
  1929.000              C
  1930.000              CCCCCCCCCCCCCCCCCCCCCCCCCCCCCCCCCCCCCCCCCCCCCCCCCCCCCCCCCCCCCC
  1931.000              C                                                            C
  1932.000              C    SUBROUTINE STEADY - CALCULATES AND PRINTS THE CREEP SOLUTION C
  1933.000              C                     CONVERGENCE PARAMETERS                 C
  1934.000              C                                                            C
  1935.000              C    DATA REQUIRED FROM COMMON BLOCKS                        C
    36.000              C                                                            C
     7.000              C    NE    = NUMBER OF ELEMENTS                              C
    38.000              C    SEYL  = ELASTIC EFFECTIVE STRESS FOR EACH ELEMENT       C
  1939.000              C    SEXYL = CHANGE IN ELASTIC EFFECTIVE STRESS FOR EACH ELEMENT C
  1940.000              C    TAV   = TIME INTERVAL FOR CURRENT CREEP INCREMENT       C
  1941.000              C                                                            C
  1942.000              C    OUTPUT STORED IN BLK15                                  C
  1943.000              C                                                            C
  1944.000              C    RHO  = MAXIMUM FRACTIONAL CHANGE IN EFFECTIVE STRESS FOR C
  1945.000              C           CURRENT CREEP INCREMENT                          C
  1946.000              C    BETA = MAXIMUM CHANGE IN EFFECTIVE STRESS PER UNIT TIME FOR C
  1947.000              C           CURRENT CREEP INCREMENT                          C
  1948.000              C                                                            C
  1949.000              CCCCCCCCCCCCCCCCCCCCCCCCCCCCCCCCCCCCCCCCCCCCCCCCCCCCCCCCCCCCCC
  1950.000              C
  1951.000              C
  1952.000     0002          REAL*8 SEXYL,SEYL,TAV
  1953.000              C
  1954.000     0003          COMMON /BLK8/ SEYL(300),SEXYL(300)
  1955.000              C
  1956.000     0004          COMMON /BLK11/ NN,NE,NUE,NUC,NGI,NLC,KV,NU,NB,NB1
  1957.000              C
  1958.000     0005          COMMON /BLK12/ JC,TIM,TAV,IPP
  1959.000              C
  1960.000     0006          COMMON /BLK15/ ETAO,ETA1,OMEGA,RHO,BETA
  1961.000              C
  1962.000     0007          RHO=0.0
  1963.000     0008          BETA=0.0
  1964.000              C
  1965.000     0009          DO 3 I=1,NE
  1966.000              C
  1967.000     0010          SRATIO=SEXYL(I)/SEYL(I)
  1968.000     0011          IF(SRATIO.LT.RHO)GOTO 1
  1969.000     0012          RHO=SRATIO
  1970.000     0013          IELM1=I
  1971.000     0014        1 CONTINUE
  1973.000     0015          SRATE=SEXYL(I)/TAV
```

```
MTS  FORTRAN IV G COMPILER(21.8) WITH SDS SUPPORT          STEADY       04-21-80     11:35:53          PAGE 0002

 1974.000     0016                IF(SRATE.LT.BETA)GOTO 2
 1975.000     0017                BETA=SRATE
 1976.000     0018                IELM2=I
 1977.000     0019          2     CONTINUE
 1978.000                   C
 1979.000     0020          3     CONTINUE
 1980.000                   C
 1981.000     0021                WRITE(6,4)RHO,IELM1,BETA,IELM2
 1982.000                   C
 1983.000     0022          4     FORMAT(/5X,'STEADY STATE CONTION CHECKS:'/7X,'MAXIMUM ',
 1984.000                        &      'FRACTIONAL CHANGE IN EFFECTIVE STRESS     =',1PE11.3,
 1985.000                        &      ' OCCURS IN ELEMENT',I5/7X,'MAXIMUM CHANGE IN EFFECTIVE ',
 1986.000                        &      'STRESS PER UNIT TIME =',1PE11.3,' OCCURS IN ELEMENT',I5)
 1987.000                   C
 1988.000     0023                RETURN
 1989.000     0024                END
```

```
MTS  FORTRAN IV G COMPILER(21.8) WITH SDS SUPPORT        MAIN        04-21-80     11:35:55         PAGE 0001

  1990.000               C
  1991.000               C
  1992.000               C     ************************************************************
  1993.000               C     *                                                          *
  1994.000               C     *                         FINAL                            *
  1995.000               C     *                                                          *
  1996.000               C     ************************************************************
  1997.000               C
  1998.000               C
  1999.000    0001             SUBROUTINE FINAL
  2000.000               C
  2001.000               C
  2002.000               CCCCCCCCCCCCCCCCCCCCCCCCCCCCCCCCCCCCCCCCCCCCCCCCCCCCCCCCCCCCCCCC
  2003.000               C                                                              C
  2004.000               C     SUBROUTINE FINAL - PRINTS OUT THE CREEP SOLUTION RESULTS FOR C
  2005.000               C                        THE FINAL TIME STEP AND ALSO WRITES ALL THE C
  2006.000               C                        NECESSARY DATA ON TAPE REQUIRED FOR A   C
  2007.000               C                        CONTINUATION RUN IF ßESIED AT A LATER DATE C
  2008.000               C                                                              C
  2009.000               C     THE FOLLOWING LIST OF VARIABLES AND ARRAYS ARE STORED ON  C
  2010.000               C     UNIT JTAPE FOR RETREIVAL AT A FUTURE DATE                C
  2011.000               C        NN        NE        NUE       NUC       KV        NU    C
  2012.000               C        NB        NB1       ND        NODES     EI        UI    C
  2013.000               C        COEF1     COEF2     EXP1      EXP2      EXP3      F     C
  2014.000               C        SM        JC        TIM       TAV       ETAO      ETA1  C
  2015.000               C        OMEGA     RHO       BETA      DX        DY        EX    C
  2016.000               C        EY        EXY       EXC       EYC       EZC       EXYC  C
  2017.000               C        FS1       FS2       FS3       SEX       SEY       SEZ   C
  2018.000               C        SEXY      SNX       SNY       SNXY      SEYL      SEXYL C
  2019.000               C        EEFFC                                                 C
  2020.000               C     ALL THE DATA STORED ON UNIT 1 IS ALSO WRITTEN ON UNIT JTAPE C
  2021.000               C                                                              C
  2022.000               CCCCCCCCCCCCCCCCCCCCCCCCCCCCCCCCCCCCCCCCCCCCCCCCCCCCCCCCCCCCCCCC
  2023.000               C
  2024.000               C
  2025.000    0002             REAL*8 TAV,EI,UI,FN,F,COEF1,COEF2,EXP1,EXP2,EXP3,EX,EY,EXY,
  2026.000                    &       EXL,EYL,EZL,EXYL,SEX,SEY,SEZ,SEXY,SEYL,SEXYL,EEFFC,SM,
  2027.000                    &       EXC,EYC,EZC,EXYC,PT(9),ARR
  2028.000    0003             REAL*8 START/'START   '/,RSTART/'RSTART  '/,RUN/'RUN     '/,
  2029.000                    &       STOP/'STOP    '/,PLOT/'PLOT    '/,CONTIN/'CONTIN  '/,
  2030.000                    &       CODE1,CODE2
  2031.000    0004             INTEGER*2 ND,MET,MMET,NODES,NP(6)
 *2032.000               C
  2033.000    0005             COMMON /BLK1/ ND(200,2)
  2034.000               C
  2035.000    0006             COMMON /BLK2/ MET(300),EI(20),UI(20)
  2036.000               C
  2037.000    0007             COMMON /BLK3/ FN(400),F(400)
  2038.000               C
  2039.000    0008             COMMON /BLK4/ DX(200),DY(200),DXI(200),DYI(200),
  2040.000                    &              VELX(200),VELY(200)
  2041.000               C
  2042.000    0009             COMMON /BLK6/ EX(300),EY(300),EXY(300),
  2043.000                    &              EXL(300),EYL(300),EZL(300),EXYL(300),
  2044.000                    &              EXC(300),EYC(300),EZC(300),EXYC(300),
```

FINE PRINT

```
MTS  FORTRAN IV G COMPILER(21.8) WITH SDS SUPPORT        FINAL       04-21-80     11:35:55         PAGE 0002
  2045.000                      &              FS1(300),FS2(300),FS3(300)
  2046.000               C
  2047.000     0010              COMMON /BLK7/ SEX(300),SEY(300),SEZ(300),SEXY(300),
  2048.000                      &              CXI(200),CYI(200),CXYI(200),CNC(200),
  2049.000                      &              SNX(200),SNY(200),SNXY(200)
  2050.000               C
  2051.000     0011              COMMON /BLK8/ SEYL(300),SEXYL(300),EEFFC(300)
  2052.000               C
  2053.000     0012              COMMON /BLK11/ NN,NE,NUE,NUC,NGI,NLC,KV,NU,NB,NB1
  2054.000               C
  2055.000     0013              COMMON /BLK12/ JC,TIM,TAV,IPP,ITAPE,JTAPE
  2056.000               C
  2057.000     0014              COMMON /BLK13/ SM(5000)
  2058.000               C
  2059.000     0015              COMMON /BLK14/ NODES(300,3)
  2060.000               C
  2081.000     0016              COMMON /BLK15/ ETAO,ETA1,OMEGA,RHO,BETA
  2062.000               C
  2063.000     0017              COMMON /BLK16/ MMET(300),COEF1(20),COEF2(20),EXP1(20),EXP2(20),
  2064.000                      &              EXP3(20)
  2065.000               C
  2066.000     0018              COMMON /BLK17/ CODE1,CODE2
  2067.000               C
  2068.000               C-----PRINT OUT THE NODAL DISPLACEMENTS, ELEMENT STRESSES AND STRAINS
  2069.000               C     AND THE NODAL STRESSES FOR THE LAST TIME STEP
  2070.000               C
  2071.000     0019              WRITE(6,600)
  2072.000     0020              WRITE(6,605)JC,TAV,TIM
  2073.000               C
  2074.000     0021              WRITE(6,610)JC
  2075.000     0022              DO 5 I=1,NN
  2076.000     0023              WRITE(6,615)I,DXI(I),DYI(I),DX(I),DY(I),VELX(I),VELY(I)
  2077.000     0024        5     CONTINUE
  2078.000               C
  2079.000     0025              WRITE(6,620)JC
  2080.000     0026              DO 10 J=1,NE
  2081.000     0027              CALL SMAX(SEX(J),SEY(J),SEXY(J),XM1,XM2,XM3,XM4)
  2082.000     0028              WRITE(6,621)J,EX(J),EY(J),EXY(J),SEX(J),SEY(J),SEXY(J),
  2083.000                      &             XM1,XM2,XM3,XM4
  2084.000     0029              WRITE(6,622)FS1(J),FS2(J),FS3(J)
  2085.000     0030              WRITE(6,623)EXC(J),EYC(J),EZC(J),EXYC(J)
  2086.000     0031              WRITE(6,624)SEYL(J),SEZ(J)
  2087.000     0032       10     CONTINUE
  2088.000               C
  2089.000     0033              WRITE(6,630)JC
  2090.000     0034              DO 20 J=1,NN
  2091.000     0035              CALL SMAX(SNX(J),SNY(J),SNXY(J),XM1,XM2,XM3,XM4)
  2092.000     0036              WRITE(6,635)J,SNX(J),SNY(J),SNXY(J),XM1,XM2,XM3,XM4
  2093.000     0037       20     CONTINUE
  2094.000               C
  2095.000               C-----WRITE ALL DATA ON TAPE REQUIRED FOR A CONTINUATION RUN
  2096.000               C     AT A LATER DATE
  2097.000               C
  2098.000     0038              IF(CODE2.EQ.RUN)RETURN
  2099.000     0039              REWIND JTAPE
```

FINE PRINT

```
MTS  FORTRAN IV G COMPILER(21.8) WITH SDS SUPPORT        FINAL       04-21-80     11:35:55           PAGE 0003

 2100.000      0040               WRITE(JTAPE)NN,NE,NUE,NUC,KV,NU,NB,NB1
 2101.000      0041               WRITE(JTAPE)((ND(I,J),J=1,2),I=1,NN)
 2102.000      0042               WRITE(JTAPE)((NODES(I,J),J=1,3),MET(I),MMET(I),I=1,NE)
 2103.000      0043               WRITE(JTAPE)(EI(I),UI(I),I=1,NUE)
 2104.000      0044               WRITE(JTAPE)(COEF1(I),COEF2(I),EXP1(I),EXP2(I),EXP3(I),I=1,NUC)
 2105.000      0045               WRITE(JTAPE)(F(I),I=1,NU)
 2106.000      0046               NV=NB1*NU
 2107.000      0047               WRITE(JTAPE)(SM(I),I=1,NV)
 2108.000      0048               WRITE(JTAPE)JC,TIM,TAV
 2109.000      0049               WRITE(JTAPE)ETAO,ETA1,OMEGA,RHO,BETA
 2110.000      0050               WRITE(JTAPE)(DX(I),DY(I),I=1,NN)
 2111.000      0051               WRITE(JTAPE)(EX(I),EY(I),EXY(I),I=1,NE)
 2112.000      0052               WRITE(JTAPE)(EXC(I),EYC(I),EZC(I),EXYC(I),I=1,NE)
 2113.000      0053               WRITE(JTAPE)(FS1(I),FS2(I),FS3(I),I=1,NE)
 2114.000      0054               WRITE(JTAPE)(SEX(I),SEY(I),SEZ(I),SEXY(I),I=1,NE)
 2115.000      0055               WRITE(JTAPE)(SNX(I),SNY(I),SNXY(I),I=1,NN)
 2116.000      0056               WRITE(JTAPE)(SEYL(I),SEXYL(I),EEFFC(I),I=1,NE)
 2117.000      0057               DO 30 I=1,NE
 2118.000      0058               READ(1)(NP(K),K=1,6),(PT(K),K=1,9),ARR
 2119.000      0059               WRITE(JTAPE)(NP(K),K=1,6),(PT(K),K=1,9),ARR
 2120.000      0060         30    CONTINUE
 2121.000      0061               WRITE(6,640)JC,JTAPE
 2122.000                   C
 2123.000                   C-----FORMAT STATEMENTS
 2124.000                   C
 2125.000      0062        600    FORMAT('1')
 2126.000      0063        605    FORMAT(///2X,'COMPLETE GRID OUTPUT FOR FINAL TIME STEP'//5X,
 2127.000                        &      'CREEP INCREMENT NUMBER',I5,5X,'INCREMENT OF TIME  = ',
 2128.000                        &      1PE12.3/5X,27('*'),5X,'TOTAL ELAPSED TIME = ',1PE12.3)
 2129.000      0064        610    FORMAT(///5X,'NODAL DISPLACEMENTS AND DISPLACEMENT RATE DUE TO ',
 2130.000                        &      'CREEP INCREMENT',I5//18X,'INCREMENT OF DISPLACEMENT',8X,
 2131.000                        &      'TOTAL ACCUMULATED DISPLACEMENT',14X,'DISPLACEMENT RATE'/
 2132.000                        &      5X,'NODE',1X,2('    X-DISPLACEMENT    Y-DISPLACEMENT'),
 2133.000                        &      8X,'X-VELOCITY',8X,'Y-VELOCITY'/)
 2134.000      0065        615    FORMAT(5X,I4,1X,6(1PE18.4))
 2135.000      0066        620    FORMAT(///5X,'ELEMENT STRAINS AND STRESSES DUE TO CREEP ',
 2136.000                        &      'INCREMENT',I4/7X,'( FIRST LINE GIVES TOTAL )'//5X,
 2137.000                        &      'ELEMENT   X-STRAIN   Y-STRAIN  XY-STRAIN   X-STRESS',
 2138.000                        &      '   Y-STRESS  XY-STRESS  MAXSTRESS  MINSTRESS   MAXSHEAR',
 2139.000                        &      '  DIRECTION'/)
 2140.000      0067        621    FORMAT(5X,I5,2X,9(1PE11.3),OPF10.2)
 2141.000      0068        622    FORMAT(12X,3(1PE11.3),'  (TOTAL ELASTIC STRAIN)')
 2142.000      0069        623    FORMAT(12X,4(1PE11.3),'  (TOTAL ACCUMULATED CREEP STRAIN, ',
 2143.000                        &      'X, Y, Z & XY COMPONENTS)')
 2144.000      0070        624    FORMAT(14X,'EFFECTIVE STRESS = ',1PE11.3,14X,'SIGMA-Z = ',
 2145.000                        &      1PE11.3/)
 2146.000      0071        630    FORMAT(///5X,'AVERAGE NODAL STRESSES FOR CREEP INCREMENT',I4//
 2147.000                        &      5X,'NODE    X-STRESS     Y-STRESS    XY-STRESS  MAX STRESS',
 2148.000                        &      '  MIN STRESS   MAX SHEAR   DIRECTION'/)
 2149.000      0072        635    FORMAT(5X,I4,6(1PE12.3),OPF11.2)
 2150.000      0073        640    FORMAT(//2X,'RESULTS FOR CREEP INCREMENT #',I4,' WRITTEN ON ',
 2151.000                        &      'TAPE',I3,'1')
 2152.000                   C
 2153.000      0074               REWIND 1
 2154.000      0075               REWIND JTAPE
```

FINE PRINT

```
MTS  FORTRAN IV G COMPILER(21.8) WITH SDS SUPPORT          FINAL       04-21-80     11:35:55         PAGE 0004
  2155.000     0076                RETURN
  2156.000     0077                END
```

```
MTS  FORTRAN IV G COMPILER(21.8) WITH SDS SUPPORT        MAIN        04-21-80      11:35:59          PAGE 0001
      C
      C
      C     ****************************************************************
      C     *                                                              *
      C     *                           INPUT                              *
      C     *                                                              *
      C     ****************************************************************
      C
      C
0001        SUBROUTINE INPUT
      C
      C
      CCCCCCCCCCCCCCCCCCCCCCCCCCCCCCCCCCCCCCCCCCCCCCCCCCCCCCCCCCCCCCCCCCCCCCCC
      C                                                                      C
      C     SUBROUTINE INPUT - READS IN ALL THE DATA OFF OF TAPE THAT IS    C
      C                       REQUIRED FOR A CONTINUATION OF A PREVIOUSLY   C
      C                       RUN PROBLEM                                   C
      C                                                                      C
      C     THE FOLLOWING LIST OF VARIABLES AND ARRAYS IS READ FROM         C
      C     UNIT ITAPE FOR RESTARTING A PROBLEM TERMINATED EARLY            C
      C       NN        NE        NUE       NUC       KV        NU          C
      C       NB        NB1       ND        NODES     EI        UI          C
      C       COEF1     COEF2     EXP1      EXP2      EXP3      F           C
      C       SM        JC        TIM       TAV       ETAO      ETA1        C
      C       OMEGA     RHO       BETA      DX        DY        EX          C
      C       EY        EXY       EXC       EYC       EZC       EXYC        C
      C       FS1       FS2       FS3       SEX       SEY       SEZ         C
      C       SEXY      SNX       SNY       SNXY      SEYL      SEXYL       C
      C       EEFFC                                                         C
      C     ALL THE DATA REQUIRED ON UNIT 1 IS ALSO READ FROM UNIT JTAPE    C
      C                                                                      C
      CCCCCCCCCCCCCCCCCCCCCCCCCCCCCCCCCCCCCCCCCCCCCCCCCCCCCCCCCCCCCCCCCCCCCCCC
      C
      C
0002        REAL*8 TAV,EI,UI,FN,F,COEF1,COEF2,EXP1,EXP2,EXP3,EX,EY,EXY,
           &     EXL,EYL,EZL,EXYL,SEX,SEY,SEZ,SEXY,SEYL,SEXYL,EEFFC,SM,
           &     EXC,EYC,EZC,EXYC,PT(9),ARR
0003        INTEGER*2 ND,MET,MMET,NODES,NP(6)
      C
0004        COMMON /BLK1/ ND(200,2)
      C
0005        COMMON /BLK2/ MET(300),EI(20),UI(20)
      C
0006        COMMON /BLK3/ FN(400),F(400)
      C
0007        COMMON /BLK4/ DX(200),DY(200)
      C
0008        COMMON /BLK6/ EX(300),EY(300),EXY(300),
           &              EXL(300),EYL(300),EZL(300),EXYL(300),
           &              EXC(300),EYC(300),EZC(300),EXYC(300),
           &              FS1(300),FS2(300),FS3(300)
      C
0009        COMMON /BLK7/ SEX(300),SEY(300),SEZ(300),SEXY(300),
           &              CXI(200),CYI(200),CXYI(200),CNC(200),
           &              SNX(200),SNY(200),SNXY(200)
```

FINE PRINT

```
MTS  FORTRAN IV G COMPILER(21.8) WITH SDS SUPPORT        INPUT       04-21-80     11:35:59          PAGE 0002
  2212.000                    C
  2213.000     0010                  COMMON /BLK8/ SEYL(300),SEXYL(300),EEFFC(300)
  2214.000                    C
  2215.000     0011                  COMMON /BLK11/ NN,NE,NUE,NUC,NGI,NLC,KV,NU,NB,NB1
  2216.000                    C
  2217.000     0012                  COMMON /BLK12/ JC,TIM,TAV,IPP,ITAPE,JTAPE
  2218.000                    C
  2219.000     0013                  COMMON /BLK13/ SM(5000)
  2220.000                    C
  2221.000     0014                  COMMON /BLK14/ NODES(300,3)
  2222.000                    C
  2223.000     0015                  COMMON /BLK15/ ETAO,ETA1,OMEGA,RHO,BETA
  2224.000                    C
  2225.000     0016                  COMMON /BLK16/ MMET(300),COEF1(20),COEF2(20),EXP1(20),EXP2(20),
  2226.000                         &                EXP3(20)
  2227.000                    C
  2228.000     0017                  REWIND ITAPE
  2229.000     0018                  READ(ITAPE)NN,NE,NUE,NUC,KV,NU,NB,NB1
  2230.000     0019                  READ(ITAPE)((ND(I,J),J=1,2),I=1,NN)
  2231.000     0020                  READ(ITAPE)((NODES(I,J),J=1,3),MET(I),MMET(I),I=1,NE)
  2232.000     0021                  READ(ITAPE)(EI(I),UI(I),I=1,NUE)
  2233.000     0022                  READ(ITAPE)(COEF1(I),COEF2(I),EXP1(I),EXP2(I),EXP3(I),I=1,NUC)
  2234.000     0023                  READ(ITAPE)(F(I),I=1,NU)
  2235.000     0024                  NV=NB1*NU
  2236.000     0025                  READ(ITAPE)(SM(I),I=1,NV)
  2237.000     0026                  READ(ITAPE)JC,TIM,TAV
  2238.000     0027                  READ(ITAPE)ETAO,ETA1,OMEGA,RHO,BETA
  2239.000     0028                  READ(ITAPE)(DX(I),DY(I),I=1,NN)
  2240.000     0029                  READ(ITAPE)(EX(I),EY(I),EXY(I),I=1,NE)
  2241.000     0030                  READ(ITAPE)(EXC(I),EYC(I),EZC(I),EXYC(I),I=1,NE)
  2242.000     0031                  READ(ITAPE)(FS1(I),FS2(I),FS3(I),I=1,NE)
  2243.000     0032                  READ(ITAPE)(SEX(I),SEY(I),SEZ(I),SEXY(I),I=1,NE)
  2244.000     0033                  READ(ITAPE)(SNX(I),SNY(I),SNXY(I),I=1,NN)
  2245.000     0034                  READ(ITAPE)(SEYL(I),SEXYL(I),EEFFC(I),I=1,NE)
  2246.000     0035                  DO 5 I=1,NE
  2247.000     0036                  READ(ITAPE)(NP(K),K=1,6),(PT(K),K=1,9),ARR
  2248.000     0037                  WRITE(1)(NP(K),K=1,6),(PT(K),K=1,9),ARR
  2249.000     0038           5      CONTINUE
  2250.000     0039                  REWIND 1
  2251.000     0040                  REWIND ITAPE
  2252.000                    C
  2253.000     0041                  WRITE(6,600)JC,ITAPE,TIM
  2254.000     0042                  WRITE(6,610)JC
  2255.000                    C
  2256.000     0043                  WRITE(6,615)
  2257.000     0044                  DO 10 I=1,NN
  2258.000     0045          10      WRITE(6,616)I,DX(I),DY(I)
  2259.000                    C
  2260.000     0046                  WRITE(6,620)
  2261.000     0047                  DO 20 I=1,NE
  2262.000     0048                  WRITE(6,621)I,EX(I),EY(I),EXY(I)
  2263.000     0049                  WRITE(6,622)FS1(I),FS2(I),FS3(I)
  2264.000     0050                  WRITE(6,623)EXC(I),EYC(I),EZC(I),EXYC(I)
  2265.000     0051                  WRITE(6,624)SEX(I),SEY(I),SEZ(I),SEXY(I)
  2266.000     0052          20      WRITE(6,625)SEYL(I),EEFFC(I)
```

FINE PRINT

```
MTS  FORTRAN IV G COMPILER(21.8) WITH SDS SUPPORT         INPUT       04-21-80     11:35:59          PAGE 0003
  2267.000                C
  2268.000     0053                WRITE(6,630)
  2269.000     0054                DO 25 I=1,NN
  2270.000     0055       25       WRITE(6,631)I,SNX(I),SNY(I),SNXY(I)
  2271.000                C
  2272.000                C-----FORMAT STATEMENTS
  2273.000                C
  2274.000     0056       600  FORMAT(///2X,26('*')/2X,'*',24X,'*'/2X,'* CREEP SOLUTION RESULTS *
  2275.000                   &        '/2X,'*',24X,'*'/2X,26('*')//5X,'CONTINUATION FROM A ',
  2276.000                   &        'PREVIOUS RUN '/5X,'CREEP INCREMENT # ',I4,' RESULTS READ ',
  2277.000                   &        'FROM TAPE',I3/5X,'TOTAL ELAPSED TIME = ',1PE10.3)
  2278.000     0057       610  FORMAT(///5X,'NODAL AND ELEMENT DATA READ FROM TAPE FOR CREEP ',
  2279.000                   &        'INCREMENT # ',I4)
  2280.000     0058       615  FORMAT(///5X,'ACCUMULATED NODAL DISPLACEMENT'//5X,'NODE',1X,
  2281.000                   &        2('     X-DISPLACEMENT     Y-DISPLACEMENT')/)
  2282.000     0059       616  FORMAT(5X,I4,2(1PE18.4))
  2283.000     0060       620  FORMAT(///5X,'ELEMENT STRESS AND STRAIN DATA'/)
  2284.000     0061       621  FORMAT(5X,'ELEMENT ',I3,4X,'TOTAL ELEMENT STRAIN (X, Y AND XY ',
  2285.000                   &        'COMPONENTS)',T75,3(1PE12.3))
  2286.000     0062       622  FORMAT(20X,'ELASTIC ELEMENT STRAIN (X, Y AND XY COMPONENTS)',
  2287.000                   &        T75,3(1PE12.3))
  2288.000     0063       623  FORMAT(20X,'ACCUMULATED CREEP STRAIN (X, Y, Z AND XY ',
  2289.000                   &        'COMPONENTS)',T75,4(1PE12.3))
  2290.000     0064       624  FORMAT(20X,'ELASTIC ELEMENT STRESS (X, Y, Z AND XY COMPONENTS)',
  2291.000                   &        T75,4(1PE12.3))
  2292.000     0065       625  FORMAT(20X,'EFFECTIVE STRESS = ',1PE12.3,10X,'EFFECTIVE CREEP ',
  2293.000                   &        'STRAIN = ',1PE12.3/)
  2294.000     0066       630  FORMAT(///5X,'NODAL STRESSES'//5X,'NODE',5X,'     SIGMA-X',
  2295.000                   &        '      SIGMA-Y     SIGMA-XY'/)
  2296.000     0067       631  FORMAT(5X,I4,5X,3(1PE12.3))
  2297.000                C
  2298.000     0068       30       RETURN
  2299.000     0069                END
```

APPENDIX E

THICK WALL CYLINDER CLOSED FORM SOLUTION

APPENDIX E

THICK WALL CYLINDER CLOSED FORM SOLUTION

This appendix presents a comparison of the finite element results predicted by the programme CREEP and the closed form steady state creep of a thick wall cylinder subjected to a uniform internal pressure.

The finite element grid is shown in Figure E-1. The mesh consists of 90 elements and 61 nodes. The ratio of outer to inner radius is equal to 2.0. The vertical and horizontal boundaries are placed on roller supports which allow translation in the radial direction only.

The inner radius is subjected to a uniform pressure of 100 kPa. The elastic material properties are:

$$E = 10 \times 10^6 \text{ kPa}$$
$$\nu = 0.495$$

The flow law of the material is;

$$\dot{\varepsilon} = (1.0 \times 10^{-14})\sigma^{4.5} \qquad \text{(E-1)}$$

where the units are $\text{kPa}^{-4.5}$ and hr^{-1}.

The steady state creep velociy for the inner radius is shown in Figure E-2. The closed form solution neglects elastic response and thus maintains a constant value. After approximately 0.75 hr of creep simulation, the finite element solution predicts a constant velocity 2.2% lower than the closed form solution.

The closed form and finite element elastic and steady state effective stresses are compared in Figure E-3. As shown in the figure, there is very good agreement for both elastic and steady state creep stresses.

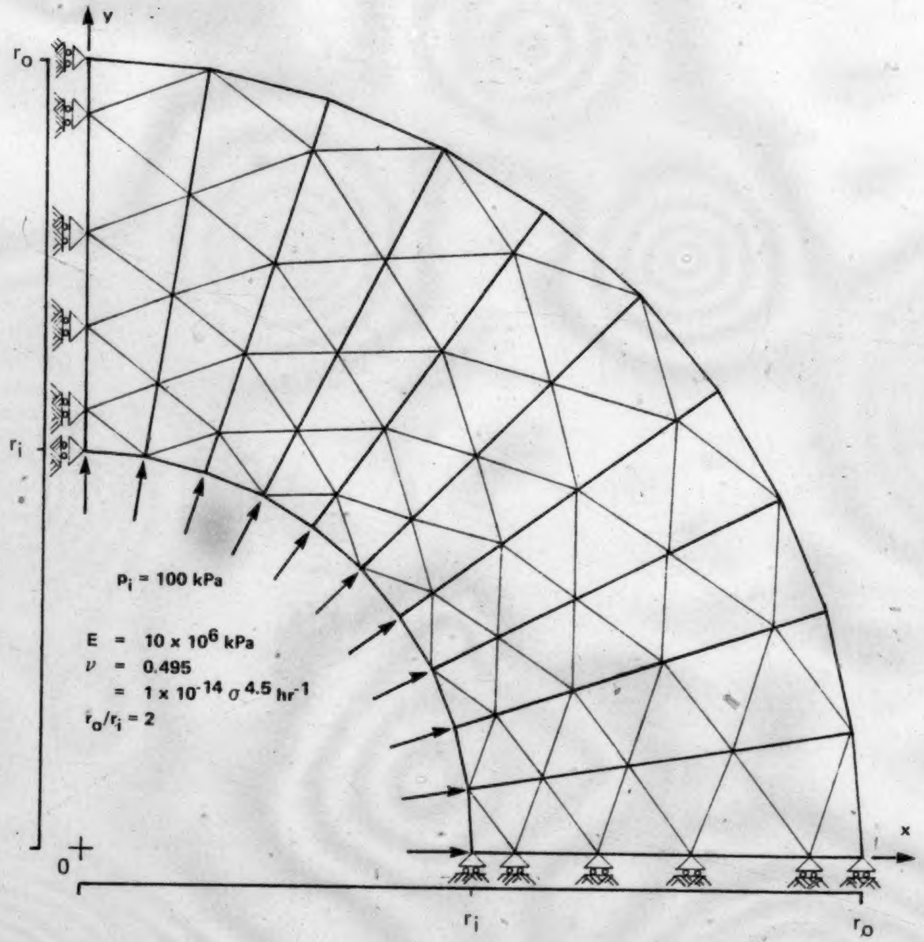
y
r_o
r_i
p_i = 100 kPa
E = 10 x 10^6 kPa
ν = 0.495
= 1 x 10^{-14} $\sigma^{4.5}$ hr^{-1}
r_o/r_i = 2
0
x
r_i
r_o

FIGURE E-1 THICK WALL CYLINDER FINITE ELEMENT MESH

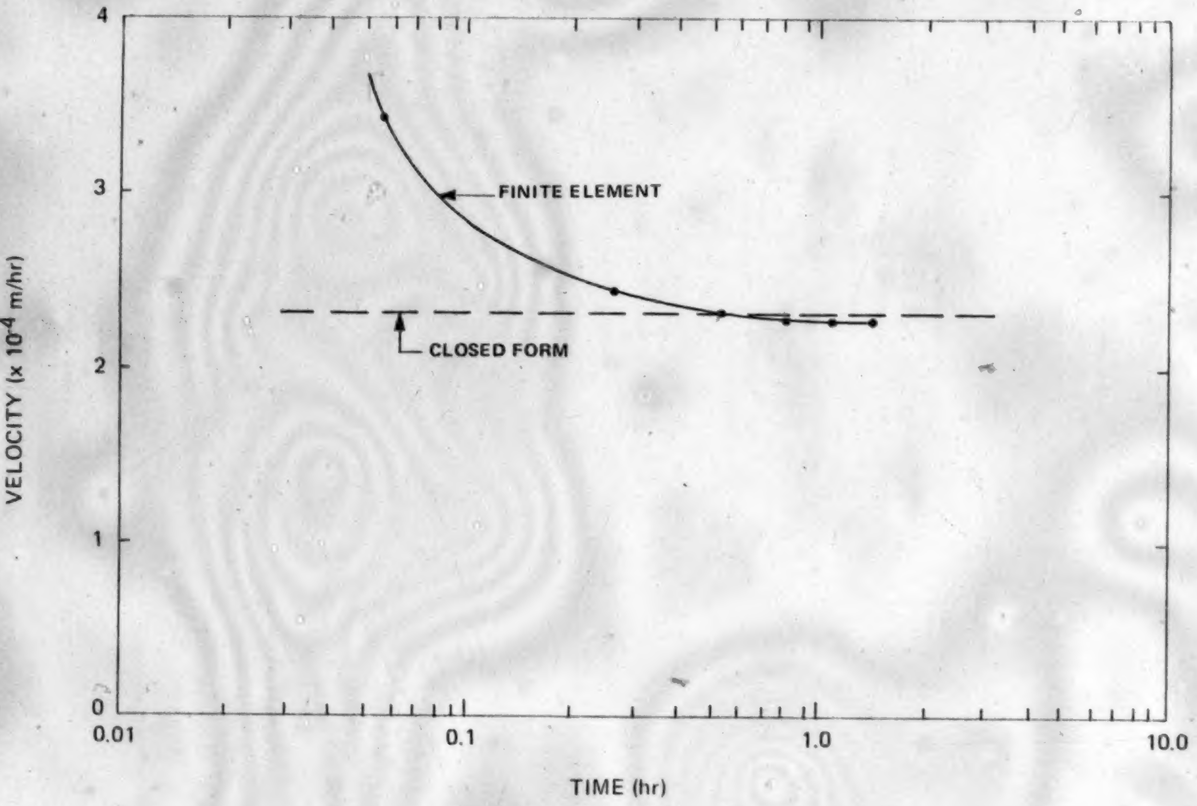

FIGURE E-2 STEADY - STATE CREEP VELOCITY